FACULTY OF PHARMACEUTICAL SCIENCES
UNIVERSITY OF COPENHAGEN

PhD thesis

Martin Hansen

Design and Synthesis of Selective Serotonin Receptor Agonists for Positron Emission Tomography Imaging of the Brain

Academic advisor: Associate Professor, Jesper Langgaard Kristensen

Submitted: 2010-12-16

Author: Martin Hansen

Title: Design and Synthesis of Selective Serotonin Receptor Agonists for Positron Emission Tomography Imaging of the Brain (revised edition)

Print: Det Samfundsvidenskabelige Fakultets Reprocenter

ISBN: 978-87-92719-00-3

Advisors: Jesper Langgaard Kristensen (primary advisor)
Department of Medicinal Chemistry
Faculty of Pharmaceutical Sciences
University of Copenhagen

Mikael Begtrup
Department of Medicinal Chemistry
Faculty of Pharmaceutical Sciences
University of Copenhagen

Thomas Balle
Department of Medicinal Chemistry
Faculty of Pharmaceutical Sciences
University of Copenhagen

Nic Gillings
PET and Cyclotron Unit
Copenhagen University Hospital (Rigshospitalet)

Assessment committee: Markus Piel
Department of Nuclear Chemistry
Johannes Gutenberg University Mainz

Jan Kehler
H. Lundbeck A/S

Rasmus Prætorius Clausen
Department of Medicinal Chemistry
Faculty of Pharmaceutical Sciences
University of Copenhagen

Abstract

Serotonin (5-HT) is an important neurotransmitter that is responsible for the regulation of a number of behavioral effects such as mood, appetite and sleep. Abnormalities in the serotonin system are associated with a broad range of disorders in the central nervous system (CNS) such as schizophrenia, depression, anxiety and migraine. The 5-HT_{2A} receptor is the primary excitatory 5-HT receptor in the human brain and mediates the hallucinogenic effects of drugs such as lysergic acid diethylamide (LSD) and is the target of atypical antipsychotics.

Positron emission tomography (PET) is a powerful technique to study receptors in the living brain and is widely used for investigating 5-HT receptors in both human and animal studies. Currently, only antagonist PET tracers are in use for the 5-HT_{2A} receptor. Agonist PET tracers could selectively label 5-HT_{2A} receptors in the high-affinity state and thereby serve as a better functional measure of 5-HT_{2A} receptor function. Furthermore, agonist PET tracers are potentially more sensitive to changes in endogenous neurotransmitter levels than antagonist tracers.

The aims of this project were: 1) To design and synthesize new 5-HT_{2A} agonists with the aim to increase affinity and selectivity for 5-HT_{2A} receptor. 2) To synthesize, radiolabel and evaluate a number of 5-HT_{2A} agonists for use as PET tracers. These were based on some known 5-HT_{2A} agonists from the literature as well as newly designed compounds.

We synthesized four groups of compounds derived from the *N*-benzylphenethylamine scaffold. Group 1, 2 and 4 compounds were synthesized by a general strategy comprising reductive amination of the appropriate phenethylamine and benzaldehyde building blocks. The more complicated Group 3 compounds were synthesized by a variety of methods.

Group 1 compounds focused on the 4-position of the phenethylamine-moiety with minor variations in the *N*-benzyl moiety. We found that most compounds had high affinity for the 5-HT_{2A}, 5-HT_{2B} and 5-HT_{2C} receptors. Compounds containing a cyano-group in the 4-position showed high selectivity towards the 5-HT_{2A} receptor, a property that has previously been elusive.

Group 2 compounds were designed with the aim to further investigate the 2'- and 3´-position of the *N*-benzyl moiety and many of these were designed as benzo-fused heterocycles. When necessary, the required aldehydes were synthesized *de novo*. The preliminary biological screening showed a mix of good and passable compounds. Some of these compounds have the highest affinity for the 5-HT_{2A} receptor when compared to known compounds from the literature.

Group 3-compounds were designed as conformationally restricted analogues of the known agonists 25B-NBOMe and 25B-NB. Most of the compounds had significantly lower binding affinity at the 5-HT_{2A} when compared to group 2 or 3 compounds, but the study gave valuable information on the binding conformation of *N*-benzylphenethylamines. One compound (**4.7**) showed good selectivity for the 5-HT_{2A} receptor as well as high affinity.

Group 4 compounds were designed using a homology model of the 5-HT_{2A} receptor made using a template from an *in silico*-activated model of the human β_2-adrenergic receptor. The predicted compounds were synthesized and submitted for biological evaluation. The results obtained so far, however, show that the predicted affinity does not correlate well with the experimental results, necessitating further refinement of the model.

A total of nine compounds were selected for *in vivo* evaluation as PET-tracers in pigs. **6.1** ([^{11}C]-CIMBI-5) was able to label 5-HT_{2A} receptors in the brain and the cortical binding of **6.1** was blocked by treatment with the antagonist ketanserin. **6.1** had a non-displaceable binding potential (BP_{ND}) in the pig brain comparable to [^{18}F]-altanserin. Using **6.1** as the lead compound, eight other compounds as well as the **6.1** isotopomer **6.2,** were synthesized and tested. Compound **6.7** ([^{11}C]-CIMBI-36) showed both better brain uptake and higher target-to-background ratio than **6.1**. The cortical BP_{ND} of **6.7** was decreased by ketanserin, indicating high selectivity for 5-HT_{2A} receptors.

Abstrakt

Serotonin (5-HT) er et vigtigt signalstof som er ansvarligt for regulering af en række adfærdsmæssige karaktertræk såsom humør, appetit og søvn. Uregelmæssigheder i serotoninsystemet er sammenkædet med en lang række lidelser i centralnervesystemet (CNS) såsom skizofreni, depression, angst og migræne. 5-HT_{2A}-receptoren er den primære excitatoriske 5-HT-receptor i menneskets hjerne og tilvejebringer de hallucinogene påvirkninger medført af stoffer såsom lysergsyre diethylamid (LSD) og er et molekylært mål for atypiske antipsykotika.

Positronemissionstomografi (PET) er en effektiv metode til studier af receptorer i hjernen og er vidt udbredt til undersøgelse af 5-HT receptorer i både mennesker og forsøgsdyr. Hidtil, har kun antagonist PET sporstoffer været anvendt til studier af 5-HT_{2A}-receptoren. Agonist PET sporstoffer er i stand til selektivt at radiomærke 5-HT_{2A}-receptorer i højaffinitetstilstanden og dermed udgøre en bedre funktionel målemetode for 5-HT_{2A} receptorfunktion. Agonist PET sporstoffer er endvidere potentielt mere følsomme overfør ændringer i koncentration af endogene signalstoffer end antagonist sporstoffer.

Formålet med dette projekt har været: 1) At syntetisere, radiomærke og evaluere en række 5-HT_{2A}-agonister som PET sporstoffer. Disse stoffer var baseret på kendte 5-HT_{2A}-agonister fra litteraturen så vel som nyligt designede stoffer. 2) At designe og syntetisere nye 5-HT_{2A}-agonister med henblik på at øge affinitet og sektivitet for 5-HT_{2A}-receptoren.

Vi syntetiserede fire grupper af stoffer baseret på *N*-benzylphenethylamin-skelettet. Gruppe 1-, 2- og 4-stoffer blev syntetiseret udfra en general strategi bestående af reduktiv aminering af de tilsvarende phenethylamin og benzaldehyd byggeblokke. De mere komplicerede Gruppe 3-stoffer blev syntetiseret ved hjælp af en række metoder.

Gruppe 1-stofferne fokuserede på 4-stillingen af phenethylamin-kernen med mindre variationer af *N*-benzyl-delen. De fleste af disse stoffer viste sig at have høj affinitet for 5-HT_{2A}, 5-HT_{2B} and 5-HT_{2C} receptorer. Stoffer indeholdende en cyano-gruppe i 4-stillingen udviste god selektivitet for 5-HT_{2A}-receptorer, en egenskab der hidtil har været vanskelig at opnå.

Gruppe 2-stofferne blev designet med henblik på yderligere undersøgelser af 2'- og 3'-stillingen i *N*-benzyl-delen og mange af disse blev designet som benzannelerede heterocykler. De anvedte aldehyder blev om nødvendigt syntetiseret *de novo*. De indtil videre opnåede resultater fra den biologiske screening viste en blanding af gode og middelmådige stoffer. Nogle af disse stoffer udviste den højest målte affinitet for 5-HT_{2A}-receptoren sammenlignet med stoffer kendt fra litteraturen.

Gruppe 3-stofferne blev designet som konformationelt begrænsede analoger af de kendte 5-HT_{2A} agonister 25B-NBOMe og 25B-NB. De fleste af stofferne havde betydelig lavere bindingsaffinitet for 5-HT_{2A}-receptoren sammenlignet med gruppe 2- og 3-stofferne, men undersøgelsen gav vigtig information om den aktive bindingskonformation af *N*-

benzylphenethylaminerne. Et af stofferne (**4.7**) udviste både god affinitet samt høj selektivitet for 5-HT_{2A}-receptoren.

Gruppe 4-stofferne blev designet ved hjælp af en homologimodel af 5-HT_{2A}-receptoren lavet ved brug af en skabelon af en computeraktiveret model af den humane β_2-adrenerge receptor. De foreslåede stoffer blev syntetiseret og underkastet biologisk evaluering. De hidtil opnåede resultater viste imidlertid at den beregnede affinitet ikke stemte særlig godt overens med de eksperimentelle resultater hvilket betyder at yderligere udvikling af modellen er nødvendig.

Ni stoffer blev udvalgt til evaluering som PET-sporstoffer i levende grise. **6.1** ([^{11}C]CIMBI-5) var i stand til at radiomærke 5-HT_{2A}-receptorer i hjernen og den kortikale binding blev blokeret ved behandling med antagonisten ketanserin. **6.1** havde et ikke-displacérbart bindingspotentiale (BP_{ND}) der var sammenligneligt med [^{18}F]altanserin i grisehjernen. På baggrund af **6.1**-strukturen blev otte andre stoffer designet, syntetiseret og testet og ligeså blev **6.1**-isotopomeren **6.2**. Stof **6.7** ([^{11}C]CIMBI-36) havde både et højere optag i hjernen samt forbedret target-to-background-forhold sammenlignet med **6.1**. Det kortikale BP_{ND} af [^{11}C]CIMBI-36 kunne blokeres med ketanserin, hvilket indikerer at **6.7**-binding er specifik for 5-HT_{2A}-receptorer.

Acknowledgements

The work presented in this thesis could not have been realized without the help and contributions from the many people I have had the privilege to work with and get to know during my three years as a graduate student. To fully express my gratitude to all these people would require a document of near equal length to this thesis.

First of all I would like to thank my two main supervisors Professor Mikael Begtrup and Associate Professor Jesper L. Kristensen. Mikael served as my main supervisor from November 2007 until his retirement in April 2010 but continues to offer his help and encouragement. Jesper has served as my day-to-day supervisor for most of the project and has filled in for Mikael as my main supervisor after Mikaels retirement. I owe both of them a lot of thanks for their guidance and encouragement throughout this project.

I would also like to thank my two co-supervisors Associate Professor Thomas Balle and Dr. Nic Gillings. Thomas has together with David Gloriam and Vignir ìsberg worked on the modeling part of the project and they were responsible for the development of the 5-HT_{2A} homology model. Nic and his group of radiochemists; Jacob, Kjell, Matthias and Szabolcs have been responsible the radiochemistry part of the project and the work with metabolites.

Many thanks go to Lars Kyhn Rasmussen and James Paine who both served as postdocs on this project in parallel with my PhD-work and whose many inputs and ideas have become an integral part of this thesis.

Anders Ettrup, Mikael Palner, Martin Santini and Gitte M. Knudsen have been responsible for PET-experiments, in vitro and in vivo experiments and I thank them for their co-operation throughout this project.

I would also like to thank the Master and Bachelor students which have contributed to this project. Thanks to all my fellow students and co-workers in the department through the years for a friendly and inspiring environment.

Special thanks goes to Morten for kindly allowing me to use the fancy hydrogenation apparatus at Novo Nordisk, and to Rune for running 600 Mhz spectra at Lundbeck.

I owe a great thanks to Professor David E. Nichols at Purdue University for the opportunity to join his group and allowing me to work on one of his projects. Dr. Nichols knowledge and expertise in the area of 5-HT_{2A}-receptors is unsurpassed, and his continuing inputs and comments on this project have been invaluable. Thanks also to the rest of the Nichols group; José, Fernando, Alia, Lisa, John, Ben, Alex, Aubrie, Danuta and Stewart for making my stay very enjoyable. My housemates in the 'Rugby House'; Amber, Maciej and Alfonso also deserves thanks for a cozy and memorable environment.

I would also like to thank the people who have been helpful with administrative and practical details; Marianne and Pia from the PhD-administration and Heidi, Anja and Tina from Department of Medicinal Chemistry and everybody from the workshop.

Last but not least thanks to my family and friends for your continuing support and encouragement.

Preface

This revised edition thesis describes research carried out as part of a PhD-program at the Faculty of Pharmaceutical Sciences, University of Copenhagen from November 2007 to November 2010, but includes some additional biological data not present at the time of submission. The additional biological data concerns binding affinities of compounds described en chapters 2, 3 and 5 and serves to give a more complete characterization of the compounds.

The experimental work described in this thesis was carried out primarily at the Department of Medicinal Chemistry, Faculty of Pharmaceutical Sciences, University of Copenhagen between January 2009 and November 2010 under the supervision of Mikael Begtrup and Jesper L. Kristensen.

The experimental work described in Chapter 4 was carried out at the Department of Medicinal Chemistry and Molecular Pharmacology, Purdue University, West Lafayette, Indiana between June 2008 and December 2008 under the supervision of David E. Nichols.

References are numbered consecutively throughout the entire thesis and appear in superscript, whereas compounds are numbered according to which chapter they appear in in boldface: e.g. **2.14** is compound no. 14 in Chapter 2.

Protein residues are referred to by their one-letter codes followed by their full sequence number. Ballesteros-Weinstein numbers are shown in parenthesis following the full sequence number were applicable.

List of Publications

This PhD project has so far resulted in the two publications enclosed at the end of the thesis as appendix 2 and 3

Appendix 2

Anders Ettrup, Mikael Palner, Nic Gillings, Martin A. Santini, Martin Hansen, Birgitte R. Kornum, Lars K. Rasmussen, Kjell Någren, Jacob Madsen, Mikael Begtrup, and Gitte M. Knudsen. Radiosynthesis and Evaluation of ^{11}C-CIMBI-5 as a 5-HT_{2A} Receptor Agonist Radioligand for PET. *Journal of Nuclear Medicine* **2010**, *51*(11), 1763-1770

Appendix 3

Anders Ettrup, Martin Hansen, Martin Andreas Santini, James Paine, Nic Gillings, Mikael Palner, Szabolcs Lehel, Matthias M. Herth, Jacob Madsen, Jesper Kristensen, Mikael Begtrup and Gitte Moos Knudsen. Radiosynthesis and in vivo evaluation of a series of substituted ^{11}C-phenethylamines as 5-HT_{2A} agonist PET tracers. *European Journal of Nuclear Medicine and Molecular Imaging* (published online, DOI: 10.1007/s00259-010-1686-8)

Abbreviations

2-AG	2-arachidonylglycerol
2C-B	2-(4-bromo-2,5-dimethoxyphenyl)ethanamine
2C-C	2-(4-chloro-2,5-dimethoxyphenyl)ethanamine
2C-CN	4-(2-aminoethyl)-2,5-dimethoxybenzonitrile
2C-D	2-(2,5-dimethoxy-4-methylphenyl)ethanamine
2C-E	2-(4-ethyl-2,5-dimethoxyphenyl)ethanamine
2C-F	2-(4-fluoro-2,5-dimethoxyphenyl)ethanamine
2C-I	2-(4-iodo-2,5-dimethoxyphenyl)ethanamine
2C-P	2-(4-iodo-2,5-dimethoxyphenyl)ethanamine
2C-T	2-(2,5-dimethoxy-4-(methylthio)phenyl)ethanamine
2C-T2	2-(4-(ethylthio)-2,5-dimethoxyphenyl)ethanamine
2C-T7	2-(2,5-dimethoxy-4-(propylthio)phenyl)ethanamine
2C-TFM	2-(2,5-dimethoxy-4-(trifluoromethyl)phenyl)ethanamine
25B-NB	*N*-benzyl-2-(4-bromo-2,5-dimethoxyphenyl)ethanamine
25B-NBOMe	2-(4-bromo-2,5-dimethoxyphenyl)-*N*-(2-methoxybenzyl)ethanamine
25I-NBOMe	2-(4-iodo-2,5-dimethoxyphenyl)-*N*-(2-methoxybenzyl)ethanamine
5-CT	5-carboxamidotryptamine
5-HIAA	5-hydroxylindoleacetic acid
5-HT	5-hydroxytryptamine (serotonin)
5-HTP	5-hydroxytryptophan
5-MeO-DMT	5-methoxy-*N*,*N*-dimethyltryptamine
AA	arachidonic acid
AADC	aromatic amino acid decarboxylase
Ac	acetyl
AC	adenylate cyclase
acac	acetylacetonate
ADP	adenosine diphosphate
Arf	ADP ribosylation factor
Boc	*tert*-butoxycarbonyl
Bn	benzyl
BP_{ND}	non-displaceable binding potential
Bu	*n*-butyl
cAMP	3'-5'-cyclic adenosine monophosphate
CIMBI	Center for Integrated Molecular Brain Imaging
CNS	central nervous system
DAG	diacylglycerol
DDQ	2,3-dichloro-5,6-dicyano-1,4-benzoquinone
dec	decomposition
DIBAL	diisobutylaluminium hydride
DMAP	*N*,*N*-dimethyl-4-aminopyridine
DME	1,2-dimethoxyethane
DMF	*N*,*N*-dimethylformamide
DMSO	dimethyl sulfoxide
DMT	*N*,*N*-dimethyltryptamine
DNA	deoxyribonucleic acid
DOB	1-(4-bromo-2,5-dimethoxyphenyl)propan-2-amine
DOCN	4-(2-aminopropyl)-2,5-dimethoxybenzonitrile
DOI	1-(4-iodo-2,5-dimethoxyphenyl)propan-2-amine
dppe	1,2-bis(diphenylphosphino)ethane

ELK1	Ets-like gene 1
ERK	extracellular signal-regulated kinase
Et	ethyl
FDG	fluorodeoxyglucose
GC-MS	gas chromatography-mass spectrometry
GDP	guanosine diphosphate
GPCR	guanine nucleotide-binding protein coupled receptor
Grb2	growth factor receptor-bound protein 2
GRK	GPCR kinase
GTP	guanosine triphosphate
HPLC	high performance liquid chromatography
i-Pr	isopropyl
IBX	2-iodoxybenzoic acid
IP_3	inositol triphosphate
IP3R	inositol triphosphate receptor
LDA	Lithium diisopropylamide
LDBBA	lithium diisopropyl *tert*-butoxyaluminium hydride
LiTMP	lithium 2,2,6,6-tetramethylpiperidide
LSD	*d*-lysergic acid diethylamide
K_D	equilibrium dissociation constant
K_i	equilibrium dissociation constant determined in a competitive binding assay
MAO	monoamine oxidase
MAP	mitogen-activated protein
m-CPBA	*meta*-chloroperoxybenzoic acid
MDMA	3,4.-methylenedioxymethamphetamine
Me	methyl
MEK	MAPK ERK kinase (MAP kinase kinase)
MIF	molecular interaction field
MKK	MAP kinase kinase
m/z	mass-to-charge ration
NBS	*N*-bromosuccinimide
NIMH	National Iinstitute of Mental Health
NMO	*N*-methylmorpholine *N*-oxide
NMP	*N*-methyl-2-pyrrolidone
NMR	nuclear magnetic resonance
p38	p38 mitogen-actived protein kinase
PA	phosphatidic acid
PDSP	Psychoactive Drug Screening Programme
PET	positron emission tomography
Ph	phenyl
Phth	phthaloyl
PI	Phosphatidylinositol
PIP_2	phosphatidylinositol bisphosphate
PKC	protein kinase C
PKN	protein kinase N
PL	phospholipid
PLA_2	phospholipase A_2
PLC	phospholipase C
PLD	phospholipase D
PPA	polyphosphoric acid
Pr	*n*-propyl

Red-Al	sodium bis(2-methoxyethoxy) borohydride
RNA	ribonucleic acid
rt	room temperature
SERT	serotonin transporter
Shc	Src homology-2 domain containing transforming protein
Sos	son-of-sevenless, a guanine nucleotide exchange factor
SRE	serum response element
Srf	serum response factor
t-Bu	*tert*-butyl
TBAF	tetra-*n*-butylammonium fluoride
TBDMS	*tert*-butyldimethylsilyl
Tf	trifluoromethanesulfonyl (triflyl)
TFA	trifluoroacetic acid
TFAc	trifluoroacetyl
TH	tryptophan hydroxylase
THF	tetrahydrofuran
TLC	thin layer chromatography
TMEDA	*N, N, N',N'*-tetramethylethane-1,2-diamine
TMH	trans-membrane helix
TPAP	tetra-*n*-propylammonium perruthenate
Tr	triphenylmethyl (trityl)
Ts	*para*-toluenesulfonyl (tosyl)

Table of Contents

Chapter 1

Introduction

1.1 The Serotonin system

Serotonin (5-hydroxytryptamine, 5-HT) is an important monoamine neurotransmitter in both the peripheral and central nervous system (CNS). In the CNS, 5-HT modulates a plethora of diverse processes such as cognition, memory processing, mood, anxiety, circadian behavior and appetite. In the neuronal cells 5-HT is synthesized from the essential amino acid tryptophan in two steps. The enzyme tryptophan hydroxylase (TH) oxidizes the 5-position of tryptophan to give 5-hydroxytryptophan (5-HTP). 5-HTP is converted to 5-HT by the enzyme aromatic amino acid decarboxylase (AADC). The rate-limiting step in serotonin biosynthesis is tryptophan hydroxylation and inhibition of TH decreases 5-HT synthesis leading to serotonin depletion. The 5-HT is stored in secretory vesicles and released into the synaptic cleft upon neuronal activation. The released 5-HT binds to 5-HT receptors on the postsynaptic neuron and initiates downstream signaling cascades through various effector systems which ultimately result in a physiological response and regulation of gene expression. Neurotransmission is terminated by reuptake of 5-HT by the serotonin transporter (SERT). The 5-HT is then recycled and incorporated into new storage vesicles or oxidized by monoamine oxidases (MAOs) to 5-hydroxyindoleacetic acid (5-HIAA).

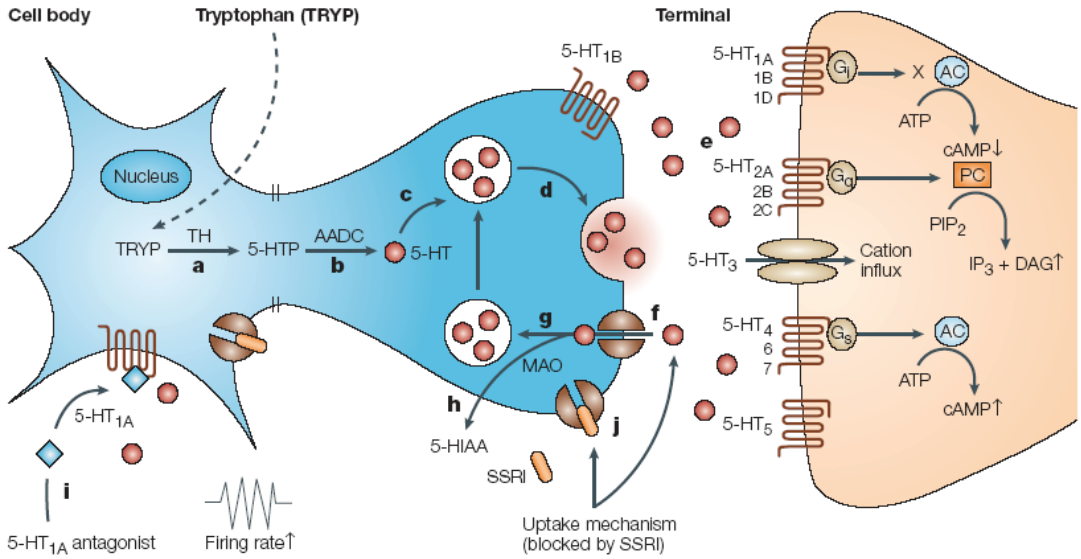

Figure 1: Diagram of the serotonergic neurotransmission. a| Tryptophan hydroxylase (TH) catalyses the conversion of tryptophan (TRYP) to 5-hydroxytryptophan (5-HTP) in the pre-synaptic neuron. b| Aromatic amino acid decarboxylase (AADC) catalyses the conversion of 5-HTP to 5-hydroxytryptamine (5-HT, serotonin). c| 5-HT is taken up into storage vesicles. d| 5-HT is released from storage vesicles into the synaptic cleft upon neuronal activation. e| 5-HT can activate subtypes of the seven existing 5-HT receptor families, which couple with their respective system of signal transduction inside the post-synaptic neuron. f| 5-HT is taken up into the pre-synaptic 5-HT terminals by the 5-HT transporter (SERT). g,h| Within the pre-synaptic 5-HT terminals, 5-HT would either be taken up by the storage vesicles or degraded by monoamine oxidase (MAO). i| 5-HT activates the pre-synaptic somatodendritic 5-HT$_{1A}$ autoreceptor, which can be blocked by selective 5-HT$_{1A}$ antagonists. j| Selective serotonin reuptake inhibitors (SSRIs) inhibit the 5-HT transporter. Figure adapted from Wong et al.[1]

The cell bodies of serotonergic neurons in the brain are localized in clusters in the brain stem known as the raphe nuclei[2]. Although the cell bodies are located in the raphe nuclei, the serotonergic neurons send projections to almost every part of the CNS.

1.2 5-HT receptors

Today there are 15 known 5-HT receptor subtypes[3]. Fourteen of these belong to the superfamily of guanine nucleotide-binding protein-coupled receptors (GPCRs), while the last, the 5-HT_3 receptor is a ligand-gated ion channel. The classification of 5-HT receptors has changed several times during the last few decades to accommodate new subtypes and changes in the general knowledge of the receptors. The earliest classification divided 5-HT receptors into a D and an M category[4], thus named because D-receptors were inhibited by dibenzyline and M-receptors by morphine. In 1979 two different types of 5-HT receptors were identified in brain homogenate[5]. The first had high affinity for LSD and 5-HT and was named the 5-HT_1 receptor. The other had high affinity for LSD and for spiperone and was called the 5-HT_2 receptor. In the late 1980s there was evidence of several types of 5-HT_2 receptors from autoradiographic and ligand-based assays. The first receptor to have its DNA cloned was the 5-HT_{1A} receptor[6,7] and following this discovery the other 5-HT receptors were also identified by cloning. The 5-HT_{5B} gene is present in the human DNA and has been cloned, but stop codons prevent the expression of a functional protein in humans whereas the functional receptor is present in rodents[8].

The 5-HT receptor family is further diversified by receptor isoforms arising from differential splicing, RNA-editing and single nucleotide polymorphisms[9,10]. The consequences of this diversification have been associated with a number of conditions such as anxiety[11], depression[12] schizophrenia, and are especially pronounced with the 5-HT_{2C} receptor[13,14].

The current classification of 5-HT receptors was formalized by IUPHAR in 1994[15]. The 5-HT receptors were divided into seven types based on their operational, structural and transductional characteristics. Some these properties are listed in Table 1 along a selection of agonists and antagonists for each receptor where applicable.

Subtype	First cloned	Primary effector system	Primary localization in the CNS	Agonists Selective in bold	Antagonists Selective in Bold
5-HT$_{1A}$	1987[6,7]	$G_{i/o}$ ↓cAMP	Dorsal and median raphe, hippocampus, septum, cortex	LSD, 8-OH-DPAT **F-15,599**	WAY-100,135 WAY-100,635
5-HT$_{1B}$	1992[16-18]	$G_{i/o}$ ↓cAMP	Basal ganglia, substantia nigra	Ergotamine, **CGS-12066A**	GR-125,743 **SB-216,641**
5-HT$_{1D}$	1991[19]	$G_{i/o}$ ↓cAMP	Basal ganglia, substantia nigra	Sumatriptan, **CP-135,807**	Ziprasidone,
5-HT$_{1E}$	1992[20]	$G_{i/o}$ ↓cAMP	Hippocampus, entorhinal cortex, subiculum,	BRL-54443	
5-HT$_{1F}$	1993[21]	$G_{i/o}$ ↓cAMP	Globus pallidus, substantia nigra, spinal cord	BRL-54443, **LY-334,370**	
5-HT$_{2A}$	1988[22,23]	$G_{q/11}$ ↑IP_3	Cortex, neocortex, claustrum	LSD, DOI, psilocin	Ketanserin, **MDL-100,907**
5-HT$_{2B}$	1992[24]	$G_{q/11}$ ↑IP_3	Inferior collicolus, cohlea	LSD, DOI, psilocin, **BW-723C86**	Sarpogrelate, **RS-127,445**
5-HT$_{2C}$	1988[25]	$G_{q/11}$ ↑IP_3	choroid plexus	LSD, DOI, mCPP, **Lorcaserin**	Mesulergine, **RS-102,221**
5-HT$_{3}$	1993[26]	*	Spinal trigeminal nerve nucleus, area postrema, solitary tract nucleus	2-methyl-5-HT, **RS-56812**	**Ondansetron, Palonosetron**
5-HT$_{4}$	1995[27]	G_s ↑cAMP	hippocampus, basal ganglia, cortex, substantia nigra	Cisapride, **Tegaserod**	Piboserod
5-HT$_{5A}$	1994[28]	$G_{i/o}$ ↓cAMP	olfactory bulb, medial habenula, neocortex	Valerenic acid, LSD,5-CT	Latrepirdine, **SB-699,551**
5-HT$_{5B}$	1993[29,30]	$G_{i/o}$ ↓cAMP	**	5-CT, LSD	Methiothepin
5-HT$_{6}$	1993[31-33]	G_s ↑cAMP	striatum, cortex nucleus accumbens	**WAY-181,187 EMD-386,088**	Latrepirdine, **Lu AE58054**
5-HT$_{7}$	1993[34-37]	G_s ↑cAMP	thalamus, hippocampus hypo-thalamus, cortex	5-CT, 8-OH-DPAT,	Mesulergine, Methysergide

Table 1: Information on the 15 5-HT receptor subtypes. *The HT_3 receptor is a cation-selective ion channel. **The 5-HT_{5B} receptor is not expressed as a functional protein in humans.

1.3 The 5-HT$_{2A}$ receptor

The 5-HT_{2A} receptor is the most abundant excitatory 5-HT receptor in the human brain. It is believed to be responsible for the remarkable psychopharmacological effects exerted by hallucinogens such as LSD[38,39]. The effects of atypical antipsychotics are partly mediated by antagonism at the 5-HT_{2A} receptor[40,41].

1.3.1 The ternary complex model – high and low affinity states

Activation of GPCRs like the 5-HT_{2A} receptor is often explained by the use of the ternary complex model[42] which posits that the receptor exist in four species in dynamic equilibrium: the free GPCR, the G-protein/GPCR complex, the agonist/GPCR complex and finally the agonist/GPCR/G-protein complex (see Figure 2). This model however did not explain why agonists such as DOB bind to a smaller population of 5-HT_{2A} receptors than the antagonist ketanserin. Initially this discrepancy was attributed to ketanserin binding to other hitherto unknown receptors. With the advent of cloned receptors this possibility was eliminated and it was found that 5-HT_{2A} receptors exist in a high-affinity and a low-affinity state[23,43,44]. The original ternary complex model did not accommodate different affinity states, but a modified ternary complex model was proposed to account for different affinity states[45]. The modified ternary complex model also explains the phenomenon of inverse agonism stating that binding of an inverse agonist stabilizes the inactive state of the receptor and decreases constitutive activity[46]. A cubic ternary complex model has also been devised to produce a complete equilibrium description of the three-way interactions between ligand, receptor and G-proteins[47-49].

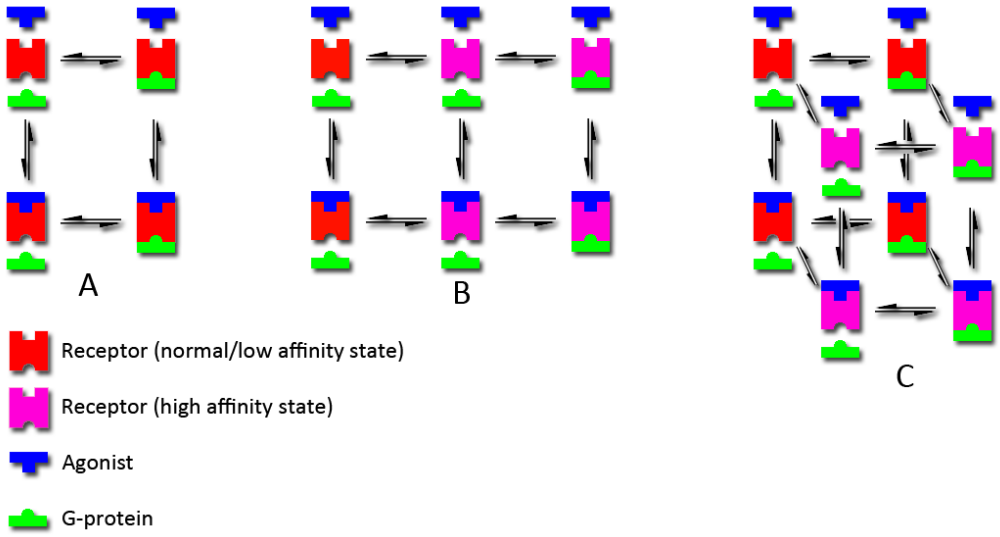

Figure 2: A| The ternary complex model. B| The modified ternary complex model. C| the cubic ternary complex model. Adapted from Limbird 2004[50]

When an agonist binds the GDP bound to the G-protein is exchanged for GTP. This results in disengagement of the G-protein from the receptor/agonist/G-protein complex and dissociation of the G-protein into G_{α} and $G_{\beta\gamma}$ subunits. These initiate an intracellular signaling cascade that is responsible for neuronal activation and regulation of gene expression. It has been known for a while that 5-HT_{2A} receptors activate more than one signaling pathway via different G-proteins and that the differentiation between signaling pathways is dependent on the agonist. This phenomenon which is known as “agonist-directed trafficking of receptor stimulus”, “biased agonism” or “functional selectivity” has in some ways rendered the classic receptor models obsolete[51-55]. The elucidation of the different downstream signaling pathways is a complex task and often diverging results are obtained due to differences in tissue type and species.

1.3.2 The PLC-pathway

The link between 5-HT receptors and phosphoinositide turnover was first established in 1984 when Conn and Sanders-Bush found that 5-HT_2 antagonists inhibited phosphatidylinositol(PI) metabolism in rat cerebral cortex[56] and soon after it was found that agonists stimulated PI-metabolism[57,58]. The regulation of intracellular Ca^{2+} levels was also tied to 5-HT_{2A} activation but was initially thought to be independent of PI-hydrolysis[59]. However, it was quickly realized that Ca^{2+}-mobilization was dependent on accumulation of inositol triphophate (IP_3)[60] generated by hydrolysis of PIP_2. Indeed, IP_3 binds to the IP_3-receptor which is a cation-specific ion channel situated in the membrane of the endoplasmic reticulum. Upon activation Ca^{2+} is released from the endoplasmic reticulum into the cytosol[61].

Hydrolysis of phosphoinositides also produces diacylglycerol (DAG), another secondary messenger. Both DAG and Ca^{2+} are coupled to protein kinase C (PKC). PKC is coupled to mitogen activated protein kinases (MAP kinases) specifically extracellular signal-regulated kinases 1 and 2 (ERK1/2) through the Ras-Raf-MEK cascade[62,63]. It is known that ERK1/2 activates Ets-like gene 1 (ELK1) which combines with serum response factor (Srf) and serum response element (SRE) to give a complex that promotes transcription of the immediate early gene *c-fos*[64,65]. Activation of 5-HT_{2A} receptors has been linked to induction of *c-fos* but the pathway through which this happens is not yet elucidated[66].

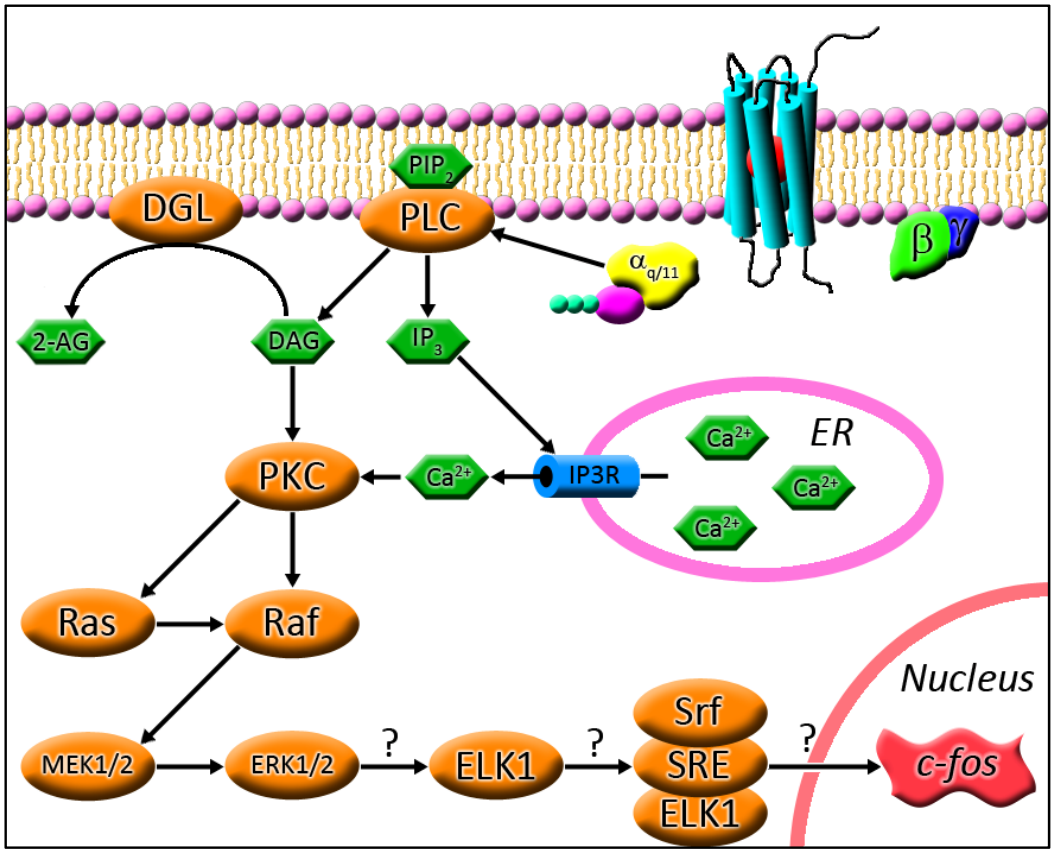

Figure 3: Illustration of the $G_{q/11}$-PLC pathway in the 5-HT_{2A} receptor. ER = endoplasmic reticulum

The PLC-pathway has mainly been linked to dissociation of $G_{q/11}$ proteins from the receptor. But an interesting observation that remains to be elucidated has recently been made concerning this link[67]. It appears that $G_{q/11}$-activation and Ca^{2+}-release was differentiated in a group of structurally diverse agonists suggesting that $G_{q/11}$-activation is not the sole determinant in PLC-activation. Another explanation could be that although closely related both structurally as well as functionally there could be differences between G_q and G_{11} proteins[68] that were not accounted for.

Parrish and Nichols showed that DAG is converted to 2-arachidonoylglycerol (2-AG) by DAG lipase and that this transformation is PLC dependent and not connected to PLD or phosphatidylcholine-sensitive PLC[69]. 2-AG is an endocannabinoid but the downstream effects of 2-AG in relation to 5-HT_{2A} are not fully described.

1.3.3 The PLA_2-cascades

Activation of the 5-HT_{2A} receptor has also been shown to couple to phospholipase A_2 (PLA_2) with resulting accumulation of arachidonic acid (AA)[70,71]. PLA_2-activation has been proved to be independent of PLC-activation in several cell lines[72,73]. The link between receptor activation and PLA_2 –activation is significantly more complex than the PLC-pathway

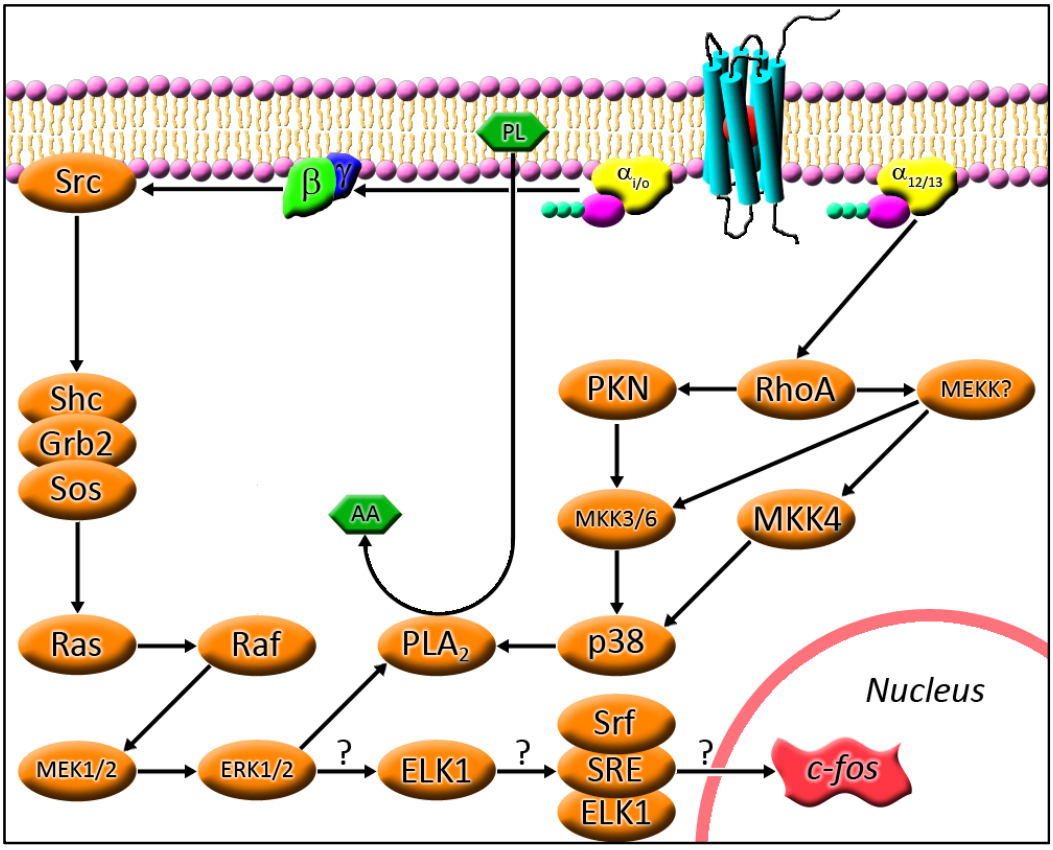

Figure 4: Illustration of the two PLC-independent parallel pathways leading to PLA2-activation. Adapted from Kurrasch-Orbaugh et al.[74]

In an elegant study Kurrasch-Orbaugh et al.[74] showed that PLA_2-activation can occur by at least two different pathways. Activation of the Ras-Raf-MEK1/2-ERK1/2 cascade by the Shc-Gbr2-Sos

ternary complex leads to AA-accumulation. By employing different inhibitors and scavengers the Ras-Raf-MEK1/2-ERK1/2 cascade was linked to the βγ-subunit of the $G_{i/o}$ proteins. It is believed that the βγ-subunits activate Src which in turn phosphorylates Shc and leads to formation of the Shc-Grb2-Sos complex.

Another pathway where PLA_2 was activated by p38 MAP kinase was also identified and linked to another class of G-proteins, $G_{12/13}$. Interestingly, inhibition of both pathways did not abolish AA-accumulation. It is possible that AA-accumulation can be the result of ERK1/2 activation via the PLC-pathway although AA-accumulation has been shown to be independent of PLC-activity[70,74]. Another explanation could be activation of Src by β-arrestins as it is known from the β_2-adrenergic receptor[75,76].

1.3.4 Regulation of gene expression

The curious case of the non-hallucinogenic 5-HT_{2A} agonist lisuride has spawned a lot research into the signaling of 5-HT_{2A} receptors[77-81]. With the accumulating evidence in favor of functional selectivity pharmacologists hoped to find a signaling pathway exclusively activated by hallucinogens but unaffected by lisuride, however until recently no such pathway had been identified.

A recent study identified transcriptome fingerprints unique to hallucinogenic 5-HT_{2A} agonists and distinct from lisuride[82]. The follow up study found that LSD, DOI and lisuride all activated 5-HT_{2A} receptors resulting in induction of *c-fos* transcription but only LSD and DOI induced *egr1* and *egr2* expression[83]. By using different inhibitors the study found that inhibition of PLC abolished 5-HT_{2A}-mediated induction of *c-fos, egr1* and *egr2* by LSD, DOI and lisuride. Inhibition of the $G_{i/o}$ protein attenuated the induction of *c-fos, egr1* and *egr2* by LSD and DOI.Furthermore, inhibition of Src which is downstream of $G_{i/o}$ (Figure 4) attenuated LSD and DOI-induced *c-fos* expression to lisuride levels and completely abolished induction of *egr1* and *egr2*. When combined with the results of Kurrasch-Orbaugh et al. these results suggest that co-activation of $G_{q/11}$-PLC and the $G_{i/o}$-Src-MEK1/2-ERK1/2 pathway is required for hallucinogenesis. It also follows that induction of *c-fos* is partially dependent on Src-activation but could also be the result of $G_{q/11}$-PLC activation.

1.3.5 Other signaling mechanisms

Not only do GPCRs couple differentially to various G-proteins upon activation, in the last decade there has been increasing evidence of downstream signaling by GPCRs initiated by other effectors than G-proteins[84]. A few of these have been linked specifically to 5-HT_{2A} receptors, namely β-arrestins and ADP ribosylation factor (Arf).

β-arrestins are structural proteins that are implicated in GPCR desensitization and internalization *(vide infra)* but also have effects on signal transduction[85-89]. A recent study showed that the head-twitch response elicited by 5-HT and the hallucinogenic 5-HT_{2A} agonist DOI were differentiated in β-arrestin knock-out mice[90]. In the knock-out mice the head-twitch response resulting from 5-HT was abolished while DOI-treated mice still elicited head-twitch behavior. Interestingly, while the head-twitch response is commonly regarded as a behavioral proxy of hallucinogenesis[83], increase in 5-HT, which is not considered hallucinogenic, still resulted in increased head-twitch behavior in wildtype mice. ERK-activation was also found to dependent

on the presence of β-arrestin. The knock-out mice treated with 5-HT showed greatly diminished ERK-activation compared to the wildtype while DOI treatment resulted in the same level of ERK activation. When 5-HT or DOI were co-administered along with a PLC inhibitor no ERK activation was observed. These results suggest that β-arrestin is important in endogenous signaling while DOI-activated receptors signal mainly through G-protein mediated cascades.

Arf-proteins are small proteins related to G proteins. 5-HT_{2A} receptors interacts preferentially with Arf1 which activates phospholipase D (PLD) resulting in accumulation of phosphatidic acid[91-93]. There is no research related to the downstream signaling arising from PLD-activation of 5-HT_{2A} receptors although phosphatidic acids are known to activate a number of signaling cascades[94].

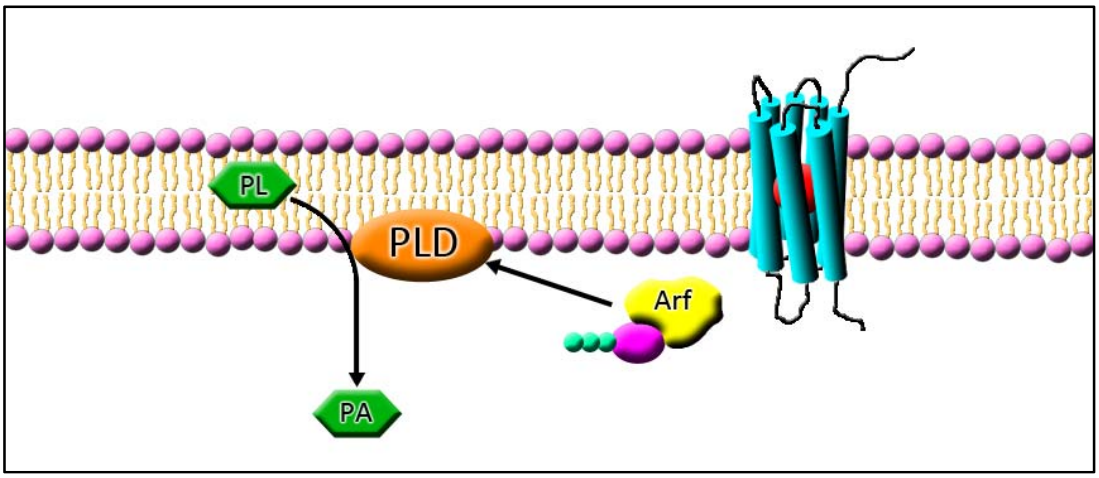

Figure 5: Illustration of the Arf-PLC signaling pathway

1.3.6 Densensitization and internalization

As mentioned above β-arrestins play a key role in desensitization and internalization of GPCRs[86,95-97]. After receptor activation and G protein-dissociation the receptor is phosphorylated by GPCR kinases (GRKs) which only act on agonist-bound receptors[97].

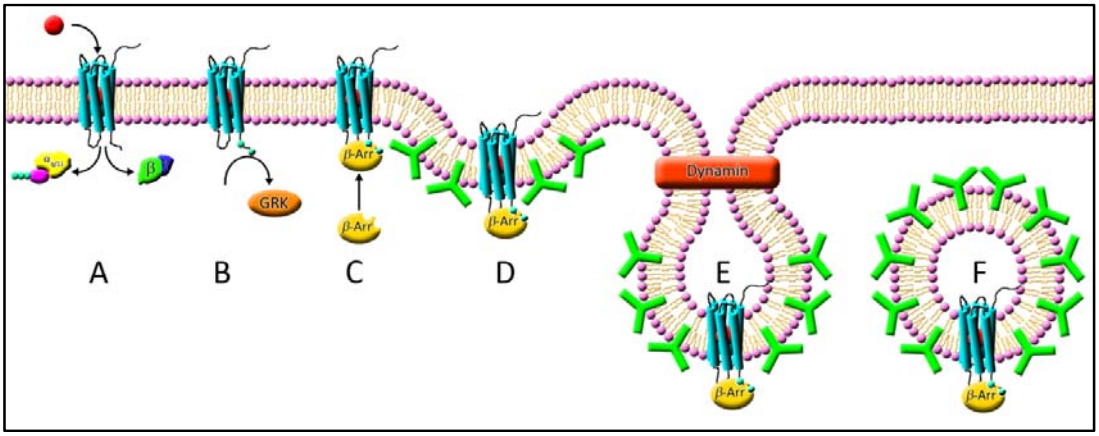

Figure 6: Desensitization and internalization of GPCRs. A| Activation and G protein dissociation. B| Phophorylation by GRKs. C| Association with β-arrestin. D| Formation of clathrin-coated pit. E| Dynamin-mediated endocytosis. F| Internalized receptor.

The phosphorylated receptor attracts β-arrestin which desensitizes the receptor and recruits the cellular endocytosis machinery. Clathrins are incorporated into the cell membrane around the receptor to form a pit which is closed off by dynamin to form an endosome. The receptor can then be returned to the cell membrane for activation or degraded. After endocytosis the β-arrestin disengages from the receptor and can then engage another phosphoylated receptor or participate in downstream signaling *(vide supra)*.

1.4 5-HT$_{2A}$ agonists

1.4.1 5-HT$_{2A}$ agonists, hallucinogens and psychedelic drugs

Today there is an increasing body of evidence that the hallucinogenic effects of certain drug such as LSD, psilocybin and DOI are mediated by agonistic action on the 5-HT$_{2A}$ receptor. This conclusion has been based mainly on animal studies where behavioral activity was perturbed by hallucinogenic drugs. The changes in behavioral activity correlated well with binding affinity and efficacy at the 5-HT$_{2A}$ receptor[98,99]. Furthermore, these behavioral traits could be blocked with selective 5-HT$_{2A}$ antagonists[100].

Human studies with hallucinogenic drugs have for the last 40 years almost exclusively been conducted well outside the controlled environment of the research lab. However, these anecdotal reports give little insight into the pharmacology of hallucinogenic drugs. In 1997 the first clinical human studies with hallucinogens in almost three decades was performed by Vollenweider et al.[101] This study was followed by a long series of experiments with psilocybin in humans[102-112]. One of these showed that psilocybin-induced psychosis in humans was blocked by pretreatment with the 5-HT$_{2A}$ selective antagonist ketanserin[102]. This observation provides additional, if not conclusive, evidence that hallucinogens act on the 5-HT$_{2A}$ receptor

Most 5-HT$_{2A}$ receptor agonists are hallucinogenic although a few are not. Similarly, most hallucinogenic compounds are 5-HT$_{2A}$ agonists, but there are exceptions.

3,4-methylenedioxymethamphetamine (MDMA, 'ecstacy') is often described as a hallucinogenic but MDMA is only a weak agonist at the 5-HT$_{2A}$ and its effects are generally attributed to the release of dopamine, norepinephrine and serotonin by disruption of intracellular storage vesicles[113]

Another exception is salvinorin A, a diterpene isolated from the herb *Salvia divinorum*. Salvinorin A is a selective κ-opioid receptor agonist devoid of 5-HT$_{2A}$ activity and activity at other monoamine receptors and transporters[114].

Nichols recently defined hallucinogens as "compounds that have a psychopharmacology similar to LSD and mescaline and which exert their effect on the CNS by an agonist (or partial agonist) effect on the 5-HT$_{2A}$ receptor.[38]" For the purposes in this thesis the term 'hallucinogenic drug' shall be defined as described above.

1.4.2 Historical perspective

Hallucinogens and other psychoactive substances have been used by man since ancient times. Especially the native peoples of the New World were known to use and worship different plants and fungi containing hallucinogens. These drugs had profound impacts on the development of religion and philosophy of these early cultures.

Mescaline from the peyote cactus *Lophophora williamsii*[115] has been used for centuries and is still the active ingredient in concoctions used by the Indian tribes of Mexico and Southwestern USA to commune with gods and spirits. *N,N'*-Dimethyltryptamine (DMT) is a naturally occurring hallucinogen present in a variety of plants all over the world[116]. DMT is orally inactive due to rapid metabolism by monoamine oxidases (MAOs). The indigenous peoples of the Amazon basin found that when certain plants that, which alone were inactive, were combined in a brew called *ayahuasca* and ingested they experienced something which to their simple everyday lives must have seemed supernatural or divine. The native Amazonians had accidentally mixed DMT-containing plants with plants containing harmala alkaloids which are MAO-inhibitors of the β-carboline class[117,118]. The presence of the MAOIs made the *ayahuasca* orally active. Other indigenous people found that the bark of trees of the *Virola* genus when used as a snuff produced a similar effect. Because the *Virola*-snuff was administered intranasally there was no need for MAOI-containing plants. The main hallucinogenic component in *Virola*-snuff is 5-methoxy-DMT[119] although other tryptamines are also present.

Hallucinogenic mushrooms were well known by indigenous groups in Mexico prior to the Spanish Conquest, but were unknown to science until the middle of the 20th century. The mushrooms were known as *teonanácatl* meaning "flesh of the gods' and were a central part of religious rites[120].

Sources of hallucinogens were not confined to the plant and fungal kingdoms. Certain species of toad secrete venom from their parotoid glands which contain bufotenin (5-hydroxy-*N,N*-dimethyltryptamine) among other toxins. These toads are believed to have been used by Mesoamerican tribes for ritual intoxication[121,122].

Other naturally occurring substances that do not fit the above definition of hallucinogens, but which are certainly psychoactive have been used by different cultures throughout history. Most notable among these are the use of various preparations of *Cannabis spp.* which appears to have been widespread throughout the old world as early 3000 BC. The use of opium (*Papaver somniferum*) also has an equally long history[123]. Chewing of coca (*Erythroxylon coca*) leaves in South America[124] and khat (*Catha edulis*) on the Arabian Peninsula and the Horn of Africa[125]. Even the use of Fly Agaric (*Amanita muscaria*) by the vikings to induce a trance-like fury called 'going berserk'[126,127].

Figure 7: Plant and animal sources of naturally occurring hallucinogens. 1| *Lophophora williamsii* a mescaline-containing cactus. 2| Hawaiian Baby Woodrose, *Argyreia nervosa*, a natural source of ergot-alkaloids. 3| *Psilocybe azurescens* one of many species of psilocybin-containing mushrooms. 4| The ergot fungus C*laviceps purpurea* from whence the ergotamine which was eventually turned into LSD came. 5| Several toad species have venom that contains the hallucinogens 5-MeO-DMT and bufotenin. 6| The bark of trees from the *Virola* genus also contain 5-MeO-DMT. 7| *Psochotria viridis* and 8| *Mimosa hostilis* are both traditional sources of DMT among the indigenous people of the Amazonian rainforest. 9| The 'Jaguar Vine' *Banisteriopsis caapi* provide the MAO-inhibiting harmala alkaloids that are essential in the *ayahuasca*.

1.4.3 Classification

The chemical structures of 5-HT_{2A} agonists have traditionally been divided into three categories: (1) the ergolines, (2) the tryptamines and (3) the phenethylamines. The ergolines and tryptamines are sometimes combined into one class because the tryptamine scaffold is part of the ergoline scaffold. The archetypical member of the ergoline class is LSD (**1.1**), which is a semisynthetic derivative made from lysergic acid. There are a number of other hallucinogenic ergolines all of which are closely related analogues of LSD. The ergoline class also contains many psychoactive but non-hallucinogenic drugs. Most of these are antagonists or inverse agonists at the 5-HT_{2A} receptor but like LSD they also interact with other 5-HT and dopamine receptors. One of the more interesting compounds in this class is lisuride which is a non-hallucinogenic 5-HT_{2A} agonist.

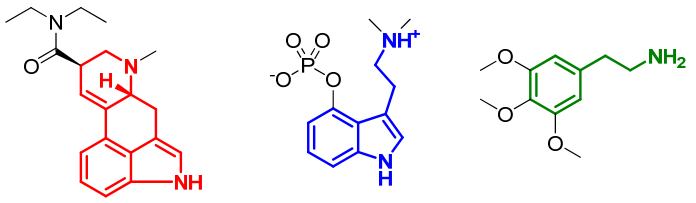

1.1 1.2 1.3

Scheme 1: Three classes of hallucinogens. LSD (1.1) with the ergoline scaffold outlined in red. Psilocybin (1.2) with the tryptamine scaffold in blue. Mescaline (1.3) with the phenethylamine scaffold in green

The tryptamine class is home to the endogenous neurotransmitter, 5-HT and the active component of magic mushrooms, psilocybin (**1.2**). Tryptamines are agonists at 5-HT_2 receptor subtypes as well as 5-HT_{1A} receptors.

Mescaline (**1.3**) is the only naturally occurring 5-HT_{2A} agonist of the phenethylamine class. Mescaline itself has a low potency but served as a lead molecule for the development of some very potent substituted phenethylamines and amphetamines *(vide infra)*. Phenethylamines are selective agonists for the 5-HT_2 receptor subtypes but with little to no subtype selectivity.

1.4.4 Evolution of 5-HT_{2A} agonists

Ergolines and tryptamines

The modern study of hallucinogens began on April 16, 1943 when Albert Hofmann, a chemist working at Sandoz Pharmaceuticals in Switzerland noted some unusual effects due to accidental exposure to a new compound he was working with, LSD-25[128,129]. Hofmann was puzzled by the "remarkable but not unpleasant state of intoxication" and by the profound effects on visual perception. Three days later Hofmann decided to try to ingest the compound. Not knowing the dose or how much he accidentally administered three days earlier Hofmann ingested 250 µg of LSD, the lowest dose he thought could possibly elicit a response. At the time no compound was known to be active at such a low dose and Hofmann expected to increase the dose in the following days until the effects were marked.

Today we know that 250 µg is a quite hefty dose and it is not hard to believe that Hofmann had trouble riding his bicycle home from work. Sandoz was initially skeptical about LSD but eventually began distributing it among experimental psychiatrists and psychologists where it quickly gained a reputation for its extraordinary effects.

LSD was quickly tied to the contemporary discovery of the neurotransmitter serotonin[130,131]. Woolley and Shaw proposed that the effects of LSD were a result of interference with the action of serotonin in the brain[132]. Throughout the 1950s and the first half of the 1960s research on LSD was widely publicized and regularly appeared in mainstream news[133-136]. Some researchers found that other substances produced effects closely related to those of LSD. Timothy Leary and Richard Alpert were among the first to use psilocybin-containing mushrooms in psychological experiments at Harvard University. Psilocybin also caught the interest of Hofmann who published several papers on its structure, synthesis and pharmacology[137-140]. Hofmann was also working on analogues of LSD and psilocybin but none of these were quite as potent[141-143].

Indeed, most of the ergolines developed since the 1950s have been antagonists or inverse agonists and only few LSD-analogues have been successful agonists. Among these are a series of analogues where the *N*-methyl group has been replaced with various saturated and unsaturated substituents (**1.5**)[144]. Finally, tying up the diethylamide moiety into a dimethylazetidide (**1.6**) has been used to map the binding orientation of LSD in computer generated models[145]. As mentioned earlier LSD binds to a multitude of neuroreceptors and analogues of LSD have not been developed with selectivity for 5-HT_{2A} in mind.

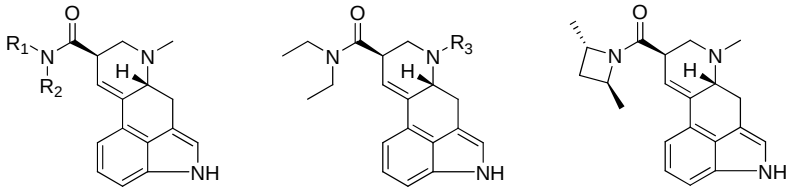

1.4 (Hofmann 1955) **1.5** (Hoffman 1985) **1.6** (Nichols 2002)

Scheme 2: LSD-analogues

While tryptamines are more selective then LSD they still have high affinities for 5-HT_{1A} which make them uninteresting as selective 5-HT_{2A} agonists and the development of tryptamines has been for different purposes. Shulgin developed a large number of tryptamines which have been described in his book 'TIHKAL'[146].

Recently, a new class of 5-HT_2 agonists has been discovered that bears close resemblance with the tryptamines but which are selective for 5-HT_2 subtypes[147,148]. The compounds (Scheme 3) have an indazole core instead of the indole in tryptamines. These compounds are currently being investigated for the treatment of glaucoma and therefore focus is on making analogues that do not cross the blood-brain barrier.

1.7 (May 2006) **1.8** (May 2009)

Scheme 3: New indazole-based 5-HT_2-selective agonists

Phenethylamines

Aldous Huxley is often credited with the rediscovery of mescaline as described in his book 'The Doors of Perception'[149]. Mescaline had in fact been known as a constituent of peyote cactus since its isolation and characterization by Heffter in the late 19th century[150,151]. However, only scattered reports on the 'mescaline psychosis' were published before 1950[152-155].

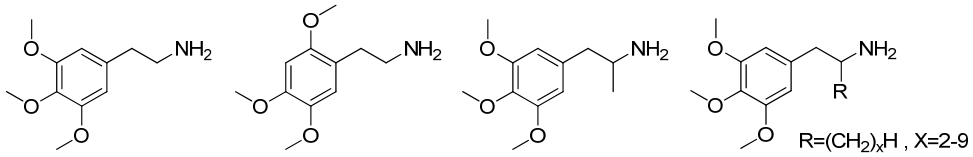

1.3 Mescaline (Heffter 1896) | **1.9** TMPEA (Jansen 1931) | **1.10** TMA (Hey 1947) | **1.11** (Shulgin 1963)

Scheme 4: Mescaline and some early analogues

The first synthetic analogue of mescaline was reported by Jansen in 1931[156]. The 2,4,5-isomer TMPEA (**1.9**) was not active and it took another 16 years before another analogue, the α-methyl homologue TMA (**1.10**), was synthesized by Hey[157]. Hey did not describe the effects of the compound and no bioassay was reported until by Peretz et al. in 1955[158]. Alexander Shulgin became interested in the compound and described its effects in 1961[159] and also described the higher α-homologues of TMA (**1.11**) which were all inactive[160].

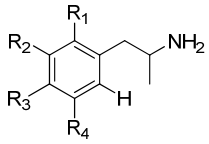

MMDA compounds (Shulgin 1964)

	R_1	R_2	R_3	R_4
1.12 (MMDA)	H	OMe	O-CH_2-O	
1.13 (MMDA-2)	OMe	H	O-CH_2-O	
1.14 (MMDA-3a)	OMe	O-CH_2-O		H
1.15 (MMDA-3b)	O-CH_2-O		OMe	H

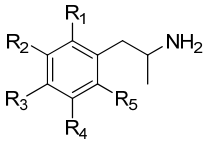

TMA compounds (Shulgin 1966)

	R_1	R_2	R_3	R_4	R_5
1.16 (TMA)	H	OMe	OMe	OMe	H
1.17 (TMA-2)	OMe	H	OMe	OMe	H
1.18 (TMA-3)	OMe	OMe	OMe	H	H
1.19 (TMA-4)	OMe	OMe	H	OMe	H
1.20 (TMA-5)	OMe	OMe	H	H	OMe
1.21 (TMA-6)	OMe	H	OMe	H	OMe

Scheme 5: MMDA and TMA compounds

In the following years Shulgin synthesized and evaluated MMDA (**1.12**)[161-163], its analogues MMDA-2 (**1.13**), MMDA-3a (**1.14**) and MMDA-3b (**1.15**)[164] as well as the five other possible trimethoxyamphetamines (**1.16**-**1.21**)[165]. He later worked on the ethoxy analogues of TMA-2[166] and found that the 4-ethoxy homologue, MEM (**1.22**) was the most potent. Shulgin first synthesized DOM (**1.25**) in 1963[167], however, in 1967 it appeared as a street drug during the Summer of Love under the name STP[168,169] unbeknownst to Shulgin who was still investigating its potential therapeutical applications.

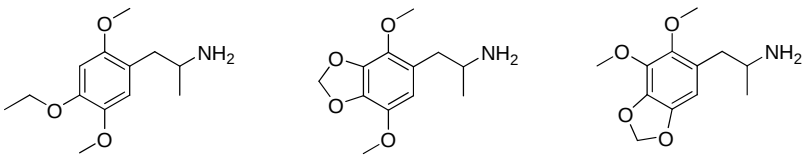

1.22 (MEM) | **1.23** (DMMDA) | **1.24** (DMMDA-2)

(Shulgin 1967)

Scheme 6: MEM, DMMDA and DMMDA-2

Meanwhile, Shulgin published a paper on DMMDA (**1.23**) and DMMDA-2 (**1.24**)[170] and a comprehensive review on structure-activity relationships of substituted phenethylamines[171]. This was followed up by Ho and co-workers who published two papers on DOM analogues in 1970[172,173]. In 1971 Shulgin et al.[174] and Barfknec and Nichols[175] independently described DOB (**1.29**) for the first time. Soon after DOI (**1.30**) and DOC (**1.31**) were described by Coutts and Malicky[176] who also described some rigidified analogues of DOM[177]. Barfknec and co-workers also published some rigidified analogues of 2,5-DMA[178,179] and DOM[180]. Cooper and Walters investigated the effects of the conformationally restricted *cis* and *trans*-cyclopropyl analogues of TMA (**1.49**)[181-183].

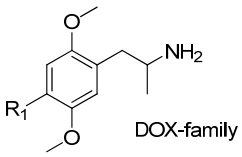

DOX-family

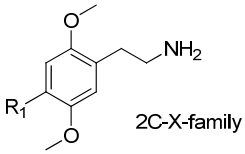

2C-X-family

	R_1	
1.25 (DOM)	Me	(Shulgin 1964)
1.26 (DOEt)	Et	(Shulgin 1970)
1.27 (DOPr)	Pr	(Shulgin 1970)
1.28 (DOBu)	Bu	(Shulgin 1970)
1.29 (DOB)	Br	(Shulgin 1971)
1.30 (DOI)	I	(Coutts and Malicky 1973)
1.31 (DOC)	Cl	(Coutts and Malicky 1973)
1.32 (DON)	NO_2	(Coutts and Malicky 1973)
1.33 (DOIp)	*i*Pr	(Aldous 1974)
1.34 (DOEf)	CH_2CH_2F	(Shulgin 1988
1.35 (DOCN)	CN	(Seggel 1990)
1.36 (DOTFM)	CF_3	(Nichols 1994

	R_1	
1.37 (2C-D)	Me	(Shulgin 1975)
1.38 (2C-B)	Br	(Shulgin 1975)
1.39 (2C-I)	I	(Shulgin 1977)
1.40 (2C-T)	SMe	(Shulgin 1976)
1.41 (2C-E)	Et	(Glennon 1979)
1.42 (2C-C)	Cl	(Cheng 1984)
1.43 (2C-CN)	CN	(Cheng 1984)
1.44 (2C-P)	Pr	(Shulgin 1991)
1.45 (2C-T2)	SEt	(Shulgin 1991)
1.46 (2C-T7)	SPr	(Shulgin 1991)
1.47 (2C-N)	NO_2	(Shulgin 1991)
1.48 (2C-TFM)	CF_3	(Nichols 1994)

Scheme 7: Some compounds in the DOX and 2C-X families

The early 1970s also saw the first asymmetric synthesis of hallucinogenic phenethylamines[184,185]. 2C-D (**1.37**) and 2C-B (**1.38**) were first reported by Shulgin in 1975[186] and the same year a paper on 4-alkyl homologues of DOM (**1.26-1.28**) was published[187,188] although some of these were patented back in 1969[189] and 1970[190]. 2C-I (**1.39**) was first published in 1977 for use as a radioligand[191] while a synthesis 2C-C (**1.42**) was not published until 1984[192]. Between 1976 and 1984 Shulgin and co-workers published a series of papers on sulfur analogues[193-197] of many of the previously described psychedelics. Meanwhile, the cyclopropyl series was extended to incorporate the cyclopropyl version of DOM called DMCPA (**1.50**)[198,199] and later a ring-methylated version of DMCPA[200].

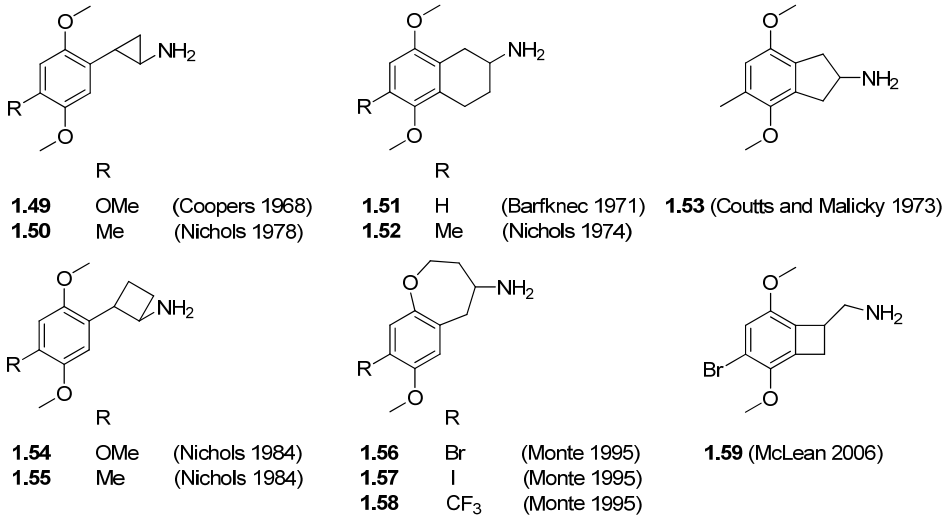

Scheme 8: Examples of conformationally restricted phenethylamines

Cyclobutane-variants (**1.54**, **1.55**) were published by Nichols in 1984, but lacked activity. New analogues with constrained side-chains appeared in 1995 (**1.56-1.58**) and 2006 with **1.59** being the most successful constrained analogue[201].

With the discovery of the 5-HT_{2C} and 5-HT_{2B} receptors it was quickly realized that none of the hallucinogenic 5-HT_{2A} agonists characterized thus far were selective for any of the three subtypes to any significant extent. Especially 5-HT_{2A} versus 5-HT_{2C} selectivity was practically non-existent.

In 1994 Glennon et al. published a paper describing the effects of amine substituents on 2C-B and 5-methoxytryptamine and found some remarkably selective compounds. However, none of these results have been reproduced in the literature and there was no functional data in the paper to indicate agonist activity. A paper published by the same group in 1999 compares a number DOX-compounds (**1.25**-**1.36**) at human 5-HT_{2A}, 5-HT_{2B} and 5-HT_{2C} receptors all labeled with agonists. The results showed a modest selectivity for 5-HT_{2A} versus 5-HT_{2B} for most of the DOX compounds. The 5-HT_{2A} versus 5-HT_{2C} selectivity was less than 7-fold for all compounds except DOCN (**1.35**) which was 22-fold selective for 5-HT_{2A}. However, DOCN had a binding affinity at the 5-HT_{2A} receptor almost a 100-fold lower than DOB (**1.29**). Nevertheless, DOCN was the first report of a 5-HT_{2A} agonist with a moderate selectivity. Later the Glennon-group found that 4-alkylphenyl substituted DOX-compounds were agonists at the 5-HT_{2A} receptor[202] although previous studies by the same group showed that substituents longer than butyl turned the compounds into antagonists[203].However, the agonist effect of these compounds were not blocked by the antagonist ketanserin which puts the validity of the data in question.

These incongruities did not stop the investigation of the 4-position Harms et al. published and paper in 2003[204] and Trachsel and co-workers published four papers between 2002 and 2008 with new 4-substituted phenethylamines[205-208] although only the latest paper contains biological data.

Although earlier attempts with conformationally restricted analogues of phenethylamines had had mixed results more work in this direction was done by the Nichols-group in the 1980s and

1990s. The focus switched to constraining the methoxy groups with dihydrofuran rings[209-212], oxepins[213], furans[214,215] dihydropyrans[216] and hybrids of these[217]. The benzodifuran analogue of DOB (bromo-dragonfly, **1.63**) were the most potent phenethylamine at the time of its discovery.

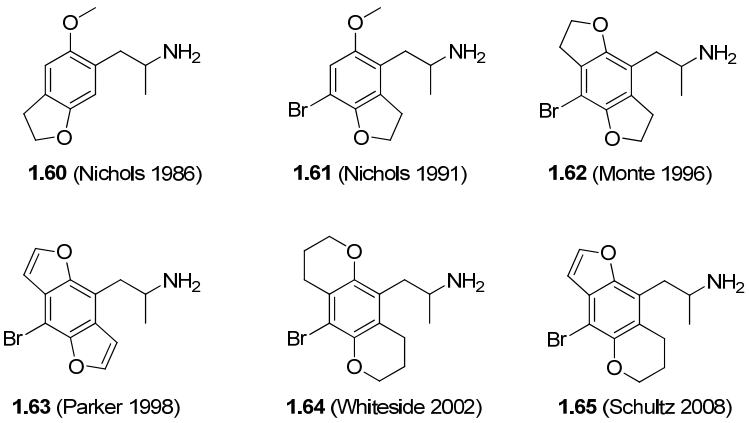

1.60 (Nichols 1986) **1.61** (Nichols 1991) **1.62** (Monte 1996)

1.63 (Parker 1998) **1.64** (Whiteside 2002) **1.65** (Schultz 2008)

Scheme 9: Phenethylamines with methoxy-groups constrained by 5 and 6-member rings

In a PhD-thesis from 2003, Ralf Heim found that adding a 2-methoxybenzyl group to phenethylamines like 2C-I and 2C-B boosted their 5-HT_{2A} activity by more than two orders of magnitude in isolated rat-tail arteries[218]. Amazingly these results never appeared in peer-reviewed literature and only a few meeting abstracts can be found[219,220]. The Nichols-group picked up on this and published their own findings on *N*-benzylphenethylamines in 2006[221] and more can be found in the PhD-thesis by Michael Braden[222].

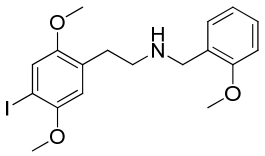

1.66 (25I-NBOMe)
(Heim 2003, Braden 2006)

Scheme 10: 25I-NBOMe (1.66), a prototypical *N*-benzylphenethylamine

1.4.5 Assaying of hallucinogens

The development of new potent and selective 5-HT_{2A}-agonists has from the beginning been reliant on assays to determine their biological activity. The evolution of these assays is no less important than the synthesis of the molecules. In the early days of hallucinogen research the most common method for assaying new chemicals was done by simple titration on human subjects until a response was noticed. This method was often employed by the chemists themselves. Hofmanns recollection of his first bioassay of LSD is well known and Shulgin reportedly performed more than 230 bioassays by the self-titration method. However, as the knowledge of the serotonin system increased more and more sophisticated methods of assaying drugs became available. In the late 1960s animal models became more common and several animal behavioral paradigms were developed along with isolated tissue models.

The simplest test was often just administration of the drug to the subject and monitoring its behavioral and physiological changes. Ho et al. used a swim-maze test and measured the effect

of DOM-isomers on barbiturate-induced sleep-time. Cheng and co-workers used isolated vascular tissue to characterize hallucinogens. Drug discrimination using the two-lever paradigm was employed Colpaert et al.[223,224] and was later used by Glennon and co-workers[98,99,225] and Nichols and co-workers[209]. Drug discrimination is still widely used today although cell based assays are becoming more prevalent. Another, behavioral assay commonly used today is the observation of the head-twitch response[226-229] associated with activation of the 5-HT_{2A} receptor by hallucinogenic 5-HT_{2A} agonists.

In the 1980s radioligand binding assays became common for determining binding affinity and selectivity. Initially homogenized brain tissue was used as the source of receptors, but later on as the technology became available cells with cloned receptors was developed. Today radioligand binding assays are a cornerstone in the pharmacological characterization of new drugs and high-throughput technology makes it possible to screen thousands of compounds in hundreds of assays within a reasonable time span.

Binding assays only measure the affinity of the compound for a receptor, but it is often necessary to determine if a ligand activates the receptor. This is done by measuring the downstream signaling from the receptor (See section 1.3 for a discussion of signal transduction).

For the 5-HT_{2A} receptor downstream signaling can be measured at different points in each signaling cascade. The first and most common method developed for this purpose is the measurement of PI-hydrolysis in the PLC-pathway. This method is still the most commonly used functional assay for 5-HT_{2A} activation. Other points of measurement in the PLC-pathway are Ca^{2+}-elevation[230], 2-AG-accumulation[69] and activity of ERK1/2[62] which are all downstream from PI-hydrolysis or activation of the G_q-protein[67] which is upstream of PLC.

With the discovery of functional selectivity and multiple signaling pathways it may be necessary to measure more than one pathway. AA-accumulation is used to measure PLA_2-activity[72,73] which can arise from at least two different signaling cascades[74]. PLD-activation has also been used to quantify receptor activation but is rarely used[92].

A relatively recent invention in assaying receptor activation is to determine changes in gene transcription, the so-called 'transcriptome fingerprint'[82,83]. Transcriptome fingerprinting uses DNA-microarrays to identify the unique distribution of gene transcripts regulated by activation of the receptors.

Functional assays are generally more sensitive to differences in tissue type and species than binding assays. There are more factors involved in signal transduction and their interconnectivity is highly dependent on the cellular milieu. It is therefore not possible to directly compare efficacies obtained with different cell types or species. A good example is a paper from 2004 that measured the intrinsic activity of several phenethylamines at cloned rat 5-HT_{2A}-receptors expressed in *Xenopus laevis* oocytes[231]. In this assay DOI was a partial agonist while 2C-B and 2C-D were antagonists. This just serves to show that one has to be careful when comparing assays especially functional assays.

1.4.6 Clinical relevance

In the 1950s, 1960s and early 1970s there were numerous clinical studies with hallucinogenic 5-HT_{2A} agonists. Most of these concerned LSD, but also other hallucinogens. However, due a shady reputation and increasingly severe restrictions on access to psychoactive drugs, research with these compounds was brought to a virtual standstill by the mid-1970s.

In recent years 5-HT_{2A} agonists have seen a resurgence of interest from the scientific community. Compounds which have been blacklisted for decades are now again being examined in clinical studies.

Psilocybin has been studied in humans for more than a decade by Vollenweider and co-workers[101-112] and these studies have been complemented by those Griffiths and co-workers[232]. There are several ongoing studies where psilocybin is being used to improve the quality of life in cancer patients[233]. Finally, psilocybin have also been evaluated in patients with obsessive-compulsive disorder (OCD)[234].

1.5 Introduction to radiochemistry and PET-imaging

Positron emission tomography (PET) is a functional nuclear imaging modality based on the decay of positron-emitting radionuclides. Certain elements have proton-rich isotopes that undergo β^+-decay i.e. a proton is converted to a neutron with the concomitant emission of a positron (β^+ or e^+) and a neutrino (ν_e). The positron is the antiparticle to the electron[235-237] and the collision of a positron and an electron results in *annihilation*, the total conversion of the particles' mass into energy. The energy is emitted as a pair of gamma photons each with energy equal to the rest mass of the positron or electron (511 keV). The two gamma photons are emitted at opposite directions (≈ 180°) and it is the coincidental observation of these photons that forms the basis of PET-imaging.

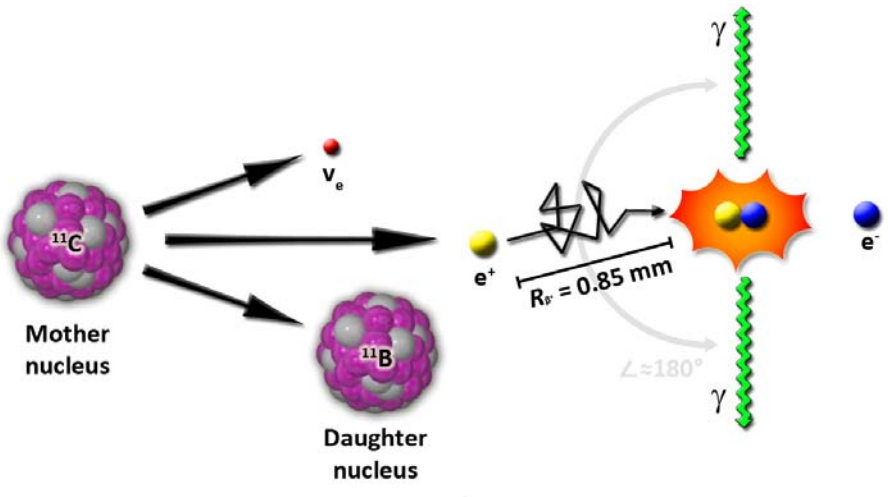

Figure 8: Illustration of the beta-plus decay of a 11C-nucleus and the resulting annihilation of the positron (e^+) with an electron (e^-).

An important parameter in PET is the half-life of the positron-emitting isotope. A very short half-life is undesirable if the radioisotope has to be generated at an off-site facility or if it has to be incorporated into a radiopharmaceutical by synthesis. Another important parameter in PET is the range *R* of the positrons emitted by a radioisotope. The range is the straight line path the positron traverses before the annihilation occurs and is dependent on energy of the positron and the density of the matter it traverses. A short range is desirable in PET in order to get a better resolution. Table 2 gives the half-life of positron-emitting radioisotopes and the energy and range of their positrons.

Radionuclide	Half-life (min)	$E_{\beta+,\,max}$ (keV)	Max. β^+-range (mm) in water	Avg. β^+-range (mm) in water
^{11}C	20.4	970	3.8	0.85
^{13}N	10	1200	5.0	1.15
^{15}O	2	1740	8.0	1.80
^{18}F	110	640	2.2	0.46
^{68}Ga	68	1900	9.0	2.15
^{82}Rb	1.25	3350	15.5	4.10

Table 2: Properties of common positron-emitting radionuclides. Adapted from Brown and Yasillo[238]

The short half-lives of ^{13}N and ^{15}O make them impractical for incorporation into radiopharmaceuticals, and they are only used in special applications. ^{11}C and ^{19}F are the most commonly used radionuclides in PET. ^{11}C has a short half-life of about 20 minutes which requires the use of an onsite cyclotron and a rapid radiosynthesis. Nonetheless, ^{11}C-labeling is still the most convenient way to generate PET-tracers. ^{19}F has better properties than ^{11}C in regards to both half-life and positron range. The long half-life makes it possible to perform more complex radiosyntheses and experiments, while the shorter β^+-range gives a better resolution. These advantages are compounded by the lack of general ways to easily introduce fluorine into precursor molecules. Also, if the desired radiopharmaceutical does not contain fluorine in its cold state, a suitable analogue has to be found that possess the same pharmacological characteristics, something which is not always possible. [^{18}F]-fluorodeoxyglucose ([^{18}F]-FDG) is used to assess glucose metabolism and is the most commonly used PET tracer. ^{68}Ga is used in cancer diagnostics where it is complexed with chelating ligands such as DOTATATE and DOTATOC. ^{82}Rb is used to assess myocardial perfusion.

1.6 PET studies in the 5-HT system

PET imaging of the 5-HT system has been conducted since 1978 when the first study using [^{11}C]5-MeO-DMT was conducted[239]. Most of the PET studies since then have been concerned with determining receptor levels in human diseases compared to binding in healthy subjects. Within the dopamine system PET-studies have more recently been used to measure changes in endogenous neurotransmitter levels induced by pharmacological challenges[240] or physiologic stimulus[241]. Several factors have been used to explain why this approach so far has not been very successful in the 5-HT system[242,243].

PET studies measuring endogenous dopamine release have been conducted successfully both using antagonist and agonist PET tracers; however agonist PET tracers have been shown to be much more sensitive to displacement by endogenous dopamine[244,245]. This is explained by the

extended ternary complex model for agonist binding[45]. The agonist PET tracer only labels the subset of receptors that are in the high-affinity state whereas an antagonist PET tracer labels all receptors regardless of affinity state. Since only the high affinity state is susceptible to competition by the endogenous dopamine it follows that the agonist PET tracer is more sensitive to endogenous dopamine release. This change in sensitivity is of course dependent on the ratio of receptors in the high and low affinity states. For the 5-HT_{2A} receptor only about 20% are in the high-affinity state[43] thus the maximum theoretical displacement of an antagonist PET tracer would be 20% compared to 100% for a full agonist PET tracer. This is however somewhat complicated by the degree of internalization of the receptor[246] and to which extent the receptor is localized extra-synaptically[247].

Recently two agonists PET tracers have been evaluated for the 5-HT_{1A} receptor: [^{11}C]CUMI-101[248,249] and [^{18}F]F15,599[250]. Neither of these tracers have yet been evaluated for their sensitivity towards changes in endogenous 5-HT levels.

Several subtype selective radioligands have been made available for imaging the 5-HT_{2A} receptors such as [^{11}C]ketanserin[251,252], [^{18}F]altanserin[253,254], [^{11}C]MDL-100,907[255,256] and [^{18}F]MH.MZ[257]. However, none of these tracers have been shown to be displaceable following pharmacological challenges that increase endogenous 5-HT. No selective 5-HT_{2A} agonists have been evaluated as PET tracers, which is perhaps not so surprising giving the lack of selective agonists in general. Interestingly, the only 5-HT_{2A} agonist PET-tracer reported in the literature is [^{11}C]5-MeO-DMT as mentioned above, but 5-MeO-DMT in unselective and has slightly higher affinity for 5-HT_{1A} receptors.

A selective 5-HT_{2A} agonist which is sensitive to endogenous changes in 5-HT levels would be a significant tool in understanding 5-HT related disorders in the CNS.

1.7 The ideal tracer

Development of PET tracers has many similarities with the drug discovery/drug development process. A candidate may fail at any given point in the development and very few tracers make it into clinical studies. Prediction of tracer performance based on in vitro data have been proposed to aid in selection of tracer candidates[258], but development of PET tracers are is still mostly based on educated guessing, trial-and-error and serendipity.

Most PET tracers are developed from compounds already described in the literature, but occasionally known compounds have to be changed slightly to accommodate radiolabeling.

A tracer candidate should have a sufficient affinity for the target. The affinity needed is dependent on the density of binding sites in the region of interest. This means that if the density of binding sites in the region of interest is low then a high-affinity tracer is needed to get at good target-to-background ratio. The tracer candidate should show selectivity for the targeted receptors, but this is again dependent on the density of the target receptor and the density of competing target receptors. The ideal candidate has zero affinity for competing targets, but this is rarely the case.

Property	Experimental method
High affinity for target	In vitro binding assay or autoradiography
Selectivity for target	In vitro binding assays and in vivo blocking experiments
Reliable radiochemical labeling at high specific radioactivity	Evaluation of chemical structure and test of radiolabeling
Penetration of the BBB	LogD measurement or calculation / in vivo scanning w/o efflux transporter blockade
No BBB penetration of radiolabeled metabolites	HPLC analysis of plasma or tissue
Suitable pharmacokinetics (observable brain uptake and washout)	In vivo PET scanning
Safe for administration in tracer doses	Toxicological testing
Low non-specific binding	In vivo PET scanning, autoradiography

Table 3: Ideal properties of a CNS PET radiotracer and methods for evaluation

The tracer candidate should be amenable to radiolabeling in a fast and efficient manner. This can usually be determined by scrutinizing the chemical structure for potential labeling sites. The labeling should preferably be the final step in the synthesis but often more than one step is required.

The tracer candidate should cross the blood-brain barrier and ideally leave all radiolabeled metabolites outside. BBB penetration is dependent on lipophilicity so $LogD_{7.4}$ values are a good preliminary parameter for selecting candidates. $LogD_{7.4}$ should be high enough for the candidate to pass through the BBB but not too high as this tends to result in non-specific binding. A tracer candidate should have a $logD_{7.4}$ within the range of 2.0-3.5[259]. Lipophilic metabolites that cross the BBB may contribute to increased background levels and non-specific binding. Fortunately, metabolism generally produces compounds less lipophilic than the parent compound to expedite elimination from the body.

The pharmacokinetics of the tracer candidate must be 'fast' i.e. the tracer has to bind reversibly during the timeframe of the PET experiment. The methods used to quantify in vivo binding do not work if binding is irreversible.

The toxicity of PET-tracers is usually not of immediate concern because tracer doses are generally insignificant compared to therapeutic doses, but toxicity screening is still required before human trials.

1.8 Project aims

This project aims to:

1) Design and synthesize new 5-HT_{2A} agonists with the aim to increase binding affinity and selectivity for the 5-HT_{2A} receptor.
2) Synthesize, radiolabel and evaluate a number of 5-HT_{2A} agonists for use as PET tracers. These may be based on compounds known from the literature or compounds found in Aim 1 which possess the desired properties.

Chapter 2

N-Benzylphenethylamines – Group 1-compounds

2.1 Aim

This part of the project aims to synthesize a focused library of *N*-benzylphenethylamines for biological evaluation. These compounds, once synthesized and evaluated, may then serve as a repository of potential PET-ligands.

2.2 Background and Introduction

It has been well known for a long time that the 4-position of hallucinogenic phenethylamines is important in determining the pharmacological characteristics of these drugs (see Section 1.4.4). The 4-position has impact on binding affinity and intrinsic activity as well as pharmacokinetic properties all of which are important for the successful development of a PET tracer.

In this project we decided to synthesize a focused library of *N*-benzylphenethylamines with different substituents in the 4-position of the phenethylamine moiety. Similar studies have been made earlier on various 4-substituted 2,5-dimethoxyamphetamines[203] (DOX-family) but not to any great extent on the corresponding phenethylamine homologues (2C-family) or *N*-benzylphenethylamines.

As it was expected that the general trends exerted by the 4-substituents in DOX-compounds would be translated to the *N*-benzylphenethylamines we decided to limit the study to the most interesting 4-substituents. The halogens I, Br, Cl and F were obvious choices as it would be logical to test Cl and F now that I and Br had already been tested. The alkyl-substituents gave the highest affinity in the earlier DOX-study, topping out at *n*-hexyl. However, alkyl-chains longer than *n*-butyl turned the compounds into antagonists or very weak partial agonists. Also, adding long alkyl chains to the already quite lipophilic *N*-benzylphenethylamines would make them uninteresting as PET-tracers due to very high LogD-values and therefore methyl, ethyl and *n*-propyl were chosen to represent alkyl chains. Very little hard data is available on thioalkyl-substituted compounds, however, anecdotal reports indicate that they are quite active and potent hallucinogens in vivo[167]. Consequently, we added *S*-methyl, *S*-ethyl and *S*-propyl to the library. The cyano group was also included, despite its relatively low affinity, because a more recent study[260] have shown DOCN (**1.35**) to be the only DOX-compound with reasonable selectivity for 5-HT_{2A} versus 5-HT_{2C} Therefore the CN-substituent was included in the hope that this property would be carried on to its *N*-benzyl analogues. Finally the trifluoromethyl-group was added to the collection, since the corresponding 2C-analogue was shown to have slightly higher affinity than 2C-I. Additionally, the additions of trifluoromethyl-groups often have remarkable impact on pharmacokinetics[261].

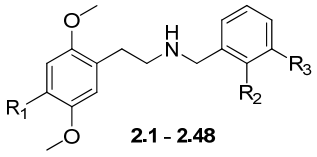

2.1 - 2.48

R_2/R_3 \ R_1	I	Br	Cl	F	Me	Et	Pr	SMe	SEt	SPr	CF_3	CN
2'-MeO	**2.1**	**2.5**	**2.9**	**2.13**	**2.17**	**2.21**	**2.25**	**2.29**	**2.33**	**2.37**	**2.41**	**2.45**
2'-OH	**2.2**	**2.6**	**2.10**	**2.14**	**2.18**	**2.22**	**2.26**	**2.30**	**2.34**	**2.38**	**2.42**	**2.46**
2'-F	**2.3**	**2.7**	**2.11**	**2.15**	**2.19**	**2.23**	**2.27**	**2.31**	**2.35**	**2.39**	**2.43**	**2.47**
2',3'-MD	**2.4**	**2.8**	**2.12**	**2.16**	**2.20**	**2.24**	**2.28**	**2.32**	**2.36**	**2.40**	**2.44**	**2.48**

Scheme 11: Group 1-compounds with structure and substitution key

To further extend the scope of the study, four different *N*-benzyl analogues were made for each 4-substituent giving a library of 48 compounds. The four *N*-benzyl substituents chosen were the 2'-methoxy, 2'-hydroxy, 2'-fluoro and 2',3'-methylenedioxy all of which had been confirmed as potent 5-HT_{2A} agonists as their 4-iodo analogues in the study of Braden et al.[221]

2.3 Synthesis of phenethylamines

Phenethylamines can be synthesized in a variety of ways, but one method seems to be used almost exclusively. This method was used in the synthesis of most of the phenethylamine compounds mentioned in Section 1.4.4 and is a simple two-step sequence. Henry-condensation[262] of an appropriately substituted aromatic aldehyde with nitromethane under base catalysis to furnish the β-nitrostyrene followed by reduction of the nitrostyrene to the phenethylamine. The reduction can be accomplished by catalytic hydrogenation[263] but is most often carried out with $LiAlH_4$[264]. If the aromatic ring is substituted with groups susceptible to reduction by $LiAlH_4$ or hydrogenation such as halogens the reduction can be carried out with DIBAL[265] or SmI_2[266].

Alternatively phenethylamines can be synthesized from the corresponding benzyl bromides by substitution with cyanide followed by reduction or by reduction of primary 2-phenylacetamides.

2.4 Synthesis of secondary amines

Secondary amines may be synthesized in a number of different ways. One of the simplest is the reductive amination. The reductive amination is a two-step reaction starting with the condensation of a primary amine with an aldehyde or ketone to form an imine or Schiff base[267]. The imine is then reduced, often with a complex hydride reducing agent[268], to give the secondary amine in a so called *indirect* reductive amination. Reductive amination can also be performed in *direct* manner with mild borohydride reagents such as $NaBH_3CN$ or $NaBH(OAc)_3$ where the borohydride is added together with the aldehyde and amine. The borohydride preferentially reduce the intermediate iminium ion without reducing the aldehyde or ketone. This approach sometimes fails when primary amines and aldehydes are used and results in dialkylation of the amine. In this case *indirect* reductive amination is a better choice. Sometimes other reducing agents are used and before the advent of borohydrides imines were commonly reduced by catalytic hydrogenation[269]. If formic acid or formates are used as reducing agents the

reaction is called the Leuckart reaction[270] or Leuckart-Wallach reaction[271] and if formaldehyde is used as the carbonyl component is it referred to as the Eschweiler-Clarke reaction[272,273].

Another approach is to first form a secondary amide, and then reducing it to the secondary amine. This method has the advantage that a number of different carbonyl compounds can be made to react with a primary amine. Carboxylic acids[274,275], acid chlorides[276], anhydrides[275,277] and esters[278] can be utilized in such a reaction. The drawback is that the resulting secondary amide requires strong reducing agent to be converted to the secondary amine. This is typically achieved using $LiAlH_4$[279], borane[280] , AlH_3[280] Red-Al or DIBAL[281]. The reduction can also be achieved by converting the amide to a thioamide[282] and treating it with Raney nickel[283].

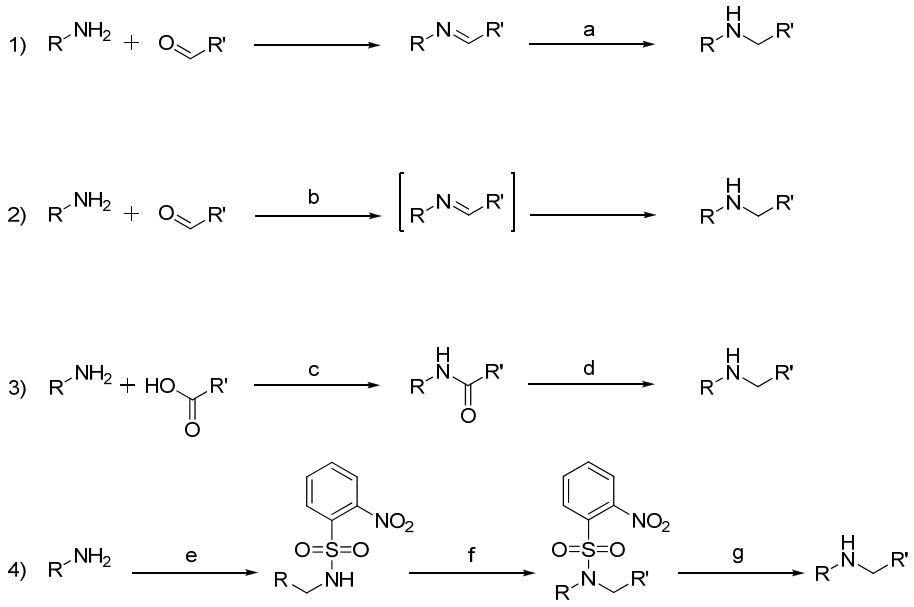

Scheme 12: Strategies and standard condition for synthesis of secondary amines. 1| Indirect reductive amination. 2| Direct reductive amination. 3| Amide synthesis and reduction. 4| Fukuyama amine synthesis. a| $NaBH_4$. b| $NaCNBH_3$. c| peptide coupling reagent. d| $LiAlH_4$. e| NsCl and base. f| alkyl halide, base. g| PhSH, base.

A third and very useful method was demonstrated by Fukuyama and co-workers[284,285]. It is well known that alkylating a primary amine with an alkyl halide, more often than not results in mixture of primary, secondary and tertiary amines and even quaternary ammonium salts. The Fukuyama-method relies on attenuating the reactivity of the primary amine by converting it into an electron-deficient sulfonamide. The sulfonamide can then be alkylated with an alkyl halide in the presence of a mild base and the sulfonamide is then removed selectively using a soft nucleophile such as thiophenol in the presence of a base.

For the purposes described in this thesis the first choice between these three possibilities was always the reductive amination. This reaction is conveniently one-pot, the reaction conditions are mild and the starting materials are easily synthesized or in some cases even commercially available. Reduction of secondary amides with strong reducing agents is problematic because not all substrates are compatible with such conditions. Also this is a two-step procedure and the work-up of the reductions can be time-consuming and messy. The Fukuyama procedure is a good alternative but comprises three reaction steps and should only be considered if the

reductive amination fails or produces side reactions, or if the required aldehyde or ketone is inaccessible

2.5 Chemical synthesis

The parent phenethylamines were, with the exception of 2C-TFM (**2.56**) synthesized according to previously described procedures[167,192]. In our hands, the Cu-mediated trifluoromethylation of TFAc-protected 2C-I (**2.49**)[286,287] did not work at all.

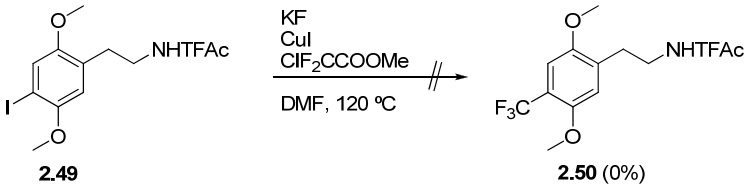

2.49 **2.50** (0%)

Scheme 13: Attempted Cu-mediated trifluoromethylation of 2.49 using literature conditions

We examined a few other trifluoromethylations using 2-bromo-1,4-dimethoxybenzene (**2.49**) or 1,4-diiodo-2,5-dimethoxybenzene (**2.51**) as the starting material. First, a relatively new procedure[288] that seemed well documented was tried. This procedure used methyl trifluoroacetate, CsF and CuI in sulfolane to generate the reactive trifluoromethyl copper.

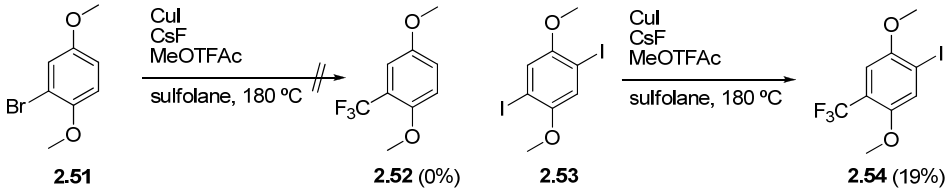

2.51 **2.52** (0%) **2.53** **2.54** (19%)

Scheme 14: Cu-mediated trifluoromethylation of aryl bromides and aryl iodides using MeOTFAc.

The reaction did not work at all with an aryl bromide (**2.51**) but with the diiodide (**2.54**) 19% conversion was reached. Next, the reaction conditions were changed to sodium trifluoroacetate and CuI in NMP[289,290] and this immediately resulted in 85% yield of the desired product (**2.52**) according to GC-MS along with some byproducts.

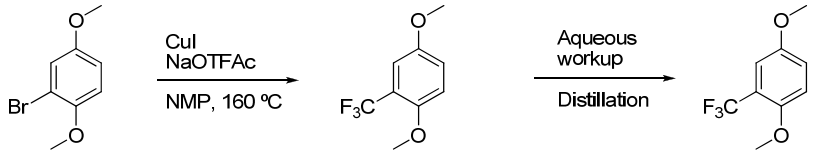

2.51 **Crude 2.52** (85 % by GC) **2.52** (40-60 %) 90 % purity

Scheme 15: Cu-mediated frifluoromethylation of aryl bromide with NaOTFAc

Unfortunately the workup and purification of this reaction turned out to be very cumbersome. The aqueous workup was hampered by the large amounts of colloidal copper waste that was contaminating everything. This was partially solved by absorbing the products on a pad of Celite and washing out the copper waste with water and then extracting the pad with diethyl ether. Purification of the crude product was made difficult because the byproducts and residual starting material were indistinguishable from the product on TLC and flash chromatography was

not able to separate the compounds. Distillation was the best option but it was not possible to get rid of all impurities with simple short-path distillation. Altogether these attempts at trifluoromethylation suggest that there is still room for improvement in this field.

A completely different strategy to synthesize **2.56** was therefore devised starting from the commercially available, but expensive, 1-fluoro-4-methoxy-2-(trifluoromethyl)benzene (**2.53**).

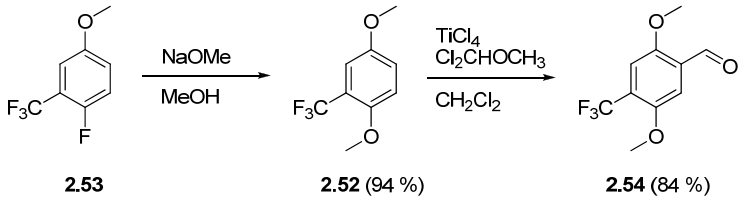

Scheme 16: Alternative synthesis of 2.52 and formylation to give 2.54

To start with, the aromatic fluorine was displaced by methoxide in a nucleophilic aromatic substitution assisted by the neighboring electron-withdrawing trifluoromethyl group[291]. The reaction was executed in excellent yield and the product (**2.52**) was easily purified by distillation. Then followed a three-step sequence familiar from many other phenethylamine syntheses. First a Lewis-acid-mediated formylation (Rieche-formylation) with dichloromethyl methyl ether[292] to give the aldehyde (**2.54**).

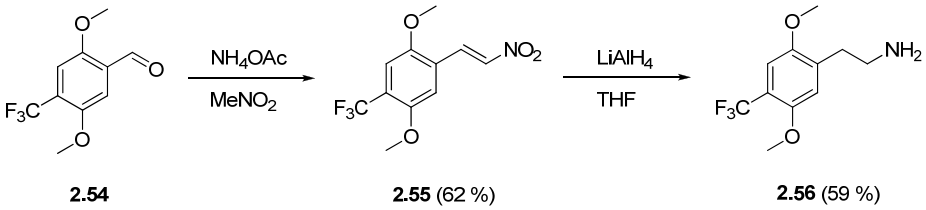

Scheme 17: Final steps in the synthesis of 2C-TFM (2.56)

Next, he aldehyde was converted to the nitrostyrene (**2.55**) utilizing a base-catalyzed Henry-condensation[262] with nitromethane and finally reduction of the nitrostyrene with $LiAlH_4$[264] afforded 2C-TFM (**2.56**).

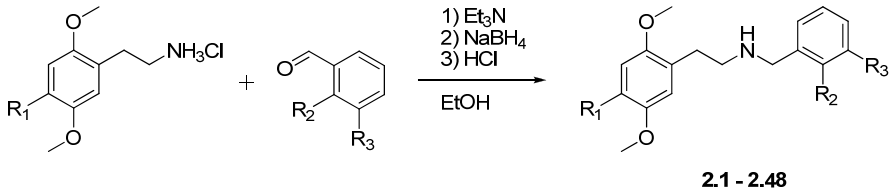

Scheme 18: Indirect reductive amination of phenethylamines and aromatic aldehydes to give the desired *N*-benzylphenethylamines which were converted to HCl salts. For a complete overview of substitution patterns refer to Scheme 11

The parent phenethylamines were subjected to reductive aminations with the appropriate aldehydes. The *indirect* reductive amination was used in all cases to avoid formation of tertiary amines. The secondary amines were converted to hydrochloride salts and isolated in 28-94% yield followed by characterization and biological evaluation.

2.6 In vitro biological evaluation

The compounds were tested for their ability to displace radioligands at 5-HT_{2A}, 5-HT_{2B} and 5-HT_{2C} receptors in heterologous cell-based assays at the National Institute of Mental Healths Psychoacitve Drug Screening Programme (NIMH-PDSP) at the University of North Carolina.

The compounds were first subjected to a primary screen were a 10 μM concentration of the compound was screened for its ability to displace radioligands at typical assay concentrations. Compounds that were able to displace at least 50% of the radioligand were subjected to secondary binding assays for determination of IC_{50} and K_i.

The 5-HT_{2A} and 5-HT_{2B} assays used cloned human receptors while 5-HT_{2C} used cloned rat receptors.

The antagonist radioligands [^{3}H]ketanserin and [^{3}H]mesulergine was used as radioligands for 5-HT_{2A} and 5-HT_{2C} receptors respectively. For 5-HT_{2B} the agonist radioligand [^{3}H]LSD was used except for compound **2.3** were [^{3}H]mesulergine was used.

Comparison of Ki-values measured against antagonists and agonists cannot be directly compared since agonists only bind receptors in the high-affinity state and the amount of receptors in the high-affinity state depends both on the type of receptor and the assay conditions. Therefore, the 5-HT_{2B} affinities in Table 4 cannot be compared directly with 5-HT_{2A} and 5-HT_{2C} affinities while the latter two can be considered comparable and selectivity can be derived. The amount 5-HT_{2B} receptors in the high-affinity state is usually around 10-20% and as a rule of thumb one can multiply the affinity with 5-10 (lowering pKi 0.5-1.0 values).

Binding affinities for 5-HT_{2A}, 5-HT_{2B} and 5-HT_{2C} receptors are presented in Table 4. A full screening at all 5-HT receptors except 5-HT_{1F} and 5-HT_{5B} can be found in appendix 1.

Compound	R_1	R_2	R_3	pK_i h5-HT_{2A} vs. [^{3}H]Ketanserin	pK_i h5-HT_{2B} vs. [^{3}H]LSD	pK_i r5-HT_{2C} vs. [^{3}H]Mesulergine
2.1 (25I-NBOMe)	I	OMe	H	8.67	8.64	8.15
2.2 (25I-NBOH)	I	OH	H	9.15	8.55	8.85
2.3 (25I-NBF)	I	F	H	8.55	7.72	7.68
2.4 (25I-NBMD)	I	O–CH_2–O		9.22	8.88	7.56
2.5 (25B-NBOMe)	Br	OMe	H	9.30	9.30	8.77
2.6 (25B-NBOH)	Br	OH	H	9.47	8.10	8.33
2.7 (25B-NBF)	Br	F	H	8.57	8.23	7.73
2.8 (25B-NBMD)	Br	O–CH_2–O		9.22	8.85	7.95
2.9 (25C-NBOMe)	Cl	OMe	H	8.80	8.95	8.27
2.10 (25C-NBOH)	Cl	OH	H	9.21	8.08	8.21
2.11 (25C-NBF)	Cl	F	H	8.12	7.57	7.43
2.12 (25C-NBMD)	Cl	O–CH_2–O		9.00	8.08	7.67
2.13 (25F-NBOMe)	F	OMe	H	8.49	8.12	7.36
2.14 (25F-NBOH)	F	OH	H	8.34	7.68	7.16
2.15 (25F-NBF)	F	F	H	7.25	7.11	6.31
2.16 (25F-NBMD)	F	O–CH_2–O		7.92	7.47	6.59
2.17 (25D-NBOMe)	Me	OMe	H	8.70	8.41	8.23
2.18 (25D-NBOH)	Me	OH	H	8.96	7.96	7.92
2.19 (25D-NBF)	Me	F	H	7.72	7.30	7.18
2.20 (25D-NBMD)	Me	O–CH_2–O		8.59	7.92	7.43
2.21 (25E-NBOMe)	Et	OMe	H	9.48	8.67	8.55
2.22 (25E-NBOH)	Et	OH	H	9.54	8.65	8.47
2.23 (25E-NBF)	Et	F	H	8.63	7.70	7.58
2.24 (25E-NBMD)	Et	O–CH_2–O		9.40	8.40	7.92
2.25 (25P-NBOMe)	Pr	OMe	H	9.20	7.70	8.79
2.26 (25P-NBOH)	Pr	OH	H	9.28	8.34	8.51
2.27 (25P-NBF)	Pr	F	H	8.51	8.78	7.88
2.28 (25P-NBMD)	Pr	O–CH_2–O		9.20	8.24	8.13
2.29 (25T-NBOMe)	SMe	OMe	H	9.27	9.04	8.15
2.30 (25T-NBOH)	SMe	OH	H	9.42	8.80	8.29
2.31 (25T-NBF)	SMe	F	H	8.10	7.84	7.16
2.32 (25T-NBMD)	SMe	O–CH_2–O		9.15	8.61	7.56
2.33 (25T2-NBOMe)	SEt	OMe	H	9.25	9.07	8.65
2.34 (25T2-NBOH)	SEt	OH	H	9.21	8.71	8.72
2.35 (25T2-NBF)	SEt	F	H	8.02	8.09	7.64
2.36 (25T2-NBMD)	SEt	O–CH_2–O		9.40	8.75	8.04
2.37 (25T7-NBOMe)	SPr	OMe	H	9.17	8.64	8.71
2.38 (25T7-NBOH)	SPr	OH	H	9.17	8.41	8.66
2.39 (25T7-NBF)	SPr	F	H	8.60	7.86	7.84
2.40 (25T7-NBMD)	SPr	O–CH_2–O		9.02	8.16	8.06
2.41 (25TFM-NBOMe)	CF_3	OMe	H	9.32	8.96	8.57
2.42 (25TFM-NBOH)	CF_3	OH	H	9.18	8.46	8.49
2.43 (25TFM-NBF)	CF_3	F	H	7.99	7.80	7.74
2.44 (25TFM-NBMD)	CF_3	O–CH_2–O		9.00	8.34	7.93
2.45 (25CN-NBOMe)	CN	OMe	H	8.34	7.68	7.25
2.46 (25CN-NBOH)	CN	OH	H	8.88	7.21	6.88
2.47 (25CN-NBF)	CN	F	H	7.20	6.41	6.20
2.48 (25CN-NBMD)	CN	O–CH_2–O		7.79	7.00	6.86

Table 4: Binding affinities of Group 1-compounds at 5-HT_{2A}, 5-HT_{2B} and 5-HT_{2C} receptors.* vs. [^{3}H]mesulergine.

In general most of the compounds had high affinity for the 5-HT_{2A} receptor with K_i values in the low-nanomolar to sub-nanomolar range. A typical trend was that the 2'-fluoro compounds had significantly lower affinity than the other *N*-benzyl substituents especially when paired with lower affinity 4-substituents. Another observation is that 4-fluoro, 4-cyano and 4-methyl had slightly lower affinity than the other 4-substituents. This in accord with previous observations of 4-subtituents by Nelson et al.[260] It does however appear that the *N*-benzyl substituents seem to attenuate the effect on affinity by the 4-substituents. In previous studies on the effect of 4-subtituents on 2,5-dimethoxyamphetamines 4-fluoro has 27–70-fold lower affinity than 4-bromo and 4-cyano has 58–76-fold lower affinity than 4-bromo[203,260]. With 2'-hydroxybenzyl substituents the difference is 15-fold for 4-fluoro versus 4-bromo and just 4-fold for 4-cyano versus 4-bromo.

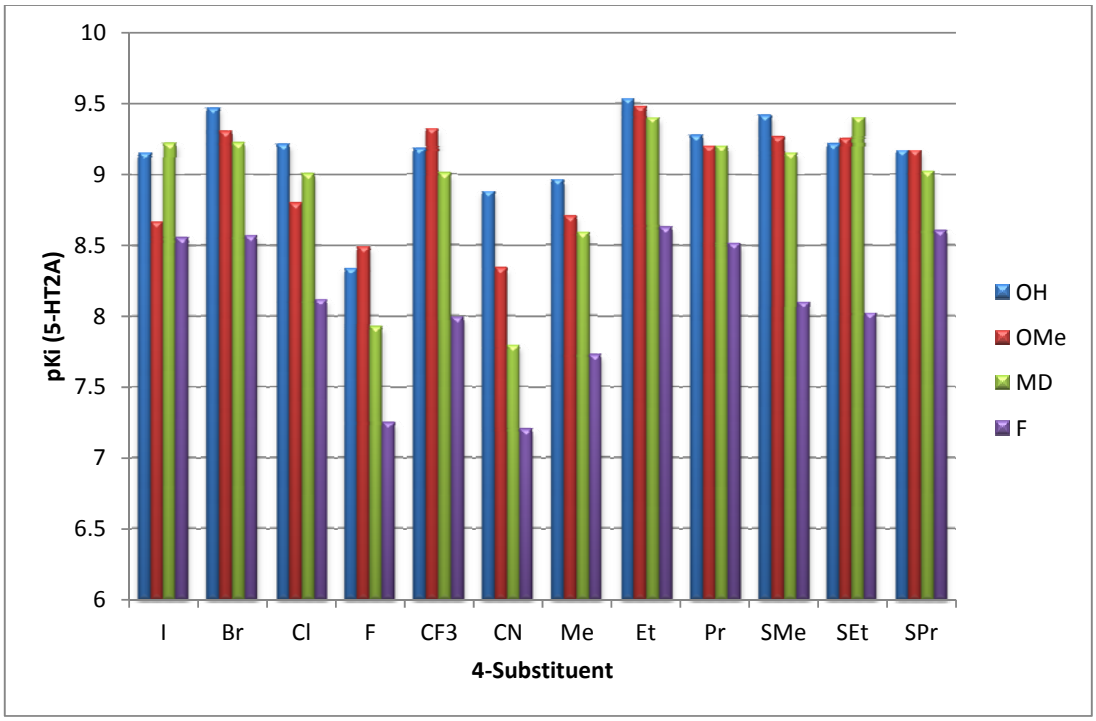

Figure 9: Graphical representation of pKi-values of Group 1-compounds

The affinities for the 5-HT_{2B} receptor was generally a bit lower than for 5-HT_{2A}. The 5-HT_{2B} affinities are, however, measured against LSD meaning that the radiolabeled receptors are in the high affinity-state. This means that the values cannot be directly compared with the 5-HT_{2A} and 5-HT_{2C} affinities which are measured by displacement of antagonist radioligands. The affinities of **2.1–2.4** were previously reported by Braden et al. for displacement of the agonist DOI at 5-HT_{2A} receptor and are 10-50-fold lower than when measured against ketanserin[221]. For PET purposes the 5-HT_{2B} affinity is of little concern because of the low expression of 5-HT_{2B} receptors in the brain.

The affinity for the 5-HT_{2C} receptor is more important because these receptors are present in some brain areas most notably in the choroid plexus. Until now only moderate selectivity for a 5-HT_{2A} agonist has been reported for DOCN with 22-fold selectivity for 5-HT_{2A} versus 5-HT_{2C}[260]. But

because of the low affinity of DOCN compared to other DOX compounds it has never been in use as a selective agonist.

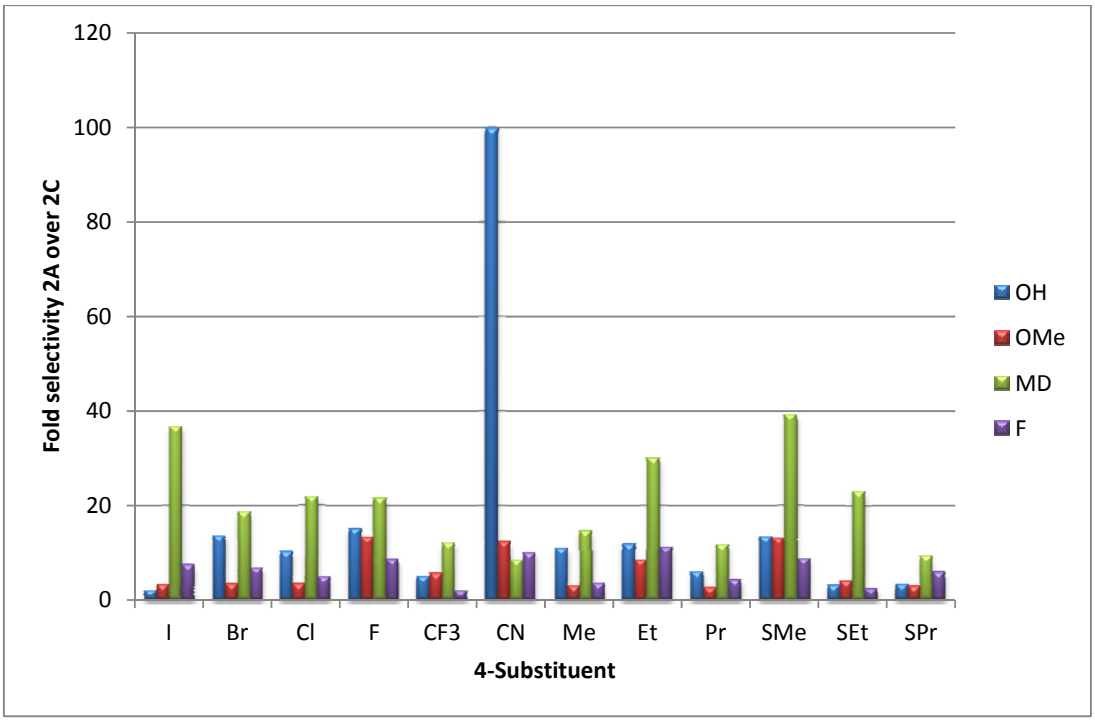

Figure 10: Chart showing the 5-HT_{2A} versus 5-HT_{2C} selectivities for the Group 1-compounds

The *N*-benzyl-substituted phenethylamines in Group 1 all showed selectivity for 5-HT_{2A} receptors but this was generally low to moderate for 2'-methoxy, 2'-hydroxy and 2'-fluoro compounds. The 2',3'-methylenedioxy compounds all showed moderate to good selectivity towards 5-HT_{2A}.

The most striking result however was **2.46** which had a 100-fold selectivity for 5-HT_{2A} versus 5-HT_{2C} while retaining a high affinity of 1.32 nM. **2.46** also had good selectivity for 5-HT_{2A} versus 5-HT_{2B} being 46-fold selective for 5-HT_{2A}. If **2.46** was also able to activate the 5-HT_{2A}-receptor it would become the first truly selective 5-HT_{2A} agonist to be disclosed. **2.46** may perhaps be superseded by **2.48** when the data are available. **2.48** has significantly lower affinity for 5-HT_{2C} than **2.46** and if the 5-HT_{2A}-affinities follows the general trend then **2.48** should have an affinity around 1–3 nM making it even more selective for 5-HT_{2A}. These results seem to confirm that the 4-cyano substituent confers selectivity and that this selectivity is augmented by selectivity conferred by the *N*-benzyl-substituent.

2.47 did not show the selectivity in the same range as **2.46** and this seems to be due to its low affinity for the 5-HT_{2A}-receptor. It appears that when 4-fluoro or 4-cyano-substituents are combined with the 2'-fluorobenzyl group the poor affinity of corresponding non-benzylated phenethylamines are not amplified.

The compounds that were selected for radiolabeling and PET experiments were examined for their ability to initiate hydrolysis of PIP_2 into DAG and PIP_3. These results would confirm whether the compounds were agonists at the 5-HT_{2A} receptor. Because these results were measured at the rat 5-HT_{2A} receptor the binding affinities at this receptor are also displayed.

Compound	Ki±SEM (nM) r5-HT_{2A} vs. [^{3}H]MDL-100,907	EC_{50}±SEM (nM) r5-HT_{2A} PI-hydrolysis	(% 5-HT) Intrinsic activity
2.1	1.49±0.35	1.02±0.08	91
2.2	1.12±0.08	0.19±0.03	99
2.3	12.5±3.11	50.7±12.3	86
2.4	1.36±0.37	29.7±2.82	93
2.5	1.01±0.17	0.51±0.19	87
2.9	2.89±1.05	2.31±0.11	88
2.41	0.35±0.05	0.96±0.18	92

Table 5: Functional characterization of selected Group 1-compounds

All of the tested compounds had high intrinsic activity confirming that they are all agonists at the 5-HT_{2A} receptor. Potency varied significantly with **2.2** being the most potent at 0.19 nM. The potency of **2.1**, **2.2**, and **2.3** corresponded well with previously published data by Braden et al.[221] but the potency of **2.4** was unexpectedly low. This could theoretically be attributed to the different cell types since functional assays are more sensitive to changes in cell and tissue type.

These data can of course not be extrapolated to cover all 48 compounds in this chapter but we think there is good reason to believe that they will be agonists based on these preliminary results as well as the structural homology of the compounds.

Chapter 3

Investigation of the *N*-Benzyl moiety – Group 2-compounds

3.1 Aim

This chapter is concerned with exploring ligand-receptor interactions of the *N*-benzyl binding cavity. Focus will be on designing ligands with various 2,3-substitutions patterns but other combinations will also be considered

3.2 Ligand design

It was obvious from the beginning of this project that the *N*-benzylphenethylamine-scaffold has great potential for modifications. The *N*-benzyl moiety in particular is pretty much unexplored. It is however evident from the present data that a hydrogen-bond acceptor in the 2-position of the *N*-benzyl substituent increases binding affinity by at least an order of magnitude. Furthermore, as shown in Chapter 2, the 2',3'-methylenedioxy group seems to confer a moderate selectivity for 5-HT_{2A} over 5-HT_{2C}. This selectivity is of course good, but further investigation of the space which the methylenedioxy group fills might produce a ligand of even better selectivity.

For the phenethylamine part of the molecules we decided to use 2C-B (**1.38**) because it was the most easily synthesized phenethylamine of the 12 compounds used in Chapter 2.

We decided to first look at the other positions of the *N*-benzyl moiety by using a methoxy group to probe each of the other positions while keeping a second methoxy group in the 2-position. Two other compounds focusing on the 2- and 3-positions were included in this group since their aldehydes were readily available commercially (Scheme 19).

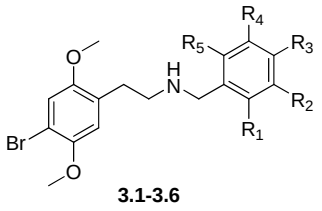

3.1-3.6

	R_1	R_2	R_3	R_4	R_5
3.1	OMe	OMe	H	H	H
3.2	OMe	H	OMe	H	H
3.3	OMe	H	H	OMe	H
3.4	OMe	H	H	H	OMe
3.5	OH	OMe	H	H	H
3.6	F	OMe	H	H	H

Scheme 19: Ligands designed to explore substitution patterns of the *N*-benzyl moiety

In order to further explore the 2- and 3-positions, a series of compounds containing heterocycles in the *N*-benzyl substituents and a hydrogen-bond acceptor in the 2-position were designed (Scheme 20). Most of these were designed as benzo-fused 5-membered heterocycles containing N, O or S as hetero-atoms to provide the hydrogen bond acceptor. In addition to these compounds a number of pyridines and pyridine-derived substituents were also included in this group of heterocycles.

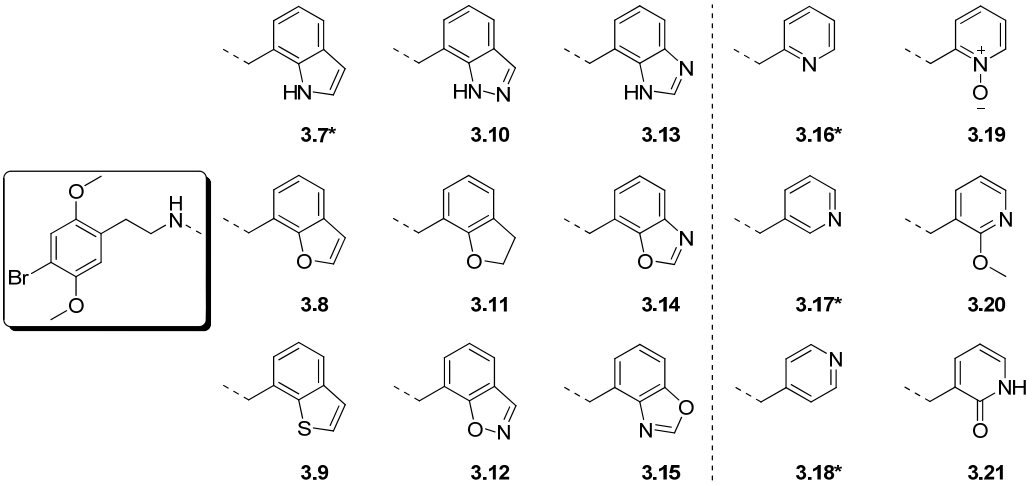

Scheme 20: Structures and compound numbers of heterocyclic Group 3-compounds. *Denotes that the aldehyde is commercially available.

3.3 Chemical synthesis

As explained in Chapter 2 the preferred method of synthesizing these compounds was to use indirect reductive amination to couple the phenethylamine with the substituted benzaldehyde. For a number of the desired compounds this was relatively straightforward as the aldehydes were commercially available. Consequently, **3.1-3.7**, **3.16**, **3.17** and **3.18** were synthesized by reductive amination of 2C-B (**1.38**) with the respective commercially available aldehydes. For the remaining compounds the required aldehydes had to be synthesized *de novo* from simpler starting materials.

3.3.1 Synthesis of aldehydes

Dihydrobenzofuran

The dihydrobenzofuran-aldehyde (**3.23**) was synthesized from 2.3-dihydrobenzofuran (**3.22**) by TMEDA-accelerated ortholithiation[293,294] followed by a DMF-quench (Scheme 21).

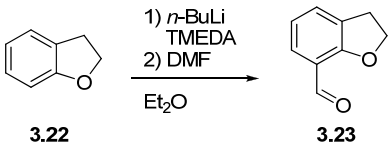

Scheme 21: Synthesis of aldehyde 3.23

The role of TMEDA in this reaction was to assist in de-agglomeration of the *n*-BuLi-hexamer and polarize the C-Li bond further to increase basicity.

Benzofuran and benzothiophene

Initially we attempted to synthesize the benzofuran aldehyde (**3.26**) from the dihydrobenzofuran-aldehyde (**3.23**) by oxidation with DDQ[295], but although this reaction looked good on GC-MS, no product was recovered after flash chromatography. Instead, the 7-formylated benzofuran (**3.32**) and benzothiophene (**3.33**) were synthesized using a parallel strategy[296] with only slightly different conditions. First the starting materials, 2-iodophenol **(3.24**) and 2-bromothiophenol (**3.27**) were alkylated with 2-bromoacetaldehyde diethyl acetal

using standard conditions. The resulting products (**3.25** and **3.28**) were then cyclized using a Friedel-Craft type acylation by refluxing the compounds in a two-phase mixture of polyphosphoric acid and chlorobenzene (Scheme 22).

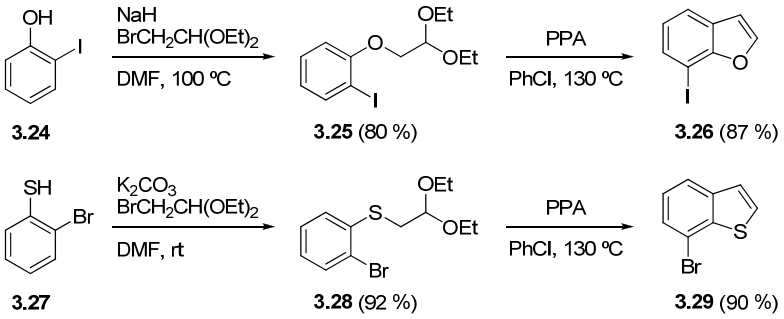

Scheme 22: Synthesis of benzofuran 3.26 and benzothiophene 3.29

Halogen-lithium exchange of the iodobenzofuran (**3.26**) followed by a DMF-quench gave surprisingly the 2-formylated product (**3.30**) instead of the 7-isomer (**3.32**) (Scheme 23). Apparently the hydride-shift is fast enough even at -78 °C to completely convert the 7-lithio-derivative to the 2-lithio derivative within 60 minutes. Nevertheless, the 2-formylbenzofuran was isolated in 21 % yield and the corresponding *N*-benzylphenethylamine was added to the Group 2-compounds.

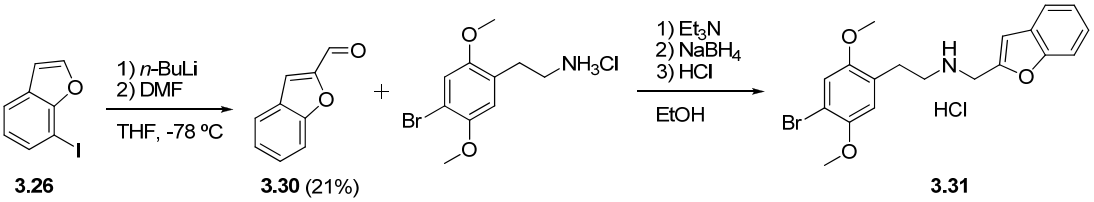

Scheme 23: Unexpected formation of benzofuran-2-carbaldehyde (3.30) and reductive amination to give 3.31

The formylation was instead accomplished using the Bouveault-procedure[297], first converting the aryl halide to the Grignard reagent and the quenching with DMF. The Grignard reagent did not show any sign of rearranging in refluxing THF and the synthesis of **3.32** was accomplished in 71% yield. The Bouveault-procedure was also used to make the benzothiophene-aldehyde (**3.33**) and resulted in 72% yield of the desired product (Scheme 24).

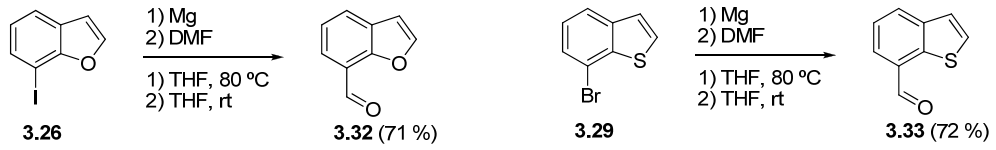

Scheme 24: Synthesis of aldehydes 3.32 and 3.33 via the Bouveault-procedure

Benzimidazole

The benzimidazole aldehyde (**3.41**) was synthesized from 2-nitrophthalic anhydride (**3.34**) in seven steps (Scheme 25). The first five steps in this sequence were adopted from literature procedures[298,299].

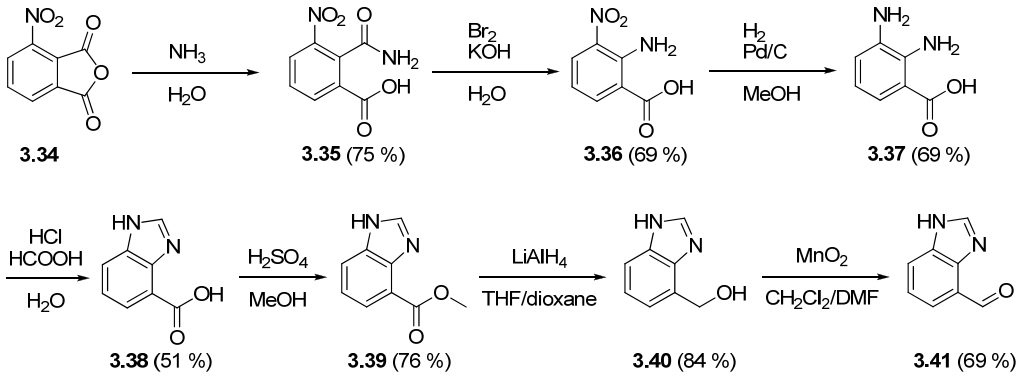

Scheme 25: Synthesis of benzimidazole-4-carbaldehyde (3.41) from 3-nitrophthalic anhydride (3.34)

The sequence began with a regioselective opening of the 2-nitrophthalic anhydride with aqueous ammonia. The phthalamic acid (**3.35**) was then subjected to a Hofmann-rearrangement[300] to give the anthranilic acid (**3.36**). The nitro-group was reduced by catalytic hydrogenation to give the diaminobenzoic acid (**3.37**). Cyclization using the Phillips benzimidazole synthesis[301] afforded the benzimidazole carboxylic acid (**3.38**).

Direct reduction of **3.38** with $LiAlH_4$ to **3.40** would have been preferable but **3.38** was only soluble in solvents that were incompatible with strong reducing agents i.e. MeOH and DMSO. It was therefore necessary first to convert the carboxylic acid to its methyl ester (**3.39**) under standard Fischer-conditions which were accomplished in 76% yield. The more soluble methyl ester (**3.39**) was reduced to the alcohol with $LiAlH_4$ in good yield. For the oxidation to the aldehyde (**3.41**) many reagents are available. TPAP/NMO[302] which is generally a very useful oxidant only gave yields of about 15%. Pyridinium dichromate (PDC)[303] worked fine but due to the presence of DMF as a co-solvent the purification became problematic as PDC always co-eluted with the product on a column. Activated MnO_2[304] turned out to be the best option since the purification could be accomplished simply by filtration through a pad of Celite, evaporation of the filtrate and recrystallization of the solids to give **3.41**.

Indazole

The indazole aldehyde (**3.50**) was synthesized from *o*-toluidine (**3.42**) in 8 steps. First the *o*-toluidine was converted to 7-methylisatin (**3.44**) using the two-step Sandmeyer isatin synthesis[305,306] (Scheme 26).

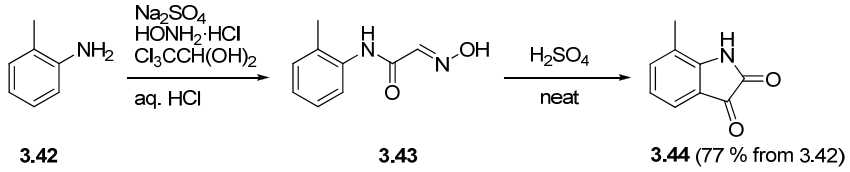

Scheme 26: Sandmeyer isatin synthesis of 7-methylisatin 3.44

The isatin was then exposed to H_2O_2 under basic conditions[307] to afford the anthranilic acid (**3.45**). This reaction was also tried in methanolic solution with a higher concentration of H_2O_2 which should give the methyl ester directly[308] but resulted in a 1:1 mixture of the acid and ester. Instead the acid was esterified afterwards. Fischer-esterification gave yields around 50% but TMS-diazomethane accomplished the task in 93% yield (Scheme 27).

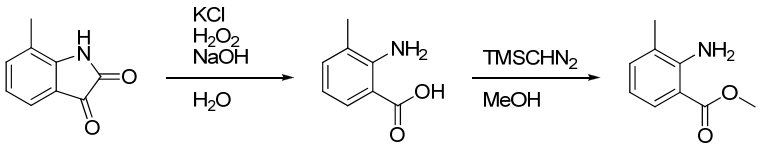

Scheme 27: Oxidative scission of 7-methylisatin 3.44 and esterification to methyl anthanilate 3.46

The next step in the sequence was the crucial indazole cyclization[309] (Scheme 28). The first step in this two-stage synthesis was a simple diazotation which was performed with $NaNO_2$ in aqueous HBF_4. Diazonium tetrafluoroborates are generally considered to be more stable than chlorides and can be handled without the risk of explosion. The isolated and dried diazonium salt (**3.47**) was treated with anhydrous KOAc in $CHCl_3$ in presence of 18-crown-6 to effect the cyclization. Interestingly, the 3-methyl ester has been prepared according to patent literature without the need of a base to bring about the cyclization[310].

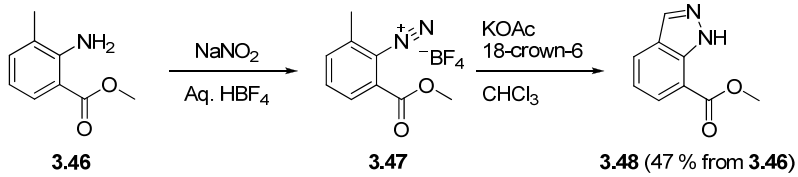

Scheme 28: Diazotation of methyl anthranilate 3.46 and cyclization of diazonium salt 3.47 into indazole 3.48

The final steps towards the desired aldehyde were accomplished in the same manner as with the benzimidazole (**3.41**). Reduction with $LiAlH_4$ to the benzylic alcohol (**3.49**) followed by oxidation with activated MnO_2 gave **3.50** in a decent yield (Scheme 29).

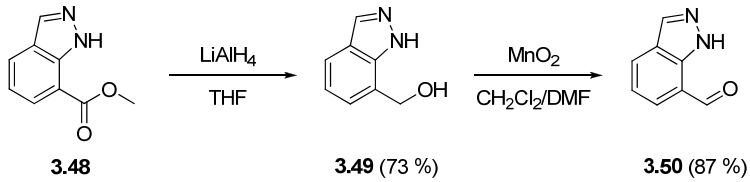

Scheme 29: Final steps in the synthesis of 1*H*-indazole-7-carbaldehyde 3.50

Benzoxazoles

The two isomeric benzoxazole aldehydes were planned to be synthesized in a parallel manner and the strategy was composed mainly of functional group conversions and the benzoxazole-cyclization. First the starting materials (**3.51** and **3.54**) were converted into the regioisomeric aminophenols (**3.52** and **3.56**). This only required a Fischer-esterification for **3.52** while **3.54** also required a hydrogenation of the nitro-group (Scheme 30).

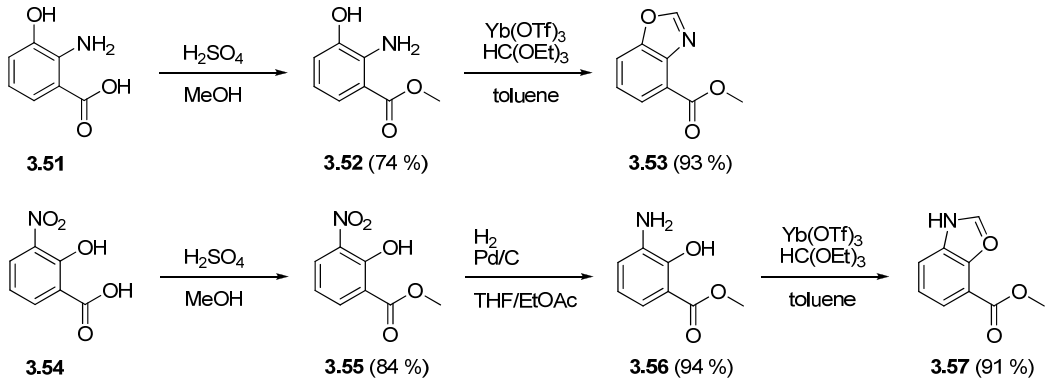

Scheme 30: Synthesis of regioisomeric benzoxazoles

The cyclization was accomplished using triethyl orthoformate in the presence of a Lewis acid catalyst[311] and gave excellent yields for both substrates (Scheme 30). Next up was the reduction of the methyl esters which gave very different results with the two substrates (Scheme 31). It is known that benzoxazoles can undergo ring-opening under reductive conditions[312], yielding the corresponding *N*-methylanilines. Indeed, when treated with DIBAL-H both substrates underwent reductive ring-opening to give *N*-methylanilines (**3.58** and **3.59**). Surprisingly, the even stronger reagent $LiAlH_4$ gave a different result. Reduction of **3.57** with $LiAlH_4$ gave a 2.5:1 mixture of the alcohol (**3.60**) and the *N*-methylaniline (**3.59**). When $LiAlH_4$ was used in the reduction of **3.53** however, the sole product was the *N*-methylaniline (**3.58**).

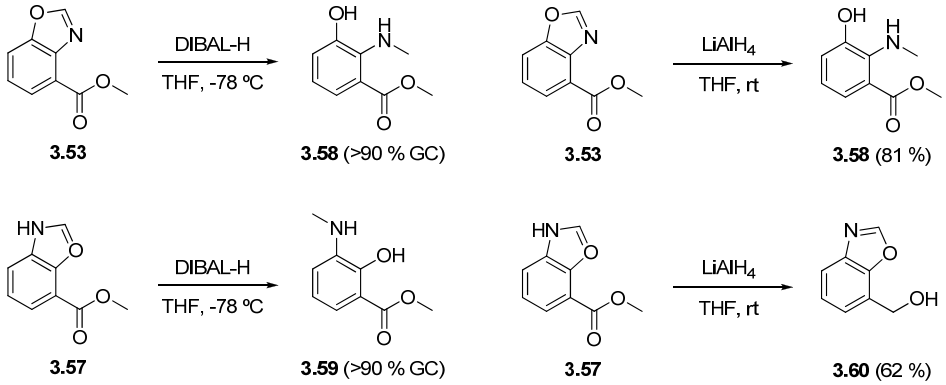

Scheme 31: Reduction of regioisomeric benzoxazoles with DIBAL and $LiAlH_4$

Other reducing agents were applied in the attempt reduce **3.53**. Red-Al[313,314] and LDBBA[315] both gave the same result as DIBAL. No further progress with **3.53** was made at the time but it was clear that the strategy would have to be revised. It might have been possible to reduce the ester before the benzoxazole cyclization and then do the final oxidation. Another possibility was to choose an ester that could be reduced with milder reagents.

The primary alcohol (**3.60**) was oxidized with TPAP/NMO to the desired aldehyde in 56% yield (Scheme 32). This yield was deemed sufficient but it might be improved using other reagents, especially MnO_2 which worked well for the benzimidazole and indazole.

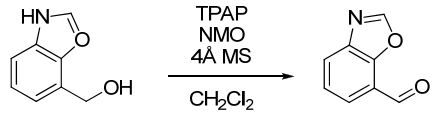

3.60 **3.61** (56 %)

Scheme 32: Oxidation of 3.60 with TPAP/NMO.

Benzisoxazole

The first attempt at synthesizing the benzisoxazole-aldehyde (**3.12**) began with 2,6-dimethoxyphenol **3.62** which was protected as its acetate ester in excellent yield.

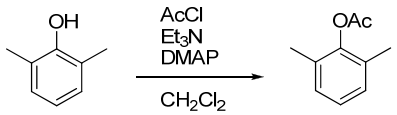

3.62 **3.63** (91 %)

Scheme 33: Acylation of 3.62

The acetate was then subjected to free-radical bromination[316] to obtain the tribrominated product (**3.64**). Despite some early success, this reaction tended to give some erratic product distributions and frequently mixtures of dibromo (**3.65**), tribromo (**3.64**) and tetrabromo (**3.65**) compounds were recovered.

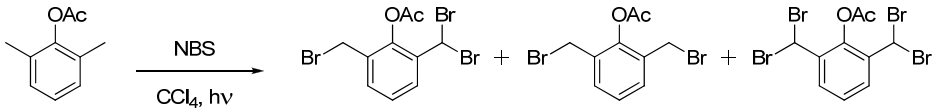

3.63 **3.64** (50%) **3.65** (25%) **3.66** (25%)

Scheme 34: Free-radical bromination of 3.63

The outcome of the subsequent reaction was dependent on a pure starting material but purification was difficult. The compounds were very close on TLC and flash chromatography was not useful in separating the mixtures. Distillation was also tried, but despite a relatively large gap between the boiling points several runs were necessary to get a pure product. The best way to purify the compound was to recrystallize it from heptanes and toluene, but this only worked when the crude compound was relatively pure and did not work for statistical mixtures. Despite these problems, a good quantity of **3.64** was synthesized mainly, from the few batches that gave a favorable product distribution. It was never determined exactly what conditions gave tribromination exclusively. When conditions that yielded a batch of almost pure **3.64** were repeated the result was completely different. A more rigorous examination of reaction conditions might reveal exactly what affects product distribution

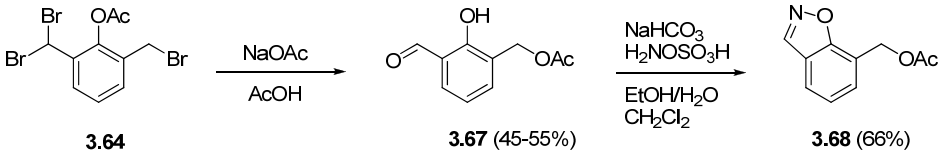

3.64 **3.67** (45-55%) **3.68** (66%)

Scheme 35: Acetolysis/hydrolysis of 3.64 and isoxazole formation

The tribromide (**3.64**) was converted into the salicylaldehyde (**3.67**) by boiling in acetic acid with excess sodium acetate. This reaction not only converted to geminal dibromide to an aldehyde, but also deprotected the phenol and effected an S_N2-substitution on the benzyl(mono)bromide, converting it to an acetate ester (Scheme 35). This compound was then set up for the benzisoxazole cyclization using an established procedure[317] which gave the desired benzisoxazole **3.68** in 66% yield. The only remaining steps were to remove the acetyl protecting group and oxidize the liberated benzylic alcohol (**3.69**) to the corresponding aldehyde (**3.70**) (Scheme 36).

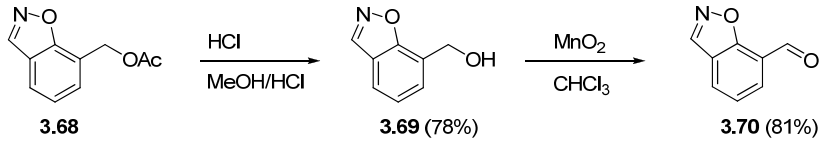

Scheme 36: Final steps in the synthesis of 3.70

These operations were accomplished in 78% and 81% yields respectively. While this synthetic strategy was ultimately effective, it was not as efficient as originally hoped and only a tiny amount of aldehyde was produced, mainly due to the problems with the radical bromination. With the problems arising in the previously described strategy to synthesize **3.70** a backup strategy was devised and carried out. 3-methylsalicylic acid (**3.71)** was esterified using Fischer conditions and the phenol (**3.72**) was protected as its acetate ester (**3.73**) (Scheme 37).

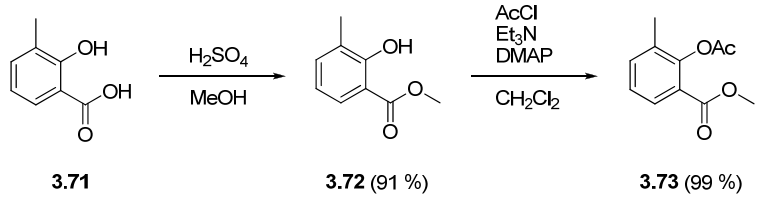

Scheme 37: Synthesis of 3.73

This compound was then subjected to the same radical bromination as described earlier, only this time chlorobenzene was used as solvent because carbon tetrachloride was no longer in supply. The radical bromination of this particular substrate did not prove difficult as excess NBS could be used without the possibility of overbromination (Scheme 38).

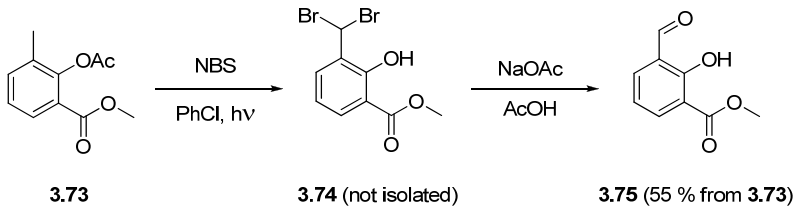

Scheme 38: Free-radical bromination of 3.73 and hydrolysis to give 3.75

The geminal dibromide (**3.74**) was hydrolyzed using the same conditions as earlier described[316], giving the salicylaldehyde (**3.75**) (Scheme 38). We tried to improve the yield of the hydrolysis using different conditions such as DMSO[318], pyridine[319], $AgNO_3$[320,321], NH_4CO_3[322] and $CaCO_3$[323]. None of these gave better results and various problems were encountered in their use.

The salicylaldehyde (**3.75**) was converted to the benzisoxazole (**3.76**) using the same procedure as before. The next step was potentially the most problematic in this strategy. Since we had already encountered problems when reducing esters in the presence of the benzoxazole (**3.53**) (Scheme 31) we anticipated that this could be problematic. Luckily the first reagent tried was LDBBA in the hope that it might be possible to obtain the aldehyde by partial reduction of the ester. While the aldehyde was initially formed according to TLC it was quickly reduced to the alcohol and it was not possible to get clean conversion to the aldehyde. The ester was instead reduced all the way to the alcohol and then oxidized with activated MnO_2 to give the desired aldehyde (Scheme 39).

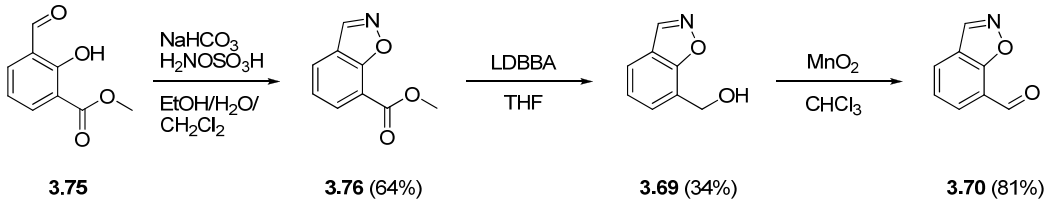

Scheme 39: Benzisoxazole formation, reduction and oxidation to synthesize 3.70

The two pathways to this compound both comprise seven steps, but the latter was overall a better solution. The hydrolysis step and reduction could both be improved but in the short amount of time available for this synthesis the result was acceptable.

2-pyridone and 2-methoxy pyridine

These two aldehydes have been prepared in the literature and this method was followed with a few adjustments. There are several literature procedures describing the synthesis of 3-formyl-2-chloropyridine from 2-chloropyridine[324,325]. These use LDA to selectively lithiate 2-chloropyridine in the 3-position followed by quenching with a formyl donor like DMF or ethyl formate. We found that lithiation with LiTMP followed by quench with excess ethyl formate gave moderately improved yields over the previously described procedures.

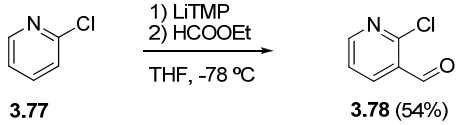

Scheme 40: Improved synthesis of 3-formyl-2-chloropyridine

3.78 was then converted to **3.79** and **3.80** using the literature procedures.

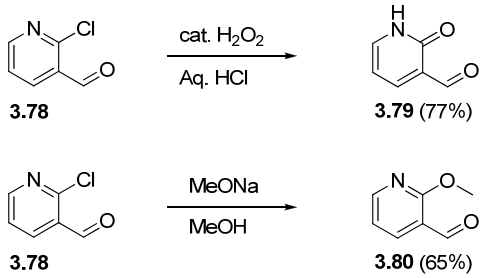

Scheme 41: Synthesis of aldehydes 3.79 and 3.80

The nucleophilic substitution with MeONa resulted in a substantial amount of a byproduct resulting from reduction of the aldehyde **3.80**. Otherwise, the reactions proceeded without problems.

3.3.2 Reductive aminations

The final products were assembled by reductive amination except for **3.19** which was supposed to be made by oxidation of **3.16**. Unfortunately, time was short and **3.19** was not synthesized within the timespan of the project.

The reductive aminations generally went smoothly and the secondary amines were converted to hydrochloride salts. The hydrochloride salt of **3.14** turned out to be so hygroscopic that the crystals dissolved in the filter paper while air-drying. **3.14** was instead converted to its hemioxalate salt which was completely stable. The synthesis of **3.12** went smooth enough but an interesting development took place while the crude amine was analyzed by NMR. The compound slowly transformed into a slightly different compound while the NMR was recorded. The benzoxazole proton simply disappeared over time. It is known that benzoxazole can undergo ring opening when treated with strong base but we had not anticipated that the secondary amine was strong enough to deprotonate the benzoxazole and convert it into the corresponding 2-cyanophenol (**3.81**).

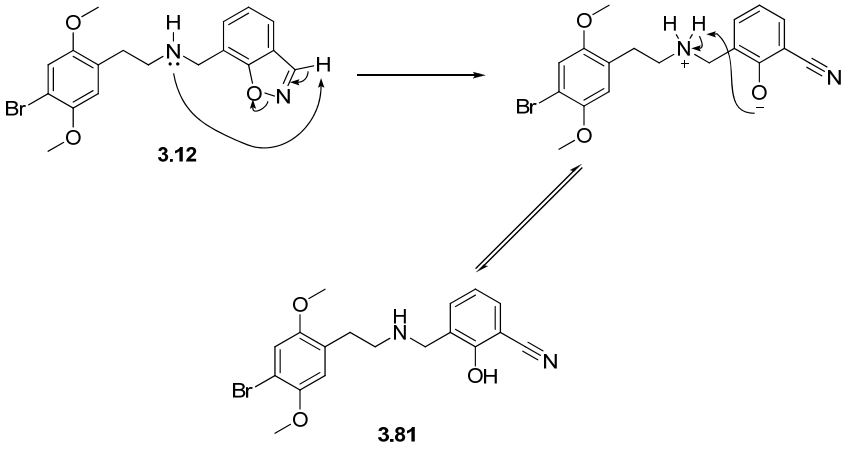

Scheme 42: Proposed mechanism for rearrangement of benzisoxazole (3.12) into cyanophenol (3.81)

Since it still possessed a desirable substitution pattern, **3.81** was isolated, characterized and submitted for biological evaluation along with the remaining compounds.

3.4 In vitro biological evaluation

The compounds were submitted for biological evaluation at the PDSP as previously described. So far we have only obtained data on binding affinity and none of the compounds have yet been tested for efficacy in a functional assay.

Beware that as in Chapter 2, 5-HT_{2B} affinites are measured against an agonist and therefore not directly comparable to the measured 5-HT_{2A} and 5-HT_{2C} affinities.

Compound	pK_i h5-HT_{2A} vs. [^{3}H]Ketanserin	pK_i h5-HT_{2B} vs. [^{3}H]LSD	pK_i r5-HT_{2C} vs. [^{3}H]Mesulergine
3.1 (2,3-DiMeO)	8.51	8.07	7.63
3.2 (2,4-DiMeO)	7.70	7.99	7.57
3.3 (2,5-DiMeO)	7.51	7.30	7.11
3.4 (2,6-DiMeO)	6.50	8.05	7.75
3.5 (2-OH;3-MeO)	9.64	8.92	8.20
3.6 (2-F;3-MeO)	8.48	8.20	7.25
3.7 (indole)	7.89	8.39	7.18
3.8 (benzofuran)	9.22	8.66	8.60
3.9 (benzothiophene)	8.77	8.16	8.11
3.10 (indazole)	7.92	8.27	7.62
3.11 (coumaran)	9.70	9.22	8.47
3.12 (benzisoxazole)	n/a	n/a	n/a
3.13 (benzimidazole)	8.11	8.33	8.03
3.14 (benz-7-oxazole)	7.96	7.39	7.49
3.15 (benz-4-oxazole)	n/a	n/a	n/a
3.16 (2-pyridine)	7.41	7.14	7.38
3.17 (3-pyridine)	7.08	6.89	6.92
3.18 (4-pyridine)	6.85	6.49	6.81
3.19 (2-pyridine oxide)	n/a	n/a	n/a
3.20 (2-MeO-3-Pyr)	7.10	7.20	7.15
3.21 (2-pyridon)	6.91	7.11	6.92

Table 6: Binding affinites for Group 2-compounds at 5-HT_{2A}, 5-HT_{2B} and 5-HT_{2C} receptors. TBD: to be determined

2',3'-disubstitution (**3.1**) seems well tolerated which we already knew from the 2',3'-methylenedioxy compounds in Chapter 2. 2',4'-, 2',5'- and 2',6'-disubstitution (**3.2-4**) reduces 5-HT_{2A} affinity by a 10-100-fold but retains some affinity for 5-HT_{2B} and 5-HT_{2C}. **3.5** on the other hand has the highest affinity for the 5-HT_{2A} reported in this thesis and also has a decent selectivity for 5-HT_{2A} versus 5-HT_{2C}. **3.11** also has very high affinity but selectivity is not as good as **3.5**. The other benzo-fused heterocycles have slightly lower affinities for 5-HT_{2A} but mediocre selectivities vs. 5-HT_{2C}. Pyridines and 2-substituted pyridines have poor affinity for 5-HT_{2A} and this might be caused by the electron-poor heterocycle forming weaker π-interactions with a phenylalanine (F339) as previously described by Braden. For future PET studies **3.5** and possibly **3.11** should be the prime candidates from this group of compounds. Some of the benzo-fused heterocycles may have value in metabolism studies since these often have different metabolic profiles which could be of benefit for future studies.

Chapter 4

Conformationally restricted *N*-benzylphenethylamines

(Group 3-compounds)

4.1 Aim

The project described in this chapter is concerned with the synthesis of compounds that constitute a subset of a larger group of conformationally restricted *N*-benzylphenethylamines designed and synthesized by the Nichols-group at Purdue University.

4.2 Introduction

The discovery of the *N*-benzylphenethylamines as potent 5-HT_{2A} agonists was the latest breakthrough in the research into 5-HT_{2A} agonists. One of the best ways to expand upon this breakthrough was to design, synthesize and evaluate structurally rigid analogues of these compounds. The Nichols group has a long history of making structurally rigid analogues of simple phenethylamines, among these are the FLY compounds and 2C-BCB (Scheme 43).

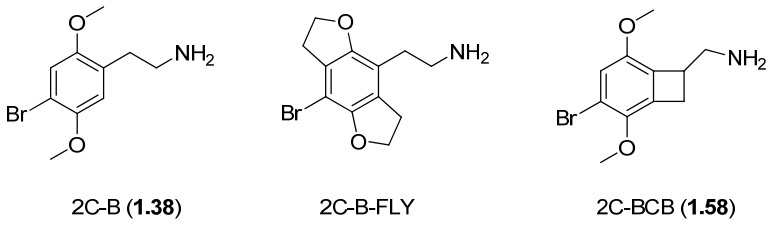

Scheme 43: Structurally rigid analogues of 2C-B (1.38)

Expanding this concept was easily achieved by making the *N*-benzyl analogues of 2C-B-FLY and 2C-BCB, but disappointingly both of these turned out to have slightly lower affinity than 25I-NBOMe at the 5-HT_{2A} receptor[222]. It would seem like the more flexible 25I-NBOMe had an easier time of adopting a suitable binding conformation and it was possible the affinity had been pushed to the limit. There was however still the question of selectivity. All of these compounds retain a relatively high affinity for the 5-HT_{2C} receptor. The Nichols group designed a new set of compounds based on 25B-NB and 25B-NBOMe (**2.5**) (Scheme 44) in which the *N*-benzyl moiety had been constricted so that the amount of binding conformations had been reduced significantly (Scheme 45). Bromine was chosen over iodine in the 4-position of the phenethylamine because electrophilic aromatic bromination is much more easily accomplished than iodination and does not require the use of protecting groups on the basic nitrogen.

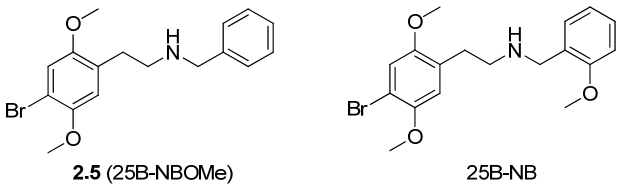

Scheme 44: 25B-NBOMe (2.5) and 25B-NB which serve as flexible templates

Some of the target compounds are analogues 25B-NB, and while these were expected to have lower affinity than 25B-NBOMe-analogues, it should still be possible to determine if the conformational restriction confers any selectivity or not.

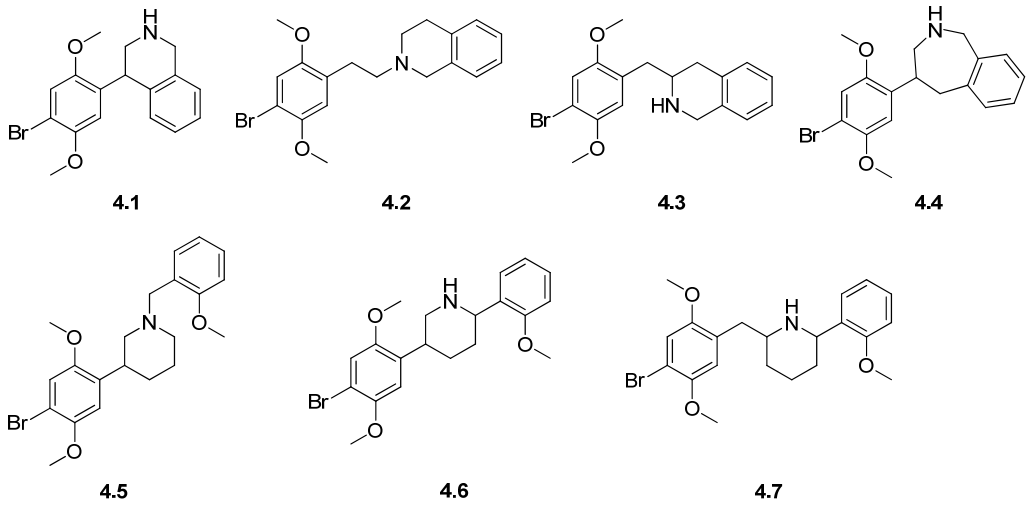

Scheme 45: Conformationally restricted analogues of 25B-NBOMe (2.5) and 25B-NB

4.3 Chemical synthesis

Of the seven proposed compounds (**4.1-4.7**) three were synthesized in this project (**4.3**, **4.5** and **4.6**) although the final steps of **4.6** were completed by Jose Juncosa of the Nichols group.

4.3.1 Synthesis of tetrahydroisoquinoline (4.3)

The synthesis of **4.3** proved to be a challenging task. Tetrahydroisoquinolines can be synthesized in a variety of ways, most of which involve the Pictet-Spengler reaction[326] or the related Bischler-Napieralski reaction[327]. Both these reactions were however not very well suited for this particular tetrahydroisoquinoline because those cyclizations generally occur onto electron-rich aromatic rings. Furthermore, adding the 2,5-dimethoxybenzyl group at the 3-position of the tetrahydroisoquinoline at a later stage did not look like a promising endeavor. A search in the literature gave few good results, but did produce a promising paper on synthesis of 3-substituted tetrahydroisoquinoline derivatives *via* heteroatom-directed lateral lithiation of Boc-protected 2-methylbenzylamine[328].

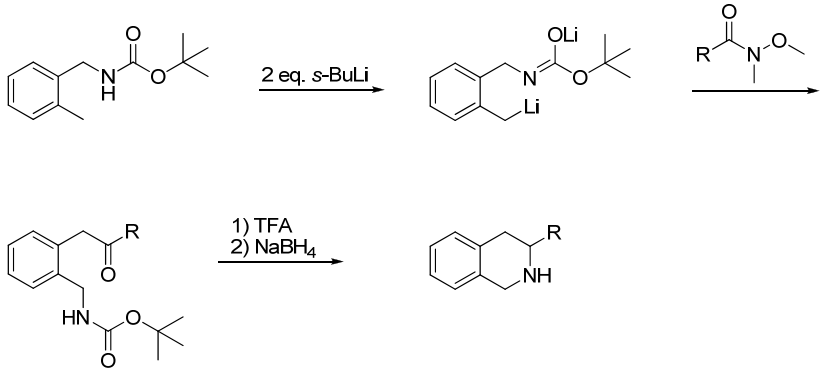

Scheme 46: Methodology for the synthesis of 3-substituted tetrahydroisoquinolines

The methodology is relatively straightforward: The Boc-protected 2-methylbenzylamine is lithiated with 2 equivalents of *sec*-butyllithium and the dilithiated species is combined with a Weinreb-amide[329] containing the desired 3-substituent. The resulting ketone is then deprotected with concomitant imine-formation followed by reduction with $NaBH_4$ to give the tetrahydroisoquinoline (Scheme 46).

The necessary starting materials for this reaction were synthesized in a few steps. The Boc-protected benzylamine (**4.11**) was synthesized from *o*-toluic acid (**4.6**) in four steps and the Weinreb-amide (**4.13**) was synthesized from 2,5-dimethoxyphenylacetic acid (**4.12**) in two steps (Scheme 47).

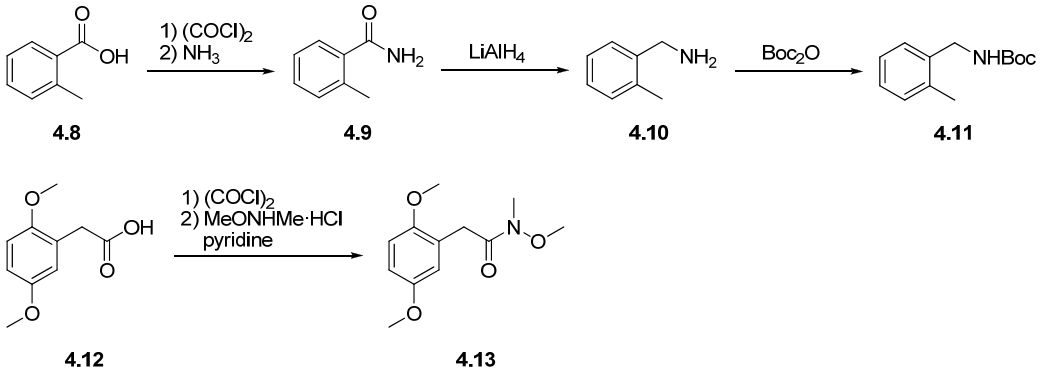

Scheme 47: Synthesis of starting materials for the lateral lithiation-Weinreb ketone synthesis

With the starting materials in hand, experimentation on the lateral lithiation-ketone synthesis could commence. The literature procedure was applied with some success but the yields varied between 15% and 40%. The reason for these variations in yields was not determined, but insufficient drying of glassware and solvents seemed to be the likely cause. The best results for the lithiation-ketone synthesis was obtained by adding *sec*-butyllithium to a solution of **4.11** at -40 °C until the solution started turning orange, indicating formation of the dilithiated species. At this point an additional 1.1 eq. of *sec*-butyllithium was added to ensure complete formation of the dilithiated species (Scheme 48).

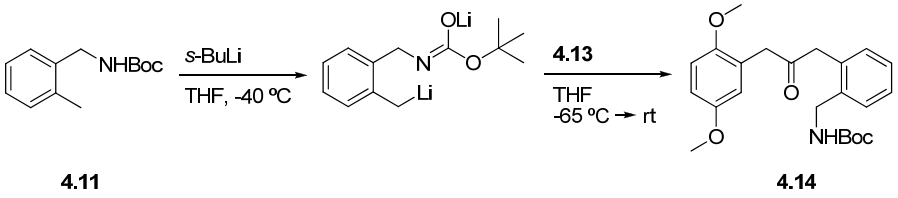

Scheme 48: Synthesis of the key intermediate 4.14

The reaction was then cooled to -65 °C and the Weinreb amide (**4.13**) was added and reaction was allowed to reach room temperature over the course of 2 hours. This resulted in consistent yields of about 35-40% ketone and better scalability, ensuring that enough material was available for the final steps.

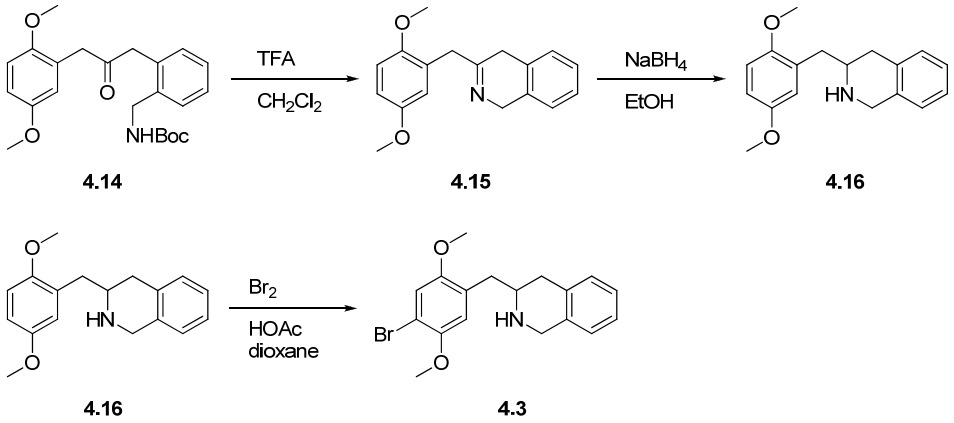

Scheme 49: Final steps in the synthesis of the tetrahydroisoquinoline (4.3)

The TFA-promoted deprotection-cyclization proceded smoothly and reduction of the intermediate dihydroisoquinoline (**4.15**) with $NaBH_4$ gave the tetrahydroisoquinoline **4.16** in 75% yield from the ketone (**4.14**) (Scheme 49). The final step required a regioselective bromination at the 4-position, a reaction that had proved troublesome on **4.2** resulting in bromination of the tetrahydroisoquinoline ring. Fortunately the last step was achieved with Br_2 in AcOH/dioxane, without any byproducts.

4.3.2 Synthesis of *N*-benzylphenylpiperidine (4.5)

The tricyclic skeleton of **4.5** was synthesized in five steps from 1,4-dimethoxybenzene (**4.17**) (Scheme 50 and 51). The starting material was converted to the boronic acid (**4.18)** using a literature procedure[330]. Suzuki cross-coupling[331] of the boronic acid and 3-bromopyridine gave the phenylpyridine (**4.19**) in 78% yield. This compound had been synthesized previously[332] by a Kumada-coupling, but in a miserable yield of 20%, showing that the substrate scope of the Suzuki couping was superior in this case (Scheme 50).

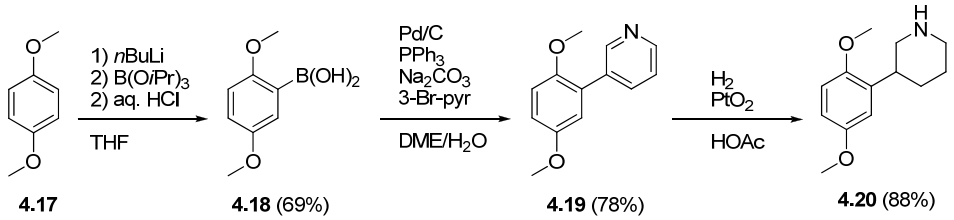

Scheme 50: Synthesis of phenylpiperidine (4.20)

Pt-catalysed reduction of **4.19** with H_2 under elevated pressure afforded the phenylpiperidine (**4.20**) which was converted to **4.21** using a standard bromination procedure. The final step was reductive amination with 2-methoxybenzaldehyde which was accomplished in 66% yield (Scheme 51).

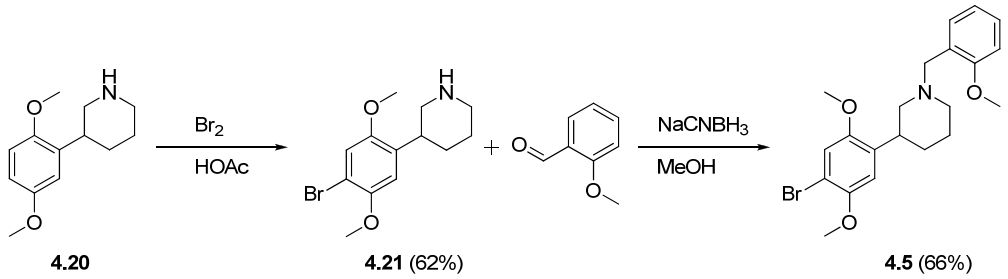

Scheme 51: Final steps in the synthesis of 4.5

4.3.3 Partial synthesis of diphenylpiperidine (4.6)

The synthesis of the final compound (**4.6**) was expected to be relatively simple, since two of the synthetic steps were very similar to the ones in the synthesis of **4.5**. The first two steps were relatively unproblematic. Suzuki-coupling of the previously synthesized boronic acid (**4.18)** and 3-bromo-5-chloropyridine (**4.22**) did not work with Pd/C and PPh_3 but required the preformed catalyst $Pd(PPh_3)_4$. The yield of 62% was lower than expected but acceptable. The ensuing Kumada-coupling[333] proceeded smoothly in good yield (Scheme 52).

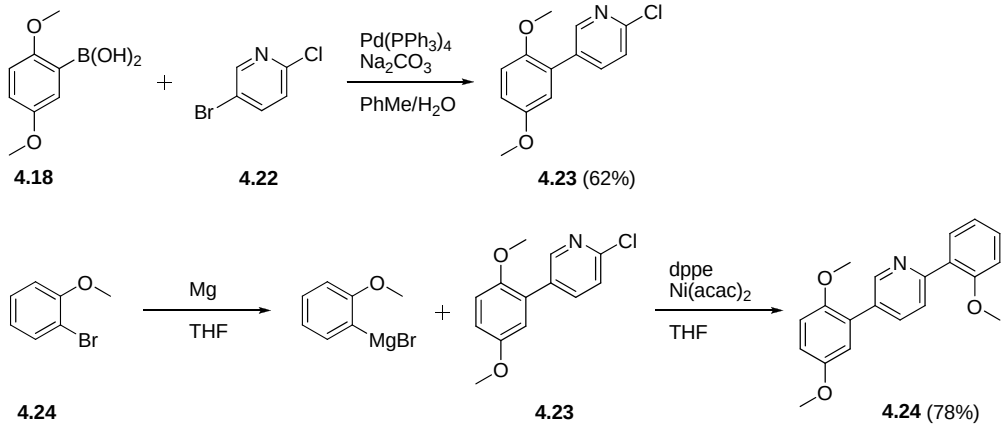

Scheme 52: Synthesis of diphenylpyridine (4.24)

Reduction of the diphenylpyridine proved to be a difficult task. The substrate was inert to the usual catalytic hydrogenation conditions. A number of experimental conditions listed in Table 7 were tried without resulting in the desired 2,5-disubstituted piperidine (**4.39**).

Conditions	Results
H_2 (80 psi), PtO_2, HOAc, 2-100+ hrs	No reaction
H_2 (0.1 psi), $Pd(OH)_2$, HOAc, 24 hrs	No reaction
H_2 (0.1 psi), RaNi, HOAc, 24 hrs	No reaction
H_2 (0.1 psi), Rh/C, HOAc, 24 hrs	No reaction
$HCOONH_4$, PtO_2, HOAc, 60 °C, 5 hrs	No reaction
$HCOONH_4$, PtO_2, HOAc, 170 °C, µW, 5 hrs	No reaction
H_2 (1000 psi), PtO_2, HOAc, 3 hrs	Some reduction of phenyl rings
$NaBH_4$, MeOH	No reaction
$NaBH_4$, HOAc	No reaction
$NaBH_4$, BnBr, DCM	No reaction
$LiBHEt_3$, THF	No reaction
Na, EtOH	No reaction
$Na(CF_3COO)BH_3$	No reaction
*m*CPBA then $NaBH_4$, EtOH	No reaction
*m*CPBA then Pt/C, $HCOONH_4$, EtOH, 110 °C, µW, 1 hr	*N*-oxide was reduced back to the pyridine
*m*CPBA then DIBAL, THF	*N*-oxide was reduced back to the pyridine

Table 7: Different reaction conditions employed in the attempted reduction of the diphenylpyridine (4.24)

With no apparent solution to the reduction problem in sight, a different approach was needed. The reason for the reduction being so difficult was attributed to the two phenyl-rings. With the phenyl-rings being ortho-substituted and perpendicular to the pyridine ring, reducing agents and especially heterogenous catalysts would have had a hard time approaching the pyridine due to steric hindrance. However, if one of the phenyl rings were absent at the time of reduction it might be easier to accomplish.

A simpler substrate (**4.27**) was synthesized via Suzuki-coupling of 2-methoxyphenylboronic acid (**4.25**) and 5-bromo-3-hydroxypyridine (**4.26**) (Scheme 53).

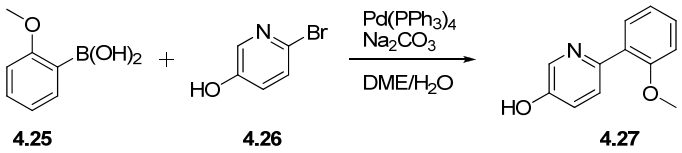

4.25 **4.26** **4.27**

Scheme 53: Synthesis of 3-hydroxypyridine (4.27)

Unfortunately, when this compound was subjected to some of the previously mentioned reduction conditions the results were the same. This substrate was also subjected to the conditions shown in Scheme 54 which have been showed to reduce 3-hydroxypyridines in good yields[334].

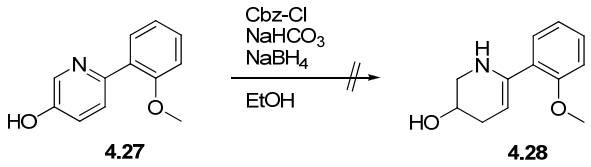

Scheme 54: Attempted reduction of 3-hydroxypyridine (4.27)

These conditions did not work any better than those previously mentioned. However, the paper in which these conditions were described gave some inspiration to devise an alternative method to synthesizing 2,5-disubstituted piperidines. An alternative strategy was created starting from 3-hydroxypyridine (**4.29**). Comprising 11 steps, it was a significant detour compared to the original strategy. Reduction of 3-hydroxypyridine with $NaBH_4$ using methyl chloroformate as an electrophilic activator gave the carbamate protected enamine (**4.30**) which was converted to the N,O-acetal (**4.31**) and the secondary alcohol was protected as the acetate (**4.32**). The next step involved the addition of an aryl cuprate to the *N*-acyliminium ion generated from (**4.32**) by the action of BF_3. The addition was accomplished in good yield and deprotection of the acetate followed by Swern-oxidation gave the ketone (**4.35**) (Scheme 55).

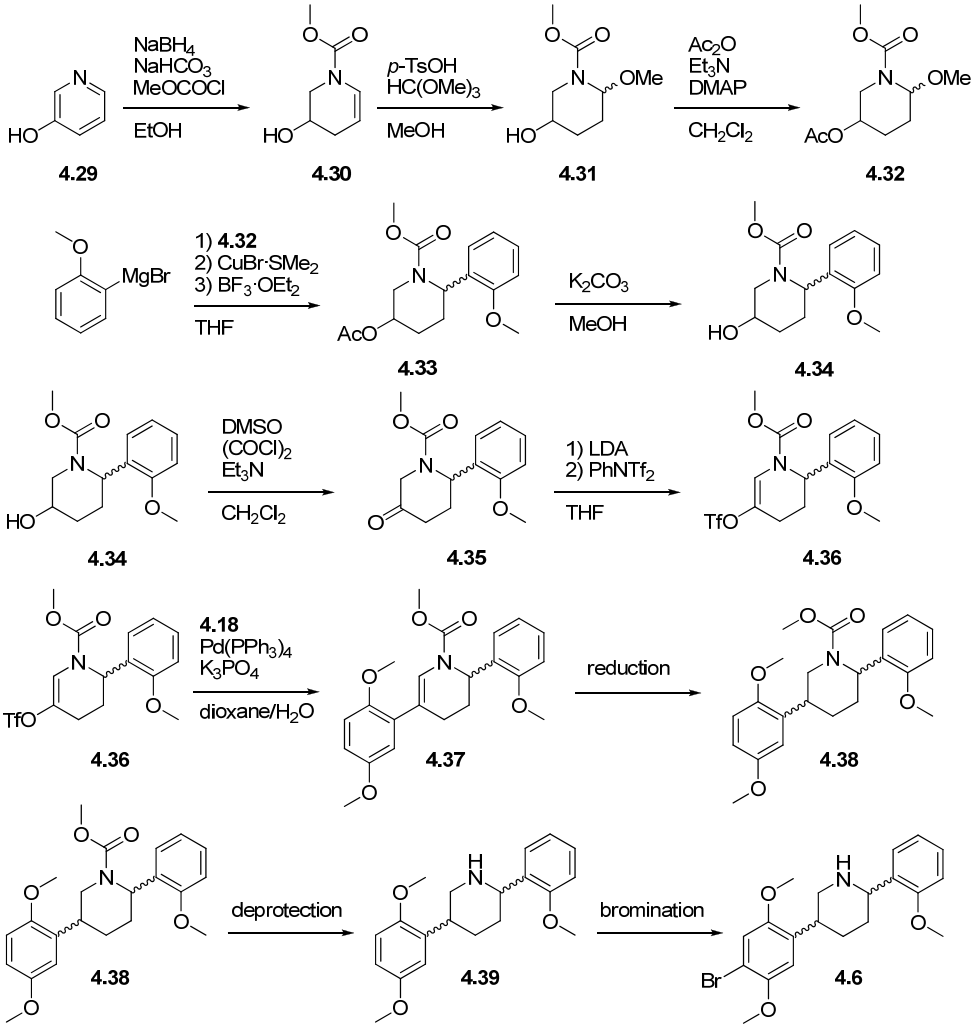

Scheme 55: Alternative synthetic strategy for the synthesis of 4.6

However, no further work in this direction was accomplished because the reduction problem with **4.24** had been solved in the meantime. A colleague at the Nichols-group working on **4.7** found a way of reducing the diphenylpyridine. Compound **4.7** was made from a 2,6-disubstituted pyridine in a similar fashion to **4.6**, but unlike **4.6** this compound was susceptible to catalytic hydrogenation although this gave exclusively the *cis*-product. The *trans*-isomer was obtained by treatment with 64 equivalents of sodium in refluxing ethanol which gave a 1:1 ratio of *cis* and *trans* products that could be separated by column chromatography (Scheme 56). The same procedure was already tried with **4.24** albeit at ambient temperature and with less sodium but without any noticeable reaction. In refluxing EtOH the reduction worked as advertised and the synthesis of both diastereomers of **4.6** was completed at the Nichols lab. The final bromination proved to be relatively straightforward, although purification by flash chromatography required some experimentation.

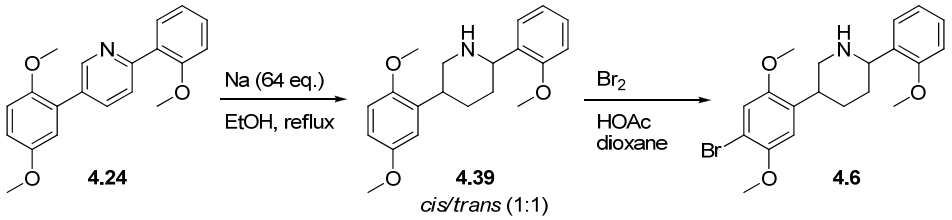

Scheme 56: Final steps in the synthesis of the diphenylpiperidine (4.6)

4.4 In vitro biological evaluation

The compounds were evaluated in a radioligand competition assay using [^{3}H]Ketanserin as radioligand for 5-HT$_{2A}$ receptors and [^{3}H]mesulergine as radioligand for 5-HT$_{2C}$. Selected compounds were also tested in 5-HT$_{2A}$ and 5-HT$_{2C}$ receptors labeled with the agonist DOI.

Compound	pKi h5-HT$_{2A}$ vs. [^{3}H]Ketanserin	pKi h5-HT$_{2C}$ vs. [^{3}H]Mesulergine	pKi h5-HT$_{2A}$ vs. [^{125}I]DOI	pKi h5-HT$_{2C}$ vs. [^{125}I]DOI
Cinanserin	7.59	n/a	n/a	n/a
Mianserin	n/a	7.89	n/a	n/a
±DOI	n/a	n/a	8.37	8.28
2C-B	7.01	6.62	8.33	8.60
2.5	8.22	7.44	9.17	9.19
4.1	6.15	5.07	n/a	n/a
4.2	5.80	4.11	n/a	n/a
4.3	5.78	5.17	n/a	n/a
4.4	6.34	5.49	n/a	n/a
4.5	4.67	4.23	n/a	n/a
***cis*-4.6**	5.54	4.41	n/a	n/a
***trans*-4.6**	5.07	3.51	n/a	n/a
***cis*-4.7**	5.09	4.15	n/a	n/a
***trans*-4.7**	7.35	5.29	8.70	7.11

Table 8: Binding affinities of Group 3-compounds at 5-HT$_{2A}$ and 5-HT$_{2C}$ receptors

The assays were performed at Purdue University with different cell lines and species than the results obtained from PDSP presented in the other chapters. It is therefore not possible to directly compare these values with those presented in Chapter 2, 3 and 5. Even so, the affinities of **2.5** at antagonist labeled receptors are very close to those reported in Chapter 2.

Upon immediate inspection of the binding affinities it was clear that none of these compounds have an affinity that is comparable with **2.5**. However, there was clearly one compound that stands out both in terms of binding affinity and selectivity towards the 5-HT_{2A} receptor. *trans*-**4.7** has a binding affinity an order of magnitude better than the next best compound (**4.4**) but better than the pharmcological standard, DOI. However, the selectivity for 5-HT_{2A} was 115-fold over 5-HT_{2C} when measured at antagonist assays. This selectivity was reduced somewhat in agonist labeled assays but was still 39-fold. *trans*-**4.7** is clearly a compound that is worth further investigation and isolating the enantiomers to determine the optimal stereochemistry would be valuable to determine the absolute binding orientation in the computational model. The right enantiomer would most likely also have a better binding affinity and possibly even better selectivity. *trans*-**4.7** was also tested for its ability to activate the 5-HT_{2A} receptor by measuring its ability to initiate PI-hydrolysis and was found to be a partial agonist with an intrinsic activity of 70% of 5-HT.

Compounds **4.1** and **4.4** also deserves mention because they do not possess the 2-methoxy-group on the *N*-benzyl moiety that boosts the affinity and it would be interesting to see those two compounds with a methoxy or hydroxy group in what amounts to the 2'-position.

The compounds synthesized as part this thesis **4.3**, **4.5** and **4.6** did not fare as well as *trans*-**4.7** but were nonetheless important in order explore as many conformations as possible and to create a sufficient dataset. The fact that only one compound performed so well did confirm that the binding conformation is very important in determining binding affinity and selectivity.

Another noteworthy point was that binding affinities at agonist-labeled receptors were at least an order of magnitude higher at than the antagonist-labeled receptors which confirm the two-state theory presented in Section 1.3.1.

Chapter 5

Structure-Based Design and Synthesis of 5-HT$_{2A}$-agonists

(Group 4-compounds)

5.1 Aim

To synthesize and evaluate novel agonists for the 5-HT$_{2A}$ receptor designed using a homology model of the receptor to predict novel ligand-receptor interactions.

5.2 Introduction

Structure-based drug design is the use of three-dimensional models of target proteins to design novel ligands and is considered the state of the art in drug design.

The three dimensional structure of the target protein is usually obtained by X-ray crystallography or in some cases by NMR-spectroscopy. If the structure of the protein in question has not determined experimentally it might be possible to generate a homology model by using the template from a related protein. The quality of a homology model depends on many factors but the sequence homology between the template and the target protein should be as good as possible.

If the protein has been co-crystallized with a ligand it is possible to visualize the protein-ligand interactions in the 3D-model and use a number of computational tools to visualize the binding site and predict other favorable interactions that may be exploited in the design of a new ligand. Putative ligands may be evaluated in the model using 'docking' and 'scoring' and it is possible to use this method as a virtual screening procedure.

The three dimensional structure of the 5-HT$_{2A}$ receptor has not yet been determined, which is due to the general problems involved in crystallizing GPCRs. Since GPCRs are membrane proteins they are difficult to crystallize compared to e.g. enzymes that are in solution. However, in 2000 Palczewski et al.[335] succeeded in crystallizing and determining the three dimensional structure of bovine rhodopsin, a GPCR responsible for the detection of light in the retina. This disclosure immediately spawned the development of multiple homology models of GPCRs belonging to the rhodopsin family. Chambers et al.[336] were the first to publish an *in silico*-activated homology model of the 5-HT$_{2A}$ receptor. The crystal structure of the bovine rhodopsin contained the native ligand retinal in its inactive 11-*cis*-isomer. In order to activate the receptor the ligand was isomerized to all-*trans*-retinal, and the receptor was steered with constrained molecular dynamics to adopt the active state. A homology model of the 5-HT$_{2A}$ receptor was then made using the activated bovine rhodopsin structure as the template. With the use of this model several new 5-HT$_{2A}$ agonists were designed[337,338]. While the development of a homology model of the 5-HT$_{2A}$ receptor was a big step towards structure based design, there were also problems with the model. Some compounds, among these the recently published *N*-benzylphenethylamines, fitted the receptor but the predicted score did not always correlate with the measured binding affinities. Most of these problems were attributed to marked differences between the rhodopsin-template and the 5-HT$_{2A}$ receptor. This was later confirmed

when other GPCR crystal structures were solved. Recently, structures of the human β_2-adrenergic receptor[339-341], squid rhodopsin[342,343], turkey β_1-adrenergic receptor[344], bovine opsin[345], bovine opsin bound to the C-terminus of the Gα-subunit[346] and human adenosine A_{2A} receptor[347] have been solved. This sudden abundance of structural information gave new opportunities for computational chemists to create homology models based on the template that best fitted the target structure.

5.3 Homology model of the 5-HT$_{2A}$ receptor

A homology model of 5-HT_{2A} receptor was made by the Biostructural Research Group at FARMA[348]. The model was based on structural information from the human β_2-adrenergic receptor and the G-protein bound opsin. The constraints applied between the ligand and receptor model was based on experimentally determined ligand-receptor interactions which have been identified using site-directed mutagenesis studies[221,222,349-356]. The model was validated by molecular dynamics simulation without constraints and by retrospective ligand screening of more than 9,400 compounds of which 143 were known ligands.

5.4 Binding site analysis and ligand suggestions

The binding site in the homology model was analyzed with the help of molecular interaction fields using the GRID software. The molecular interaction fields are determined using different probes for hydrophobic interactions, halogens, hydrogen-bond donors and acceptors.

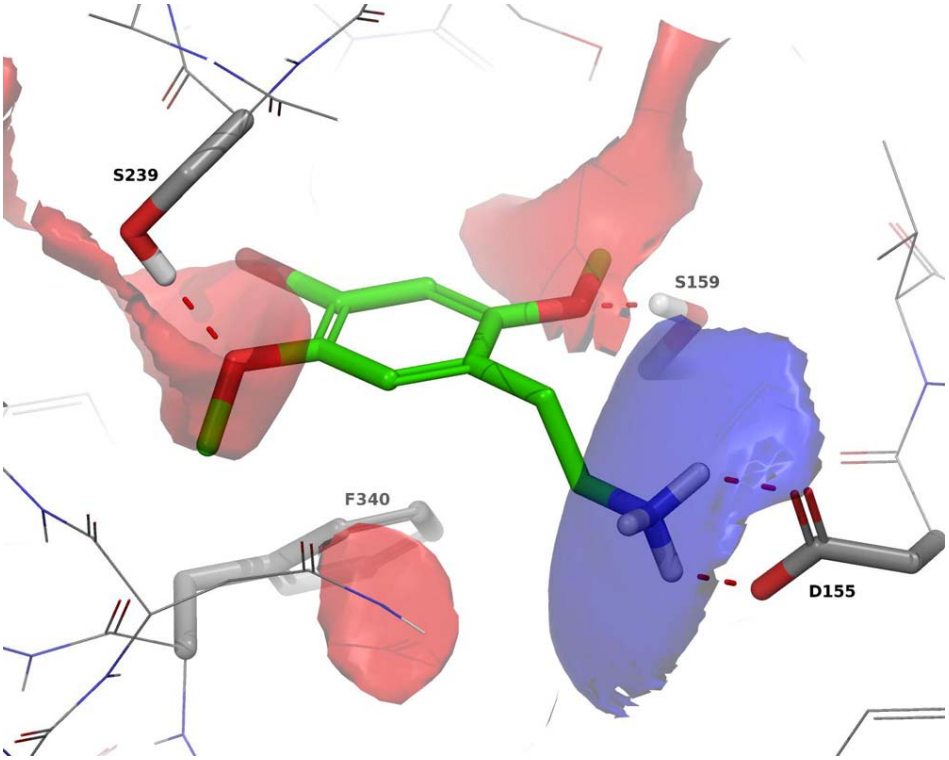

Figure 11: 2C-B (green carbons) docked into the active 5-HT_{2A} model. Hydrogen bonds are shown with red dashed lines. Hydrogen bond donor (red) and acceptor (blue) MIFs from GRID are shown. The MIFs correlate well with the protonated amine (hydrogen bond donor) and two methoxy groups (hydrogen bond acceptors) of the ligand. The interactions between the ligand and amino acid residues are shown with dashed bonds. F340 also contributes with π- π interactions with the aromatic core.

The model showed that there were several accessible parts of the binding site that were hitherto unexplored. Although several interesting structural features were observed only those concerning the *N*-benzyl moiety will be described in the following.

The GRID-analysis of the *N*-benzyl part of the binding pocket showed an extended hydrophobic cavity between TMHs 2, 6 and 7 which was partly occupied by the *N*-benzyl moiety. The cavity seemed to be able to accommodate hydrophobic substituents in the 4' and 5'-positions of the *N*-benzyl ring.

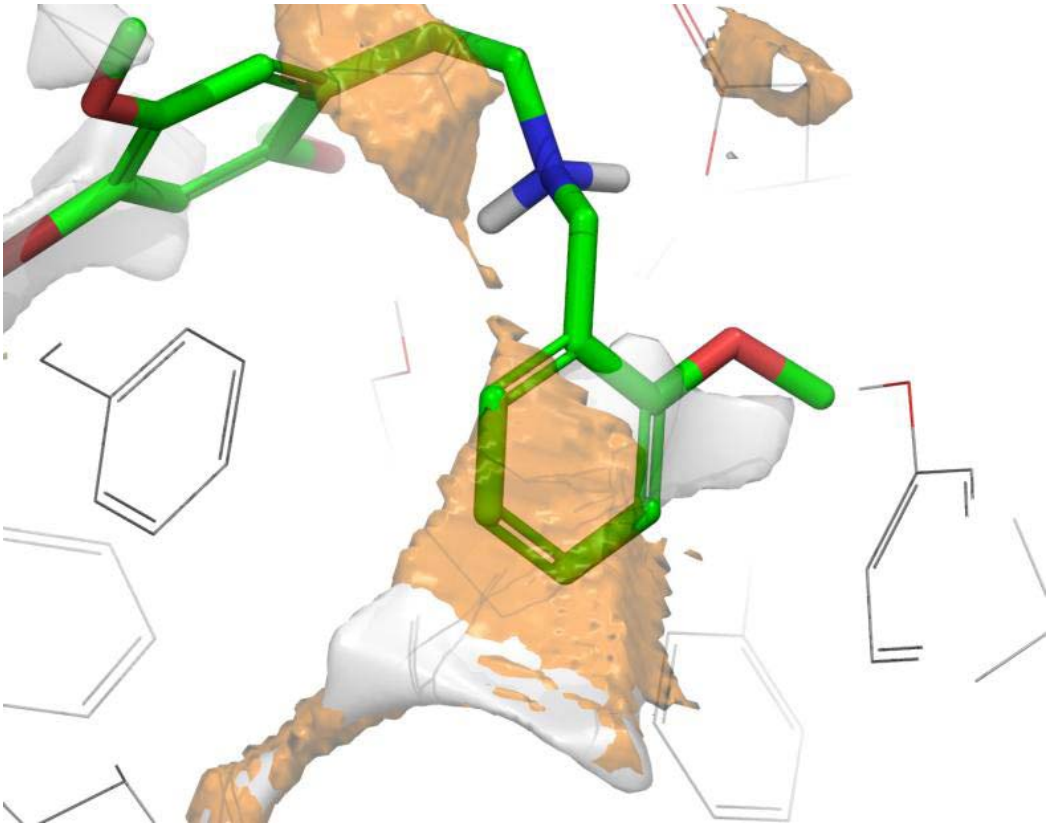

Figure 12: 25Br-NBMeO (green carbons) docked into the active 5-HT$_{2A}$ model. Hydrophobic (orange) and methyl (grey) MIFs from GRID are displayed showing a hydrophobic cavity in the extended binding site between transmembrane helices 2, 6 and 7.

A set of ligands were designed to probe this cavity and docked into the homology model and the best scoring ones were selected for synthesis and biological evaluation. The set consisted of four compounds with alkyl substituents in the 4'-position, two compounds with bromine in the 4' or 5' position and finally a 4',5'-dimethyl compound.

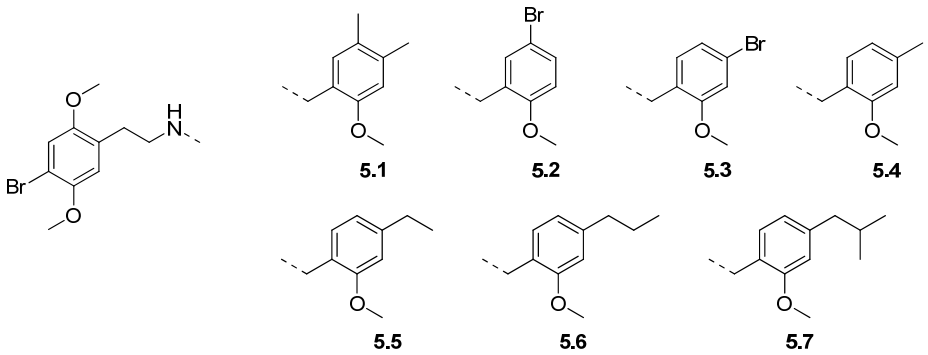

Scheme 57: Ligands designed to explore the extended hydrophobic cavity between TMHs 2, 6 and 7.

Another potentially beneficial interaction was identified in TMH 6 were the backbone carbonyl of M335(6.47) would be able to interact with a hydrogen bond donor off of the 5-position of the aromatic ring and two compounds containing hydroxy-substituted groups in the 5-position were suggested for synthesis.

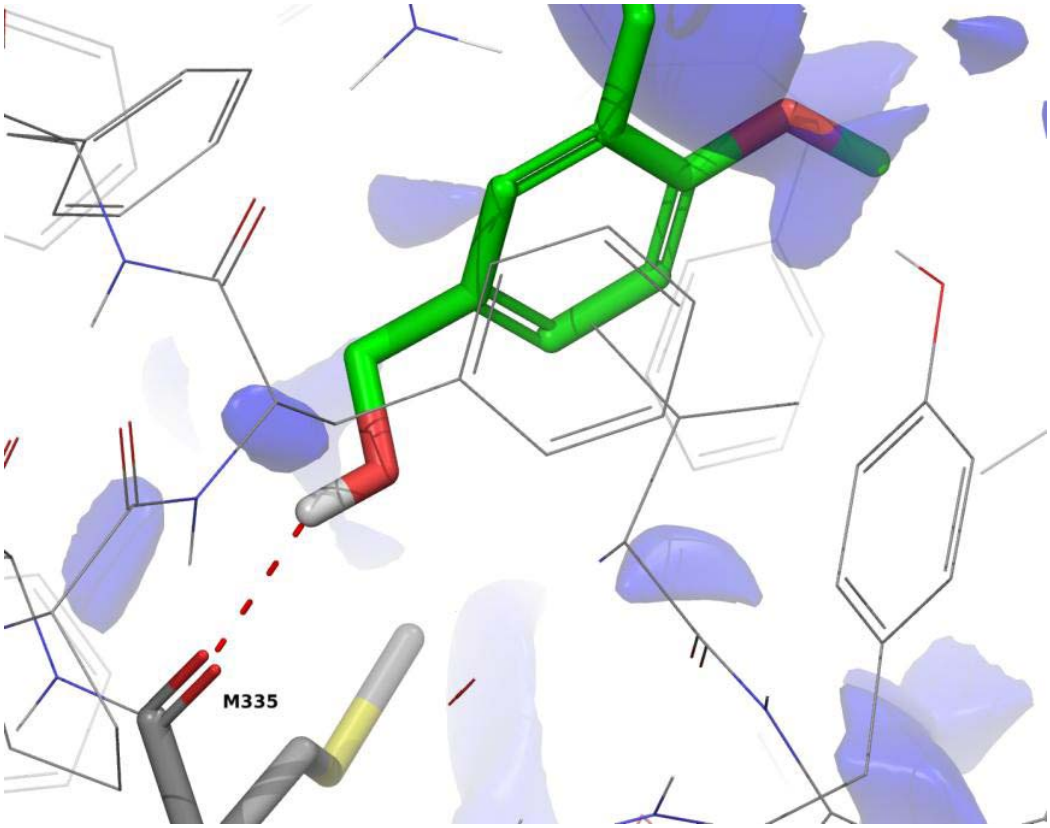

Figure 13: Compound 2C-B (green carbons, Table 18) docked into the active 5-HT_{2A} model. Hydrogen bond donor MIFs from GRID are displayed as a blue surface. The hydroxyl substituent of the ligand interacts with the backbone carbonyl of M334(6.47).

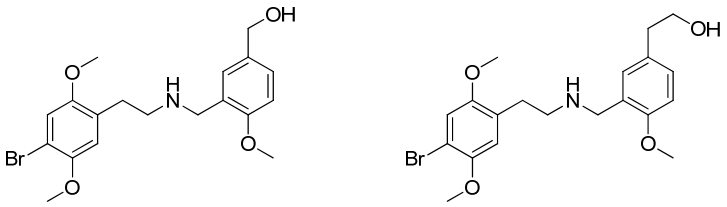

Scheme 58: Ligand suggestions for interaction with M334(6.47)

5.5 Chemical synthesis

The suggested compounds were synthesized according to the same overall strategy as employed in Chapters 2 and 3 where the phenethylamine constitutes the first building block and the appropriate aromatic aldehyde the second with the final synthetic step being a reductive amination reaction between the two building blocks. As in Chapter 3 most of the synthetic work was in the synthesis of the aldehydes which were not commercially available.

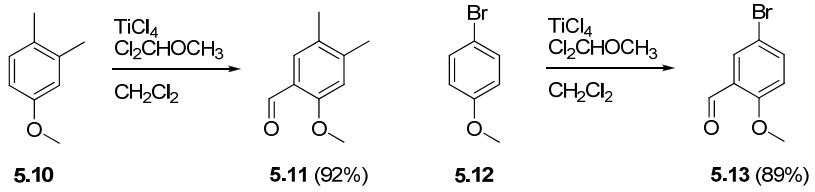

Scheme 59:Synthesis of aldehydes 5.11 and 5.13

5.11 and **5.13** were synthesized using the Rieche-formylation[292] from the corresponding starting materials (**5.10** and **5.12**). Both formylations were completely regioselective and gave good yields. **5.14** was synthesized by methylation of the commercially available 4-bromo-2-hydroxybenzaldehyde (**5.14**).

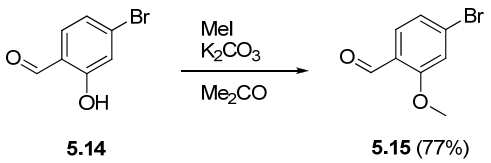

Scheme 60: Synthesis of 5.15

5.19 was synthesized by bis-methylation of 3-methylsalicylic acid (**5.16**) followed by reduction of the ester (**5.17**) with $LiAlH_4$ to the benzyl alcohol (**5.18**) which was oxidized to the benzaldehyde (**5.19**) using TPAP-NMO. Reduction of the ester with DIBAL or Red-Al at -78 °C did not result in the desired aldehyde and gave complete reduction to the benzylic alcohol. The oxidation could probably have been achieved with the significantly cheaper MnO_2 but TPAP performed the oxidation without problems.

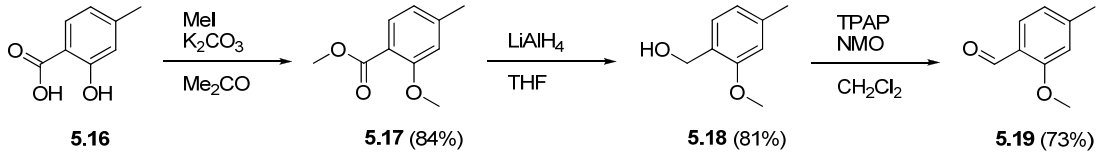

5.16 **5.17** (84%) **5.18** (81%) **5.19** (73%)

Scheme 61: Synthesis of 5.19

We envisioned **5.24**, **5.27** and **5.30** to be made in similar ways. The first strategy was to formylate the corresponding 3-alkylanisoles which would in turn be generated from 3-methoxybenzaldehyde by Wittig-reactions followed by catalytic hydrogenation of the alkene double bonds. The Wittig-reactions were executed in good yields using dimsylsodium as the base. The reduction of the double bonds went smoothly in the case of the ethyl (**5.23**) and propyl (**5.26**) compounds. The isobutyl compound (**5.29**) only reached 8 % conversion after 24 hours at 70 psi, despite literature claims of full conversion in the same time at just 50 psi[357]. The double bond was instead reduced with diimide generated in situ by $TsNHNH_2$ and NaOAc in refluxing THF[358]. And while this reaction also was slow and required replenishment of the reagents it did complete the reduction in just 6 days. Alternatively, a Birch-type reduction might have worked and we also considered hydrogenation with a homogenous catalyst like Wilkinsons catalyst[359].

With the 3-alkylanisoles in hand we tested several formylation procedures. Electrophilic formylation using the Rieche-conditions[292] gave full conversion, but also gave all three possible products although favoring the desired isomer with about 50 % according to GC. The problem was that these three isomers were essentially one spot on TLC, promising a tedious separation by column chromatography.

We hoped to increase the regioselectivity by using the Vilsmeier-Haack formylation[360] with *N*-methylformanilide as the formyl donor in the hope that the larger size of the Vilsmeier reagent would confer some regioselectivity. Unfortunately, this did not work and there was very little conversion even at elevated temperatures and prolonged reaction time. The Vilsmeier reaction did work with DMF as the formyl donor but in mediocre yields and the regioselectivity was not much better than the previously performed Riecke-formylation.

Lithiation of the 3-alkylanisoles with *n*-BuLi or *t*-BuLi followed by DMF quench gave low yields but only two regioisomers. We believe the low yields were due to competing lithiation of the benzylic position although the corresponding aldehyde could not be identified in the reaction mixture.

We instead considered using the previously synthesized methyl benzoate (**5.17**) as starting material with the basic substitution pattern already established. We envisioned a benzylic oxidation followed by a Wittig reaction and subsequent catalytic hydrogenation to install the 4-alkyl substituent. The methyl ester could then be converted to the aldehyde in the usual fashion.

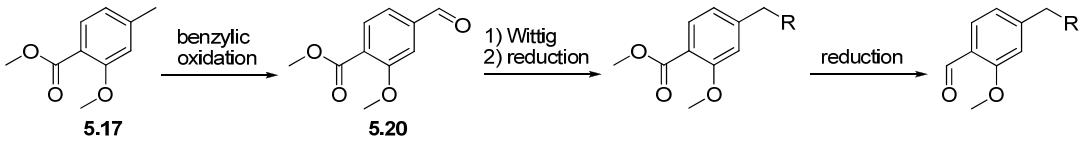

Scheme 62: Alternative synthesis of 4-alkyl-2-methoxybenzaldehydes

We tried several one-step benzylic oxidations to get the aldehyde (**5.20**). IBX has been suggested as a mild reagent to perform benzylic oxidations[361] but in this case there was absolutely no reaction. The chromium based Thiele-oxidation[362] and Etard-reaction[363] did not fare much better although the Etard reaction managed to chlorinate the methyl group. The last alternative was the two-step protocol of radical bromination of the benzylic position followed by hydrolysis, but with our previous experience with this procedure we felt that the advantage of this approach would be compromised.

We decided instead to do a thorough TLC analysis of the product mixture obtained from the previously performed Rieche-formylation, and found that 40% dichloromethane in petroleum ether gave a discernible separation. It was possible to completely separate the compounds in two runs with about 80% of the total isolated in the first run. Consequently, the three aldehydes were prepared by Rieche-formylation and the desired regioisomers were isolated by flash chromatography.

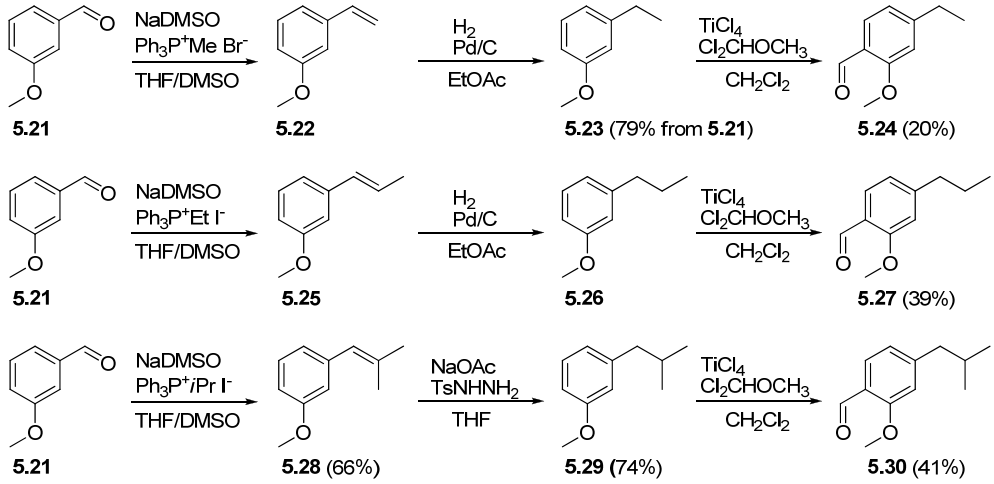

Scheme 63: Synthesis of aldehydes 5.24, 5.27 and 5.30

The aldehydes required for **5.8** and **5.9** were also made in parallel fashion. 4-methoxybenzyl alcohol (**5.31**) was readily available but the homobenzyl alcohol (**5.35**) was made from the corresponding phenylacetic acid (**5.34**) by reduction with $LiAlH_4$. The alcohols were then protected as their trityl ethers (**5.32** and **5.36**). The trityl ethers were then formylated by way of TMEDA-assisted ortholithiation followed by a DMF quench to give the aldehydes (**5.33** and **5.37**). The trityl protecting groups could be removed from the aldehydes in aqueous acid but the resulting aldehydes did not participate in reductive amination with 2C-B.

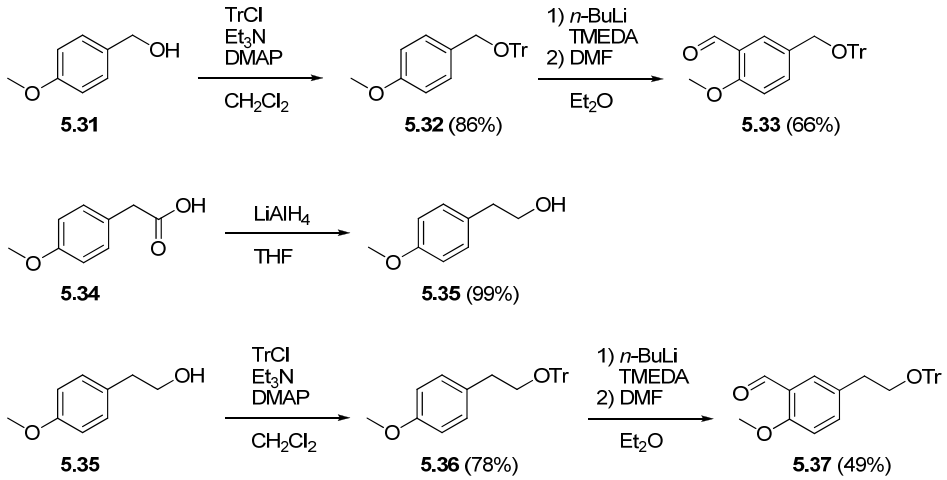

Scheme 64: Synthesis of trityl-protected aldehydes 5.33 and 5.37

5.8 and **5.9** were instead made reductive aminations of the trityl-protected aldehydes (**5.33** and **5.37**) with 2C-B and the resulting secondary amines (**5.38** and **5.39**) were treated with aqueous sulfuric acid in methanol to remove the trityl groups.

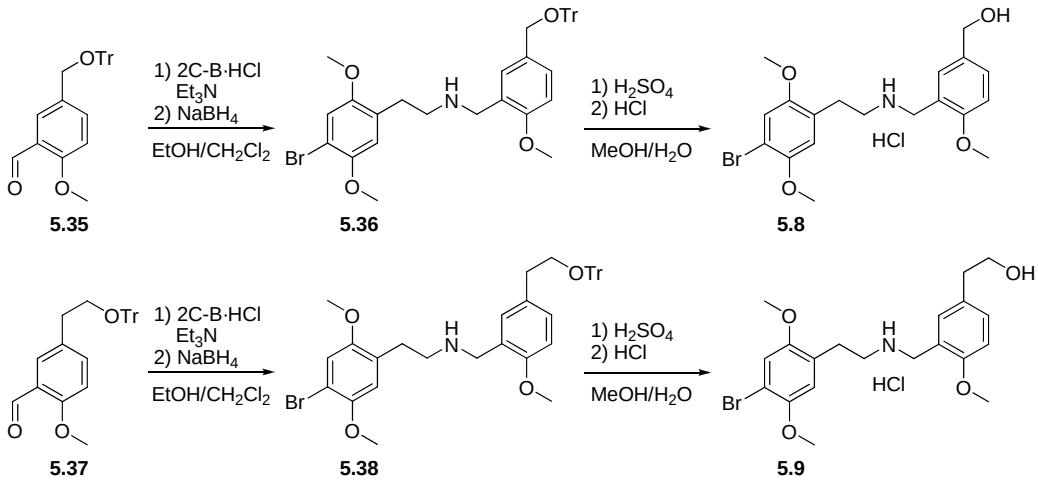

Scheme 65: Synthesis of 5.8 and 5.9

The remaining compounds **5.1-5.7** were completed in the usual fashion by reductive amination of the appropriate aldehydes with 2C-B.

5.6 In vitro biological evaluation

The compounds were submitted for biological evaluation at the PDSP as previously described. Beware that as in Chapter 2 and 3, 5-HT_{2B} affinites are measured against an agonist and therefore not directly comparable to the measured 5-HT_{2A} and 5-HT_{2C} affinities.

Compound	**pK_i h5-HT_{2A} vs. [^{3}H]Ketanserin**	**pK_i h5-HT_{2B} vs. [^{3}H]LSD**	**pK_i r5-HT_{2C} vs. [^{3}H]Mesulergine**
5.1 (2-MeO;4,5-DiMe)	6.81	8.03	7.85
5.2 (2-MeO;5-Br)	7.63	7.72	7.23
5.3 (2-MeO;4-Br)	7.17	7.05	7.28
5.4 (2-MeO;4-Me)	7.46	8.02	7.59
5.5 (2-MeO;4-Et)	7.12	8.16	7.92
5.6 (2-MeO;4-Pr)	6.70	7.55	7.77
5.7 (2-MeO;4-$_i$Bu)	6.86	7.28	7.96
5.8 (2-MeO;5-MeOH)	6.77	6.84	6.67
5.9 (2-MeO;5-EtOH)	7.00	6.61	7.02

Scheme 66: Binding affinities of Group 4-compounds at 5-HT_{2A}, 5-HT_{2B} and 5-HT_{2C} receptors

The radioligand binding results were not exactly encouraging as none of the compounds tested thus far had binding affinities comparable with Group 1-compounds. The proposed hydrophobic pocket around the 4 and 5 positions is almost certainly not solvent-accessible or the binding of these compounds simply disrupt other beneficial interactions. The same explanation can be used for compounds **5.8** and **5.9** since these would have to reach through the hydrophobic pocket to engage the backbone carbonyl in hydrogen bonding. Together these results suggest that the computational model needs further refinement and the data gathered in this study will help in this process so that the next generation of compounds designed this way may perform better.

The selectivity of these compounds were also troubling since they were actually more selective for other subtypes than 5-HT_{2A} with **5.7** actually being a fairly selective and potent 5-HT_{2C} ligand. This further underlines that more work is needed. It would be particularly helpful to have homology models of all three 5-HT_2 receptor subtypes but of course this will require a lot more work on the computational side.

Chapter 6

Synthesis of PET-precursors, radiochemistry and PET-studies

6.1 Aim

To synthesize precursors for 5-HT_{2A} agonist radiotracers that can be radiolabeled and evaluated in PET experiments. The results of the radiosyntheses and PET experiments are discussed in Paper I and Paper II, and this chapter will focus on the chemistry and summarize the results of the PET experiments

6.2 Choice of radiotracers and precursor design

In the early phase of this project, none of our own ligands had yet been subjected to *in vitro* pharmacological evaluation. Therefore our first choice of candidate for *in vivo* PET-evaluation would be chosen from the pool of 5-HT_{2A} agonists already known from the literature. With the recent disclosure of the *N*-benzylphenethylamines it was obvious to choose one of these as the first tracer candidate.

Of the compounds published by Braden et al.[221], four seemed particularly interesting. These compounds were included in the Group 1-compounds as **2.1**, **2.2**, **2.3** and **2.4** All of these compounds possessed sub-nanomolar affinity at the human 5-HT_{2A} receptor and were potent agonists. Most importantly they all have sites that are readily modified for radiochemical labeling with electrophilic [^{11}C]-labeling reagents such as [^{11}C]MeI or [^{11}C]MeOTf.

We chose three compounds from the Group 1-compounds which were simple analogues of **2.1** but with bromine (**2.5**), chlorine (**2.9**) and trifluoromethyl (**2.41**) groups in the 4-position instead of iodine. These were complemented by 2C-I (**1.39**) and 2C-BFly-NBOMe (**6.21**) which has been mentioned previously in two PhD-theses[218,222].

A general feature of all the candidate compounds is that they possess an amine which has to be protected during the radiochemical labeling and then deprotected before the radiotracer is formulated and injected into a test subject. This deprotection step has to be done as fast as possible in order to retain enough radioactivity before administration. The Boc protection group was chosen here because it can be removed swiftly with TFA, and are stable under the conditions employed in the radiolabeling procedure. For the primary amine in 2C-I (**1.39**) we decided to use the phthalimide protecting group instead of the Boc group.

For compounds **2.1**, **2.5**, **2.9**, **2.41** and **6.21** the 2'-methoxy on the *N*-benzyl moiety was the optimal choice for the labeling position and the precursors (**6.1, 6.7, 6.8, 6.9** and **6.6**) were designed accordingly.

2.2, **2.3** and **2.4** did not possess a methoxy group in the 2'-position and instead the precursors (**6.3**-**6.5**) were designed for labeling in the 2-position of the phenethylamine core. We included a second precursor (**6.2**) for **2.1** for labeling in the 2-position to compare with the 2'-labeled **6.1**.

We also decided to label 2C-I (**1.39**) in the 2-position and use the phthalimide for protection of the primary amine.

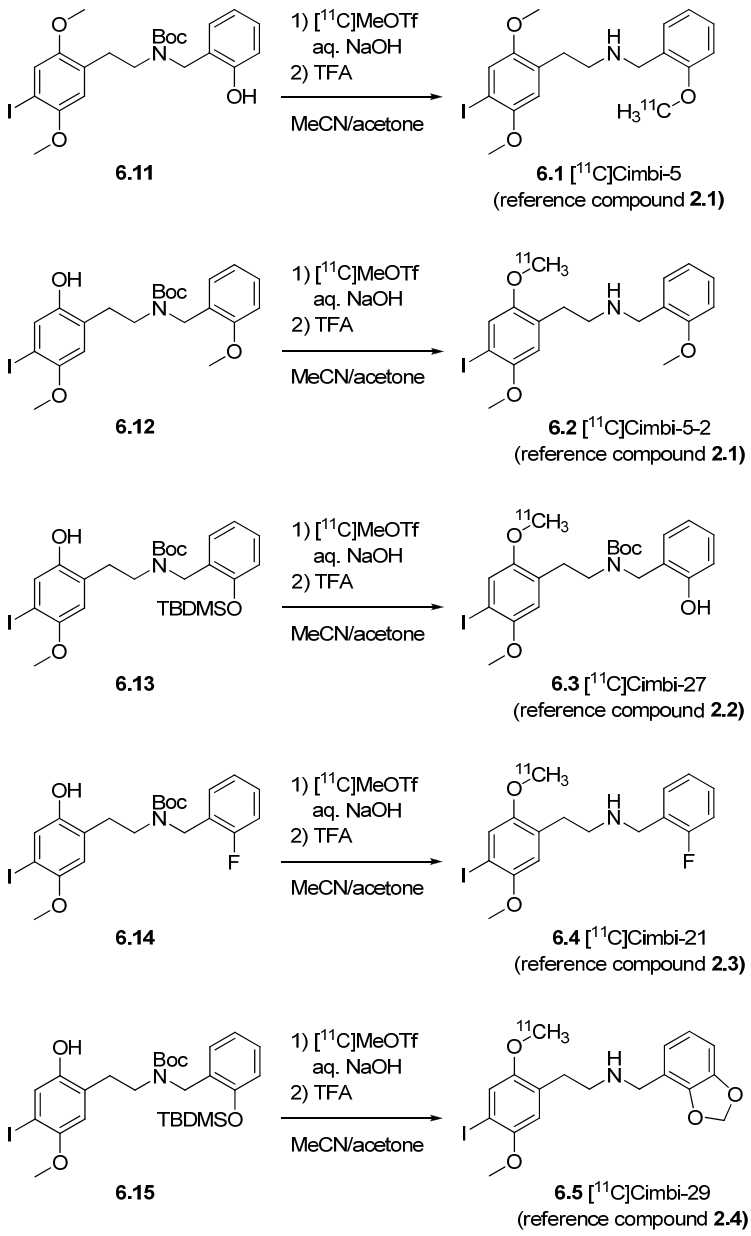

Scheme 67: Radiolabeling of precursors (6.11-6.15) to give radiotracers (6.1-6.5)

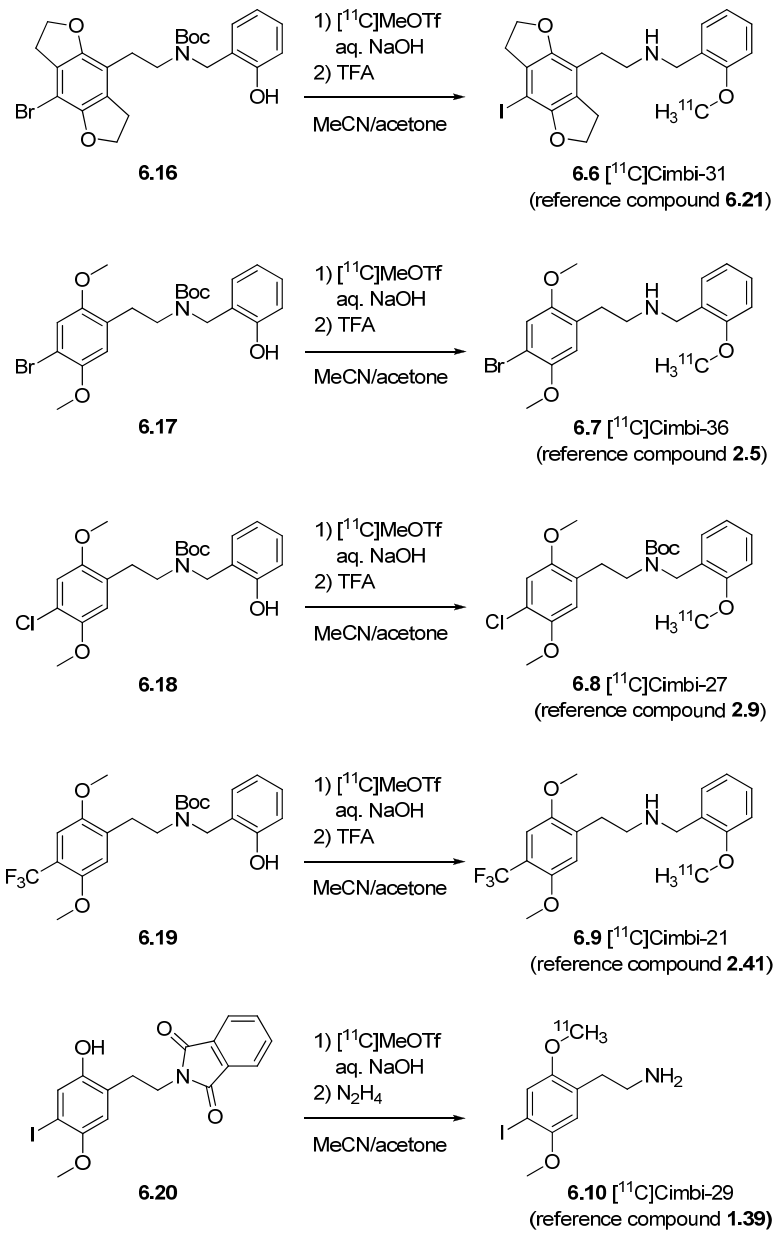

Scheme 68: Radiolabeling of precursors (6.16-620) to give radiotracers (6.6-6.10)

6.3 Synthesis of PET-precursors

6.3.1 Synthesis of precursor 6.11 for radiotracer 6.1 ([^{11}C]Cimbi-5)

The precursor **6.11** was designed to be radiolabeled on the *N*-(2-methoxy)benzyl moiety as this was the most readily synthesized precursor possible. The desired 2-*O*-demethylated, *N*-Boc-protected precursor was synthesized in three steps from 2C-I (**1.39**).

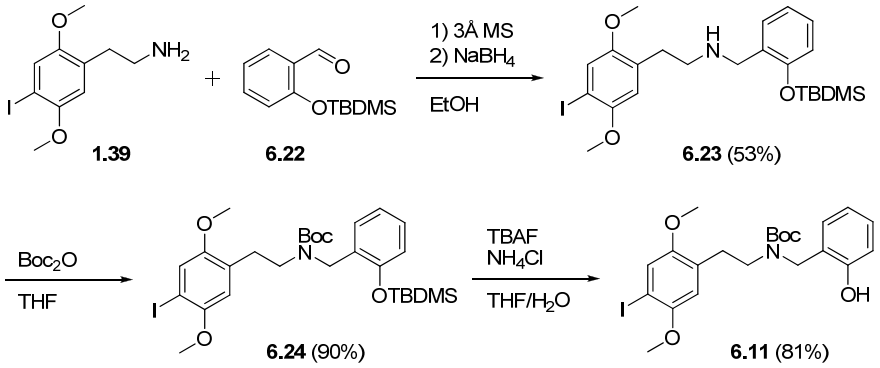

Figure 14: Synthesis of the precursor 6.11

Reductive amination with 2C-I and TBDMS-protected 2-hydroxybenzaldehyde (**6.22**)[364] gave the secondary amine (**6.23**). Boc-protection of the secondary amine followed by TBAF-assisted cleavage of the TBDMS-group gave the precursor (**6.11**).

6.3.2 Synthesis of precursors 6.12-6.15

These four precursors were all *N*-benzylphenethylamines designed to be labeled on the 2-position of the phenethylamine core. This required the synthesis of a 2-demethylated analogue of 2C-I which could be subjected to reductive amination with the respective aldehydes. The 2-desmethyl-2C-I was synthesized in 5 steps from 1,4-dimethoxybenzene.

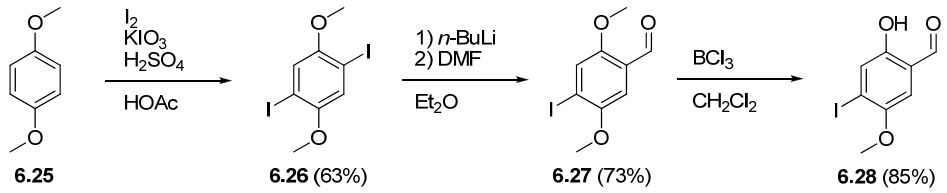

Scheme 69: Synthesis of salicylaldehyde (6.28)

Aromatic iodination of 1,4-dimethoxybenzene (**6.25**) gave the diiodoarene (**6.26**). Halogen-lithium exchange followed by a quench with DMF produced the aldehyde (**6.27**) and carbonyl-assisted demethylation of the 2-methoxy group with BCl_3 gave the salicylaldehyde (**6.28**).

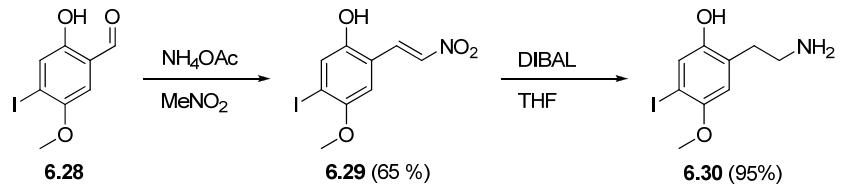

Scheme 70: Henry condensation and reduction to give 2-desmethyl-2C-I (6.30)

Elaboration of the side-chain was carried out in the usual manner with the Henry-condensation to give the nitrostyrene (**6.29**). Reduction to the phenethylamine (**6.30**), was achieved using DIBAL[265] which, in contrast to $LiAlH_4$, did not reduce the aryl iodide. The phenethylamine (**6.30**) was subjected to reductive aminations with the respective aldehydes (**6.31**-**6.34**) to produce the secondary amines (**6.35**-**6.39**). These were Boc-protected selectively on the basic nitrogen using Boc_2O under neutral conditions to give the precursors (**6.12-6.15**).

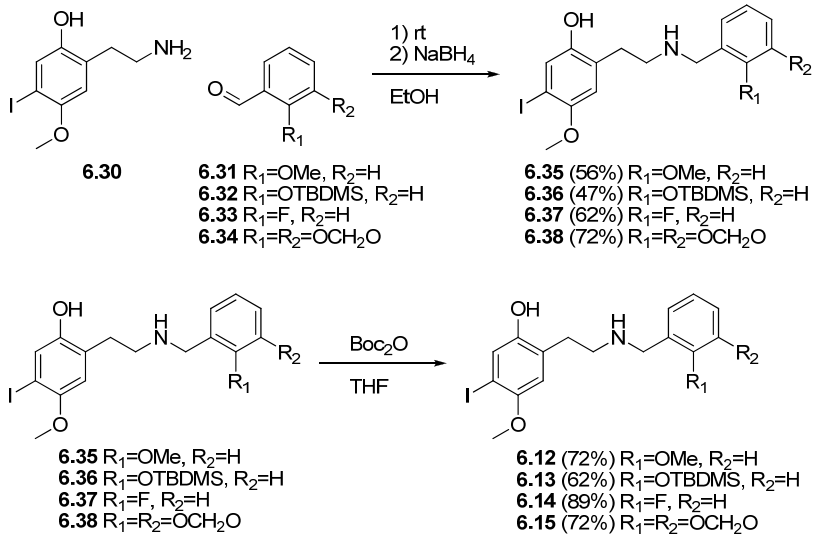

Scheme 71: Synthesis of precursors 6.12-615

6.3.3 Synthesis of precursors 6.16-6.19

The precursors **6.16**-**6.19** could be made in the same way as **6.11** but we found that using the TBDMS-protected aldehyde was unnecessary since the boc-protection was selective for the secondary amine as long no base was introduced. The secondary amines (**6.41**-**6.44**) were already synthesized in Chapter 2 as their hydrochlorides, but in this case the freebased amines were needed for the boc-protection. 2C-B-Fly (**6.39**) was synthesized according to a previously published procedure[211].

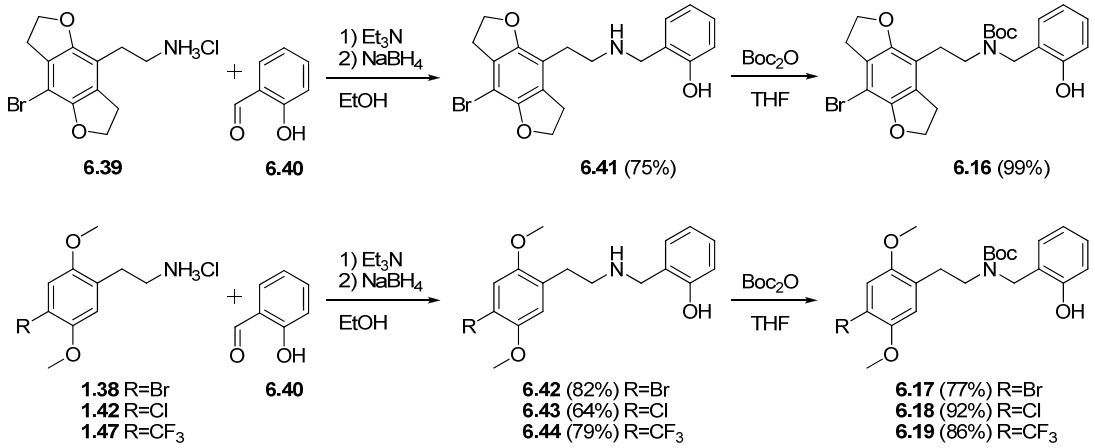

Scheme 72: Synthesis of precursors 6.16-6.19

6.3.4 Synthesis of precursor 6.20

The synthesis of **6.20** was accomplished by phthalimide protection of the previously described phenethylamine **6.45**[365] followed by aromatic iodination with ICl and finally selective deprotection of the isopropyl ether with BCl_3.

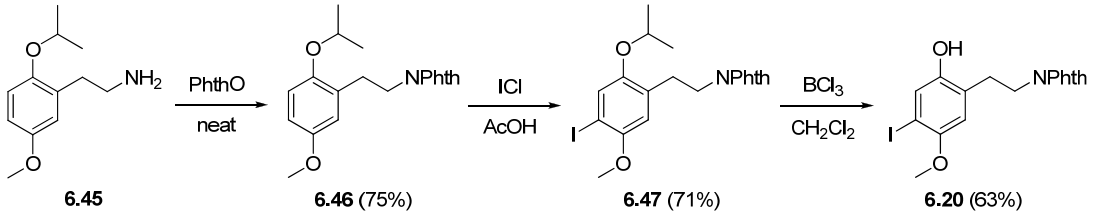

6.45 **6.46** (75%) **6.47** (71%) **6.20** (63%)

Scheme 73: Synthesis of precursor 6.20

6.4 Radiosynthesis of ^{11}C-labeled phenethylamines

The precursors were labeled with [^{11}C]MeOTf and deprotected as outlined in Schemes 67 and 68. The details of the radiosyntheses can be found in the experimental section or in Paper I and II.

6.5 PET studies

PET studies in pigs performed with the 10 radioligands (**6.1**-**6.10**) are described in detail in paper I and II. This section will present the most important data and briefly discuss the findings.

6.5.1 Radiotracer 6.1

Tracer **6.1** is the subject of Paper I and the results confirmed that **6.1** is a high affinity agonist at the 5-HT_{2A} receptor. Ex vivo rat studies showed that **6.1** entered the brain and showed specific binding which was blocked by ketanserin treatment. PET studies in pigs showed that **6.1** binds selectively to areas with high 5-HT_{2A} receptor density in the brain i.e. high binding in the cortex and low binding in the cerebellum[255]. **6.1** had a cortical binding potential of 0.46±0.12 and a target to background ratio similar to the widely used 5-HT_{2A} antagonist tracer [^{18}F]altanserin. Treatment with ketanserin reduced the cortical binding to cerebellar levels, further indicating that **6.1** binds selectively to 5-HT_{2A} receptors in the pig brain.

6.1 is a promising PET tracer for labeling and quantification of 5-HT_{2A} receptors in the human brain. Furthermore **6.1** is the first selective 5-HT_{2A} receptor to show promising results in animal studies.

The ultimate goal of a 5-HT_{2A} agonist radiotracer is to be able to measure changes in endogenous 5-HT levels. Since these are very small it is crucial to have a radioligand with a high target-to-background ratio. **6.1** was shown to be a good candidate but more efforts should be expended to identify the optimal candidate before progressing with further studies.

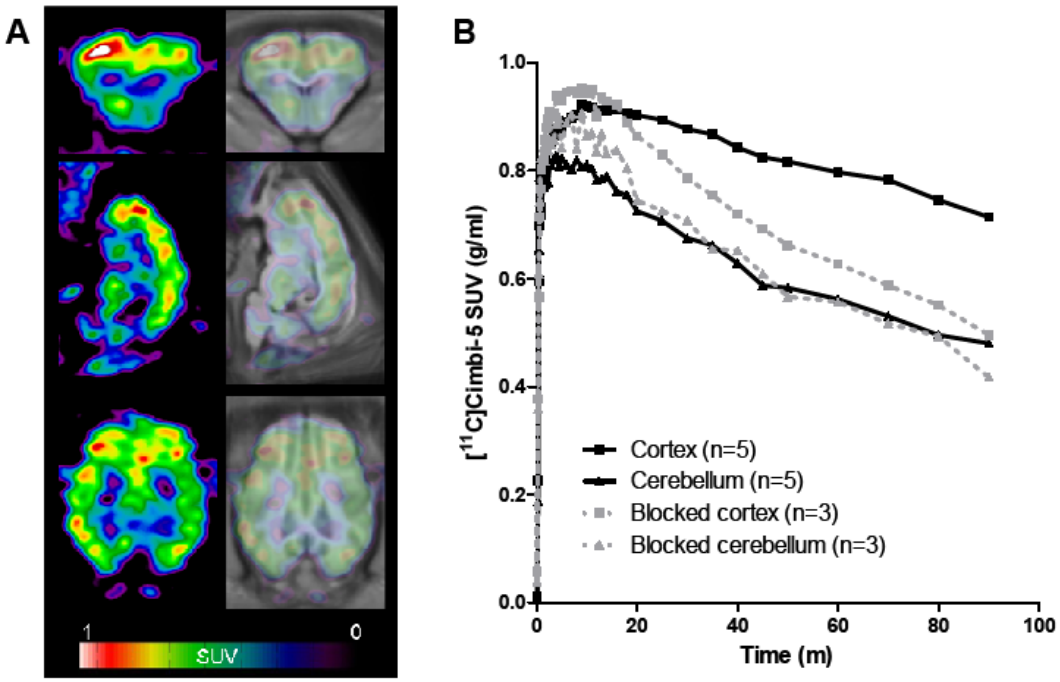

Scheme 74: A| Color coded representative coronal (top), sagittal (middle), and horizontal (bottom) standardized uptake value (SUV) PET images summed from 0-90 min scanning showing distribution of 6.1 in the pig brain. Left column show filtered PET, while right column show the same PET images aligned and overlaid on the standard pig brain after co-registration and transformation. B| Regional time-activity curves of 6.1 in the pig brain at baseline (black, solid line) or following i.v. ketanserin (3 mg/kg bolus, 1 mg/kg/h infusion) blockade (gray, dotted line). Number of pigs s indicated by the legends. Adapted from Ettrup 2010[366].

6.5.2 Radiotracers 6.2-6.10

Of the nine tracers presented in Paper II, eight were close analogues of **6.1** while the last (**6.10**) was a simple phenethylamine. The tracer properties of the first eight compounds were expected to be reasonably similar. They had all high affinity for 5-HT_{2A} receptors in vitro and their LogD-values did not differ substantially.

PET Tracer	ID / MBq	A_s / GBq/µmol	cLogD	Plasma free fraction	2TC distribution volumes		SRTM
					Cortex	Cerebellum	Cortical BP_{ND}
6.2	682	122.7	3.33	0.4	10.93	6.88	0.32
6.3	434	21.6	2.94	0.7	16.79	11.00	0.45
6.4	627	9.6	3.86	0.8	7.24	5.73	0.17
6.5	710	45.2	3.35	0.4	5.15	3.57	0.32
6.6	390	36.3	2.87	1.0	dnf	dnf	0.43
6.7	506	210.4	3.42	1.1	13.42	6.76	0.82
6.8	578	445.5	3.49	0.7	4.51	2.82	0.49
6.9	589	455.6	4.40	1.2	13.85	6.19	0.60
6.10	462	231.2	-0.24	6.5	n.d.	n.d.	0.17

Table 9: PET tracers in the pig brain. Injection data, cLogD-values, free fraction, and in vivo biodistribution as calculated by kinetic modeling. cLogD calculated with CSLogD (ChemSilico). ID; injected dose. A_s; specific activity. SRTM; simplified reference tissue model. BP_{ND}; non-dispalceable binding potential dnf; did not fit kinetic model. n.d.; not determined. Adapted from Paper II.

Nevertheless, the tracer properties of the compounds were quite distinct. **6.4** And **6.10** had the lowest binding potentials, which can perhaps be attributed to the slightly lower binding affinity of these compounds. Both compounds also had poor separation between the cortex and cerebellum time-activity curves (Figure 15). In addition, **6.10** had a negative cLogD-value which puts it well outside the 'ideal tracer' definition. **6.2**, **6.3**, **6.5**, **6.6** and **6.8** had binding potentials slightly lower or equal to that of **6.1**. With the exception of the isotopomer **6.2** they all showed slightly improved kinetics but not enough to warrant further research. **6.7** and **6.9** both had substantially better binding potentials and higher target-to-background ratios than **6.1**. Furthermore, **6.7** showed improved kinetics with a steady decline of the activity over the 90-minute experiments which is a clear indication of reversible binding.

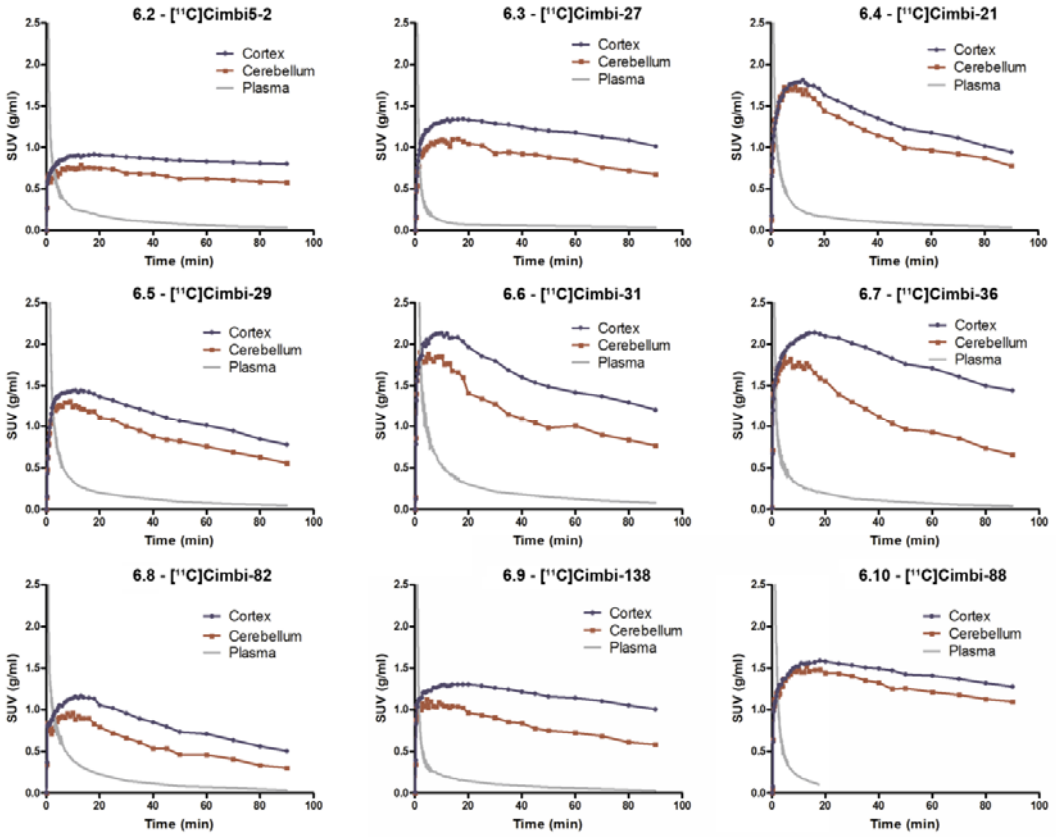

Figure 15: Regional time activity curves for cortex (blue) and cerebellum (red) of ^{11}C-labeled phenethylamines in the pig brain. Standardized uptake values (SUV) normalized to injected dose per body weight is shown. Adapted from Paper II

To show that binding of **6.7** was selective for 5-HT_{2A}, a blocking study was conducted with ketanserin. The cortical BP_{ND} dropped from 0.70 to 0.26 indicating that binding is selective for 5-HT_{2A} receptors in the pig brain (Figure 16). **6.7** is currently being tested in monkeys at the Karolinska Institute in Stockholm, Sweden and is the prime tracer candidate for further studies

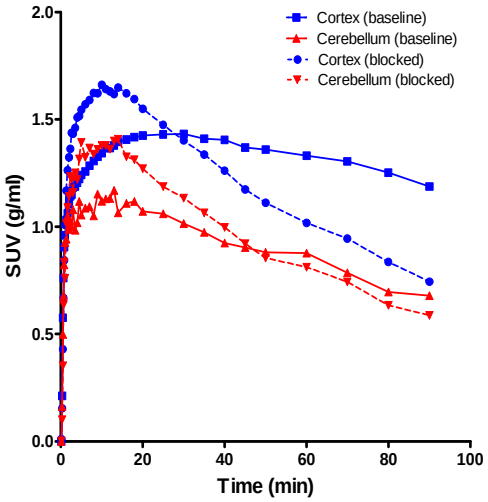

Figure 16: Cortical and cerebellar time-activity curves for 6.7 in pig brain at baseline (blue) and following pre-treatment with i.v. with ketanserin 10 mg/kg (red). Standardized uptake values (SUV) normalized to injected dose per body weight is shown. Adapted from Paper II.

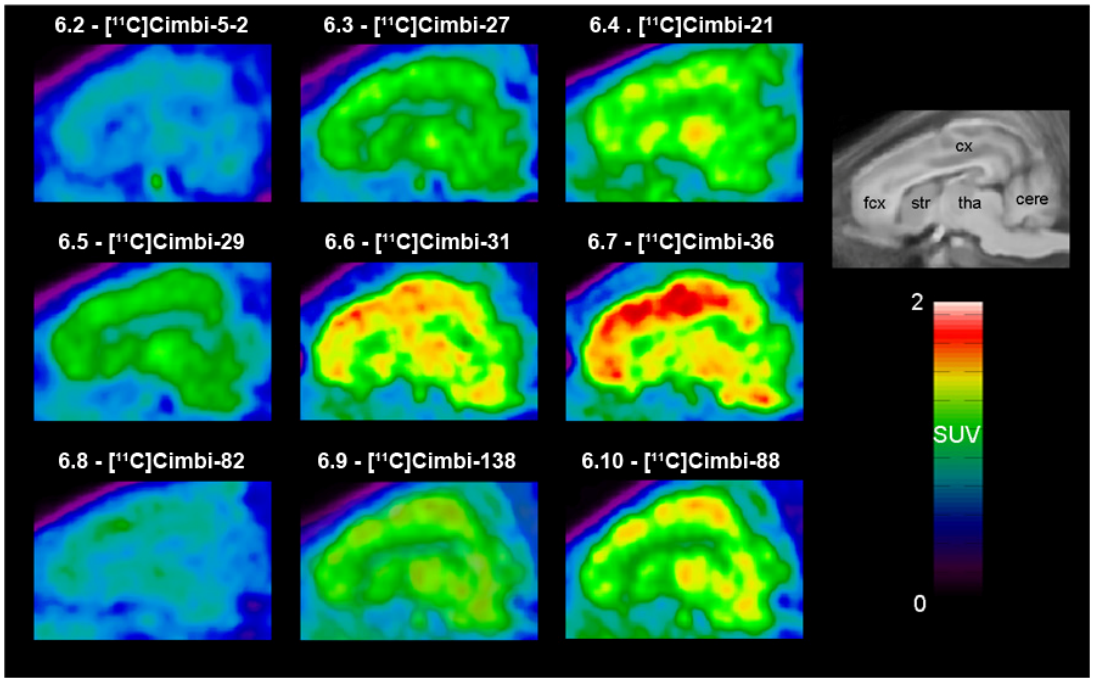

Figure 17: Averaged sagittal images from 10-90 minutes

Chapter 7

Conclusions and perspectives

The overall aims in this thesis have been the design and synthesis of 5-HT_{2A} agonists for PET-imaging. To accomplish this goal we chose to work with a new class of 5-HT_{2A} agonists, the *N*-benzylphenethylamines, which have great potential for structural modifications.

A focused library of compounds designed with modifications of the 4-substituent and minor modifications of the *N*-benzyl moiety (Group 1-compounds) were synthesized from simple starting materials using reductive amination to assemble the compounds. The vast majority of the Group 1-compounds were high-affinity ligands at the 5-HT_{2A} receptor. The compounds showed moderate to good selectivity for the 5-HT_{2A} receptor versus the 5-HT_{2C} receptor and in general compounds having a 2,3-methylenedioxy *N*-benzyl substituent had the best selectivity. The 4-cyano-2'-hydroxy substituted compound **2.46** showed a 100-fold selectivity for 5-HT_{2A} versus 5-HT_{2C} and is the first high-affinity 5-HT_{2A} selective phenethylamine to be reported. However, the intrinsic activity of this compound has yet to be determined.

The *N*-benzyl moiety was further explored by compounds containing various substituents and heterocyclic motifs in the *N*-benzyl moiety (Group 2-compounds). Some of these compounds were structurally more complex and required extensive synthetic work to access the required aldehydes for reductive amination. Not all of the compounds have yet been evaluated biologically but the preliminary results suggest that substituents in the 2' and 3'-position on the *N*-benzyl group is well tolerated but even minor differences have strong impact on affinity and selectivity.

Another set of compounds was designed as conformationally restricted *N*-benzylphenethylamines (Group 3-compounds) and the primary objective was to determine the optimum binding conformation these compounds adopt inside the receptor. The compounds were synthesized by a variety of methods and the syntheses of **4.3**, **4.5** and **4.6** have been described while the remainder were synthesized by various members of the Nichols-group at Purdue University. The only compound which distinguished itself was (*trans*-**6.7**) whose synthesis will be described elsewhere. (*trans*-**6.7**) had significantly higher affinity than the other compounds tested and also showed an unprecedented 115-fold selectivity for 5-HT_{2A} vs. 5-HT_{2C} indicating that its constrained conformation is ideal for binding at the 5-HT_{2A} receptor.

The final set of compounds (Group 4-compounds) was designed using a homology model of the 5-HT_{2A} receptor to explore novel ligand-receptor interactions. The compounds were synthesized in the same manner as the Group 1- and 2-compounds with the bulk of the synthetic work lying in the synthesis of the substituted benzaldehydes. The preliminary biological results showed significant decreases in binding affinity and poor selectivity of these compounds which suggest that further refinement of the homology model is needed.

Ten compounds were selected for in vivo PET-studies in pigs. The syntheses of the required precursors **6.1**-**6.10** were accomplished and the compounds were radiolabeled and subjected to in vivo PET-experiments in pigs. The results showed that the first candidate **6.1** ([^{11}C]Cimbi-5) entered the brain with a BP_{ND} of 0.47 and target-to-background ratio equal to that of

[^{18}F]altanserin. PET tracer **6.7** ([^{11}C]Cimbi-36) showed improved BP_{ND} and better target-to-background ratio as well as improved kinetics over **6.1**. **6.7** is now the prime candidate for evaluation as a PET tracer in humans.

Future work on this project should focus on the biological evaluation of the remaining compounds. Furthermore, most of the compounds in this study have yet to be assayed for their intrinsic activity. The functional selectivity of these compounds is also an area which has not yet been studied.

With the data at hand it will probably be difficult to design a 5-HT_{2A} agonist PET-tracer with properties superior to those of **6.7**. It would however be interesting to design and evaluate an ^{18}F-labeled agonist tracer for the 5-HT_{2A} receptor. Such a compound could potentially have superior properties compared to **6.7** but a compound which is amenable to fluorination and retains a binding profile similar to **6.7** will have to be discovered first.

Chapter 8 – Experimental

8.1 Materials and apparatus

THF was distilled from sodium/benzophenone ketyl. Et_2O was dried over sodium. All other dry solvents were dried over 3Å molecular sieves. Flash chromatography was performed on silica gel 60 (35-70 μm) according to the procedure by Still et al.[367] Radial chromatography was performed on a Harrison Research Chromatotron® 8924. Melting points were determined using a SRS Optimelt apparatus. NMR spectra were recorded on Varian Mercury 300 BB, Varian Gemini 2000 or Bruker ARX300 spectrometers and processed using MestReNova software. TMS was used as internal reference for ^{1}H-NMR spectra recorded in $CDCl_3$. Solvent residual peaks[368] were used as internal reference for all ^{13}C-NMR spectra and for ^{1}H-NMR spectra recorded in DMSO-d_6, CD_3OD and C_6D_6. GC-MS were performed on a Shimadzu

TLC was performed on Merck aluminium sheets precoated with silica F^{254}. Compounds were visualized by UV or by heating after dipping in Cemol (6.25 g $NH_4Mo_2O_7$ and 2.5 g $Ce(SO_4)_2$ in 250 mL 10% H_2SO_4), anisaldehyde (9.2 mL *p*-Anisaldehyde, 3.75 mL AcOH and 12.5 mL H_2SO_4 in 338 mL EtOH) or ninhydrin (1.5 g ninhydrin, 100 mL *n*-butanol, 3.0 mL AcOH)

Short-path distillation was performed on a Buchi KugelRohr-apparatus. The stated temperature intervals were measured by the internal probe and are not equal to the actual boiling point of the fraction.

8.2 General procedures

General procedure A - for the synthesis of secondary amine hydrochlorides

To a suspension of the amine hydrochloride (or hydrobromide) (1.0 mmol) and aldehyde (1.1 mmol) in EtOH (10 mL) was added Et_3N (1.0 mmol) and the reaction was stirred until formation of the imine was complete according to TLC or GC (30 mins to 3 hrs). $NaBH_4$ (2.0 mmol) was added to the reaction which was stirred for another 30 minutes. The reaction mixture was evaporated under reduced pressure and redissolved in EtOAc/H_2O (30 mL, 1:1). The organic layer was isolated and the aqueous layer was extracted with EtOAc (2 × 15 mL). The combined organic extracts were dried (Na_2SO_4), filtered and evaporated under reduced pressure. The residue was purified by radial chromatography (CH_2Cl_2/MeOH/NH_3 98:2:0.04). The purified free base was dissolved in EtOH (2 mL) and there was added ethanolic HCl (1M, 2 mL) and the solution was diluted with Et_2O until crystals formed. The crystals were collected by filtration and dried under reduced pressure.

General procedure B - for the synthesis of secondary amines.

To a suspension of the amine hydrochloride (or hydrobromide) (1.0 mmol) and aldehyde (1.1 mmol) in EtOH (10 mL) was added Et_3N (1.0 mmol) and the reaction was stirred until formation of the imine was complete according to TLC or GC (30 mins to 3 hrs). $NaBH_4$ (2.0 mmol) was added to the reaction which was stirred for another 30 minutes. The reaction mixture was evaporated under reduced pressure and redissolved in EtOAc/H_2O (30 mL, 1:1). The organic layer was isolated and the aqueous layer was extracted with EtOAc (2 × 15 mL). The combined organic extracts were dried (Na_2SO_4), filtered and evaporated under reduced pressure. The residue was purified by radial chromatography (CH_2Cl_2/MeOH/NH_3 98:2:0.04).

General procedure C - for Boc-protection of secondary amines

A solution of the secondary amine (1 equiv.) and Boc_2O (1.1 equiv) in THF (10 mL/mmol) was stirred until TLC showed full conversion. The reaction was concentrated under reduced pressure and purified by flash chromatography or radial chromatography.

8.2 Experimental – Chapter 2

1,4-dimethoxy-2-(trifluoromethyl)benzene (2.52)

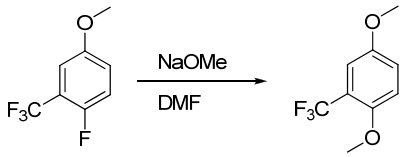

2.53 **2.52**

To a solution of NaOMe (100 mmol) in dry DMF (100 mL) was added a solution of 1-fluoro-4-methoxy-2-(trifluoromethyl)benzene (**2.53**, 9.71 g, 50 mmol) in dry DMF (150 mL). The reaction was stirred at 100 °C for 2 hrs and then concentrated to approx. 100 mL on the rotavap. The concentrate was poured into water (300 mL) and extracted with Et_2O (3 × 100 mL). The the combined organic layers were washed with water (100 mL), dried ($MgSO_4$) and evaporated to give the crude product as a yellow oil. The product was purified by short-path vacuum-distillation. The fraction collected at 75-85 °C (0.5 mmHg) contained the product, **2.52 (**9.69 g, 94%) which was obtained as a colorless oil. ^{1}H NMR (300 Mhz, $CDCl_3$) δ 7.09 (d, *J* = 3.0 Hz, 1H), 6.99 (dd, *J* = 9.0, 3.0 Hz, 1H), 6.91 (d, *J* = 9.0 Hz, 1H), 3.84 (s, 3H), 3.77 (s, 3H). ^{13}C NMR (75 MHz, $CDCl_3$) δ 152.9, 151.5 (q, $^3J_{CF}$ = 1.8 Hz), 123.5 (q, $^1J_{CF}$ = 272.0 Hz), 119.4 (q, $^2J_{CF}$ = 30.9 Hz), 118.1 (q, $^4J_{CF}$ = 1.0 Hz), 113.6, 112.9 (q, $^3J_{CF}$ = 5.4 Hz), 56.7, 56.0

2,5-dimethoxy-4-(trifluoromethyl)benzaldehyde (2.54)

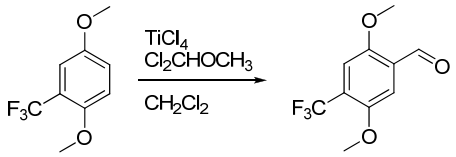

2.52 **2.54**

Dichloromethyl methyl ether (6.37 mL, 72 mmol) was added to a cooled (-78 °C) solution of **2.52** (4.94 g, 24 mmol) and $TiCl_4$ (6.58 mL, 60 mmol) in dry CH_2Cl_2 (80 mL). The reaction was allowed to slowly reach 0 °C and then poured onto ice (200 mL). After the ice had melted, the organic layer was isolated and washed with saturated aqueous $NaHCO_3$ (100 mL), dried ($MgSO_4$) and evaporated to give an off-white solid which was recrystallized from heptanes to give the title compound, **2.54** (4.72 g, 84%) as white crystals. mp. 137-140 °C. ^{1}H NMR (300 MHz, $CDCl_3$) δ 10.45 (s, 1H), 7.42 (s, 1H), 7.21 (s, 1H), 3.94 (s, 3H), 3.90 (s, 1H). ^{13}C NMR (75 MHz, $CDCl_3$) δ 188.7, 155.3, 151.33 (q, $^3J_{CF}$ = 1.4 Hz), 127.3, 124.8 (q, $^2J_{CF}$ = 31.1 Hz), 122.8 (q, $^1J_{CF}$ = 273.0 Hz), 111.5 (q, $^3J_{CF}$ = 5.4 Hz), 110.9, 56.7, 56.5.

(E)-1,4-dimethoxy-2-(2-nitrovinyl)-5-(trifluoromethyl)benzene (2.55)

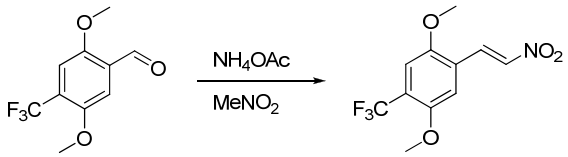

2.54 (4.995 g, 21.33 mmol) was dissolved in $MeNO_2$ (35 mL) and there was added NH_4OAc (0.164 g, 2.13 mmol). The reaction was heated to reflux and the progress was monitored by TLC. After 4 hours there was full conversion and the excess $MeNO_2$ was removed under reduced pressure. The residue was recrystallized from *i*-PrOH to give the title compound, **2.55** (3.66 g, 62%) as yellow needles. mp. 177-179 °C. ^{1}H NMR (300 Mhz, DMSO-d_6) δ 8.07 (d, J = 13.6 Hz, 1H), 7.87 (d, J = 13.6 Hz, 1H), 7.15 (s, 1H), 7.04 (s, 1H), 3.95 (s, 3H), 3.90 (s, 3H). ^{13}C NMR (75 MHz, DMSO-d_6) δ 152.8, 151.2 (q, $^3J_{CF}$ = 1.9 Hz), 140.1, 133.8, 122.9, (q, $^1J_{CF}$ = 272.6 Hz), 122.8 (q, $^4J_{CF}$ = 1.2 Hz), 122.3 (q, $^2J_{CF}$ = 31.3 Hz), 115.3, 110.5 (q, $^3J_{CF}$ = 5.5 Hz).

2-(2,5-dimethoxy-4-(trifluoromethyl)phenyl)ethanamine hydrochloride (2.56)

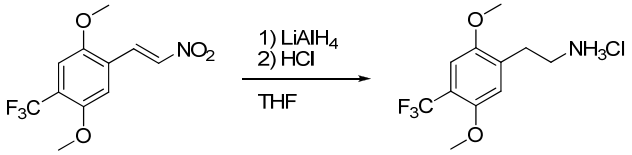

2.55 **2.56**

To a suspension of $LiAlH_4$ (3.42 g, 90.00 mmol) in dry THF (50 mL) was added a solution of the nitrostyrene, **2.55** (4.99 g, 18.00 mmol) in dry THF (100 mL) over the course of 30 minutes. The reaction was heated at reflux temperature for 3 hours and then cooled to room temperature. The excess hydride was destroyed by successive addition of water (3.5 mL), 15% NaOH (3.5 mL) and water (10.5 mL). The precipitate was loosened by addition of THF (100 mL) and filtered. The filter cake was washed thoroughly with THF (2 × 50 mL) and squeezed dry between washings. The filtrate was concentrated under reduced pressure, redissolved in Et_2O (150 mL) and extracted with 2M HCl (3 × 100 mL). The aqueous extracts were made basic to pH>11 with conc. NaOH and extracted with CH_2Cl_2 (3 × 75 mL). The combined CH_2Cl_2-extracts were dried (Na_2SO_4), filtered and evaporated under reduced pressure. The residue was purified by flash chromatography ($CHCl_3$/MeOH/NH_3 90:9:1) and the collected fractions were evaporated under reduced pressure and dissolved in EtOH (10 mL). 1M ethanolic HCl (25 mL) was added and the mixture was diluted with Et_2O (75 mL) to ensure complete crystallization. The precipitate is collected by filtration and dried under reduced pressure to afford the title compound, **2.56** (2.65 g, 59%) as white fluffy crystals. mp. 259-261 °C (Litt[286]. 260 °C), ^{1}H NMR (300 MHz, DMSO-d_6) δ 8.27 (br s, 3H), 7.18 (s, 1H), 7.11 (s, 1H), 3.84 (s, 3H), 3.80 (s, 3H), 3.06-2.91 (m, 4H). ^{13}C NMR (75 MHz, DMSO-d_6) δ 150.6 (q, $^3J_{CF}$ = 1.8 Hz), 150.4, 131.2, 123.5 (q, $^1J_{CF}$ = 271.7 Hz), 115.6, 115.4 (q, $^2J_{CF}$ = 30.3 Hz), 108.9 (q, $^3J_{CF}$ = 5.2 Hz), 56.5, 56.1, 38.0, 28.0

2-(4-iodo-2,5-dimethoxyphenyl)-*N*-(2-methoxybenzyl)ethanamine hydrochloride (2.1)

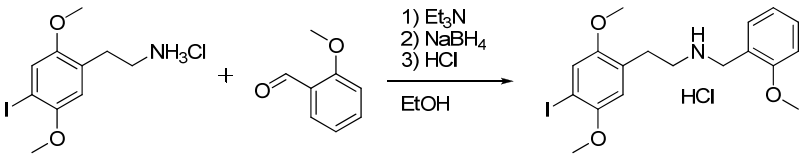

2.1

Obtained from 2C-I·HCl (**1.39**) and 2-methoxybenzaldehyde by general procedure A in 88% yield as a colorless solid, mp. 162-166 °C. ^{1}H NMR (300 MHz, DMSO-d_6) δ 9.42 (br s, 2H), 7.51 (dd, 1H, *J* = 7.4, 1.5 Hz), 7.42-7.35 (m, 1H), 7.29 (s, 1H), 7.05 (d, 1H, *J* 8.3 Hz), 6.97 (t, 1H, *J* = 7.4 Hz), 6.90 (s, 1H), 4.10 (s, 2H), 3.82 (s, 3H), 3.76 (s, 3H), 3.72 (s, 3H), 3.11-2.93 (m, 4H). ^{13}C NMR (75 MHz, DMSO-d_6) δ 157.2, 151.8, 151.6, 131.3, 130.5, 126.2, 121.2, 120.2, 119.6, 113.6, 110.9, 83.9, 56.8, 56.2, 55.6, 45.6, 44.6, 26.4.

2-((4-iodo-2,5-dimethoxyphenethylamino)methyl)phenol hydrochloride (2.2)

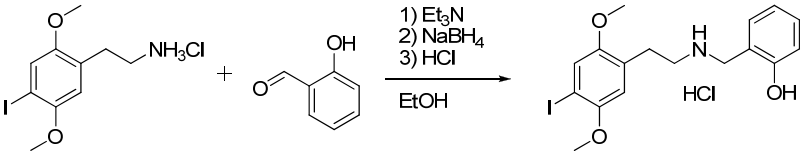

2.2

Obtained from 2C-I·HCl and salicylaldehyde by general procedure A in 81% yield as a colorless solid. mp. 197-201 °C. ^{1}H NMR (300 Mhz, DMSO-d_6) δ 10.30 (s, 1H), 9.15 (br s, 2H), 7.39 (dd, *J* = 7.4, 1.4 Hz, 1H), 7.21 (ddd, *J* = 8.1, 7.5, 1.4 Hz, 1H), 7.30 (s, 1H), 6.98 (dd, *J* = 8.1, 0.9 Hz, 1H), 6.88 (s, 1H), 6.82 (ddd, *J* =7.5, 7.4, 0.9 Hz, 1H), 4.08 (s, 2H), 3.78 (s, 3H), 3.73 (s, 3H), 3.11-2.90 (m, 4H). ^{13}C NMR (75 MHz, $CDCl_3$) δ 155.9, 151.8, 151.6, 131.5, 130.2, 126.2, 121.3, 118.9, 117.9, 115.3, 113.6, 83.9, 56.8, 56.2, 45.7, 44.9, 26.5

N-(2-fluorobenzyl)-2-(4-iodo-2,5-dimethoxyphenyl)ethanamine hydrochloride (2.3)

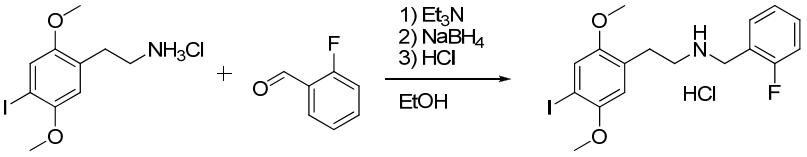

2.3

Obtained from 2C-I and 2-fluorobenzaldehyde by general procedure A in 84% yield as a colorless solid. mp 196-197 °C. ^{1}H NMR (300 MHz, DMSO-d_6) δ 9.74 (br s, 2H), 7.76 (td, *J* = 7.5, 1.5 Hz, 1H), 7.51–7.41 (m, 1H), 7.32–7.22 (m, 3H), 6.92 (s, 1H), 4.19 (br s, 2H), 3.76 (s, 3H), 3.73 (s, 3H), 3.17–3.05 (m, 2H), 3.05–2.95 (m, 2H). ^{13}C NMR (75 MHz, DMSO-d_6) δ 160.3 (d, $^{1}J_{CF}$ = 247 Hz), 151.8, 151.6, 132.3 (d, $^{3}J_{CF}$ = 3.1 Hz), 131.2 (d, $^{3}J_{CF}$ = 8.3 Hz), 126.1, 124.5 (d, $^{4}J_{CF}$ = 3.5 Hz), 121.2, 119.0 (d, $^{2}J_{C\text{-}F}$ = 14.5 Hz), 115.4 (d, $^{2}J_{CF}$ = 21.4 Hz), 113.6, 83.9, 56.8, 56.2, 45.9, 42.8, 26.5.

N-(benzo[*d*][1,3]dioxol-4-ylmethyl)-2-(4-iodo-2,5-dimethoxyphenyl)ethanamine hydrochloride (2.4)

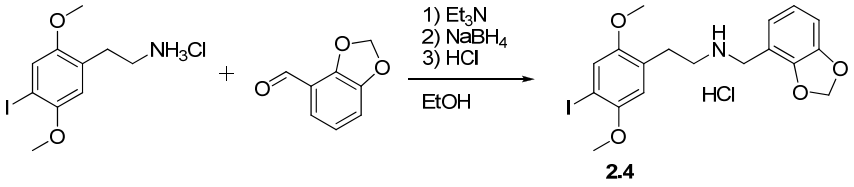

2.4

Obtained from 2C-I·HCl and 2,3-methylenedioxybenzaldehyde in 71% yield as a colorless solid, mp. 190-191 °C. ^{1}H NMR (300 MHz, DMSO-d_6) δ 9.70 (br s, 2H), 7.29 (s, 1H), 7.15 (dd, *J* = 7.8, 1.3 Hz, 1H), 6.95 (dd, *J* = 7.8, 1.3 Hz, 1H), 6.91 (s, 1H), 6.87 (t, *J* = 7.8 Hz, 1H), 6.05 (s, 2H), 4.07 (br s, 2H), 3.76 (s, 3H), 3.72 (s, 3H), 3.14–3.03 (m, 2H), 3.02-2.93 (m, 2H). ^{13}C NMR (75 MHz, DMSO-d_6) δ 151.8, 151.6, 146.9, 146.1, 126.1, 123.2, 121.6, 121.2, 113.6, 113.0, 108.9, 101.1, 83.9, 56.8, 56.2, 45.6, 43.4, 26.5.

2-(4-bromo-2,5-dimethoxyphenyl)-*N*-(2-methoxybenzyl)ethanamine hydrochloride (2.5)

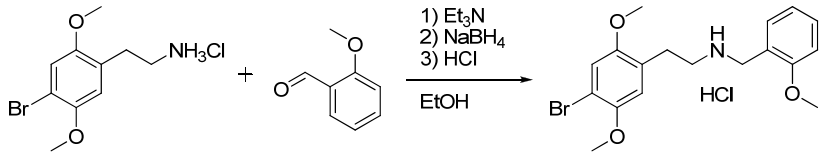

2.5

Obtained from 2C-B·HCl and 2-methoxybenzaldehyde by general procedure A in 85% yield as a colorless solid. mp. 179-181 °C. ^{1}H NMR (300 Mhz, DMSO-d_6) δ 9.34 (br s, 2H) , 7.50 (d, *J* =7.4 Hz, 1H), 7.39 (t, *J* = 8,3 Hz, 1H), 7.17 (s, 1H), 7.06 (d, *J* = 8.3 Hz, 1H), 7.01 (s, 1H), 6.98 (t, *J* = 7.4 Hz, 1H), 4.10 (s, 2H), 3.79 (s ,3H), 3.73 (s, 3H), 2.93-3.11 (m, 4H). ^{13}C NMR (75 MHz, DMSO-d_6) δ 157.3, 151.3, 149.2, 131.3, 130.6, 125.4, 120.2, 119.6, 115.7, 114.8, 110.9, 108.7, 56.6, 56.2, 55.6, 45.6, 44.7, 26.3

2-((4-bromo-2,5-dimethoxyphenethylamino)methyl)phenol hydrochloride (2.6)

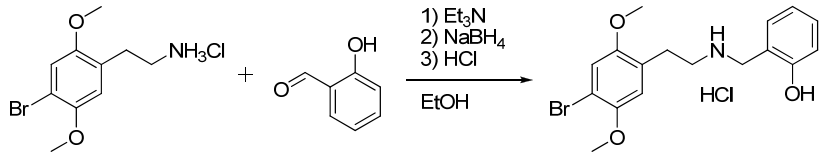

2.6

Obtained from 2C-B·HCl and salicylaldehyde by general procedure A in 79% yield as a colorless solid. mp. 188-190 °C. ^{1}H NMR (300 Mhz, DMSO-d_6) δ 2.91-3.11 (m, 4H), 3.74 (s, 3H), 3.78 (s ,3H), 4.08 (m, 2H), 6.78-6.85 (m, 1H), 6.96-7.02 (m, 1H), 6.99 (s, 1H), 7.16-7.24 (m, 1H), 7.17 (s, 1H) 7.38-7.43 (m, 1H), 9.19 (br s, 2H), 10.31 (s, 1H). ^{13}C NMR (75 MHz, DMSO d_6) δ 155.9, 151.3, 149.2, 131.5, 130.2, 125.4, 118.8, 117.9, 115.7, 115.3, 114.8, 108.7, 56.6, 56.2, 45.6, 44.8, 26.4

2-(4-bromo-2,5-dimethoxyphenyl)-*N*-(2-fluorobenzyl)ethanamine hydrochloride (2.7)

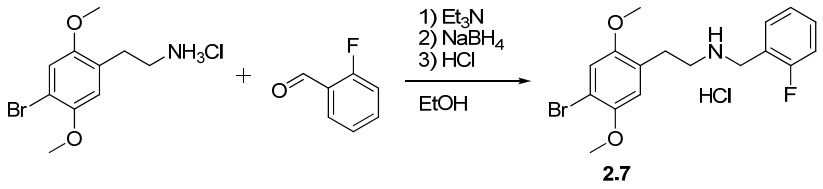

2.7

Obtained from 2C-B and 2-fluorobenzaldehyde by general procedure A in 80% yield as a colorless solid. mp. 172-174 °C. ^{1}H NMR (300 MHz, DMSO-d_6) δ^{13}C NMR (75 MHz, DMSO-d_6) δ 9.67 (br s, 2H), 7.75 (td, *J* = 7.6, 1.6 Hz, 1H), 7.51- 7.42 (m, 1H), 7.32-7.23 (m, 2H), 7.18 (s, 1H), 7.02 (s, 1H), 4.19 (s, 2H), 3.79 (s, 3H), 3.74 (s, 3H), 3.18-2.93 (m, 4H). ^{13}C NMR (75 MHz, DMSO) δ 160.3 (d, $^{1}J_{CF}$ = 246.6 Hz), 151.4, 149.2, 132.3 (d, $^{3}J_{CF}$ = 3.0 Hz), 131.2 (d, $^{3}J_{CF}$ = 8.4 Hz), 125.3, 124.5 (d, $^{4}J_{CF}$ = 3.7 Hz), 119.0 (d, $^{2}J_{CF}$ = 14.6 Hz), 115.72, 115.4 (d, $^{2}J_{CF}$ = 21.3 Hz), 114.8, 108.8, 56.6, 56.2, 45.9, 42.8 (d, $^{3}J_{CF}$ = 4.1 Hz), 26.4

N-(benzo[*d*][1,3]dioxol-4-ylmethyl)-2-(4-bromo-2,5-dimethoxyphenyl)ethanamine hydrochloride (2.8)

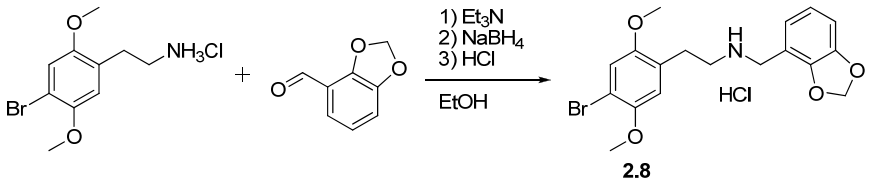

2.8

Obtained from 2C-B·HCl and 2,3-methylenedioxybenzaldehyde by general procedure A in 88% yield as a colorless solid. mp. 193-196 °C. ^{1}H NMR (300 Mhz, DMSO-d_6) δ 9.61 (br s, 2H), 7.18 (s, 1H), 7.13 (dd, 7.7, 1.3 Hz, 1H), 7.01 (s, 1H), 6.95 (dd, *J* = 7.7, 1.3 Hz, 1H), 6.88 (t, *J* = 7.7 Hz, 1H), 6.05 (s, 2H), 4.08 (s, 2H), 3.78 (s 3H), 3.74 (s, 3H), 3.15-2.91 (m, 4H). ^{13}C NMR (75 MHz, DMSO-d_6) δ 151.3, 149.2, 146.9, 146.1, 125.3, 123.2, 121.7, 115.7, 114.8, 113.0, 109.0, 101.1, 56.6, 56.2, 45.7, 43.4, 26.4.

2-(4-chloro-2,5-dimethoxyphenyl)-*N*-(2-methoxybenzyl)ethanamine hydrochloride (2.9)

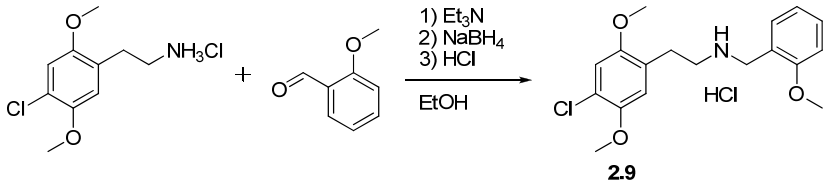

2.9

Obtained from 2C-C·HCl and 2-methoxybenzaldehyde by general procedure A in 86% yield as a colorless solid. mp. 179-181 °C. ^{1}H NMR (300 Mhz, CD_3OD) δ 7.46-7.36 (m, 2H), 7.07 (d, *J* = 8.3 Hz, 1H), 7.03-6.97 (m, 3H), 4.24 (s, 2H), 3.88 (s, 3H), 3.82 (s, 3H), 3.77 (s, 3H), 3.25-3.17 (m, 2H), 3.07-2.99 (m, 2H). ^{13}C NMR (75 MHz, CD_3OD) δ 159.1, 152.8, 150.4, 132.6, 125.1, 122.5, 121.9, 120.1, 116.4, 114.1, 111.9, 57.3, 56.6, 56.2, 47.9, 47.8, 28.2.

2-((4-chloro-2,5-dimethoxyphenethylamino)methyl)phenol hydrochloride (2.10)

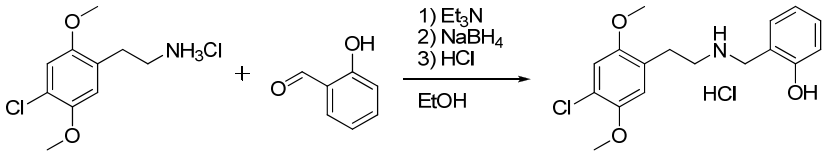

2.10

Obtained from 2C-C and salicylaldehyde by general procedure A in 83% yield as a colorless solid. mp. 167-170 °C. ^{1}H NMR (300 Mhz, DMSO-d_6) δ 10.30 (s, 1H), 9.14 (br s, 2H), 7.39 (dd, *J* = 7.5, 1.6 Hz, 1H), 7.20 (ddd, *J* = 8.1, 7.4, 1.6 Hz, 1H), 7.06 (s, 1H), 7.02 (s, 1H), 6.98 (dd, *J* = 8.1, 1.0 Hz, 1H), 6.82 (ddd, *J* = 7.5, 7.4, 1.0 Hz, 1H), 4.08 (s, 2H), 3.79 (s, 3H), 3.74 (s, 3H), 3.11-2.92 (m, 4H). ^{13}C NMR (75 MHz, DMSO-d_6) δ 155.9, 151.0, 148.2, 131.5, 130.2, 124.7, 119.4, 118.9, 117.9, 115.3, 115.0, 113.0, 56.5, 56.2, 45.7, 44.9, 26.3

2-(4-chloro-2,5-dimethoxyphenyl)-*N*-(2-fluorobenzyl)ethanamine hydrochloride (2.11)

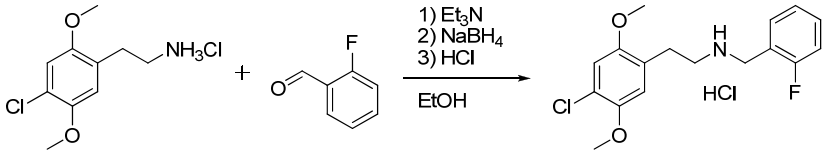

2.11

Obtained from 2C-C·HCl and 2-fluorobenzaldehyde by general procedure A in 83% yield as a colorless solid. mp. 160-162 °C. ^{1}H NMR (300 Mhz, DMSO-d_6) δ 9.73 (br s, 2H), 7.80-7.73 (m, 1H), 7.51-7.41 (m, 1H), 7.31-7.22 (m, 2H), 7.06 (s, 1H), 7.05 (s, 1H), 4.19 (s, 2H), 3.79 (s, 3H), 3.74 (s, 3H), 3.18-2.96 (m, 4H). ^{13}C NMR (75 MHz, DMSO-d_6) δ 160.3 (d, $^{1}J_{CF}$ = 246.7 Hz), 151.0, 148.2, 132.3 (d, $^{3}J_{CF}$ = 2.9 Hz), 131.23 (d, $^{3}J_{CF}$ = 8.3 Hz), 124.5 (d, $^{3}J_{CF}$ = 3.6 Hz), 124.6, 119.4, 119.0 (d, $^{2}J_{CF}$ = 14.5 Hz), 115.0, 115.4 (d, $^{2}J_{CF}$ = 21.4 Hz), 113.0, 56.5, 56.2, 46.0, 42.8 (d, $^{3}J_{CF}$ = 4.1 Hz), 26.2

N-(benzo[*d*][1,3]dioxol-4-ylmethyl)-2-(4-chloro-2,5-dimethoxyphenyl)ethanamine hydrochloride (2.12)

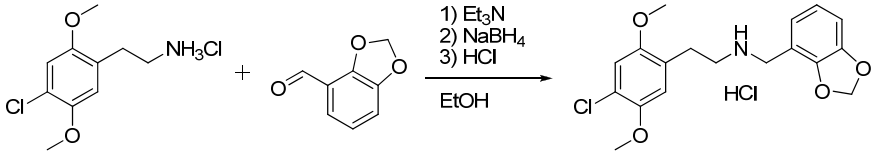

2.12

Obtained from 2C-C·HCl and 2,3-methylenedioxybenzaldehyde by general procedure A in 92% yield as a colorless solid. mp. 177-179 °C. ^{1}H NMR (300 Mhz, DMSO-d_6) δ 9.63 (br s, 2H), 7.14 (dd, *J* = 7.8, 1.0 Hz, 1H), 7.06 (s, 1H), 7.04 (s, 1H), 6.95 (dd, *J* = 7.7, 1.0 Hz, 1H), 6.88 (dd, *J* = 7.8, 7.7 Hz, 1H), 6.05 (s, 2H), 4.08 (s, 2H), 3.79, (s, 3H), 3.74 (s, 3H), 3.15-2.92 (m, 4H). ^{13}C NMR (75 MHz, DMSO-d_6) δ 151.0, 148.2, 146.9, 146.1, 124.6, 123.2, 121.7, 119.4, 115.2, 115.0, 113.0, 109.0, 101.1, 56.4, 56.2, 45.86, 43.4, 26.3

2-(4-fluoro-2,5-dimethoxyphenyl)-*N*-(2-methoxybenzyl)ethanamine hydrochloride (2.13)

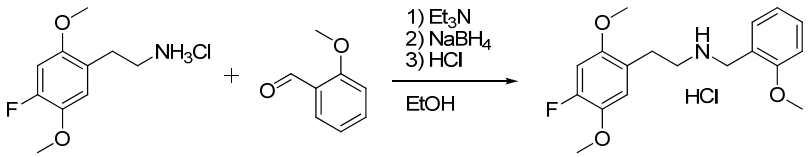

2.13

Obtained from 2C-F·HCl and 2-methoxybenzaldehyde by general procedure A in 79% yield as a colorless solid. mp. 143-146 °C. ^{1}H NMR (300 MHz, DMSO-d_6) δ 9.11 (br s, 2H), 7.47 (dd, J = 7.4, 1.3 Hz, 1H), 7.44-7.36 (m, 1H), 7.10-6.94 (m, 4H), 4.11 (br t, J = 4.5 Hz, 2H), 3.83 (s, 3H), 3.78 (s, 3H), 3.73 (s, 3H), 3.11-2.99 (m, 2H), 2.98-2.89 (m, 2H). ^{13}C NMR (75 MHz, DMSO-d_6) δ 157.3, 150.9, 150.8, 150.5 (d, $^{1}J_{CF}$ = 242 Hz), 140.2 (d, $^{2}J_{CF}$ = 10.8 Hz), 131.3, 130.5, 120.5 (d, $^{4}J_{CF}$ = 3.7 Hz), 120.2, 119.6, 116.1 (d, $^{3}J_{CF}$ = 2.9 Hz), 110.9, 100.9 (d, $^{2}J_{CF}$ = 22.2 Hz), 56.6, 56.2, 55.6, 45.8, 44.5, 25.9.

2-((4-fluoro-2,5-dimethoxyphenethylamino)methyl)phenol hydrochloride (2.14)

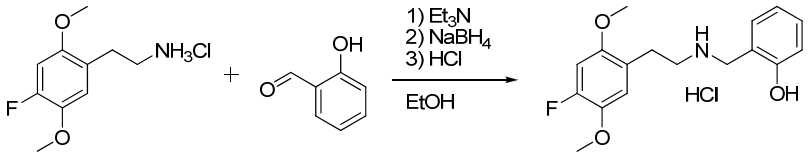

2.14

Obtained from 2C-F·HCl and salicylaldehyde by general procedure A in 66% yield as a colorless solid. mp. 190-192 °C. ^{1}H NMR (600 MHz, DMSO-d_6) δ 10.33 (br s, 1H), 9.19 (br s, 2H), 7.42 (dd, J = 7.6, 1.6 Hz, 1H), 7.24-7.20 (m, 1H), 7.03 (d, $^{3}J_{H-F}$ = 9.8 Hz, 1H), 7.02-6.99 (m, 1H), 6.97 (d, $^{4}J_{H-F}$ = 13.3 Hz, 1H), 6.83 (td, J = 7.6, 1.0 Hz, 1H), 4.08 (br s, 2H), 3.78 (s, 3H), 3.72 (s, 3H), 3.06-3.00 (m, 2H), 2.97-2.92 (m, 2H). ^{13}C NMR (150 MHz, DMSO-d_6) δ 156.1, 150.8 (d, $^{1}J_{CF}$ = 243 Hz), 151.0 (d, $^{3}J_{CF}$ = 8.2 Hz), 140.4 (d, $^{2}J_{CF}$ = 10.8 Hz), 131.7, 130.4, 120.5 (d, $^{4}J_{CF}$ = 3.6 Hz), 119.0, 118.1, 116.3 (d, $^{3}J_{CF}$ = 2.7 Hz), 115.5, 101.0 (d, $^{2}J_{CF}$ = 22.2 Hz), 56.7, 56.2, 45.9, 44.8, 26.0.

2-(4-fluoro-2,5-dimethoxyphenyl)-*N*-(2-fluorobenzyl)ethanamine hydrochloride (2.15)

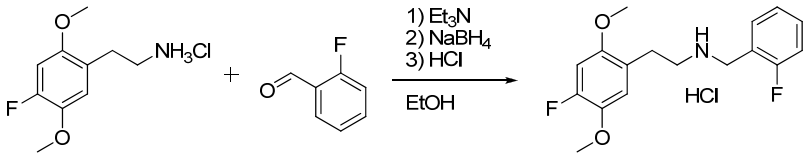

2.15

Obtained from 2C-F·HCl and 2-fluorobenzaldehyde by general procedure A in 88% yield as a colorless solid. mp. 177-179 °C. ^{1}H NMR (600 MHz, DMSO-d_6) δ 9.71 (br s, 2H), 7.77 (td, J = 7.6, 1.6 Hz, 1H), 7.50-7.46 (m, 1H), 7.31-7.26 (m, 2H), 7.06 (d, J = 9.8 Hz, 1H), 6.98 (d, J = 13.3 Hz, 1H), 4.20 (br t, J = 5.3 Hz, 2H), 3.78 (s, 3H), 3.73 (s, 3H), 3.13-3.06 (m, 2H), 3.00-2.96 (m, 2H); ^{13}C NMR (150 MHz, DMSO-d_6) δ 160.6 (d, $^{1}J_{CF}$ = 247 Hz), 151.1 (d, $^{3}J_{CF}$ = 8.3 Hz), 150.8 (d, $^{1}J_{CF}$ = 243 Hz), 140.4 (d, $^{2}J_{CF}$ = 10.8 Hz), 132.5 (d, $^{3}J_{CF}$ = 2.9 Hz), 131.4 (d, $^{3}J_{CF}$ = 8.3 Hz), 124.7 (d, $^{4}J_{CF}$ = 3.4 Hz),

120.5 (d, $^4J_{CF}$ = 3.6 Hz), 119.2 (d, $^2J_{CF}$ = 14.5 Hz), 116.3 (d, $^3J_{CF}$ = 2.7 Hz), 115.6 (d, $^2J_{CF}$ = 21.3 Hz), 101.0 (d, $^2J_{CF}$ = 22.2 Hz), 56.7, 56.2, 46.2, 42.8 (d, $^3J_{CF}$ = 3.9 Hz), 25.9.

N-(benzo[*d*][1,3]dioxol-4-ylmethyl)-2-(4-fluoro-2,5-dimethoxyphenyl)ethanamine hydrochloride (2.16)

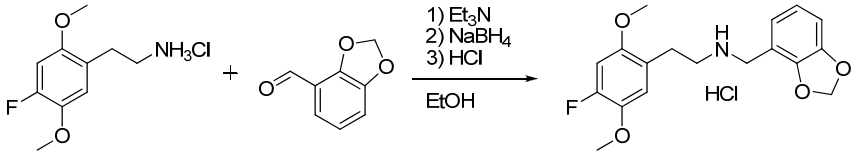

2.16

Obtained from 2C-F·HCl and 2,3-methylenedioxybenzaldehyde in 76% yield as a colorless solid. mp. 160 °C (dec). ^{1}H NMR (600 MHz, DMSO-d_6) δ 9.70 (br s, 2H), 7.17 (dd, *J* = 8.0, 1.0 Hz, 1H), 7.05 (d, *J* = 9.8 Hz, 1H), 6.97 (d, *J* = 13.3 Hz, 1H), 6.96 (dd, *J* = 8.0, 1.0 Hz, 1H), 6.89 (t, *J* = 8.0 Hz, 1H), 6.06 (s, 2H), 4.08 (br t, *J* = 5.2 Hz, 2H), 3.78 (s, 3H), 3.72 (s, 3H), 3.10-3.03 (m, 2H), 2.99-2.94 (m, 2H); ^{13}C NMR (150 MHz, DMSO-d_6) δ 151.1 (d, $^3J_{CF}$ = 8.3 Hz), 150.8 (d, $^1J_{CF}$ = 243 Hz), 147.1, 146.3, 140.3 (d, $^2J_{CF}$ = 10.7 Hz), 123.4, 121.8, 120.5 (d, $^4J_{CF}$ = 3.6 Hz), 116.3 (d, $^3J_{CF}$ = 2.7 Hz), 113.2, 109.1, 101.2, 101.0 (d, $^2J_{CF}$ = 22.1 Hz), 56.7, 56.2, 45.9, 43.4, 26.0.

2-(2,5-dimethoxy-4-methylphenyl)-*N*-(2-methoxybenzyl)ethanamine hydrochloride (2.17)

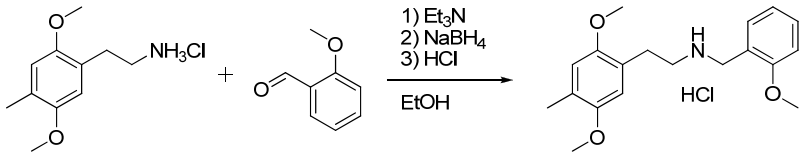

2.17

Obtained from 2C-D·HCl and 2-methoxybenzaldehyde by general procedure A in 90% yield as a colorless solid. mp. 166-168 °C. ^{1}H NMR (300 Mhz, DMSO-d_6) δ 9.36 (br s, 2H), 7.48-7.53(m, 1H), 7.35-7.42 (m, 1H), 7.04-7.08 (m, 1H), 6.94-7.01 (m, 1H), 6.80 (s, 1H), 6.76 (s, 1H), 4.10 (t, *J* = 5.3 Hz, 2H), 3.82 (s ,3H), 3.72 (s ,3H), 3.69 (s, 3H), 2.90-3.07 (m, 4H), 2.12 (s, 3H) ^{13}C NMR (75 MHz, DMSO-d_6) δ 157.3, 150.9, 150.4, 131.4, 130.5, 124.7, 122.5, 120.2, 119.6, 113.8, 112.6, 110.9, 55.83, 55.6, 55.6, 46.1, 44.6, 26.4, 16.1.

2-((2,5-dimethoxy-4-methylphenethylamino)methyl)phenol hydrochloride (2.18)

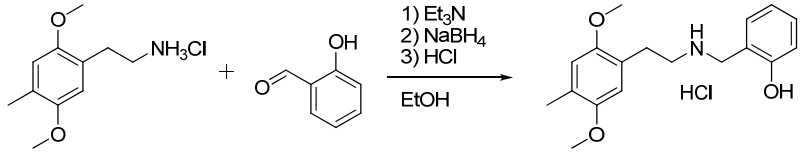

2.18

Obtained from 2C-D·HCl and salicylaldehyde by general procedure A in 78% yield as a colorless solid. mp. 174-175 °C. ^{1}H NMR (300 Mhz, DMSO-d_6) δ 2.12 (s, 3H), 2.88-3.08 (m, 4H), 3.70 (s, 3H), 3.72 (s ,3H), 4.08 (s, 2H), 6.74 (s, 1H), 6.78-6.86 (m, 1H), 6.80 (s, 1H), 6.96-7.02 (m, 1H), 7.17-7.24 (m, 1H), 7.36-7.42 (m, 1H), 9.16 (br s, 2H), 10.31 (s, 1H). ^{13}C NMR (75 MHz, DMSO-d_6) δ 155.9,

150.9, 150.4, 131.5, 130.2, 124.2, 122.5, 118.8, 118.0, 115.3, 113.8, 112.7, 55.9, 55.7, 46.1, 44.8, 26.4, 16.1

2-(2,5-dimethoxy-4-methylphenyl)-*N*-(2-fluorobenzyl)ethanamine hydrochloride (2.19)

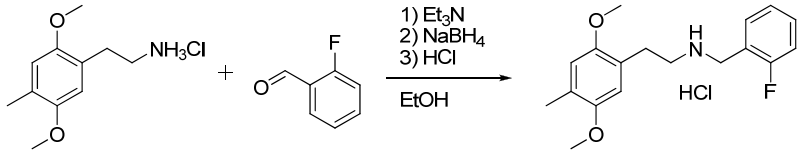

2.19

Obtained from 2C-D and 2-fluorobenzaldehyde by general procedure A in 89% yield as a colorless solid. mp. 164-166 °C. ^{1}H NMR (300 Mhz, DMSO-d_6) δ 9.72 (br s, 2H), 7.71-7.78 (m, 1H), 7.22-7.31 (m, 1H), 6.94-7.01 (m, 2H), 6.80 (s, 1H), 6.77 (s, 1H), 4.15-4-23 (m, 2H), 3.72 (s ,3H), 3.70 (s, 3H), 2.92-3.14 (m, 4H), 2.12 (s, 3H). ^{13}C NMR (75 MHz, DMSO) δ 160.4 (d, $^{1}J_{CF}$ = 246.6 Hz), 150.9, 150.5, 132.4 (d, $^{3}J_{CF}$ = 2.9 Hz), 131.2 (d, $^{3}J_{CF}$ = 8.4 Hz), 124.7, 124.5 (d, $^{4}J_{CF}$ = 3.4 Hz), 122.4, 119.1 (d, $^{2}J_{CF}$ = 14.7 Hz), 115.4 (d, $^{2}J_{CF}$ = 21.3 Hz), 113.8, 112.7, 55.8, 55.6, 46.3, 42.8, 26.4, 16.1

N-(benzo[*d*][1,3]dioxol-4-ylmethyl)-2-(2,5-dimethoxy-4-methylphenyl)ethanamine hydrochloride (2.20)

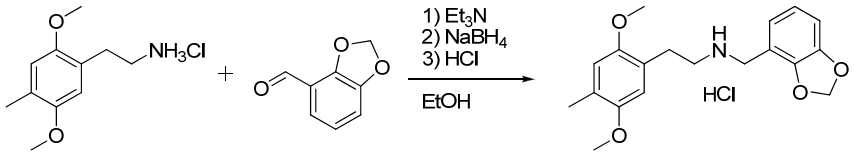

2.20

Obtained from 2C-D·HCl and 2,3-methylenedioxybenzaldehyde by general procedure A in 94% yield as a colorless solid. mp. 184-185 °C. ^{1}H NMR (300 Mhz, DMSO-d_6) δ 9.61 (br s, 2H), 7.14 (dd, *J* = 7.8, 1.2 Hz, 1H), 6.95 (dd, *J* = 7.7, 1.2 Hz, 1H), 6.88 (dd, *J* = 7.7, 7.8 Hz, 1H), 6.80 (s, 1H), 6.76 (s, 1H), 6.05 (s, 2H), 4.08 (s, 2H), 3.72 (s ,3H), 3.70 (s, 3H), 3.11-2.90 (m, 4H), 2.12 (s, 3H). ^{13}C NMR (75 MHz, DMSO-d_6) δ 150.9, 150.5, 146.9, 146.1, 124.7, 123.3, 122.4, 121.7, 113.8, 113.0, 112.7, 109.0, 101.10, 55.8, 55.6, 46.1, 43.4, 26.4, 16.1.

2-(4-ethyl-2,5-dimethoxyphenyl)-*N*-(2-methoxybenzyl)ethanamine (2.21)

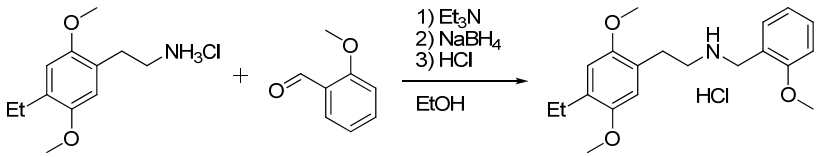

2.21

Obtained from 2C-E·HCl and 2-methoxybenzaldehyde by general procedure A in 74% yield as a colorless solid. mp. 160-161 °C. ^{1}H NMR (600 MHz, DMSO-d_6) δ 9.35 (br s, 2H), 7.51 (dd, *J* = 7.5, 1.7 Hz, 1H), 7.40 (ddd, *J* = 8.3, 7.5, 1.7 Hz, 1H), 7.08 (br d, *J* = 8.3 Hz, 1H), 6.99 (td, *J* = 7.5, 1.0 Hz, 1H), 6.80 (s, 1H), 6.79 (s, 1H), 4.11 (br s, 2H), 3.82 (s, 3H), 3.73 (s, 3H), 3.71 (s, 3H), 3.04-2.99 (m, 2H), 2.99-2.94 (m, 2H), 2.53 (q, *J* = 7.5 Hz, 2H), 1.10 (t, *J* = 7.5 Hz, 3H); ^{13}C NMR (150 MHz, DMSO-d_6) δ 157.5, 150.9, 150.7, 131.5, 131.1, 130.7, 122.8, 120.4, 119.7, 113.2, 112.5, 111.1, 55.9, 55.8, 55.6, 46.1, 44.7, 26.3, 22.9, 14.5.

2-((4-ethyl-2,5-dimethoxyphenethylamino)methyl)phenol hydrochloride (2.22)

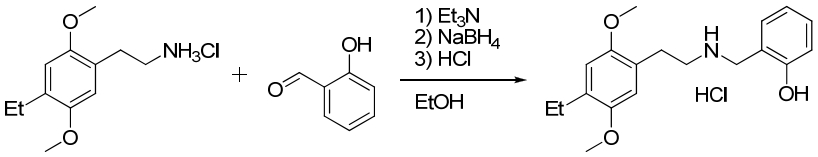

2.22

Obtained from 2C-E·HCl and salicylaldehyde by general procedure A in 78% yield as a colorless solid. mp. 189-191 °C. ^{1}H NMR (600 MHz, DMSO-d_6) δ 10.34 (s, 1H), 9.19 (br s, 2H), 7.41 (dd, *J* = 7.5, 1.5 Hz, 1H), 7.25-7.20 (m, 1H), 7.01 (dd, *J* = 8.1, 0.9 Hz, 1H), 6.83 (td, *J* = 7.5, 0.9 Hz, 1H), 6.79 (s, 1H), 6.77 (s, 1H), 4.08 (br t, *J* = 5.1 Hz, 2H), 3.73 (s, 3H), 3.71 (s, 3H), 3.05-2.99 (m, 2H), 2.96-2.92 (m, 2H), 2.53 (q, *J* = 7.5 Hz, 2H), 1.10 (t, *J* = 7.5 Hz, 3H). ^{13}C NMR (150 MHz, DMSO-d_6) δ 156.2, 150.9, 150.7, 131.7, 131.1, 130.4, 122.8, 119.0, 118.1, 115.5, 113.2, 112.5, 55.9, 55.8, 46.1, 44.8, 26.4, 22.9, 14.5.

2-(4-ethyl-2,5-dimethoxyphenyl)-*N*-(2-fluorobenzyl)ethanamine hydrochloride (2.23)

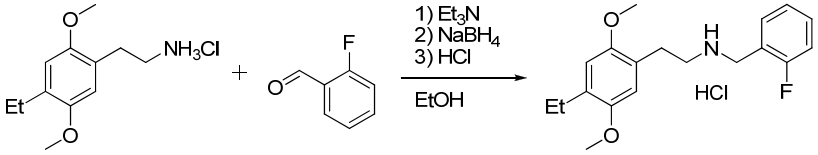

2.23

Obtained from 2C-E·HCl and 2-fluorobenzaldehyde by general procedure A in 75% yield as a colorless solid. mp. 160-162 °C. ^{1}H NMR (300 MHz, DMSO-d_6) δ 9.64 (br s, 2H), 7.74 (dt, *J* = 7.5, 1.3 Hz, 1H), 7.52-7.42 (m, 1H), 7.33-7.23 (m, 2H), 6.79 (s, 2H), 4.20 (br s, 2H), 3.73 (s, 3H), 3.72 (s, 3H), 3.15-3.03 (m, 2H), 3.01-2.92 (m, 2H), 2.53 (q, *J* = 7.5 Hz, 2H), 1.11 (t, *J* = 7.5 Hz, 3H). ^{13}C NMR (75 MHz, DMSO-d_6) δ 160.4 (d, $^{1}J_{CF}$ = 247 Hz), 150.7, 150.5, 132.4 (d, $^{3}J_{CF}$ = 2.9 Hz), 131.2 (d, $^{3}J_{CF}$ = 8.4 Hz), 130.9, 124.5 (d, $^{4}J_{CF}$ = 3.5 Hz), 122.6, 119.1 (d, $^{2}J_{CF}$ = 14.6 Hz), 115.4 (d, $^{2}J_{CF}$ = 21.4 Hz), 113.0, 112.3, 55.9, 55.8, 46.3, 42.7 (d, $^{3}J_{CF}$ = 4.0 Hz), 26.4, 22.9, 14.6.

N-(benzo[*d*][1,3]dioxol-4-ylmethyl)-2-(4-ethyl-2,5-dimethoxyphenyl)ethanamine hydrochloride (2.24)

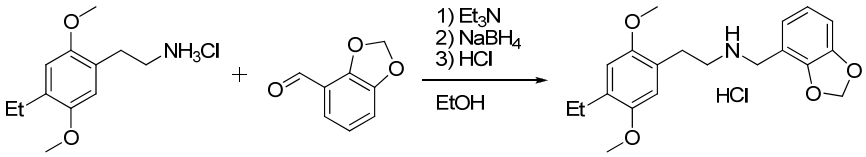

2.24

Obtained from 2C-E·HCl and 2,3-methylenedioxybenzaldehyde by general procedure A in 69% yield as a colorless solid. mp. 143-145 °C. ^{1}H NMR (600 MHz, DMSO-d_6) δ 9.66 (br s, 2H), 7.16 (dd, *J* = 7.9, 1.1 Hz, 1H), 6.96 (dd, *J* = 7.9, 1.1 Hz, 1H), 6.89 (t, *J* = 7.9 Hz, 1H), 6.80 (s, 1H), 6.79 (s, 1H), 6.06 (s, 2H), 4.09 (br t, *J* = 4.9 Hz, 2H), 3.73 (s, 3H), 3.71 (s, 3H), 3.09-3.03 (m, 2H), 2.98-2.93 (m, 2H), 2.53 (q, *J* = 7.5 Hz, 2H), 1.10 (t, *J* = 7.5 Hz, 3H). ^{13}C NMR (150 MHz, DMSO-d_6) δ 150.9,

150.7, 147.1, 146.3, 131.1, 123.4, 122.7, 121.8, 113.2, 113.2, 112.5, 109.1, 101.2, 55.9, 55.8, 46.1, 43.4, 26.4, 22.9, 14.5.

2-(2,5-dimethoxy-4-propylphenyl)-*N*-(2-methoxybenzyl)ethanamine hydrochloride (2.25)

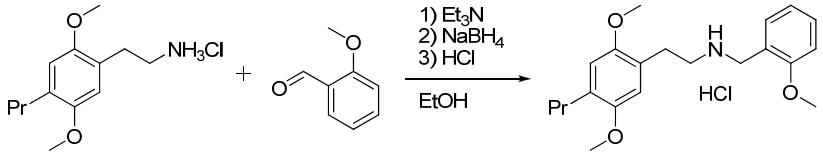

2.25

Obtained from 2C-P·HCl and 2-methoxybenzaldehyde in 68% yield as a colorless solid, mp 124-127 °C (dec). ^{1}H NMR (600 MHz, DMSO-d_6) δ 9.19 (br s, 2H), 7.49 (dd, *J* = 7.5, 1.6 Hz, 1H), 7.41 (ddd, *J* = 8.3, 7.5, 1.6 Hz, 1H), 7.09 (br d, *J* = 8.3 Hz, 1H), 7.00 (td, *J* = 7.5, 0.9 Hz, 1H), 6.78 (s, 1H), 6.78 (s, 1H), 4.12 (br s, 2H), 3.83 (s, 3H), 3.72 (s, 3H), 3.71 (s, 3H), 3.07-3.01 (m, 2H), 2.96-2.92 (m, 2H), 2.50-2.47 (m, 2H), 1.55-1.48 (m, 2H), 0.89 (t, *J* = 7.3 Hz, 3H). ^{13}C NMR (150 MHz, DMSO-d_6) δ 157.5, 150.8, 150.7, 131.5, 130.8, 129.5, 122.7, 120.4, 119.7, 113.2, 113.2, 111.1, 55.9, 55.8, 55.6, 46.2, 44.8, 31.8, 26.4, 22.8, 14.0.

2-((2,5-dimethoxy-4-propylphenethylamino)methyl)phenol hydrochloride (2.26)

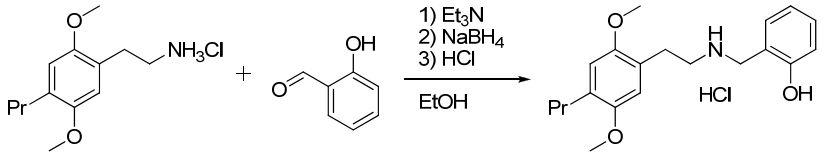

2.26

Obtained from 2C-P·HCl and salicylaldehyde by general procedure A in 46% yield as a colorless solid. mp. 159-161 °C. ^{1}H NMR (600 MHz, DMSO-d_6) δ 10.29 (br s, 1H), 9.05 (br s, 2H), 7.39 (dd, *J* = 7.6, 1.6 Hz, 1H), 7.23 (ddd, *J* = 8.1, 7.6, 1.6 Hz, 1H), 6.98 (dd, *J* = 8.1, 1.0 Hz, 1H), 6.84 (td, *J* = 7.6, 1.0 Hz, 1H), 6.78 (s, 1H), 6.77 (s, 1H), 4.09 (br s, 2H), 3.72 (s, 3H), 3.71 (s, 3H), 3.07-3.01 (m, 2H), 2.95-2.90 (m, 2H), 2.50-2.47 (m, 2H), 1.55-1.48 (m, 2H), 0.89 (t, *J* = 7.3 Hz, 3H). ^{13}C NMR (150 MHz, DMSO-d_6) δ 156.1, 150.8, 150.7, 131.7, 130.4, 129.5, 122.8, 119.0, 118.1, 115.4, 113.2, 113.2, 55.9, 55.8, 46.2, 45.0, 31.8, 26.4, 22.8, 14.0.

2-(2,5-dimethoxy-4-propylphenyl)-*N*-(2-fluorobenzyl)ethanamine hydrochloride (2.27)

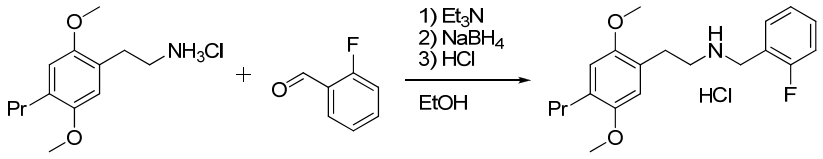

2.27

Obtained from 2C-P·HCl and 2-fluorobenzaldehyde by general procedure A in 71% yield as a colorless solid. mp. 124-125 °C. ^{1}H NMR (600 MHz, DMSO-d_6) δ 9.67 (br s, 2H), 7.76 (td, *J* = 7.5, 1.7 Hz, 1H), 7.50-7.46 (m, 1H), 7.32-7.27 (m, 2H), 6.80 (s, 1H), 6.78 (s, 1H), 4.20 (br s, 2H), 3.72 (s, 3H), 3.71 (s, 3H), 3.12-3.06 (m, 2H), 2.99-2.94 (m, 2H), 2.50-2.47 (m, 2H), 1.56-1.48 (m, 2H), 0.89

(t, *J* = 7.3 Hz, 3H). ^{13}C NMR (150 MHz, DMSO-d_6) δ 160.6 (d, $^{1}J_{CF}$ = 247 Hz), 150.8, 150.8, 132.5 (d, $^{3}J_{CF}$ = 2.8 Hz), 131.4 (d, $^{3}J_{CF}$ = 8.3 Hz), 129.5, 124.7 (d, $^{4}J_{CF}$ = 3.4 Hz), 122.7, 119.2 (d, $^{2}J_{CF}$ = 14.6 Hz), 115.6 (d, $^{2}J_{CF}$ = 21.3 Hz), 113.2 (2C), 55.9, 55.8, 46.4, 42.8 (d, $^{3}J_{CF}$ = 3.9 Hz), 31.8, 26.4, 22.8, 14.0.

N-(benzo[*d*][1,3]dioxol-4-ylmethyl)-2-(2,5-dimethoxy-4-propylphenyl)ethanamine hydrochloride (2.28)

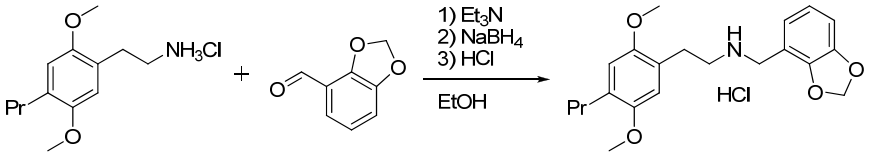

2.28

Obtained from 2C-P·HCl and 2,3-methylenedioxybenzaldehyde by general procedure A in 67% yield as a colorless solid. mp. 110 °C (dec). ^{1}H NMR (600 MHz, DMSO-d_6) δ 9.55 (br s, 2H), 7.13 (dd, *J* = 7.9, 1.1 Hz, 1H), 6.97 (dd, *J* = 7.9, 1.1 Hz, 1H), 6.90 (t, *J* = 7.9 Hz, 1H), 6.79 (s, 1H), 6.78 (s, 1H), 6.07 (s, 2H), 4.10 (br s, 2H), 3.72 (s, 3H), 3.71 (s, 3H), 3.11-3.04 (m, 2H), 2.97-2.92 (m, 2H), 2.50-2.47 (m, 2H), 1.56-1.48 (m, 2H), 0.89 (t, *J* = 7.3 Hz, 3H). ^{13}C NMR (150 MHz, DMSO-d_6) δ 150.8, 150.8, 147.1, 146.3, 129.5, 123.4, 122.7, 121.8, 113.2, 113.2, 113.2, 109.1, 101.2, 55.9, 55.8, 46.2, 43.4, 31.8, 26.4, 22.8, 14.0.

2-(2,5-dimethoxy-4-(methylthio)phenyl)-*N*-(2-methoxybenzyl)ethanamine hydrochloride (2.29)

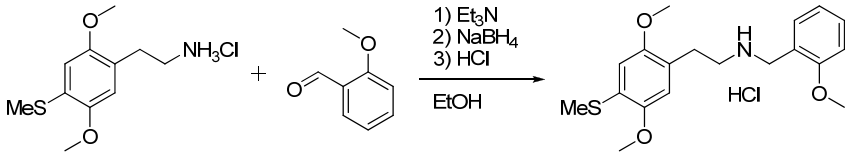

2.29

Obtained from 2C-T·HCl and 2-methoxybenzaldehyde by general procedure A in 76% yield as a colorless solid. mp. 147-153 °C. ^{1}H NMR (600 MHz, DMSO-d_6) δ 9.20 (br s, 2H), 7.50-7.48 (m, 1H), 7.41 (ddd, *J* = 8.3, 7.5, 1.7 Hz, 1H), 7.10-7.06 (m, 1H), 7.00 (td, *J* = 7.5, 1.0 Hz, 1H), 6.83 (s, 1H), 6.75 (s, 1H), 4.13-4.10 (m, 2H), 3.83 (s, 3H), 3.77 (s, 3H), 3.76 (s, 3H), 3.07-3.00 (m, 2H), 2.97-2.93 (m, 2H), 2.40 (s, 3H). ^{13}C NMR (150 MHz, DMSO-d_6) δ 157.5, 151.6, 149.5, 131.5, 130.8, 125.8, 121.6, 120.4, 119.7, 113.1, 111.1, 109.2, 56.2, 56.1, 55.6, 46.1, 44.8, 26.2, 13.7.

2-((2,5-dimethoxy-4-(methylthio)phenethylamino)methyl)phenol hydrochloride (2.30)

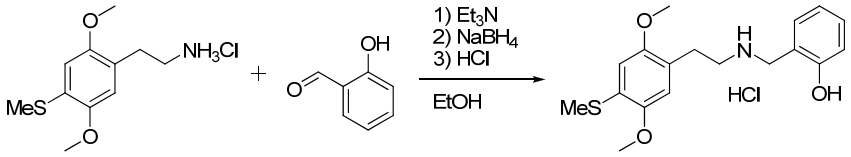

2.30

Obtained from 2C-T·HCl and salicylaldehyde by general procedure A in 68% yield as a colorless solid. mp. 221-223 °C. ^{1}H NMR (600 MHz, DMSO-d_6) δ 10.31 (s, 1H), 9.10 (br s, 2H), 7.40 (dd, *J* = 7.5, 1.6 Hz, 1H), 7.23 (ddd, *J* = 8.1, 7.5, 1.6 Hz, 1H), 6.99 (dd, *J* = 8.1, 1.0 Hz, 1H), 6.84 (td, *J* = 7.5, 1.0 Hz, 1H), 6.82 (s, 1H), 6.74 (s, 1H), 4.09 (br t, *J* = 5.4 Hz, 2H), 3.77 (s, 3H), 3.76 (s, 3H), 3.06-

3.00 (m, 2H), 2.96-2.92 (m, 2H), 2.40 (s, 3H). ^{13}C NMR (150 MHz, DMSO-d_6) δ 156.1, 151.6, 149.5, 131.7, 130.4, 125.7, 121.7, 119.0, 118.1, 115.4, 113.1, 109.2, 56.2, 56.1, 46.0, 44.9, 26.2, 13.7.

2-(2,5-dimethoxy-4-(methylthio)phenyl)-*N*-(2-fluorobenzyl)ethanamine hydrochloride (2.31)

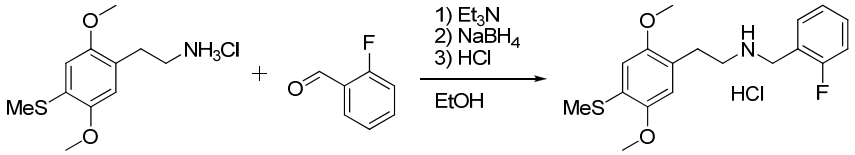

2.31

Obtained from 2C-T·HCl and 2-fluorobenzaldehyde by general procedure A in 71% yield as a colorless solid. mp. 196-198 °C. ^{1}H NMR (600 MHz, DMSO-d_6) δ 9.67 (br s, 2H), 7.76 (td, J = 7.6, 1.6 Hz, 1H), 7.51-7.46 (m, 1H), 7.32-7.27 (m, 2H), 6.85 (s, 1H), 6.75 (s, 1H), 4.20 (br s, 2H), 3.78 (s, 3H), 3.76 (s, 3H), 3.12-3.06 (m, 2H), 2.99-2.95 (m, 2H), 2.40 (s, 3H). ^{13}C NMR (150 MHz, DMSO-d_6) δ 160.6 (d, $^1J_{C\text{-}F}$ = 247 Hz), 151.6, 149.5, 132.5 (d, $^3J_{C\text{-}F}$ = 2.8 Hz), 131.4 (d, $^3J_{C\text{-}F}$ = 8.3 Hz), 125.8, 124.7 (d, $^4J_{C\text{-}F}$ = 3.5 Hz), 121.6, 119.2 (d, $^2J_{C\text{-}F}$ = 14.6 Hz), 115.6 (d, $^2J_{C\text{-}F}$ = 21.3 Hz), 113.1, 109.2, 56.2, 56.1, 46.3, 42.8 (d, $^3J_{C\text{-}F}$ = 3.8 Hz), 26.2, 13.7.

N-(benzo[*d*][1,3]dioxol-4-ylmethyl)-2-(2,5-dimethoxy-4-(methylthio)phenyl)-ethanamine hydrochloride (2.32)

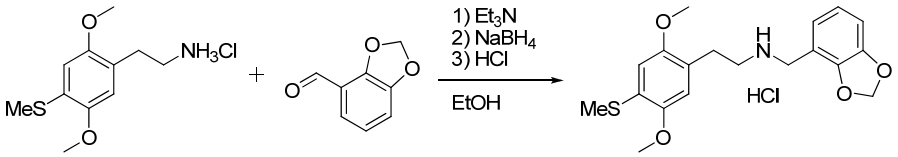

2.32

Obtained from 2C-T·HCl and 2,3-methylenedioxybenzaldehyde by general procedure A in 85% yield as a colorless solid. mp. 149-150 °C. ^{1}H NMR (600 MHz, DMSO-d_6) δ 9.57 (br s, 2H), 7.14 (dd, J = 7.9, 1.1 Hz, 1H), 6.97 (dd, J = 7.9, 1.1 Hz, 1H), 6.90 (t, J = 7.9 Hz, 1H), 6.84 (s, 1H), 6.75 (s, 1H), 6.07 (s, 2H), 4.09 (br t, J = 5.1 Hz, 2H), 3.78 (s, 3H), 3.76 (s, 3H), 3.10-3.04 (m, 2H), 2.97-2.93 (m, 2H), 2.40 (s, 3H). ^{13}C NMR (150 MHz, DMSO-d_6) δ 151.6, 149.5, 147.1, 146.3, 125.8, 123.4, 121.8, 121.5, 113.2, 113.1, 109.2, 109.1, 101.2, 56.2, 56.1, 46.1, 43.4, 26.2, 13.7.

2-(4-(ethylthio)-2,5-dimethoxyphenyl)-*N*-(2-methoxybenzyl)ethanamine hydrochloride (2.33)

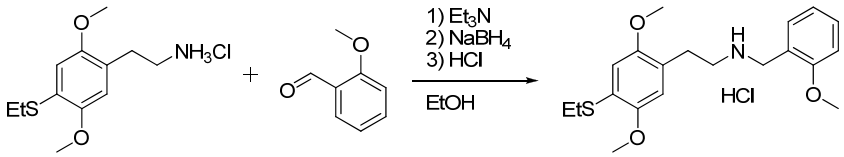

2.33

Obtained from 2C-T2·HCl and 2-methoxybenzaldehyde by general procedure A in 55% yield as a colorless solid. mp. 134-135 °C. ^{1}H NMR (600 MHz, DMSO-d_6) δ 9.18 (br s, 2H), 7.49 (dd, J = 7.5, 1.7 Hz, 1H), 7.41 (ddd, J = 8.3, 7.5, 1.7 Hz, 1H), 7.09 (br d, J = 8.3 Hz, 1H), 7.00 (td, J = 7.5, 1.0 Hz, 1H), 6.85 (s, 1H), 6.82 (s, 1H), 4.12 (br s, 2H), 3.83 (s, 3H), 3.75 (s, 3H), 3.75 (s, 3H), 3.07-3.02 (m, 2H), 2.97-2.93 (m, 2H), 2.92 (q, J = 7.3 Hz, 2H), 1.22 (t, J = 7.3 Hz, 3H). ^{13}C NMR (150 MHz, DMSO-

d_6) δ 157.5, 151.3, 150.3, 131.5, 130.8, 123.6, 122.6, 120.4, 119.7, 113.5, 111.2, 111.1, 56.2, 56.1, 55.6, 46.0, 44.8, 26.2, 24.8, 13.9.

2-((4-(ethylthio)-2,5-dimethoxyphenethylamino)methyl)phenol hydrochloride (2.34)

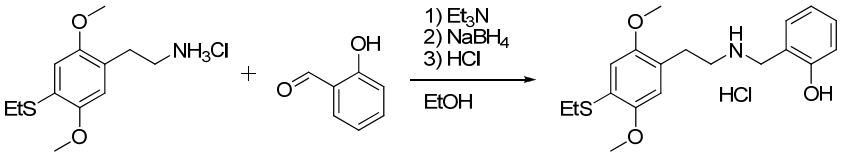

2.34

Obtained from 2C-T2 and salicylaldehyde in 69% yield as a colorless solid. mp. 190-192 °C. ^{1}H NMR (300 MHz, DMSO-d_6) δ 10.30 (s, 1H), 9.10 (br s, 2H), 7.40 (dd, J = 7.5, 1.5 Hz, 1H), 7.25-7.21 (m, 1H), 7.00-6.97 (m, 1H), 6.86-6.81 (m, 3H), 4.09 (br t, J = 5.0 Hz, 2H), 3.75 (s, 3H), 3.75 (s, 3H), 3.07-3.01 (m, 2H), 2.96-2.90 (m, 4H), 1.22 (t, J = 7.4 Hz, 3H). ^{13}C NMR (150 MHz, DMSO-d_6) δ 156.1, 151.3, 150.3, 131.6, 130.4, 123.6, 122.7, 119.0, 118.1, 115.4, 113.5, 111.2, 56.2, 56.1, 46.0, 44.9, 26.3, 24.8, 13.9.

2-(4-(ethylthio)-2,5-dimethoxyphenyl)-*N*-(2-fluorobenzyl)ethanamine hydrochloride (2.35)

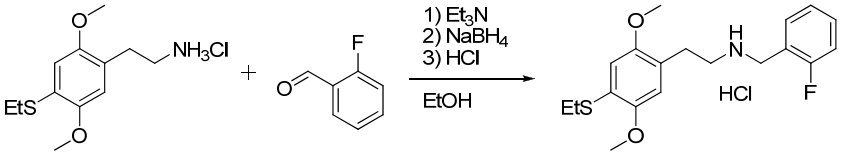

2.35

Obtained from 2C-T2·HCl and 2-fluorobenzaldehyde by general procedure A in 57% yield as a colorless solid. mp. 127-129 °C. ^{1}H NMR (600 MHz, DMSO-d_6) δ 9.68 (br s, 2H), 7.76 (td, J = 7.6, 1.6 Hz, 1H), 7.50-7.46 (m, 1H), 7.32-7.26 (m, 2H), 6.87 (s, 1H), 6.82 (s, 1H), 4.20 (br s, 2H), 3.76 (s, 3H), 3.75 (s, 3H), 3.13-3.07 (m, 2H), 3.00-2.96 (m, 2H), 2.92 (q, J = 7.4 Hz, 2H), 1.22 (t, J = 7.4 Hz, 3H). ^{13}C NMR (150 MHz, DMSO-d_6) δ 160.6 (d, $^1J_{CF}$ = 247 Hz), 151.4, 150.3, 132.5 (d, $^3J_{CF}$ = 2.8 Hz), 131.4 (d, $^3J_{CF}$ = 8.3 Hz), 124.7 (d, $^4J_{CF}$ = 3.4 Hz), 123.6, 122.6, 119.2 (d, $^2J_{CF}$ = 14.6 Hz), 115.6 (d, $^2J_{CF}$ = 21.3 Hz), 113.5, 111.2, 56.2, 56.1, 46.2, 42.8 (d, $^3J_{CF}$ = 3.9 Hz), 26.2, 24.8, 13.9.

N-(benzo[*d*][1,3]dioxol-4-ylmethyl)-2-(4-(ethylthio)-2,5-dimethoxyphenyl)-ethanamine hydrochloride (2.36)

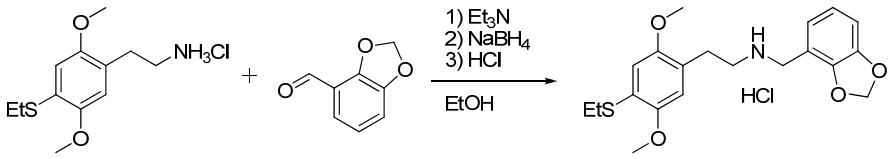

2.36

Obtained from 2C-T2·HCl and 2,3-methylenedioxybenzaldehyde by general procedure A in 69% yield as a colorless solid. mp. 149-151 °C. ^{1}H NMR (600 MHz, DMSO-d_6) δ 9.55 (br s, 2H), 7.13 (br d, J = 7.9 Hz, 1H), 6.97 (dd, J = 7.9, 1.1 Hz, 1H), 6.90 (t, J = 7.9 Hz, 1H), 6.86 (s, 1H), 6.82 (s, 1H), 6.07 (s, 2H), 4.09 (br t, J = 4.6 Hz, 2H), 3.76 (s, 3H), 3.75 (s, 3H), 3.11-3.05 (m, 2H), 2.97-2.93 (m,

2H), 2.92 (q, *J* = 7.3 Hz, 2H), 1.22 (t, *J* = 7.3 Hz, 3H). ^{13}C NMR (150 MHz, DMSO-d_6) δ 151.4, 150.3, 147.1, 146.3, 123.7, 123.4, 122.6, 121.8, 113.6, 113.1, 111.2, 109.1, 101.2, 56.2, 56.1, 46.0, 43.4, 26.3, 24.8, 13.9.

2-(2,5-dimethoxy-4-(propylthio)phenyl)-*N*-(2-methoxybenzyl)ethanamine hydrochloride (2.37)

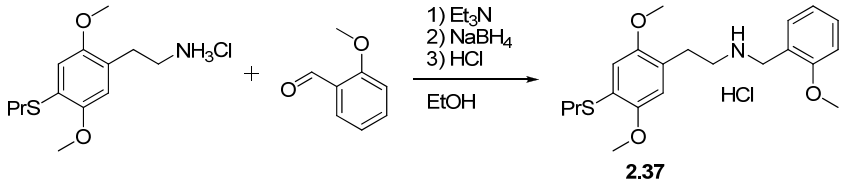

2.37

Obtained from 2C-T7·HCl and 2-methoxybenzaldehyde by general procedure A in 49% yield as a colorless solid. mp. 121-123 °C. ^{1}H NMR (600 MHz, DMSO-d_6) δ 9.19 (br s, 2H), 7.49 (dd, *J* = 7.6, 1.7 Hz, 1H), 7.41 (ddd, *J* = 8.3, 7.6, 1.7 Hz, 1H), 7.09 (br d, *J* = 8.3 Hz, 1H), 7.00 (td, *J* = 7.6, 1.0 Hz, 1H), 6.85 (s, 1H), 6.82 (s, 1H), 4.12 (br s, 2H), 3.83 (s, 3H), 3.75 (s, 3H), 3.75 (s, 3H), 3.07-3.02 (m, 2H), 2.97-2.93 (m, 2H), 2.89 (t, *J* = 7.3 Hz, 2H), 1.58 (sextuplet, *J* = 7.3 Hz, 2H), 0.98 (t, *J* = 7.3 Hz, 3H). ^{13}C NMR (150 MHz, DMSO-d_6) δ 157.5, 151.3, 150.4, 131.5, 130.8, 123.8, 122.6, 120.4, 119.7, 113.5, 111.3, 111.1, 56.2, 56.1, 55.6, 46.0, 44.8, 32.7, 26.2, 21.8, 13.3.

2-((2,5-dimethoxy-4-(propylthio)phenethylamino)methyl)phenol hydrochloride (2.38)

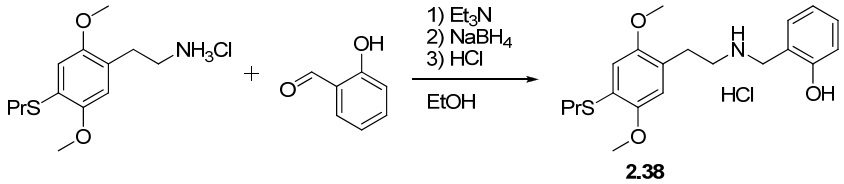

2.38

Obtained from 2C-T7·HCl and salicylaldehyde by general procedure A in 57% yield as a colorless solid. mp. 116-117 °C. ^{1}H NMR (600 MHz, DMSO-d_6) δ 10.31 (br s, 1H), 9.11 (br s, 2H), 7.40 (dd, *J* = 7.6, 1.7 Hz, 1H), 7.23 (ddd, *J* = 8.1, 7.6, 1.7 Hz, 1H), 6.99 (dd, *J* = 8.1, 1.0 Hz, 1H), 6.86-6.82 (m, 2H), 6.81 (s, 1H), 4.09 (br s, 2H), 3.75 (s, 6H), 3.06-3.02 (m, 2H), 2.96-2.92 (m, 2H), 2.88 (t, *J* = 7.3 Hz, 2H), 1.58 (sextuplet, *J* = 7.3 Hz, 2H), 0.97 (t, *J* = 7.3 Hz, 3H). ^{13}C NMR (150 MHz, DMSO-d_6) δ 156.1, 151.3, 150.4, 131.6, 130.4, 123.7, 122.7, 119.0, 118.1, 115.4, 113.5, 111.3, 56.2, 56.1, 46.0, 44.9, 32.7, 26.3, 21.8, 13.3.

2-(2,5-dimethoxy-4-(propylthio)phenyl)-*N*-(2-fluorobenzyl)ethanamine hydrochloride (2.39)

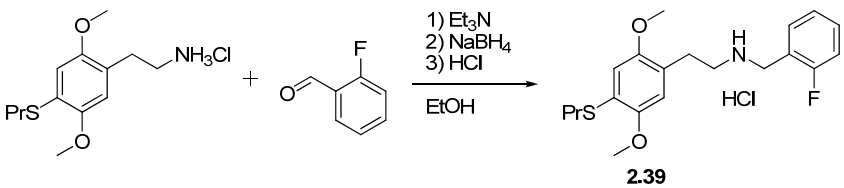

2.39

Obtained from 2C-T7·HCl and 2-fluorobenzaldehyde by general procedure A in 67% yield as a colorless solid. mp. 100-101 °C. ^{1}H NMR (600 MHz, DMSO-d_6) δ 9.74 (br s, 2H), 7.78 (td, *J* = 7.5, 1.6 Hz, 1H), 7.50-7.46 (m, 1H), 7.31-7.26 (m, 2H), 6.87 (s, 1H), 6.81 (s, 1H), 4.20 (br s, 2H), 3.75 (s,

6H), 3.12-3.07 (m, 2H), 3.00-2.96 (m, 2H), 2.88 (t, *J* = 7.3 Hz, 2H), 1.58 (sextuplet, *J* = 7.3 Hz, 2H), 0.97 (t, *J* = 7.3 Hz, 3H). ^{13}C NMR (150 MHz, DMSO-d_6) δ 160.6 (d, $^{1}J_{CF}$ = 247 Hz), 151.3, 150.4, 132.5 (d, $^{3}J_{CF}$ = 2.8 Hz), 131.4 (d, $^{3}J_{CF}$ = 8.3 Hz), 124.7 (d, $^{4}J_{CF}$ = 3.4 Hz), 123.8, 122.6, 119.2 (d, $^{2}J_{CF}$ = 14.6 Hz), 115.6 (d, $^{2}J_{CF}$ = 21.4 Hz), 113.5, 111.3, 56.2, 56.1, 46.2, 42.8 (d, $^{3}J_{CF}$ = 3.9 Hz), 32.7, 26.2, 21.8, 13.3.

N-(benzo[*d*][1,3]dioxol-4-ylmethyl)-2-(2,5-dimethoxy-4-(propylthio)phenyl)-ethanamine hydrochloride (2.40)

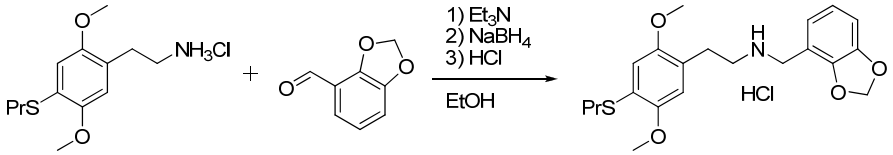

2.40

Obtained from 2C-T7·HCl and 2,3-methylenedioxybenzaldehyde by general procedure A in 28% yield as an off-white solid. mp. 116-117 °C. ^{1}H NMR (600 MHz, DMSO-d_6) δ 9.49 (br s, 2H), 7.12 (dd, *J* = 7.9, 1.1 Hz, 1H), 6.98 (dd, *J* = 7.9, 1.1 Hz, 1H), 6.90 (t, *J* = 7.9 Hz, 1H), 6.85 (s, 1H), 6.81 (s, 1H), 6.07 (s, 2H), 4.10 (br s, 2H), 3.75 (s, 6H), 3.11-3.06 (m, 2H), 2.96-2.92 (m, 2H), 2.88 (t, *J* = 7.3 Hz, 2H), 1.58 (sextuplet, *J* = 7.3 Hz, 2H), 0.98 (t, *J* = 7.3 Hz, 3H). ^{13}C NMR (150 MHz, DMSO-d_6) δ 151.3, 150.4, 147.1, 146.3, 123.8, 123.3, 122.5, 121.8, 113.6, 113.1, 111.3, 109.2, 101.2, 56.2, 56.1, 46.1, 43.5, 32.6, 26.3, 21.8, 13.3.

2-(2,5-dimethoxy-4-(trifluoromethyl)phenyl)-*N*-(2-methoxybenzyl)ethanamine hydrochloride (2.41)

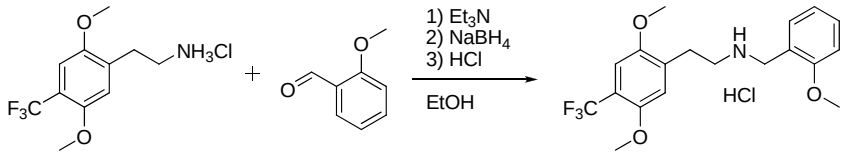

2.56 **2.41**

Obtained from 2C-TFM·HCl and 2-methoxybenzaldehyde by general procedure A in 77% yield as a colorless solid. mp. 204-205°C. ^{1}H NMR (300 Mhz, DMSO-d_6) δ 9.39 (br s, 2H), 7.49-7.54 (m, 1H), 7.36-7.42 (m, 1H), 7.18 (s, 1H) , 7.11 (s, 1H), 7.04-7.09 (m, 1H), 6.95-7.01 (m, 1H), 4.12 (s, 2H), 3.84 (s ,3H), 3.83 (s ,3H), 3.79 (s, 3H), 3.09 (s, 4H). ^{13}C NMR (75 MHz, DMSO-d_6) δ 157.3, 150.6, 150.3, 131.3, 131.1, 130.6, 123.5 (q, $^{1}J_{CF}$ = 271.6 Hz), 120.2, 119.6, 115.5, 115.4 (q, $^{2}J_{CF}$ = 30.3 Hz), 110.9, 109.0 (d, $^{3}J_{CF}$ = 5.5 Hz), 56.5, 56.1, 55.6, 45.5, 44.7, 26.5

2-((2,5-dimethoxy-4-(trifluoromethyl)phenethylamino)methyl)phenol hydrochloride (2.42)

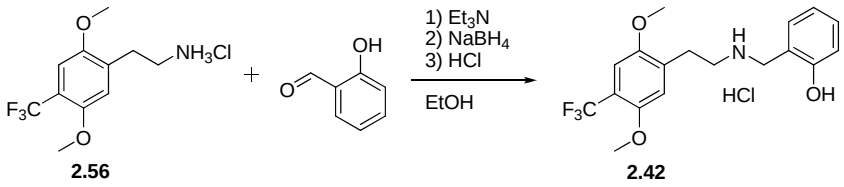

2.56 **2.42**

Obtained from 2C-TFM·HCl and salicylaldehyde by general procedure A in 69% yield as a colorless solid. mp. 209-210 °C. ^{1}H NMR (300 MHz, DMSO) δ 10.30 (s, 1H), 9.20 (br s, 2H), 7.41 (dd, *J* = 7.5, 1.6 Hz, 1H), 7.21 (ddd, 8.1, 7.4, 1.7 Hz, 1H), 7.15 (s, 1H), 7.11 (s, 1H), 6.98 (dd, *J* = 8.1, 1.1 Hz, 1H), 6.82 (ddd, *J* = 7.5, 7.4, 1.1 Hz, 1H), 4.09 (s, 2H), 3.84 (s, 3H), 3.79 (s, 3H), 3.07 (s, 4H). ^{13}C NMR (75 MHz, DMSO) δ 155.9, 150,6 (q, $^{3}J_{CF}$ = 1.6 Hz), 150.3, 131.5, 131.1, 130.2, 123.5 (q, $^{1}J_{CF}$ = 271.7 Hz) 115.5, 115.5 (q, $^{2}J_{CF}$ = 30.3 Hz) 115.3, 109.0 (q, *J* = 5.1 Hz), 56.5, 56.1, 45.5, 44.9, 26.5.

2-(2,5-dimethoxy-4-(trifluoromethyl)phenyl)-*N*-(2-fluorobenzyl)ethanamine hydrochloride (2.43)

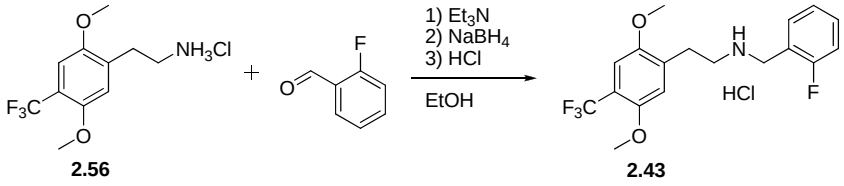

2.56 **2.43**

Obtained from 2C-TFM and 2-fluorobenzaldehyde by general procedure A in 71% yield as a colorless solid. mp. 186-188 °C. ^{1}H NMR ($CDCl_3$) δ 9.72 (bs, 2H), 7.72-7.79 (m, 1H), 7.42-7.51 (m, 1H), 7.23-7.32 (m, 2H), 7.17 (s, 1H), 7.12 (s, 1H), 4.21 (s, 2H), 3.84 (s, 3H), 3.79 (s, 3H), 3.04-3.22 (m, 4H) ^{13}C NMR (75 MHz, DMSO-d_6) δ 160.4 (d, $^{1}J_{CF}$ = 246.6 Hz), 150.6 (q, $^{3}J_{CF}$ = 1.8 Hz), 150.3, 132.3 (d, $^{3}J_{CF}$ = 3.0 Hz), 131.3 (d, $^{3}J_{CF}$ = 8.3 Hz), 131.0, 124.5 (d, $^{4}J_{CF}$ = 3.6 Hz), 123.5 (q, $^{1}J_{CF}$ = 271.7 Hz), 119.0 (d, $^{2}J_{CF}$ = 14.5 Hz), 115.5, 115.5 (q, $^{2}J_{CF}$ = 30.3 Hz), 115.4 (d, $^{2}J_{CF}$ = 21.4 Hz), 109.0 (q, $^{3}J_{CF}$ = 5.5 Hz) 56.5, 56.2, 45.7, 42.9, 26.5

N-(benzo[*d*][1,3]dioxol-4-ylmethyl)-2-(2,5-dimethoxy-4-(trifluoromethyl)phenyl)-ethanamine hydrochloride (2.44)

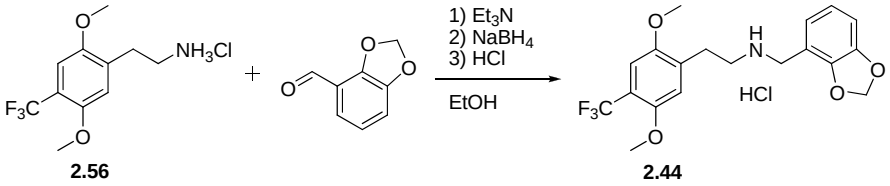

2.56 **2.44**

Obtained from 2C-TFM·HCl and 2,3-methylenedioxybenzaldehyde by general procedure A in 67% yield as a colorless solid. mp. 188-189 °C. ^{1}H NMR (300 Mhz, DMSO-d_6) δ 9.72 (br s, 2H) , 7.18 (s, 1H), 7.16 (dd, 7.7, 1.3 Hz, 1H), 7.11 (s, 1H), 6.95 (dd, *J* = 7.7, 1.3 Hz, 1H), 6.88 (t, *J* = 7.7 Hz, 1H), 6.05 (s, 2H), 4.09 (s, 2H), 3.84 (s, 3H), 3.79 (s, 3H), 3.02-3.21 (m, 4H). ^{13}C NMR (75 MHz, DMSO) δ 150.6 (q, $^{3}J_{CF}$ = 1.9 Hz), 150.3, 146.9, 146.1, 131.0, 123.5 (q, $^{1}J_{CF}$ = 271.7 Hz), 123.3,

121.6, 115.5, 115.5 (q, $^{2}J_{CF}$ = 30.6 Hz), 113.0, 109.0, 109.0 (d, $^{3}J_{CF}$ = 5.4 Hz), 101.1, 56.5, 56.1, 45.5, 43.4, 26.5

2,5-dimethoxy-4-(2-(2-methoxybenzylamino)ethyl)benzonitrile hydrochloride (2.45)

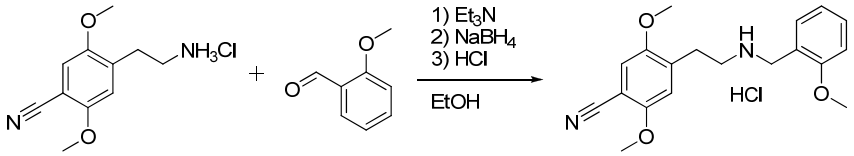

2.45

Obtained from 2C-CN·HCl and 2-methoxybenzaldehyde by general procedure A in 72% yield as a colorless solid. mp. 204-205 °C. ^{1}H NMR (300 Mhz, DMSO-d_6) δ 9.38 (br s, 2H), 7.50 (d, *J* = 7.3 Hz, 1H), 7.39 (dd, 8.3, 7.5 Hz, 1H), 7.33 (s, 1H), 7.15 (s, 1H), 7.07 (d, *J* = 8.3 Hz, 1H), 6.98 (dd, *J* = 7.5, 7.3 Hz, 1H), 4.11(s, 2H), 3.87 (s, 3H), 3.82 (s, 3H), 3.77 (s, 3H), 3.08 (s, 4H). 13C NMR (75 MHz, DMSO-d_6) δ 157.3, 155.0, 150.7, 132.9, 131.3, 130.6, 120.2, 119.5, 116.3, 114.7, 114.4, 111.0, 98.3, 56.5, 56.3, 55.6, 45.3, 44.7, 26.8

4-(2-(2-hydroxybenzylamino)ethyl)-2,5-dimethoxybenzonitrile hydrochloride (2.46)

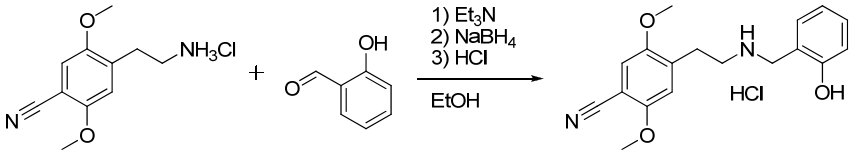

2.42

Obtained from 2C-CN·HCl and salicylaldehyde by general procedure A in 75% yield as a colorless solid. mp. 216-218 °C. ^{1}H NMR (300 Mhz, DMSO-d_6) δ 10.31 (s, 1H), 9.25 (br s, 2H), 7.41 (dd, *J* = 7.5, 1.6 Hz, 1H), 7.20 (ddd, *J* = 8.2, 7.4, 1.6 Hz, 1H), 7.31 (s, 1H), 7.14 (s, 1H), 6.99 (dd, *J* = 8.2, 0.9 Hz, 1H), 6.81 (ddd, *J* = 7.5, 7.4, 0.9 Hz, 1H), 4.08 (s, 2H), 3.86 (s, 3H), 3.76 (s, 3H), 3.07 (s, 4H). ^{13}C NMR (75 MHz, DMSO-d_6) δ 155.9, 155.0, 150.7, 133.0, 131.5, 130.2, 118.9, 117.9, 116.3, 115.3, 114.7, 114.5, 98.3, 56.5, 56.3, 45.3, 44.9, 26.9

4-(2-(2-fluorobenzylamino)ethyl)-2,5-dimethoxybenzonitrile hydrochloride (2.47)

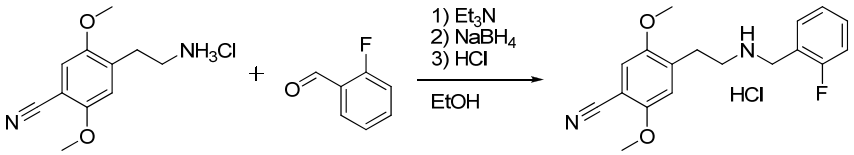

2.47

Obtained from 2C-CN·HCl and 2-fluorobenzaldehyde by general procedure A in 78% yield as a colorless solid. mp. 195-196 °C. ^{1}H NMR (300 Mhz, DMSO-d_6) δ 9.74 (br s, 2H), 7.76 (td, *J* = 7.6, 1.5 Hz, 1H), 7.51-7.41 (m, 1H), 7.33 (s, 1H), 7.31-7.23 (m, 2H) 7.17 (s, 1H), 4.20 (s, 2H), 3.87 (s, 3H), 3.77 (s, 3H), 3.23-3.04 (m, 4H). ^{13}C NMR (75 MHz, DMSO-d_6) δ 160.3 (d, $^{1}J_{CF}$ = 246.7 Hz), 155.0, 150.7, 132.3 (d, $^{3}J_{CF}$ = 2.8 Hz), 131.4 (d, $^{3}J_{CF}$ = 8.3 Hz), 124.6, 119.0 (d, $^{3}J_{CF}$ = 14.5 Hz), 116.3, 115.4 (d, $^{2}J_{CF}$ = 21.2 Hz), 114.6 (d, $^{2}J_{CF}$ = 19.1 Hz), 98.3, 56.5, 56.3, 45.6, 42.9, 26.8.

4-(2-(benzo[*d*][1,3]dioxol-4-ylmethylamino)ethyl)-2,5-dimethoxybenzonitrile hydrochloride (2.48)

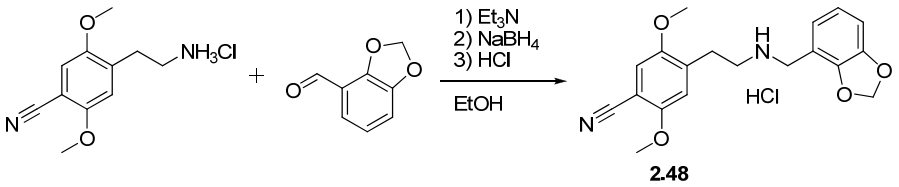

2.48

Obtained from 2C-CN·HCl and 2,3-methylenedioxybenzaldehyde by general procedure A in 71% yield as a colorless solid. mp. 214-215 °C. ^{1}H NMR (300 Mhz, DMSO-d_6) δ 9.67 (br s, 2H), 7.33 (s, 1H), 7.16 (s, 1H), 7.14 (dd, *J* = 7.9, 1.3 Hz, 1H), 6.95 (dd, *J* = 7.8, 1.3 Hz, 1H), 6.88 (dd, *J* = 7.9, 7.8 Hz, 1H), 6.05 (s, 2H), 4.08 (s, 2H), 3.87 (s, 3H), 3.77 (s, 3H), 3.21-3.01 (m, 4H). ^{13}C NMR (75 MHz, DMSO-d_6) δ 155.0, 150.8, 146.9, 146.1, 132.8, 123.2, 121.7, 116.3, 114.7, 114.5, 113.0, 109.0, 101.1, 98.3, 56.5, 56.3, 45.3, 43.5, 26.9

8.3 Experimental – Chapter 3

2-(4-bromo-2,5-dimethoxyphenyl)-*N*-(2,3-dimethoxybenzyl)ethanamine hydrochloride (3.1)

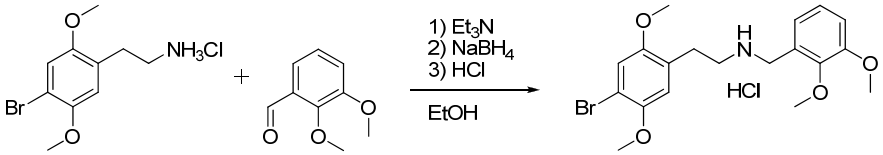

3.1

Obtained from 2C-B·HCl and 2,3-dimethoxybenzaldehyde by general procedure A in 69% yield as a colorless solid. mp. 119-120 °C. ^{1}H NMR (300 MHz, DMSO-d_6) δ 9.50 (br s, 2H), 7.23-7.16 (m, 2H), 7.12-1.08 (m, 2H), 7.01 (s, 1H), 4.12 (s, 2H), 3.82 (s, 3H), 3.79 (s, 3H), 3.79 (s, 3H) 3. 3.73 (s, 3H), 3.12-2.94 (m, 4H). ^{13}C NMR (75 MHz, DMSO-d_6) δ 152.0, 151.3, 149.2, 146.9, 125.4, 125.2, 124.0, 122.2, 115.7, 114.8, 113.6, 108.7, 60.5, 56.6, 56.2, 55.8, 45.8, 44.1, 26.3

2-(4-bromo-2,5-dimethoxyphenyl)-*N*-(2,4-dimethoxybenzyl)ethanamine hydrochloride (3.2).

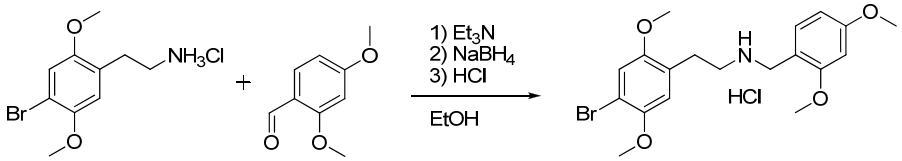

3.2

Obtained from 2C-B·HCl and 2,4-dimethoxybenzaldehyde by general procedure A in 88% yield as a colorless solid. mp. 167-168 °C. ^{1}H NMR (300 MHz, DMSO-d_6) δ 9.29 (br s, 1H), 7.41 (d, *J* = 8.3 Hz, 1H), 7.16 (s, 1H), 7.00 (s, 1H), 6.60 (d, *J* = 2.3 Hz, 1H), 6.54 (dd, *J* = 8.3, 2.3 Hz, 1H), 4.02 (s,2H), 3.81 (s, 3H), 3.78 (s, 3H), 3.77 (s,3H), 3.73 (s, 3H), 2.98 (s, 4H). ^{13}C NMR (75 MHz, DMSO-d_6) δ 161.3, 158.5, 151.3, 149.2, 132.4, 125.5, 115.7, 114.8, 111.7, 108.7, 104.8, 98.2, 56.6, 56.2, 55.7, 55.4, 45.2, 44.2, 26.3

2-(4-bromo-2,5-dimethoxyphenyl)-*N*-(2,5-dimethoxybenzyl)ethanamine hydrochloride (3.3)

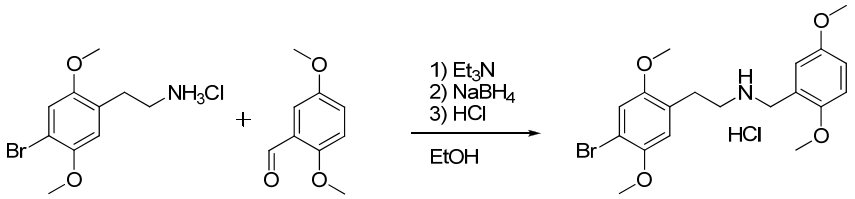

3.3

Obtained from 2C-B·HCl and 2,5-dimethoxybenzaldehyde by general procedure A in 71% yield as a colorless solid. mp. 150-151 °C. ^{1}H NMR (300 MHz, DMSO-d_6) δ 9.41 (br s, 2H), 7.23 (d, *J* = 2.9 Hz, 1H), 7.17 (s, 1H), 7.01 (s, 1H), 6.99 (d, *J* = 9.0 Hz, 1H), 6.93 (dd, *J* = 9.0, 2.9 Hz, 1H), 4.08 (s, 2H), 3.79 (s, 3H), 3.76 (s, 3H), 3.73 (s, 3H), 3.72 (s, 3H), 3.10-2.93 (m, 4H). ^{13}C NMR (75 MHz,

DMSO-d_6) δ 152.7, 151.3, 151.2, 149.2, 125.4, 120.4, 117.1, 115.7, 114.9, 114.8, 111.9, 108.7, 56.6, 56.2, 56.0, 55.5, 45.6, 44.4, 26.3

2-(4-bromo-2,5-dimethoxyphenyl)-*N*-(2,6-dimethoxybenzyl)ethanamine hydrochloride (3.4)

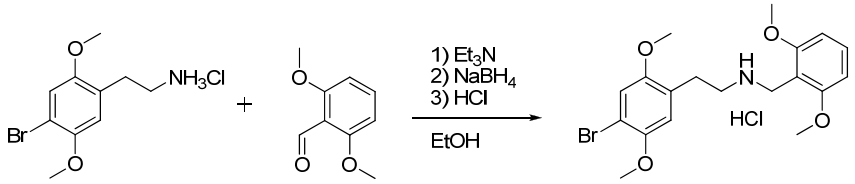

3.4

Obtained from 2C-B·HCl and 2,6-dimethoxybenzaldehyde by general procedure A in 56% yield as a colorless solid. mp. 193-194 °C. ^{1}H NMR (300 MHz, DMSO-d_6) δ 9.07 (br s, 2H), 7.36 (t, *J* = 8.4 Hz, 1H), 7.16 (s, 1H), 6.97 (s, 1H), 6.71 (d, *J* = 8.4 Hz, 2H), 4.08 (s, 2H), 3.81 (s, 6H), 3.78 (s, 3H), 3.73 (s, 3H), 2.97 (s, 4H). ^{13}C NMR (75 MHz, DMSO-d_6) δ 158.4 (2C), 151.2, 149.2, 131.1, 125.4, 115.7, 114.7, 108.7, 106.9, 103.8 (2C), 56.6, 56.2, 55.9 (2C), 45.5, 38.6, 26.3

2-((4-bromo-2,5-dimethoxyphenethylamino)methyl)-6-methoxyphenol hydrochloride (3.5)

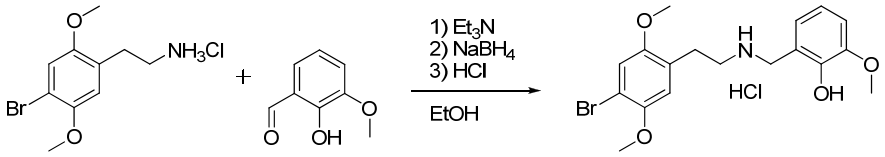

3.5

Obtained from 2C-B·HCl and 2-hydroxy-3-methoxybenzaldehyde by general procedure A in 69% yield as an off-white solid. mp. 205-206 °C. ^{1}H NMR (300 MHz, DMSO-d_6) δ 9.31 (br s, 2H), 7.16 (s, 1H), 7.05 (dd, *J* = 7.7, 1.3 Hz, 1H), 6.99 (dd, *J* = 8.1, 1.3 Hz, 1H), 6.99 (s, 1H), 6.80 (dd, *J* = 8.1, 7.7 Hz, 1H), 4.09 (s, 2H), 3.81 (s, 3H), 3.78 (s, 3H), 3.73 (s, 3H), 3.09-2.91 (m, 4H). ^{13}C NMR (75 MHz, DMSO-d_6) δ 151.3, 149.2, 147.5, 144.9, 125.4, 122.9, 118.9, 118.5, 115.7, 114.8, 112.4, 108.7, 56.6, 56.2, 55.9, 45.6, 44.4, 26.4

2-(4-bromo-2,5-dimethoxyphenyl)-*N*-(2-fluoro-3-methoxybenzyl)ethanamine hydrochloride (3.6)

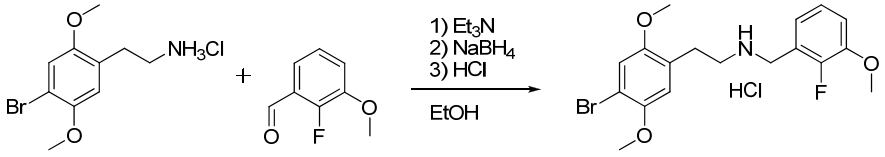

3.6

Obtained from 2C-B·HCl and 2-fluoro-3-methoxybenzaldehyde by general procedure A in 72% yield as a colorless solid. mp. 170-171 °C. ^{1}H NMR (300 MHz, DMSO-d_6) δ 9.68 (br s, 2H), 7.31-7.14 (m, 3H), 7.17 (s, 1H), 7.02 (s, 1H), 4.18 (s, 2H), 3.85 (s, 3H), 3.78 (s, 3H), 3.74 (s, 3H), 3.17-2.94 (m, 4H). ^{13}C NMR (75 MHz, DMSO) δ 151.5, 150.1 (d, $^1J_{CF}$ = 247.2 Hz), 149.3, 147.2 (d, $^2J_{CF}$ =

10.4 Hz), 125.4, 124.5 (d, $^{3}J_{CF}$ = 4.6 Hz), 122.8, 119.8 (d,$^{2}J_{CF}$ = 11.8 Hz), 115.8, 115.0, 114.5, 108.9, 56.6, 56.2, 56.2, 45.9, 42.7 (d, $^{3}J_{CF}$ = 4.8 Hz), 26.3

N-((1*H*-indol-7-yl)methyl)-2-(4-bromo-2,5-dimethoxyphenyl)ethanamine hydrochloride (3.7)

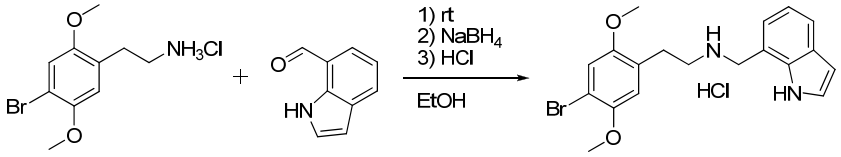

3.7

Obtained from 2C-B·HCl and 1*H*-indole-7-carbaldehyde by general procedure A in 59% yield as a light pink solid. mp. 228-229 °C. ^{1}H NMR (300 Mhz, DMSO-d_6) δ 11.81 (s, 1H), 9.45 (br s, 2H), 7.59 (d, *J* = 7.8 Hz, 1H), 7.43 (dd, *J* = 3.0, 2.5 Hz, 1H), 7.32 (dd, *J* = 7.3, 0.9 Hz, 1H), 7.16 (s, 1H), 7.03 (dd, *J* = 7.8, 7.3 Hz, 1H), 7.00 (s, 1H), 6.50 (dd, *J* = 3.0, 1.7 Hz, 1H), 4.50 (s, 2H), 3.78 (s, 3H), 3.71 (s, 3H), 3.25-3.11 (m, 2H), 3.05-2.93 (m, 2H). ^{13}C NMR (75 MHz, DMSO) δ 151.3, 149.2, 134.8, 128.1, 125.6, 125.4, 123.5, 121.0, 118.7, 115.7, 114.8, 108.7, 101.6, 56.6, 56.2, 46.4, 45.8, 26.5

N-(benzofuran-7-ylmethyl)-2-(4-bromo-2,5-dimethoxyphenyl)ethanamine hydrochloride (3.8)

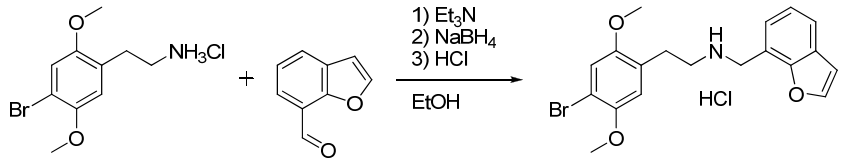

3.32 3.8

Obtained from 2C-B·HCl and **3.32** by general procedure in 77% yield as a colorless solid. mp. 200-202 °C. ^{1}H NMR (300 Mhz, DMSO-d_6) δ 9.80 (br s,2H), 8.09 (d, *J* = 2.2 Hz, 1H), 7.70 (dd, *J* = 7.7, 1.0 Hz, 1H), 7.65 (dd, *J* = 7.5, 1.0 Hz, 1H), 7.30 (dd, *J* = 7.7, 7.5 Hz, 1H), 7.17 (s, 1H), 7.03 (d, *J* = 2.5 Hz, 1H), 7.01 (s, 1H), 4.44 (s, 2H), 3.78 (s, 3H), 3.72 (s, 3H), 3.21-3.09 (m, 2H), 3.06-2.97 (m, 2H). ^{13}C NMR (75 MHz, DMSO-d_6) δ 152.5, 151.3, 149.2, 146.1, 127.3, 125.8, 125.3, 122.9, 122.1, 115.7, 115.5, 114.8, 108.8, 107.1, 56.6, 56.2, 45.9, 43.7, 26.4

N-(benzo[*b*]thiophen-7-ylmethyl)-2-(4-bromo-2,5-dimethoxyphenyl)ethanamine hydrochloride (3.9)

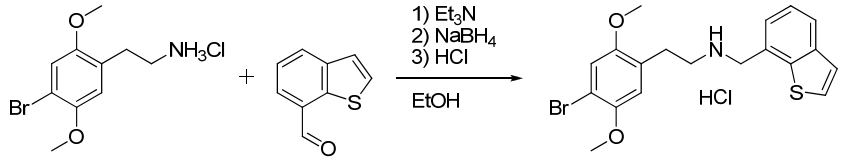

3.33 3.9

Obtained from 2C-B·HCl and **3.33** by general procedure in 55% yield as fluffy colorless crystals. mp. 219-220 °C. ^{1}H NMR (300 MHz, DMSO-d_6) δ 9.64 (br s, 1H), 7.92 (d, *J* = 7.8 Hz, 1H), 7.80 (d, *J* = 5.4 Hz, 1H), 7.70 (d, *J* = 7.2 Hz, 1H), 7.53 (d, *J* = 5.4 Hz, 1H), 7.47 (dd, *J* = 7.8, 7.2 Hz, 1H), 7.14 (s, 1H), 7.01 (s, 1H), 4.41 (s, 2H), 3.79 (s, 3H), 3.73 (s, 3H), 3.28-3.15 (m, 2H), 3.08-2.94 (m, 2H). ^{13}C

NMR (75 MHz, DMSO-d_6) δ 151.3, 149.2, 139.9, 139.3, 127.1, 126.1, 125.1, 125.0, 124.5 (2C), 124.1, 115.6, 114.8, 108.9, 56.6, 56.1, 48.7, 46.4, 26.5

N-((1*H*-indazol-7-yl)methyl)-2-(4-bromo-2,5-dimethoxyphenyl)ethanamine hydrochloride (3.10)

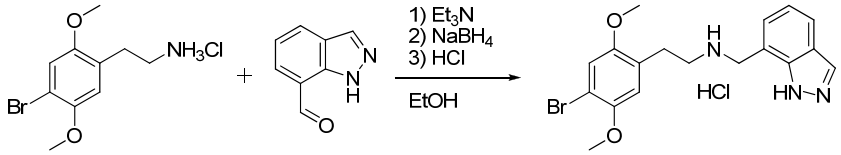

Obtained from 2C-B·HCl and **3.10** by general procedure A in 80% yield as a colorless solid. mp. 207-209 °C. ^{1}H NMR (300 Mhz, DMSO-d_6) δ 9.60 (br s, 2H), 8.14 (s, 1H), 7.80 (d, *J* = 8.1 Hz, 1H), 7.59 (d, *J* = 7.0 Hz, 1H), 7.15 (s, 1H), 7.14 (dd, *J* = 8.0, 7.1 Hz, 1H), 7.00 (s, 1H), 4.55 (s, 2H), 3.77 (s, 3H), 3.70 (s, 3H), 3.24-3.11 (m, 2H), 3.04-2.94 (m, 2H). ^{13}C NMR (75 MHz, DMSO-d_6) δ 151.3, 149.2, 139.2, 133.7, 128.5, 125.4, 123.2, 121.6, 120.2, 115.8, 114.8, 114.3, 108.8, 56.6, 56.2, 46.2, 45.9, 26.6

2-(4-bromo-2,5-dimethoxyphenyl)-*N*-((2,3-dihydrobenzofuran-7-yl)methyl)ethanamine hydrochloride (3.11)

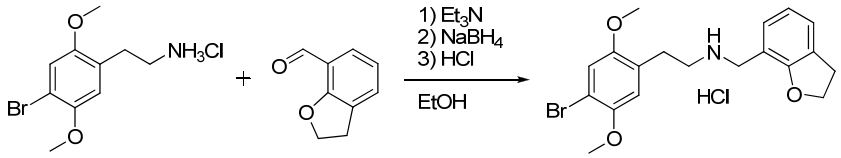

Obtained from 2C-B·HCl and **3.23** by general procedure A in 73% yield as a colorless solid. mp. 208-210 °C. ^{1}H NMR (300 Mhz, DMSO-d_6) δ 9.51 (br s, 2H), 7.36 (dd, *J* = 7.5, 0.9 Hz, 1H), 7.25 (dd, *J* = 7.3, 0.9 Hz, 1H), 7.17 (s, 1H), 7.01 (s, 1H), 6.85 (dd, *J* = 7.5, 7.3 Hz, 1H), 4.56 (t, *J* = 8.7 Hz, 2H), 4.04 (s, 2H), 3.78 (s, 3H), 3.73 (s, 3H), 3.21 (t, *J* = 8.7 Hz, 2H), 3.12-2.92 (m, 4H). ^{13}C NMR (75 MHz, DMSO-d_6) δ 158.2, 151.3, 149.2, 129.2, 127.4, 125.7, 125.3, 120.3, 115.7, 114.8, 112.9, 108.7, 71.3, 56.6, 56.2, 45.5, 44.0, 29.2, 26.4

N-((1*H*-benzo[*d*]imidazol-7-yl)methyl)-2-(4-bromo-2,5-dimethoxyphenyl)ethanamine hydrochloride (3.13)

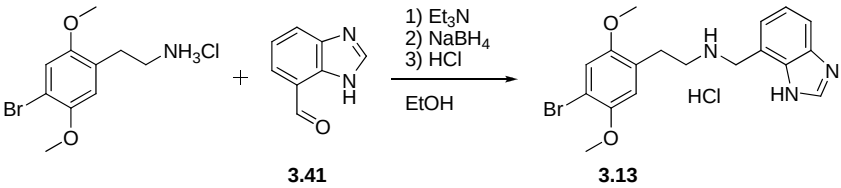

Obtained from 2C-B·HCl and **3.41** by general procedure A in 72% yield as a colorless solid. mp. 256-258 °C. ^{1}H NMR (300 MHz, DMSO-d_6) δ 9.82 (br s, 2H), 9.75 (s, 1H), 7.91–7.84 (m, 2H), 7.59 (dd, *J* = 8.0, 7.8 Hz, 1H), 7.16 (s, 1H), 7.04 (s, 1H), 4.71 (s, 2H), 3.78 (s, 3H), 3.73 (s, 3H), 3.31-3.19 (m, 2H), 3.07-2.96 (m, 2H). ^{13}C NMR (75 MHz, DMSO-d_6) δ 151.3, 149.2, 140.2, 130.8, 130.7, 128.3, 125.8, 125.3, 119.0, 115.7, 115.1, 114.8, 108.7, 56.6, 56.3, 45.9, 45.3, 26.5

N-(benzo[*d*]oxazol-7-ylmethyl)-2-(4-bromo-2,5-dimethoxyphenyl)ethanamine hemioxalate (3.14)

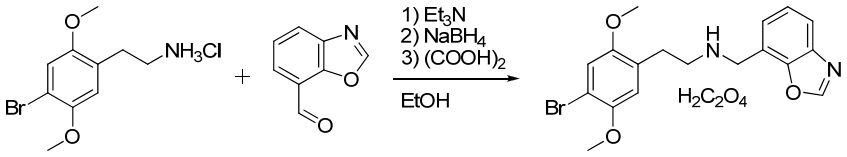

3.61 3.14

To a suspension of 2C-B·HCl (0.178 g, 0.6 mmol) and **3.61** (0.103 g, 0.7 mmol) in EtOH (10 mL) was added Et_3N (0.6 mmol) and the reaction was stirred until formation of the imine was complete according to TLC or GC (3 hours). $NaBH_4$ (1.2 mmol) was added to the reaction which was stirred for another 30 minutes. The reaction mixture was evaporated under reduced pressure and redissolved in EtOAc/H_2O (30 mL, 1:1). The organic layer was isolated and the aqueous layer was extracted with EtOAc (2 × 15 mL). The combined organic extracts were dried (Na_2SO_4), filtered and evaporated under reduced pressure. The residue was purified by radial chromatography (CH_2Cl_2/MeOH/NH_3 98:2:0.04). The purified free base was dissolved in EtOH (2 mL) and dripped slowly into a saturated solution of oxalic acid in Et_2O (10 mL). The formed precipitate was isolated by filtration and recrystallized from EtOH to give the title compound, **3.14** (0.167 g, 58%) as tan crystals. mp. 201 °C dec. ^{1}H NMR (300 Mhz, DMSO-d_6) δ 9.53 (br s, 3H), 8.83 (s, 1H), 7.83 (d, *J* = 7.8 Hz, 1H), 7.60 (d, *J* = 7.4 Hz, 1H), 7.45 (dd, *J* = 7.8, 7.4 Hz, 1H), 7.16 (s, 1H), 6.98 (s, 1H), 4.46 (s, 1H), 3.77 (s, 2H), 3.72 (s, 1H), 3.20-3.11 (m, 1H), 2.97-2.88 (m, 1H). ^{13}C NMR (75 MHz, DMSO-d_6) δ 164.4 (2C, oxalate), 154.1, 151.3, 149.2, 148.1, 139.6, 126.8, 125.5, 124.7, 120.6, 116.5, 115.7, 114.9, 108.7, 56.6, 56.2, 46.2, 44.2, 26.8

2-(4-bromo-2,5-dimethoxyphenyl)-*N*-(pyridin-2-ylmethyl)ethanamine dihydrochloride (3.16)

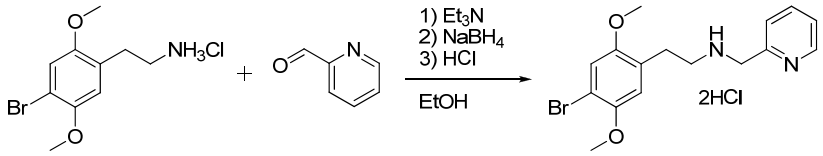

3.16

Obtained from 2C-B·HCl and picolinaldehyde by general procedure A in 76% yieldas a colorless solid. mp. 187-189 °C. ^{1}H NMR (300 Mhz, DMSO-d_6) δ 10.02 (br s, 1H), 9.97 (br s, 2H), 8.73 (ddd, *J* = 5.1, 1.7, 0.8 Hz, 1H), 8.15 (ddd, *J* = 7.8, 7.6, 1.7 Hz, 1H), 7.91 (ddd, *J* = 7.9, 1.2, 0.8 Hz, 1H), 7.64 (ddd, *J* = 7.6, 5.1, 1.2 Hz, 1H), 7.17 (s, 1H), 7.03 (s, *J* = 4.7 Hz, 1H), 4.44 (s, 2H), 3.78 (s, 3H), 3.74 (s, 3H), 3.25-3.11 (m, 2H), 3.07-2.97 (m, 2H). ^{13}C NMR (75 MHz, DMSO-d_6) δ 151.3, 150.0, 149.2, 146.4, 140.3, 125.3, 125.2, 124.8, 115.7, 114.9, 108.8, 56.7, 56.3, 48.7, 46.2, 26.4

2-(4-bromo-2,5-dimethoxyphenyl)-*N*-(pyridin-3-ylmethyl)ethanamine dihydrochloride (3.17)

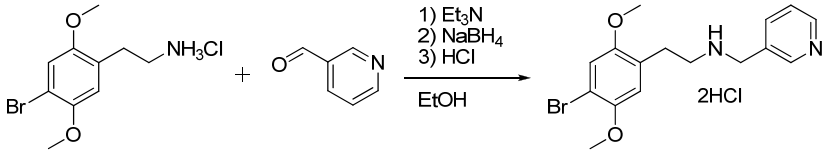

3.17

Obtained from 2C-B·HCl and nicotinaldehyde by general procedure A in 81% yield as an off-white solid. mp. 207-210 °C. ^{1}H NMR (300 Mhz, DMSO-d_6) δ 10.22 (br s, 1H), 10.17 (br s, 2H), 9.13 (dd, *J* = 1.9, 1.5 Hz, 1H), 8.91 (dd, *J* = 5.6, 1.5 Hz, 1H), 8.79 (ddd, *J* = 8.1, 1.9, 0.5 Hz, 1H), 8.05 (ddd, *J* = 8.1, 5.6, 0.5 Hz, 1H), 7.17 (s, 1H), 7.04 (s, 1H), 4.41 (s, 2H), 3.78 (s, 3H), 3.75 (s, *J* = 2.0 Hz, 3H), 3.20-3.08 (m, 2H), 3.06-2.96 (m, 2H). ^{13}C NMR (75 MHz, DMSO-d_6) δ 151.3, 149.2, 146.5, 144.0, 142.5, 131.4, 126.3, 125.2, 115.7, 114.9, 108.8, 56.7, 56.3, 46.3, 45.9, 26.4

2-(4-bromo-2,5-dimethoxyphenyl)-*N*-(pyridin-3-ylmethyl)ethanamine dihydrochloride (3.18)

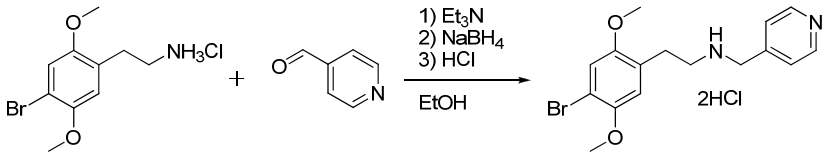

3.18

Obtained from 2C-B·HCl and isonicotinaldehyde by general procedure A in 73% yield as an off-white solid. mp. 227 °C dec. ^{1}H NMR (300 Mhz, DMSO-d_6) δ 10.38 (br s, 2H), 8.96 (d, *J* = 6.6 Hz, 2H), 8.26 (d, *J* = 6.6 Hz, 2H), 7.17 (s, 1H), 7.04 (s, 1H), 4.49 (s, 2H), 3.78 (s, 3H), 3.75 (s, 3H), 3.21-2.98 (m, 4H). ^{13}C NMR (75 MHz, DMSO-d_6) δ 151.3, 150.6, 149.2, 142.4 (2C), 127.1 (2C), 125.2, 115.7, 114.9, 108.8, 56.6, 56.35, 48.3, 46.2, 26.3

2-(4-bromo-2,5-dimethoxyphenyl)-*N*-((2-methoxypyridin-3-yl)methyl)ethanamine, dihydrochloride (3.20)

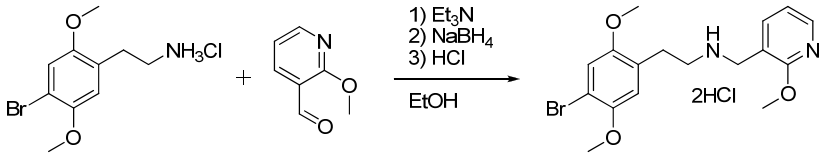

3.80 3.20

Obtained from 2C-B·HCl and **3.80** by general procedure A in 69% yield as a colorless solid. mp. 201-202 °C. ^{1}H NMR (300 Mhz, DMSO-d_6) δ 9.74 (br s, 1H), 9.59 (br s, 2H), 8.18 (dd, *J* = 5.0, 1.8 Hz, 1H), 7.97 (dd, *J* = 7.3, 1.8 Hz, 1H), 7.17 (s, 1H), 7.04 (dd, *J* = 7.3, 5.0 Hz, 1H), 7.02 (s, 1H), 4.10 (t, *J* = 5.6 Hz, 2H), 3.90 (s, 3H), 3.78 (s, 3H), 3.74 (s, 3H), 3.15-2.94 (m, 3H). ^{13}C NMR (75 MHz, DMSO-d_6) δ 161.2, 151.3, 149.2, 147.3, 140.4, 125.4, 116.9, 115.7, 114.9, 114.5, 108.8, 56.6, 56.3, 53.6, 45.9, 44.2

3-((4-bromo-2,5-dimethoxyphenethylamino)methyl)pyridin-2(1*H*)-one hydrochloride (3.21)

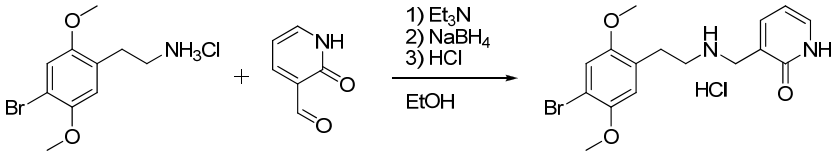

3.79 3.21

Obtained from 2C-B·HCl and **3.79** by general procedure A in 62% yield as an off-white solid. mp. 186-188 °C. ^{1}H NMR (300 Mhz, DMSO-d_6) δ 12.09 (br s, 1H), 9.20 (br s, 2H), 7.72 (dd, *J* = 6.7, 1.8 Hz, 1H), 7.47 (dd, *J* = 6.4, 1.8 Hz, 1H), 7.17 (s, 1H), 7.02 (s, 1H), 6.27 (dd, *J* = 6.7, 6.4 Hz, 1H), 3.96 (s, 2H), 3.79 (s, 3H), 3.75 (s, 3H), 3.11-2.91 (m, 4H). ^{13}C NMR (75 MHz, DMSO-d_6) δ 161.8, 151.3, 149.2, 142.2, 136.2, 125.3, 121.9, 115.7, 114.9, 108.7, 104.9, 56.6, 56.2, 45.8, 45.5, 26.3

2,3-dihydrobenzofuran-7-carbaldehyde (3.23)

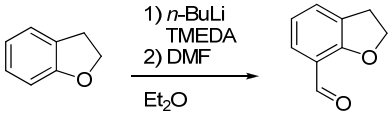

3.22 3.23

To a cooled (-20 °C) solution of 2,3-dihydrobenzofuran, **3.22** (3.61 g, 30.00 mmol)in Et_2O (50 mL) was added TMEDA (6.97 g, 60.00 mmol) followed dropwise addition of *n*-BuLi (60 mmol). The reaction was stirred for 90 minutes at -20 °C and then DMF (6.58 g, 90.00 mmol) was added. The reaction was allowed to stir for 1 hr with the cooling removed before quenching with 2N HCl (100 mL). The biphasic mixture was stirred vigorously overnight and then transferred to a separatory funnel. The organic layer was isolated and the aqueous layer was extracted with EtOAc (2 × 50 mL). The combined organic layers were dried ($MgSO_4$), filtered and evaporated under reduced pressure to give a yellow oil. The oil was purified by short-path vacuum-distillation and the fraction collected at 130-150 °C (0.3 mmHg) contained the product which solidified at room temperature. The solid was recrystallized from heptanes/EtOAc to give the title compound, **3.23** (2.34 g, 53%). mp. 55-57 °C (Litt[369]. 53-54 °C). ^{1}H NMR (300 Mhz, DMSO-d_6) δ 10.15 (s, 1H), 7.55 (m, 1H), 7.38 (m, 1H), 6.90 (dd, *J* = 7.9, 7.2 Hz, 1H), 5.72 (t, *J* = 8.8 Hz, 2H), 3.23 (t, *J* = 8.8 Hz, 2H). ^{13}C NMR (75 MHz, $CDCl_3$) δ 188.9, 162.1, 130.8, 129.4, 127.4, 120.6, 119.7, 72.8, 28.8

1-(2,2-diethoxyethoxy)-2-iodobenzene (3.25)

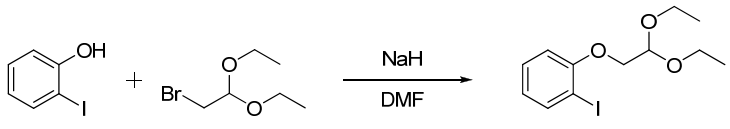

3.24 3.25

A suspension of NaH (1.60 g, 40.00 mmol of a 60% dispersion in paraffin oil, washed twice with heptane) in dry DMF (40 mL) was cooled to 0 °C. A solution of 2-iodophenol, **3.24** (7.70 g, 35.00 mmol) in dry DMF (5 mL) was added over 2 minutes and the reaction was stirred for 15 minutes. 2-bromoacetaldehyde diethylacetal (10.35 g, 52.50 mmol) was added dropwise and the reaction was heated to 100 °C and kept so for 3 hours. The reaction mixture was poured into ice-water

(200 mL) and extracted with EtOAc (2 × 150 mL). The organic extracts were washed with 1M NaOH (100 mL), water (3 × 100 mL) and brine (100 mL), dried ($MgSO_4$), filtered and evaporated under reduced pressure. The residue was purified by short-path vacuum-destillation and the fraction collected at 140-150 °C (0.07 mmHg) contained the title compound, **3.25** (9.42 g, 80%) as a colorless oil. ^{1}H NMR (300 MHz, $CDCl_3$) δ 7.74 (dd, *J* = 7.8, 1.6 Hz, 1H), 7.25 (ddd, *J* = 8.2, 7.8, 1.6 Hz, 1H), 6.80 (dd, *J* = 8.2, 1.3 Hz, 1H), 6.69 (ddd, *J* = 7.8, 7.8, 1.3, 1H), 4.87 (t, *J* = 5.2 Hz, 1H), 4.02 (d, *J* = 5.2 Hz, 2H), 3.82 (dq, *J* = 9.3, 7.0 Hz, 2H), 3.72 (dq, *J* = 9.3, 7.0 Hz, 2H), 1.26 (t, *J* = 7.0 Hz, 6H). ^{13}C NMR (75 MHz, $CDCl_3$) δ 157.2, 139.5, 129.5, 122.8, 112.3, 100.8, 86.5, 70.3, 63.6 (2C), 15.6 (2C).

7-iodobenzofuran (3.26)

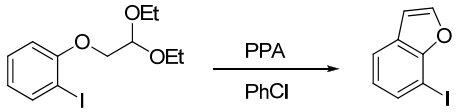

3.25 **3.26**

PPA (6.0 g) and PhCl (20 mL) was mixed and heated to reflux. A solution of **3.25** (2.70 g, 8.03 mmol) in PhCl (2 mL) was added over the course of 5 minutes. The reaction was stirred at reflux temperature for 75 minutes. The PhCl layer was decanted and there was added toluene (50 mL) and stirring was continued for 10 minutes. The toluene layer was decanted and the procedure repeated one more time. The combined organic layers were evaporated under reduced pressure and the residue was redissolved in EtOAc (100 mL), washed with water (50 mL) and saturated $NaHCO_3$ (50 mL), dried ($MgSO_4$), filtered and evaporated under reduced pressure. The residue was purified by short-path vacuum-distillation and the fraction collected at 110-125 °C (0.3 mmHg) contained the title compound, **3.26** (1.70 g, 87%) as a pink oil. ^{1}H NMR (300 MHz, $CDCl_3$) δ 7.66 (d, *J* = 2.2 Hz, 1H), 7.64 (dd, *J* = 7.7, 1.0 Hz, 1H), 7.53 (dd, *J* = 7.7, 1.0 Hz, 1H), 6.97 (dd, *J* = 7.7, 7.7 Hz, 1H), 6.85 (d, *J* = 2.2 Hz, 1H). ^{13}C NMR (75 MHz, $CDCl_3$) δ 155.2, 145.2, 133.3, 127.5, 124.6, 121.4, 107.7, 75.2

(2-bromophenyl)(2,2-diethoxyethyl)sulfane (3.28)

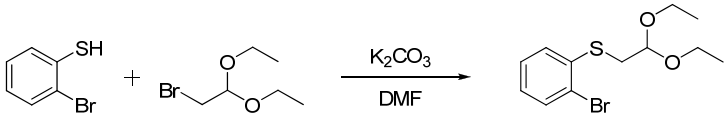

3.27 **3.28**

To a suspension of K_2CO_3 (8.186 g, 59.23 mmol) in DMF (70 mL) was added 2-bromothiophenol, **3.27** (7.00 g, 37.02 mmol) followed by 2-bromoacetaldehyde diethyl acetal (7.821 g, 40.72 mmol). The reaction was stirred at room temperature for 5 hours and then partitioned between water (100 mL) and EtOAc (100 mL). The organic layer was isolated and washed with water (5 × 50 mL). The combined aqueous layers were extracted with EtOAc (100 mL) and the combined organic layers were dried ($MgSO_4$), filtered and evaporated under reduced pressure. The residue was purified by short-path vacuum-distillation and the fraction collected at 130-140 °C (0.2 mmHg) contained the title compound, **3.28** (10.42 g, 92%) as a colorless oil. ^{1}H-NMR (300 MHz, $CDCl_3$) δ 7.51 (dd, *J* = 7.9, 1.3 Hz, 1H), 7.34 (dd, *J* = 7.9, 1.5 Hz, 1H), 7.26-7.20 (m, 1H), 7.04-6.97 (m, 1H), 4.69 (t, *J* = 5.5 Hz), 3.69 (dq, *J* = 9.2, 7.0 Hz, 2H), 3.56 (dq, *J* = 9.2, 7.0 Hz, 2H), 3.14 (d, *J* =

5.5 Hz, 2H), 1.20 (t, *J* = 7.0 Hz, 6H). ^{13}C-NMR (75 MHz, $CDCl_3$) δ 137.7, 133.0, 128.8, 127.7, 126.8, 123.8, 101.63, 62.4, 37.0, 15.5

7-bromobenzo[*b*]thiophene (3.29)

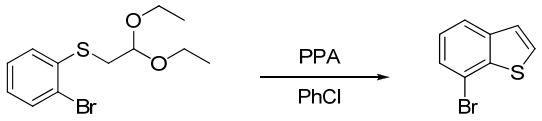

3.28 **3.29**

To a gently refluxing mixture of PPA (22.2 g) and PhCl (75 mL), was added a solution of **3.28** (10.00 g, 32.76 mmol) in PhCl (15 mL) over the course of 20 minutes. The reaction was stirred at reflux temperature for 4 hours. The PhCl layer was decanted and to the PPA-layers there was added toluene (50 mL) and stirring was continued for 10 minutes. The toluene layer was decanted and the procedure repeated one more time. The decanted organic layers were evaporated under reduced pressure and redissolved in EtOAc (100 mL). The organic layer was washed with saturated aqueous $NaHCO_3$ (50 mL), water (50 mL), brine (50 mL), dried ($MgSO_4$), filtered and evaporated under reduced pressure. The residue was purified by short-path vacuum-distillation and the fraction collected at 100-110 °C (0.2 mmHg) contained the title compound, **3.29** (6.32 g, 90%) as a yellow oil. ^{1}H-NMR (300 MHz, $CDCl_3$) δ 7.73 (d, *J* = 7.9 Hz, 1H), 7.52-7.37 (m, 3H), 7.21 (t, *J* = 7.8 Hz, 1H). ^{13}C-NMR (75 MHz, $CDCl_3$) δ 141.6, 140.6, 127.3, 127.1, 125.6, 124.8, 122.6, 116.0

Benzofuran-2-carbaldehyde (3.30)

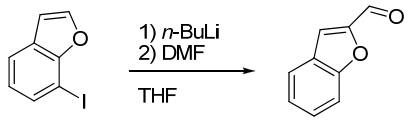

3.26 **3.30**

To a cooled (-78 °C) solution of **3.26** (1.343 g, 5.50 mmol) in dry THF (10 mL) was added *n*-BuLi (6.60 mmol). The reaction was stirred for 1 hour at -78 °C and then quenched with DMF (1.206 g, 16.51 mmol) and allowed to reach room temperature. The reaction mixture was partitioned between 0.1M KH_2PO_4 (50 mL) and Et_2O (50 mL). The organic layer was isolated and the aqueous layer was extracted with Et_2O (2 × 50 mL). The combined organic layers were dried (Na_2SO_4), filtered and evaporated under reduced pressure. The residue was purified by flash chromatography (petroleum ether/EtOAc 10:1) to afford the title compound, **3.30** (0.170 g, 21%) as a pale yellow oil. ^{1}H NMR (300 MHz, $CDCl_3$) δ 9.85 (s, 1H), 7.74 (ddd, *J* = 7.9, 1.3, 0.8 Hz, 1H), 7.59 (ddd, *J* = 8.4, 1.9, 1.0 Hz, 1H), 7.55 (d, *J* = 1.0 Hz, 1H), 7.50 (ddd, *J* = 8.4, 7.0, 1.3 Hz, 1H), 7.33 (ddd, *J* = 8.1, 7.0, 1.1 Hz, 1H). ^{13}C NMR (75 MHz, $CDCl_3$) δ 179.7, 156.2, 152.7, 129.2, 126.7, 124.2, 123.7, 117.8, 112.7

N-(benzofuran-2-ylmethyl)-2-(4-bromo-2,5-dimethoxyphenyl)ethanamine hydrochloride (3.31)

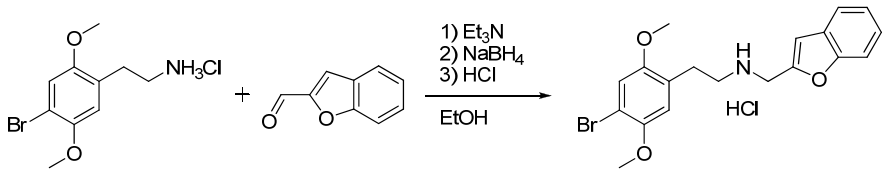

3.30 **3.31**

Obtained from 2C-B·HCl and **3.30** by general procedure A in 63% yield as a colorless solid. mp. 156-157 °C. ^{1}H NMR (300 Mhz, DMSO-d_6) δ 9.90 (br s, 2H), 7.70-7.66 (m, 1H), 7.60-7.56 (m, 1H), 7.38-7.31 (m, 1H), 7.30-7.24 (m, 1H), 7.17 (s, 1H), 7.15 (d, *J* = 0.8 Hz, 1H), 7.02 (s, 1H), 4.41 (s, 2H), 3.78 (s, 3H), 3.72 (s, 3H), 3.21-3.09 (m, 2H), 3.04-2.95 (m, 2H). ^{13}C NMR (75 MHz, DMSO) δ 155.2, 152.3, 150.1, 149.7, 128.3, 126.2, 126.0, 124.1, 122.5, 116.7, 115.9, 112.0, 109.8, 109.5, 57.6, 57.2, 46.6, 43.5, 27.4

Benzofuran-7-carbaldehyde (3.32)

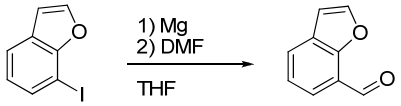

3.26 **3.32**

To a suspension of Mg turnings in dry THF (5 mL) was added a drop of 1,2-dibromoethane. The reaction was stirred and a solution of **3.26** (1.783 g, 7.306 mmol) in dry THF (20 mL) was added. The reaction was heated to reflux and kept so for 90 minutes. The reaction mixture was cooled to 0 °C and DMF (1.602 g, 21.52 mmol) was added. The reaction was stirred for 30 minutes at room temperature and the quenched by addition of 0.1M KH_2PO_4 (25 mL). The mixture was extracted with EtOAc (3 × 50 mL) and the organic extracts were dried ($MgSO_4$), filtered and evaporated under reduced pressure. The residue was purified by flash chromatography (petroleum ether/EtOAc 10:1) to give the title compound, **3.32** (0.753 g, 71%) as a yellow oil. ^{1}H NMR (300 MHz, $CDCl_3$) δ 10.41 (s, 1H), 7.85 (dd, *J* = 7.7, 1.2 Hz, 1H), 7.78 (ddd, *J* = 7.7, 1.2, 0.6 Hz), 7.76 (d, *J* = 2.2 Hz), 6.85 (dd, *J* =2.2, 0.6 Hz, 1H). ^{13}C NMR (75 MHz, $CDCl_3$) δ 188.8, 153.7, 146.3, 129.2, 127.7, 126.3, 123.0, 121.3, 106.5

benzo[*b*]thiophene-7-carbaldehyde (3.33)

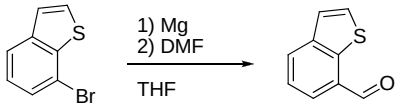

3.29 **3.33**

To a suspension of Mg turnings (0.341 g, 14.04 mmol) in dry THF (20 mL) was added a drop of 1,2-dibromoethane. The reaction was stirred and a solution of **3.29** (2.494 g, 11.70 mmol) in dry THF (2 mL) was added. The reaction was heated to reflux temperature and kept so for 90 minutes. The reaction mixture was cooled to room temperature and added to cooled (0 °C) solution of DMF (2.565 g, 35.10 mmol) in dry THF (10 mL). The reaction was stirred for 30 minutes at 0 °C and then allowed to reach room temperature. The reaction was quenched by addition of saturated NH_4Cl (25 mL). The mixture was extracted with EtOAc (3 × 50 mL) and the

organic extracts were dried ($MgSO_4$), filtered and evaporated under reduced pressure. The residue was purified by flash chromatography (petroleum ether/EtOAc, 20:1) to give the title compound, **3.33** (0.753 g, 71%) as a yellow oil. ^{1}H NMR (300 MHz, $CDCl_3$) δ 10.19 (s, 1H), 8.06 (dd, *J* = 7.9, 1.2 Hz, 1H), 7.83 (dd, *J* = 7.2, 1.2 Hz, 1H), 7.62 (d, *J* = 5.5 Hz, 1H), 7.53 (dd, *J* = 7.9, 7.2 Hz, 1H), 7.40 (d, *J* = 5.5 Hz, 1H). ^{13}C NMR (75 MHz, $CDCl_3$) δ 191.1, 141.1, 136.8, 131.3, 130.6, 130.3, 129.7, 124.1, 122.8

2-carbamoyl-3-nitrobenzoic acid (3.35)

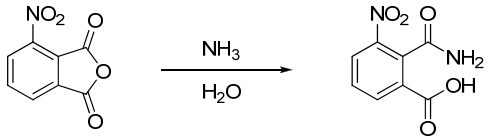

3.34 **3.35**

3-Nitrophthalic anhydride, **3.34** (22.3 g, 115 mmol) was added slowly to a well-stirred flask containing conc. NH_3 (28%, 33.5 mL). After complete addition the flask was cooled to 0 °C with ensuing precipitation. The precipitate was collected by filtration and suspended in water and acidified to pH < 3. The suspension was filtered and the precipitate was washed with water and dried to give the title compound, **3.35** (18.23 g, 75%) as white crystals. mp. 214-216 °C (Litt[370]. 217 °C). ^{1}H NMR (300 MHz, DMSO-d_6) δ 8.16 (dd, *J* = 8.1, 1.2 Hz, 1H), 8.10 (dd, *J* = 7.8, 1.2 Hz, 1H), 8.01 (br s, 1H), 7.69 (dd, *J* = 7.8, 8.1 Hz, 1H), 7.60 (br s, 1H). ^{13}C NMR (75 MHz, DMSO-d_6) δ 166.1, 165.7, 147.2, 134.2, 133.0, 132.0, 129.6, 126.9

2-amino-3-nitrobenzoic acid (3.36)

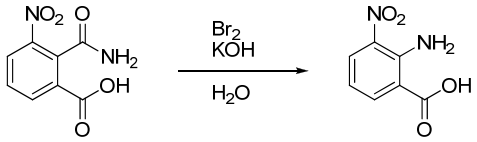

3.35 **3.36**

To a cooled (0 °C) solution of KOH (37.7 g, 78 mmol) in water (185 mL) was added Br_2 (3.84 mL, 75 mmol) followed by **3.35** (15.0 g, 78 mmol). The reaction was heated at 60 °C for 3 hours and then stirred at room temperature overnight. The orange precipitate was isolated by filtration and dissolved in the minimum amount of water to give a red solution. pH was adjusted to 4 with conc. HCl to give a yellow precipitate which was isolated by filtration and recrystallized from water to give the title compound, **3.36** (9.8 g, 69%) as bright yellow crystals. mp. 206-208 °C (Litt[371]. 209 °C). ^{1}H NMR (300 MHz, DMSO-d_6) δ 8.46 (br s, 2H), 8.26 (dd, *J* = 8.4, 1.5 Hz, 1H), 8.18 (dd, *J* = 7.6, 1.5 Hz, 1H), 6.67 (dd, *J* = 8.4, 7.6 Hz, 1H). ^{13}C NMR (75 MHz, DMSO-d_6) δ 168.5, 146.6, 139.6, 132.3, 131.6, 114.6, 113.8

2,3-diaminobenzoic acid (3.37)

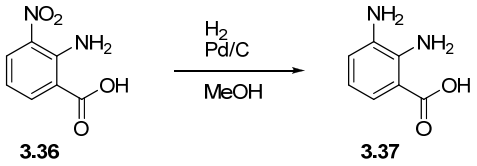

3.36 3.37

3.36 (9.36 g, 51.4 mmol) was dissolved in MeOH (100 mL) and there was added 10% Pd/C (2.0 g). The reaction was stirred under H_2-atmosphere (ambient pressure) until absorption ceased. The reaction was filtered through a pad of Celite and the filtrate was evaporated under reduced pressure. The product was purified by flash chromatography (CH_2Cl_2/MeOH 5:1) and the collected fractions were evaporated to give the title compound, **3.37** (5.40 g, 69%) as a dark brown solid. mp. 199 °C dec. (Litt[372]. 201 °C dec.). ^{1}H NMR (300 MHz, DMSO-d_6) δ 7.09 (dd, *J* = 8.0, 1.5 Hz, 1H), 6.67 (dd, *J* = 7.4, 1.5 Hz, 1H), 6.34 (dd, *J* = 8.0, 7.4 Hz, 2H), 6.32 (br s, 4H). ^{13}C NMR (75 MHz, DMSO-d_6) δ 170.5, 139.6, 135.6, 119.4, 117.0, 114.9, 110.3

1*H*-benzo[*d*]imidazole-4-carboxylic acid (3.38)

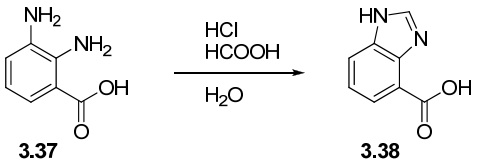

3.37 3.38

To a solution of HCOOH (0.75 mL, 20.0 mmol) in 4M HCl (20 mL) was added **3.37** (1.00 g, 6.6 mmol). The reaction was heated at reflux temperature for 2 hours and then cooled to room temperature. The pink precipitate was isolated by filtration and dissolved in hot MeOH and treated with activated charcoal and stirred for 10 minutes. The suspension was filtered and the solvent evaporated under reduced pressure to give the title compound, **3.38** (0.542 g, 51%) as white crystals. mp. 266-268 °C. ^{1}H NMR (300 MHz, DMSO-d_6) δ 9.64 (s, 1H), 8.11 (dd, *J* = 8.2, 0.9 Hz, 1H), 8.07 (dd, *J* = 7.6, 0.9 Hz, 1H), 7.65 (dd, *J* = 8.2, 7.6, 1H). ^{13}C NMR (75 MHz, DMSO-d_6) δ 165.2, 142.0, 132.3, 129.3, 127.6, 125.6, 119.7, 117.6

Methyl 1*H*-benzo[*d*]imidazole-4-carboxylate (3.39)

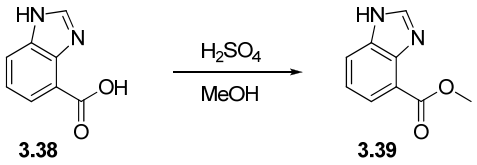

3.38 3.39

To a solution of **3.38** (1.136 g, 7.02 mmol) in MeOH (115 mL) was added conc. H_2SO_4 (0.86 mL, 15.45 mmol). The reaction was heated at reflux temperature until TLC showed full conversion (24-36 hrs). The reaction was concentrated to a few mL and pH was adjusted to 8.5 with 1M K_3PO_3. The resulting precipitate was isolated by filtration and dried under reduced pressure to afford the title compound, **3.39** (0.940 g, 76%) as a white solid. mp. 211-213 °C (Litt[299]. 204 °C). ^{1}H NMR (300 MHz, DMSO-d_6) δ 8.31 (s, 1H), 7.95 (dd, *J* = 8.0, 0.9 Hz, 1H), 7.83 (dd, *J* = 7.6, 0.9 Hz, 1H), 7.29 (dd, *J* = 8.0, 7.6 Hz, 1H). ^{13}C NMR (75 MHz, DMSO-d_6) δ 165.5, 144.1, 143.6, 132.3, 124.7, 124.3, 121.0, 113.8

(1*H*-benzo[*d*]imidazol-4-yl)methanol (3.40)

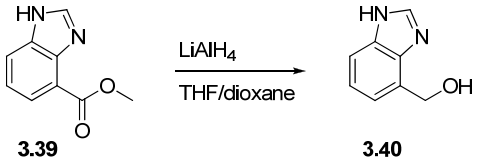

3.39 3.40

3.39 (0.504 g, 2.861 mmol) was dissolved in THF/dioxane (3:2, 50 mL). A 1.0 M solution $LiAlH_4$ in THF (3.00 mL, 3.00 mmol) was added slowly and the reaction was left to stir for 1 hour. The reaction was quenched by successive addition of water (114 µL), 15% NaOH (114 µL) and water (342 µL). The suspension was stirred for 5 minutes and Na_2SO_4 (3.0 g) was added and the stirring was continued for 10 minutes. The suspension was filtered and the filter cake washed with THF (2 × 15 mL). The combined filtrates were evaporated under reduced pressure to give the title compound, **3.40** (0.356 g, 84%) as a white solid. mp. 159-161 °C. ^{1}H NMR (300 MHz, CD_3OD) δ 8.13 (s, 1H), 7.51 (dd, *J* = 7.4, 1.7 Hz, 1H), 7.26 (dd, *J* = 7.3, 1.7 Hz, 1H), 7.21 (dd, *J* = 7.3, 7.4 Hz, 1H), 5.07 (br s, 2H), 4.98 (s, 3H). ^{13}C NMR (75 MHz, CD_3OD) δ 142.2, 139.2, 136.0, 129.5, 123.5, 121.7, 115.5, 61.8.

1*H*-benzo[*d*]imidazole-4-carbaldehyde (3.41)

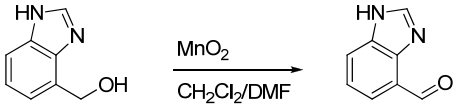

3.40 3.41

To a solution of **3.40** (0.356 g, 2.40 mmol) in CH_2Cl_2/DMF (1:1, 50 mL) was added activated MnO_2 (2.086 g, 24.00 mmol). The reaction was stirred at room temperature until TLC showed full conversion (4 hours). The reaction was filtered through a tight-packed pad of Celite and the pad was washed with CH_2Cl_2 (2 × 15 mL). The filtrate was evaporated and the solids were recrystallized from EtOAc/heptanes to give the title compound, **3.41** (0.277 g, 79%) as pale yellow crystals. mp. 163-164 °C. ^{1}H NMR (300 MHz, DMSO-d_6) δ 10.24 (s, 1H), 8.33 (s, 1H), 8.00 (dd, *J* = 8.0, 1.0 Hz, 1H), 7.83 (dd, *J* = 7.4, 1.0 Hz, 1H), 7.40 (dd, *J* = 8.0, 7.4 Hz,, 1H). ^{13}C NMR (75 MHz, DMSO) δ 191.7, 144.2, 142.5, 127.0, 124.6, 122.2, 121.4

7-Methylindoline-2,3-dione (3.44)

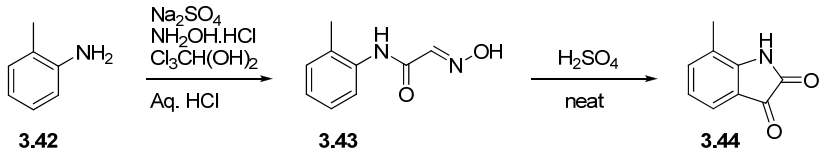

3.42 3.43 3.44

Chloral hydrate (14.7 g, 88.8 mmol) was added to a 1L round-bottomed flask containing a suspension of hydroxylamine hydrochloride (18.5 g, 266 mmol), sodium sulfate (84 g, 590 mmol) and *o*-toluidine (7.95 mL, 74 mmol) in water (500 mL) and 2M HCl (25 mL). This was heated at 55 °C overnight with mechanical stirring and. The resultant precipitate was collected by filtration and the solid was washed with water and dried under vacuum to give the isonitrosoacetanilide, **3.43**. It was then added in small portions to an Erlenmeyer flask containing concentrated sulfuric acid (45 mL) which had been preheated to 55 °C. At no point was the temperature allowed to

exceed 70 °C. After the addition was complete the solution was heated at 80 °C for 10 minutes and then cooled to room temperature, poured onto crushed ice (225 mL) and allowed to stand for 30 minutes. The precipitate was collected by filtration, washed with water and dried to yield the title compound, **3.44** (10.2 g, 77%) as a brick-red solid. mp. 268-270 °C (Litt[373]. 270-273 °C). ^{1}H NMR (300 MHz, DMSO-d_6) δ 11.04 (s, 1H), 7.37 (d, *J* = 7.6 Hz, 1H), 7.28 (d, *J* = 7.4 Hz, 1H), 6.94 (dd, *J* = 7.6, 7.4 Hz, 1H), 2.16 (s, 3H). ^{13}C NMR (75 MHz, DMSO-d_6) δ 184.5, 159.8, 149.1, 139.3, 122.5, 121.9, 121.5, 117.4, 15.5.

2-Amino-3-methylbenzoic acid (3.45)

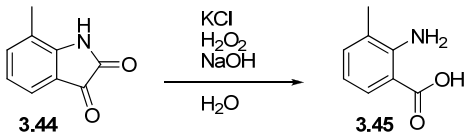

A solution of **3.44** (7.08 g, 44 mmol), NaOH (1.77 g, 44 mmol) and KCl (7.08 g, 95 mmol) in water (80ml) was cooled to 0 °C and 33% H_2O_2 (6.02 mL, 0.66 mmol) was added dropwise over 1.5 hours. After an additional 45 minutes at room temperature the addition of acetic acid (16 mL) caused precipitation of the product. Recrystallization from water gave the title compound, **3.45** (5.26 g, 80%) as a pale brown solid. mp 162-164 °C (Litt[374]. 174-176 °C). ^{1}H NMR (300 MHz, DMSO-d_6) δ 7.61 (dd, *J* = 8.0, 1.3 Hz, 1H), 7.13 (dd, *J* = 7.1, 1.3 Hz, 1H), 6.45 (dd, *J* = 8.0, 7.1 Hz, 1H), 2.10 (s, 3H). ^{13}C NMR (75 MHz, DMSO-d_6) δ 169.9, 149.6, 134.3, 129.0, 122.9, 114.3, 109.3, 17.7

Methyl 2-amino-3-methylbenzoate (3.46)

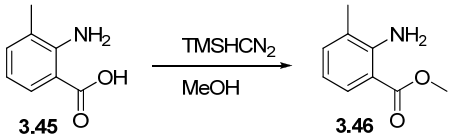

To a solution of **3.45** (3.41 g, 27.1 mmol) in MeOH (70 mL) was added a 2.0M solution of $TMSHCN_2$ in hexanes (15 mL, 30.0 mmol). The reaction was stirred for 30 minutes and then evaporated under reduced pressure to give the title compound, **3.46** (4.17 g, 93%) as a brown oil. ^{1}H NMR (300 MHz, DMSO) δ 7.61 (d, *J* = 7.4 Hz, 1H), 7.14 (d, *J* = 7.4 Hz, 1H), 6.45 (t, *J* = 7.4 Hz, 1H), 3.78 (s, 3H), 2.10 (s, 3H). ^{13}C NMR (75 MHz, DMSO) δ 169.9, 149.6, 134.3, 129.0, 122.9, 114.2, 109.3, 51.5, 17.6.

Methyl 1*H*-indazole-7-carboxylate (3.48)

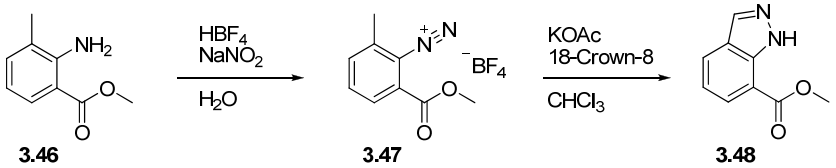

A cooled (5 °C) solution of sodium nitrite (1.670 g, 24.21 mmol) in water (3.3 mL) was added to a cooled (0 °C) solution of **3.46** (4.00 g, 24.21 mmol) in 50% HBF_4 (10 ml). After complete addition the mixture was stirred for 1 hour at room temperature. The resultant precipitate was isolated by filtration and washed with Et_2O. The diazonium intermediate (**3.47**) was then added in one

portion to a stirred mixture of dried and powdered potassium acetate (4.752 g, 48.42 mmol) and 18-crown-6 (0.32 g, 0.4 mmol) in dry chloroform (40 mL). After 1 hour the precipitate was removed and the filtrate was washed with water (20 mL), dried ($MgSO_4$) and evaporated under reduced pressure. Recrystallization of the residue from heptanes gave the title compound, **3.48** (2.017 g, 47%) as a pale orange powder. mp. 110-112 °C. ^{1}H NMR (300 MHz, $CDCl_3$) δ 11.54 (s, 1H), 8.14 (d, *J* = 1.5 Hz, 1H), 8.05 (dd, *J* = 7.3, 1.0 Hz, 1H), 7.96 (ddd, *J* = 8.0, 1.5, 1.0 Hz, 1H), 7.21 (dd, *J* = 8.0, 7.3 Hz, 1H), 4.03 (s, 3H). ^{13}C NMR (75 MHz, $CDCl_3$) δ 166.7, 138.8, 135.0, 129.2, 126.8, 124.5, 120.5, 112.6, 52.5

(1*H*-indazol-7-yl)methanol (3.49)

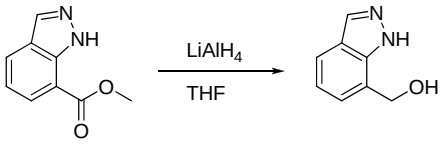

3.48 **3.49**

To a solution of **3.48** (0.182 g, 1.033 mmol) in dry THF (10 mL) was added a 1.0M solution of $LiAlH_4$ (2.1 mL, 2.10 mmol). The reaction was stirred for 30 minutes and then quenched by successive addition of water (210 µL), 15% NaOH (210 µL) and water (630 µL). The suspension was diluted with THF (10 mL) and there was added $MgSO_4$. The suspension was stirred for 10 minutes and filtered. The filter cake was washed with EtOAc (10 mL) and $CHCl_3$/MeOH (1:1, 10 mL) and the combined filtrates were evaporated under reduced pressure to afford the title compound, **3.49** (0.112 g, 73%) as a white solid. ^{1}H NMR (300 MHz, DMSO-d_6) δ 8.05 (s, 1H), 7.62 (d, *J* = 8.0 Hz, 1H), 7.30 (d, *J* = 6.9 Hz, 1H), 7.06 (dd, *J* =8.0, 6.9 Hz, 1H), 4.80 (2H, s). ^{13}C NMR (75 MHz, DMSO-d_6) δ 133.4, 133.3, 124.8, 122.9, 122.8, 120.1, 118.8, 59.8

1*H*-indazole-7-carbaldehyde (3.50)

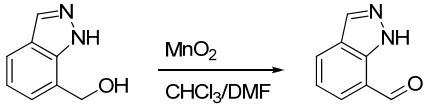

3.49 **3.50**

To a solution of **3.49** (0.173 g, 1.17 mmol) in CH_2Cl_2/DMF (4:1, 50 mL) was added activated MnO_2 (1.02 g, 11.7 mmol). The reaction was stirred overnight at room temperature. The reaction was filtered through a tight-packed pad of Celite and the pad was washed with CH_2Cl_2 (2 × 15 mL). The filtrate was evaporated under reduced pressure and the residue was purified by radial chromatography (petroleum ether/EtOAc) to give the title compound, **3.50** (0.149 g, 87%) as off-white crystals. mp. 120-122 °C. ^{1}H NMR (300 MHz, $CDCl_3$) δ 12.02 (s, 1H), 10.15 (s, 1H), 8.19 (s, 1H), 8.05 (dd, *J* = 8.0, 0.9 Hz, 1H), 7.85 (dd, *J* = 7.1, 0.9 Hz, 1H), 7.31 (dd, *J* = 8.1, 7.1 Hz, 1H). ^{13}C NMR (75 MHz, $CDCl_3$) δ 192.2, 136.7, 134.9, 133.2, 128.4, 124.4, 120.7, 120.4

Methyl 2-amino-3-hydroxybenzoate (3.52)

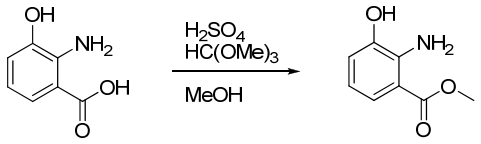

3.51 3.52

2-amino-3-hydroxybenzoic acid, **3.51** (4.83 g, 31.54 mmol) was dissolved in dry MeOH (250 mL) and there was added $HC(OMe)_3$ (10.04 g, 94.62 mmol) followed by conc. H_2SO_4 (5.8 mL, 104.1 mmol). The reaction was heated at reflux temperature until TLC showed full conversion (48 hours). pH was adjusted to 4 with saturated aqueous $NaHCO_3$ and the excess MeOH was evaporated under reduced pressure. The residue was partitioned between water (50 mL) and CH_2Cl_2 (50 mL) and the organic layer was isolated. The aqueous layer was extracted with CH_2Cl_2 (2 × 50 mL) and the combined organic layers were dried ($MgSO_4$), filtered and evaporated under reduced pressure. The residue was purified by dry column vacuum chromatography (EtOAc/petroleum ether, 1:3) and the product recrystallized from heptanes to give the title compound, **3.52** (3.90 g, 74%) as colorless filmy strips. mp. 98-100 °C (Litt[375]. 97-98 °C). ^{1}H NMR (300 MHz, $CDCl_3$) δ 7.45 (dd, *J* = 8.2, 1.3 Hz, 1H), 6.80 (dd, *J* = 7.6, 1.3 Hz, 1H), 6.48 (dd, *J* = 8.2, 7.6 Hz, 1H), 5.80 (br s, 3H), 3.86 (s, 3H). ^{13}C NMR (75 MHz, $CDCl_3$) δ 168.9, 143.3, 140.5, 123.2, 118.1, 115.4, 111.5, 51.9

methyl benzo[*d*]oxazole-4-carboxylate (3.53)

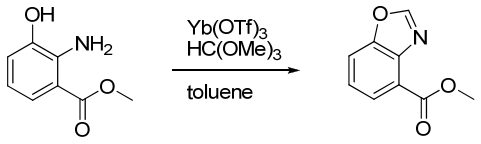

3.52 3.53

Methyl 3-amino-2-hydroxybenzoate, **3.52** (2.18 g, 13.04 mmol) was suspended in toluene (2 mL) in a microwave vial. $HC(OMe)_3$ (2.08 g, 19.60 mmol) and $Yb(OTf)_3$ (0.004 g, 0.0065 mmol) were added and the reaction was heated at 100 °C for 2 hours in the microwave. The reaction mixture was evaporated under reduced pressure and the residue was purified by flash chromatography (petroleum ether/EtOAc 4:1) to give the title compound, **3.53** (2.15 g, 93%) as large white crystals. mp. 109-110 °C (Litt[376]. 107-109 °C). ^{1}H NMR (300 MHz, $CDCl_3$) δ 8.24 (s, 1H), 8.06 (dd, *J* = 7.7, 1.1 Hz, 1H), 7.78 (dd, *J* = 8.2, 1.1 Hz, 1H), 7.46 (t, *J* = 8.0 Hz, 1H), 4.05 (s, 3H). ^{13}C NMR (75 MHz, $CDCl_3$) δ 165.5, 153.9, 150.5, 139.2, 127.4, 125.2, 122.7, 115.5, 52.7

Methyl 2-hydroxy-3-nitrobenzoate (3.55)

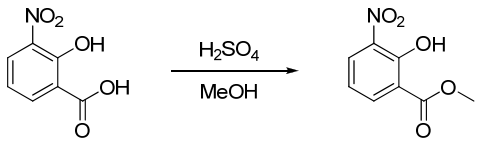

3.54 3.55

2-hydroxy-3-nitrobenzoic acid, **3.54** (4.42 g, 24.14 mmol) were dissolved in dry MeOH (250 mL) and there was added conc. H_2SO_4 (2.7 mL, 48.28 mmol). The reaction was heated at reflux

temperature until TLC showed full conversion (36 hours). pH was adjusted to 4 with saturated aqueous $NaHCO_3$ and the excess MeOH was evaporated under reduced pressure. The residue was partitioned between water (50 mL) and CH_2Cl_2 (50 mL) and the organic layer was isolated. The aqueous layer was extracted with CH_2Cl_2 (2 × 50 mL) and the combined organic layers were dried ($MgSO_4$), filtered and evaporated, to give a pale yellow solid. Recrystallization from EtOH gave the title compound, **3.55** (4.00 g, 84%) as pale yellow needles. mp. 130-131 °C (Litt[377]. 130-132 °C). ^{1}H-NMR (300 MHz, $CDCl_3$) δ 11.96 (s, 1H), 8.10-8.16 (m, 2H), 6.99 (t, *J* = 8.0 Hz, 1H), 4.01 (s, 3H). ^{13}C-NMR (75 MHz, $CDCl_3$) δ 169.2, 155.6, 138.0, 135.8, 131.4, 118.4, 115.9, 53.3

Methyl 3-amino-2-hydroxybenzoate (3.56)

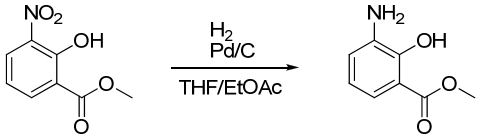

3.55 3.56

Methyl 2-hydroxy-3-nitrobenzoate, **3.55** (3.90 g, 19.78 mmol) was dissolved in THF/EtOAc (1:1, 100 mL) in a hydrogenation bottle and there was added Pd/C (0.390 g). The reaction was shaken under H_2-atmosphere (50 psi) in a Parr hydrogenation apparatus for 2½ hours. The reaction mixture was filtered through a pad of Celite and the filtrate was evaporated under reduced pressure. The residue was purified by dry column vacuum chromatography (petroleum ether → EtOAc) and the collected fractions were evaporated to give the title compound, **3.56** (3.10 g, 94%), as white needles. mp. 88-89 °C (Litt[377]. 88-89 °C). ^{1}H-NMR (300 MHz, $CDCl_3$) δ 10.85 (d, *J* = 0.6 Hz, 1H), 7.21 (dd, *J* = 8.0, 1.6 Hz, 1H), 6.85 (ddd, *J* = 7.7, 1.6, 0.6 Hz, 1H), 6.69 (dd, *J* = 8.0, 7.7 Hz, 1H), 3.92 (s, 3H), 3.88 (br s, 3H). ^{13}C-NMR (75 MHz, $CDCl_3$) δ 171.1, 149.7, 135.8, 119.7, 119.1, 118.8, 111.8, 52.4

Methyl benzo[*d*]oxazole-7-carboxylate (3.57)

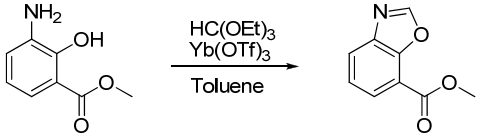

3.56 3.57

Methyl 3-amino-2-hydroxybenzoate, **3.56** (1.69 g, 10.13 mmol) was suspended in toluene (2 mL) in a microwave vial. $HC(OEt)_3$ (1.80 g, 12.15 mmol) and $Yb(OTf)_3$ (0.003 g, 0.005 mmol) was added and the reaction was heated at 100 °C for 1 hour in the microwave. The reaction mixture was evaporated and purified by flash chromatography (petroleum ether/EtOAc 4:1) to give the title compound, **3.57** (1.63 g, 91%) as pale yellow crystals. mp. 116-118 °C (Litt[378]. 77 °C). ^{1}H-NMR (300 MHz, $CDCl_3$) δ 8.21 (s, 1H), 8.04 (dd, *J* = 7.8, 1.2 Hz, 1H), 7.99 (dd, *J* = 8.0, 1.2 Hz, 1H), 7.44 (dd, *J* = 8.0, 7.8 Hz), 3.76 (s, 3H). ^{13}C-NMR (75 MHz, $CDCl_3$) δ 180.9, 164.4, 153.4, 141.4, 128.0, 125.6, 124.5, 115.4, 52.6

benzo[*d*]oxazol-7-ylmethanol (3.60)

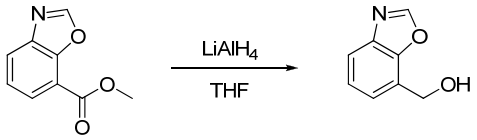

3.57 3.60

Methyl benzo[*d*]oxazole-7-carboxylate, **3.57** (1.57 g, 8.86 mmol) was dissolved in dry THF (50 mL) and there was added a 1.0M solution of $LiAlH_4$ in THF (5 mL, 5 mmol). The reaction was stirred at room temperature for 30 minutes at which point TLC indicated full conversion. The reaction was quenched by addition of water (50 mL) and there was added saturated aqueous Rochelle salt (50 mL) and Et_2O (50 mL). The reaction was stirred vigorously for 15 minutes and then transferred to a separatory funnel. The organic layer was isolate and the aqueous layer was extracted with Et_2O (2 × 100 mL). The combined organic layers were washed with saturated aqueous Rochelle salt (50 mL) and water (50 mL), dried ($MgSO_4$), filtered and evaporated under reduced pressure. The crude compound was purified by flash chromatography (petroleum ether/EtOAc 3:1) to give the title compound, **3.60** (0.823 g, 62%) as a colorless oil. ^{1}H-NMR (300 MHz, $CDCl_3$) δ 8.07 (s, 1H), 7.69 (dd, *J* = 7.7, 1.3 Hz, 1H), 7.40 (dd, *J* = 7.7, 1.3 Hz, 1H), 7.33 (t, *J* = 7.7 Hz), 5.00 (s, 2H), 2.51 (br s, 1H). ^{13}C-NMR (75 MHz, $CDCl_3$) δ 153.4, 145.4, 140.0, 124.8, 124.7, 124.4, 119.9, 60.3

Benzo[*d*]oxazole-7-carbaldehyde (3.61)

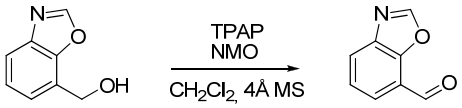

3.60 3.61

Benzo[*d*]oxazol-7-ylmethanol, **3.60** (0.746 g, 5.00 mmol) was dissolved in dry CH_2Cl_2 (25 mL). There was added powdered activated 4Å molecular sieves (2.5 g), TPAP (0.088 g, 0.25 mmol) and NMO (0.937 g, 8.00 mmol). The reaction was stirred for 30 minutes and the crude reaction mixture was poured onto a column of silica and eluted with petroleum ether/EtOA (3:1). The fractions containing the product were evaporated to give the title compound, **3.61** (0.415 g, 56%) as a pale yellow solid. mp. 114-116 °C. ^{1}H-NMR (300 MHz, $CDCl_3$) δ 10.33 (s, 1H), 8.26 (s, 1H), 8.06 (d, *J* = 7.9 Hz, 1H), 7.89 (d, *J* = 7.6 Hz, 1H), 7.54 (dd, *J* = 7.9, 7.7 Hz, 1H) ^{13}C-NMR (75 MHz, $CDCl_3$) δ 187.8, 153.6, 148.5, 141.6, 127.9, 126.8, 124.9, 121.5

benzo[d]isoxazol-7-ylmethanol (3.69)

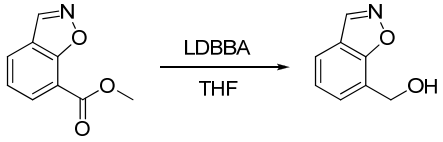

3.76 3.69

To a cooled (-20 °C) solution of **3.76** (0.532, 3.00 mmol) in THF (20 mL) was added a 1 M solution of LDBBA in THF (12.0 mL, 12.0 mmol) and the reaction was stirred for 4 hours. The reaction was quenched by addition of 1M HCl (20 mL) and extracted with CH_2Cl_2 (3 × 15 mL). The combined

extracts were dried ($MgSO_4$), filtered and evaporated. The residue was purified by flash chromatography (petroleum ether/EtOAc, 4:1) to give the title compound, **3.69** (0.152 g, 34%) as a white solid. ^{1}H NMR (300 MHz, $CDCl_3$) δ 8.69 (s, 1H), 7.63 (d, *J* = 7.9 Hz, 1H), 7.57 (d, *J* = 7.2 Hz, 1H), 7.29 (t, *J* = 7.5 Hz, 1H), 5.03 (s, 3H), 2.73 (s, 2H). ^{13}C NMR (75 MHz, $CDCl_3$) δ 160.0, 146.3, 128.3, 124.2, 123.7, 121.3, 121.2, 60.1

benzo[*d*]isoxazole-7-carbaldehyde (3.70)

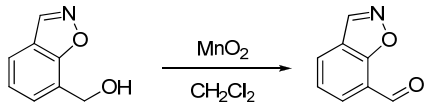

3.69 **3.70**

To a solution of **3.69** (0.299 g, 2.00 mmol) in CH_2Cl_2 (20 mL) was added activated MnO_2 (1.74 g, 20 mmol). The reaction was stirred overnight at room temperature. The reaction was filtered through a tight-packed pad of Celite and the pad was washed with CH_2Cl_2 (2 × 15 mL). The filtrate was evaporated under reduced pressure and the residue was purified by radial chromatography (petroleum ether/EtOAc) to give the title compound, **3.70** (0.178 g, 61%) as off-white crystals. mp. 112-114 °C. ^{1}H NMR (300 MHz, $CDCl_3$) δ 10.47 (s, 1H), 8.83 (s, 1H), 8.08 (dd, *J* = 7.4, 1.1 Hz, 1H), 8.03 (dd, *J* = 7.9, 1.1 Hz, 1H), 7.51 (dd, *J* = 7.9, 7.4 Hz, 1H). ^{13}C NMR (75 MHz, $CDCl_3$) δ 187.3, 160.8, 145.9, 131.4, 128.5, 124.3, 123.4, 120.2

Methyl 2-hydroxy-3-methylbenzoate (3.72)

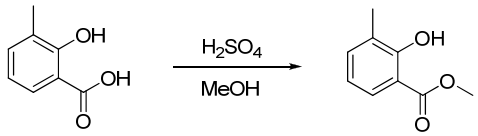

3.71 **3.72**

To a solution of 3-methylsalicylic acid, **3.71** (61.5 g, 400 mmol) in MeOH (1 L) was added conc. H_2SO_4 (194 mL, 3.49 mol) in small portions to avoid bumping. After complete addition the reaction was heated to reflux temperature and stirred overnight. The reaction mixture was poured into ice-water (2.3 L) and the mixture was extracted with CH_2Cl_2 (3 × 600 mL). The combined extracts were dried ($MgSO_4$), filtered and evaporated under reduced pressure. The product was purified by fractionated vacuum distillation and the fraction boiling at 66 °C (0.3 mmHg) contained the title compound, **3.72** (60.5 g, 91%) as a colorless liquid. ^{1}H NMR (300 MHz, $CDCl_3$) δ 10.98 (d, *J* = 0.5 Hz, 1H), 7.68-7.63 (m, 1H), 7.31-7.26 (m, 1H), 6.75 (dd, *J* = 7.8, 7.5 Hz, 1H), 3.92 (s, 3H), 2.25 (s, 3H). ^{13}C NMR (75 MHz, $CDCl_3$) δ 171.0, 160.0, 136.5, 127.4, 126.6, 118.5, 111.7, 52.4, 15.9

Methyl 2-acetoxy-3-methylbenzoate (3.73)

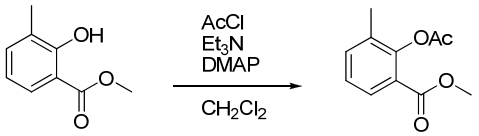

3.72 **3.73**

To a solution of **3.72** (8.31 g, 50.0 mmol) in CH_2Cl_2 (100 mL) was added Et_3N (7.08 g, 70.0 mmol) and DMAP (0.12 g, 1.0 mmol). The reaction was cooled to 0 °C and AcCl (4.71 g, 60.0 mmol) was added slowly. The reaction was stirred for 1 hour and then poured into ice-water (200 mL). The organic layer was isolated and the aqueous layer was extracted with CH_2Cl_2 (2 × 100 mL). The combined organic extracts were dried ($MgSO_4$), filtered and evaporated under reduced pressure. The residue was purified by short-path vacuum-distillation and the fraction collected at 140 °C (0.2 mmHg) contained the title compound, **3.73** (10.4 g, 99%) as a colorless liquid. ^{1}H NMR (300 MHz, $CDCl_3$) δ 7.82 (dd, *J* = 7.8, 1.7 Hz, 1H), 7.40 (ddd, *J* = 7.5, 1.7, 0.8 Hz, 1H), 7.17 (dd, *J* = 7.8, 7.5 Hz, 1H), 3.84 (s, 3H), 2.37 (s, 3H), 2.22 (s, 3H). ^{13}C NMR (75 MHz, $CDCl_3$) δ 169.2, 165.1, 149.2, 135.4, 132.1, 129.4, 125.6, 122.9, 52.3, 21.0, 16.4

Methyl 3-formyl-2-hydroxybenzoate (3.75)

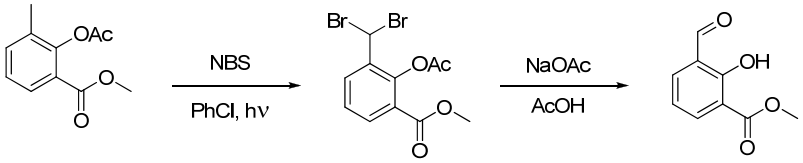

3.73 **3.74** **3.75**

To a solution of **3.73** (5.00 g, 24.0 mmol) in PhCl (80 mL) was added NBS (10.66 g, 60.0 mmol). The reaction was irradiated with a 500 W tungsten lamp until GC-MS showed full conversion. The reaction mixture was allowed to cool to room temperature and the precipitate was removed by filtration. The filtrate was concentrated under reduced pressure and the residue was dissolved in EtOAc (100 mL). The organic layer was washed with water (3 × 100 ml), dried ($MgSO_4$), filtered and evaporated under reduced pressure. The residue was dissolved in AcOH (80 mL) and NaOAc (15.0 g, 183 mmol) was added. The reaction was heated at reflux temperature for 2 hours and then allowed to cool to room temperature. The reaction mixture was diluted with EtOAc (70 mL) and filtered. The filtrate was evaporated under reduced pressure and the residue was partitioned between water (50 mL) and EtOAc (50 mL). The organic layer was isolated and the aqueous layer extracted with EtOAc (2 × 50 mL). The combined organic extracts were dried ($MgSO_4$), filtered and evaporated under reduced pressure. The residue was purified by flash chromatography (petroleum ether/EtOAc, 10:1) to give the title compound, **3.75** (2.38 g, 55%) as fluffy white crystals. mp. 82-84 °C (Litt[379]. 87 °C). ^{1}H NMR (300 MHz, $CDCl_3$) δ 11.49 (s, 1H), 10.46 (d, *J* = 0.6 Hz, 1H), 8.07 (dd, *J* = 7.8, 1.9 Hz, 2H), 7.98 (dd, *J* = 7.7, 1.9 Hz, 2H), 6.97 (ddd, *J* = 7.7, 7.8, 0.6 Hz, 1H), 3.98 (s, 3H). ^{13}C NMR (75 MHz, $CDCl_3$) δ 189.0, 169.8, 163.7, 136.4, 134.7 124.3, 119.1, 114.1, 52.9

methyl benzo[*d*]isoxazole-7-carboxylate (3.76)

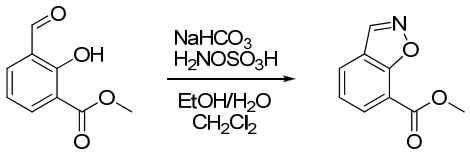

3.75 **3.76**

3.75 (1.35 g, 7.50 mmol) was dissolved in EtOH (10 mL) and hydroxylamine-*O*-sulfonic acid (1.27 g, 11.25 mmol) was added. The reaction was stirred a few minutes and CH_2Cl_2 (50 mL) was added followed by saturated $NaHCO_3$ (25 mL). The reaction was stirred vigorously for 5 minutes and then transferred to a separatory funnel. The organic layer was isolated and the aqueous layer was extracted with CH_2Cl_2 (2 × 15 mL). The combined organic extracts were set aside and the aqueous layer was stirred with CH_2Cl_2 (50 mL) for 30 minutes and the extractions were repeated. The combined organic extracts were dried ($MgSO_4$), filtered and evaporated under reduced pressure. The residue was purified by flash chromatography (CH_2Cl_2) to give the title compound, **3.76** (0.944 g, 71%) as white needles. ^{1}H NMR (300 MHz, DMSO) δ 9.34 (s, 1H), 8.18 (dd, *J* = 6.0, 1.2 Hz, 1H), 8.15 (dd, *J* = 5.8, 1.2 Hz, 1H), 7.49 (dd, *J* = 6.0, 5.8 Hz, 1H), 3.95 (s, 3H). ^{13}C NMR (75 MHz, DMSO) δ 163.6, 159.3, 147.1, 132.2, 128.5, 124.1, 119.3, 113.2, 52.5

2-Chloronicotinaldehyde (3.78)

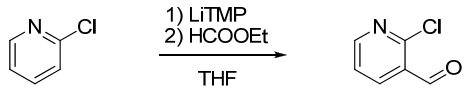

3.77 **3.78**

A solution of TMP (4.66 g, 33.00 mmol) in dry THF (60 mL) was cooled to -78 °C and there was added *n*-BuLi (30.00 mmol). The reaction was stirred at 0 °C for 30 minutes and then cooled to -78 °C again. 2-chloropyridine, **3.77** (2.84 g, 25.00 mmol) was added over the course of 5 minutes and the reaction was stirred at -78 °C for 2½ hours. Ethyl formate (9.26 g, 125 mmol) was added and the reaction was allowed to reach -40 °C over the course of 30 minutes. At -40 °C the reaction was quenched by addition of 10% water in THF (10 mL) followed by water (50 mL). The mixture was extracted with Et_2O (2 × 50 mL) and the combined organic layers were washed with 0.1M KH_2PO_4 (3 × 100 mL), dried ($MgSO_4$), filtered and evaporated to give the crude product. Purification by flash column chromatography (petroleum ether/EtOAc 6:1) followed by recrystallization from heptane/toluene afforded the title compound, **3.78** (2.02 g, 57%) as pale yellow needles. mp. 52-53 °C (Litt[380]. 50 °C). ^{1}H NMR (300 Mhz, $CDCl_3$) δ ^{1}H NMR (300 MHz, $CDCl_3$) δ 10.42 (d, *J* = 0.7 Hz, 1H), 8.59 (dd, *J* = 4.7, 2.1 Hz, 1H), 8.22 (dd, *J* = 7.6, 2.1 Hz, 1H), 7.41 (ddd, *J* = 7.6, 4.7, 0.7 Hz, 1H). ^{13}C NMR (75 MHz, $CDCl_3$) δ 189.1, 154.2, 153.6, 138.0, 128.9, 123.3

Pyridin-2(1*H*)-one-3-carbaldehyde (3.79)

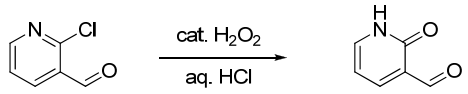

3.78 **3.79**

2-Chloronicotinaldehyde, **3.78** (0.283 g, 2.00 mmol) was suspended 3M aqueous HCl (2 mL). 4 drops of 3% H_2O_2 was added and the mixture was heated in a sealed vial for 2 hours at 100 °C in the microwave. After cooling to room temperature the product crystallized and the suspension was neutralized by addition of solid K_2CO_3. The precipitate was isolated by filtration and recrystallized from the minimum volume of EtOH to furnish the title compound, **3.79** (0.190 g, 77%). mp. 224-225 °C (Litt[381]. 224 °C). ^{1}H NMR (300 MHz, DMSO-d_6) δ 12.37 (br s, 1H), 10.05 (d, *J* = 0.7 Hz, 1H), 7.95 (dd, *J* = 7.1, 2.3 Hz, 1H), 7.80 (dd, *J* = 6.3, 2.3 Hz, 1H), 6.36 (ddd, *J* = 7.1, 6.3, 0.7 Hz, 1H). ^{13}C NMR (75 MHz, DMSO-d_6) δ 189.0, 162.0, 143.4, 142.6, 124.2, 105.3

2-Methoxypyridine-3-carbaldehyde (3.80)

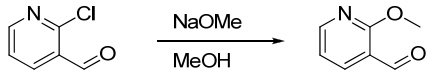

3.78 **3.80**

Elemental sodium (0.35 g, 15.0 mmol) was added to dry MeOH (6 mL) at 0 °C and allowed to dissolve completely. A solution of **3.78** (0.708, 5.0 mmol) in dry MeOH (2 mL) was added via syringe and the reaction was heated at reflux temperature for 5 hours. The reaction mixture was cooled to room temperature and evaporated under reduced pressure. The residue was taken up in water (10 mL), neutralized with dilute HCl and extracted with Et_2O (3 × 10 mL). The organic extracts were dried ($MgSO_4$), filtered and evaporated under reduced pressure. The residue was purified by flash chromatography (petroleum ether/EtOAc, 4:1) to give the title compound, **3.80** (0.473, 69%),as a colorless oil. ^{1}H NMR (300 MHz, $CDCl_3$) δ 10.34 (d, *J* = 0.8 Hz, 1H), 8.36 (dd, *J* = 4.9, 2.1 Hz, 1H), 8.09 (dd, *J* = 7.4, 2.1 Hz, 1H), 7.00 (ddd, *J* = 7.4, 4.9, 0.8 Hz, 1H), 4.07 (s, 3H). ^{13}C NMR (75 MHz, $CDCl_3$) δ 189.1, 164.4, 152.8, 137.6, 118.8, 117.3, 54.0

3-((4-bromo-2,5-dimethoxyphenethylamino)methyl)-2-hydroxybenzonitrile hydrochloride (3.81)

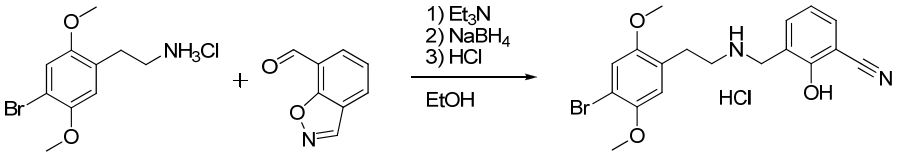

3.70 **3.81**

Obtained from 2C-B·HCl and **3.70** by standard procedure A in 24% yield as a colorless solid. ^{1}H NMR (300 MHz, DMSO-d_6) δ ^{1}H NMR (300 MHz, DMSO) δ 11.05 (br s, 1H), 9.35 (br s, 2H), 7.80 (dd, *J* = 7.7, 1.6 Hz, 1H), 7.69 (dd, *J* = 7.7, 1.6 Hz, 1H), 7.18 (s, 1H), 7.05 (t, *J* = 7.7 Hz, 1H), 7.01 (s, 1H), 4.26 (s, 2H), 3.79 (s, 3H), 3.75 (s, 3H), 3.22-3.07 (m, 2H), 3.02-2.91 (m, 2H). ^{13}C NMR (75 MHz, DMSO-d_6) δ ^{13}C NMR (75 MHz, DMSO) δ 158.0, 151.3, 149.2, 137.4, 134.3, 125.3, 121.3, 120.4, 116.7, 115.7, 114.8, 108.8, 101.7, 56.6, 56.2, 46.0, 44.7, 26.5.

Experimental – Chapter 4

3-(4-bromo-2,5-dimethoxybenzyl)-1,2,3,4-tetrahydroisoquinoline (4.3)

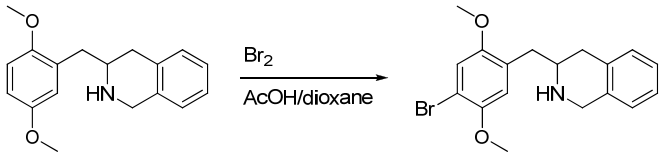

A flame dried flask containing a solution of **4.16** (0.180 g, 0.635 mmol) in AcOH/dioxane 1:1 (5 mL) was cooled with magnetic stirring to 0 °C and wrapped in aluminium foil. A 0.206 M solution of Br_2 in AcOH/Dioxane 1:1 (4.0 mL, 0.826 mmol) was added drop wise and the reaction was stirred for 48 hours at room temperature. KOAc (0.100 g) was added to quench excess HBr and the reaction mixture was poured onto ice (ca. 50 mL) and stirred until all ice had melted. Saturated aqueous $NaHSO_3$ (5 mL) was added to quench excess Br_2. The mixture was made basic (pH > 10) by addition of conc. NaOH. The mixture was extracted with Et_2O (4 × 20 mL) and the organic extracts were dried (Na_2SO_4), filtered and evaporated under reduced pressure. The crude product was purified by flash chromatography (EtOAc/hexanes/Et_3N 70:30:1) to give the title compound, **4.3** (0.117 g, 51%) as a colorless oil. ^{1}H-NMR (300 MHz, $CDCl_3$) δ 7.14-6.98 (m, 5H), 6.81 (s, 1H), 4.03 (s, 2H), 3.86 (s, 3H), 3.78 (s, 3H), 3.25-3.13 (m, 1H), 2.92-2.55 (m, 4H), 1.77 (br s, 1H). ^{13}C-NMR (75 MHz, $CDCl_3$) δ 153.4, 152.2, 135.5, 135.0, 129.2, 128.5, 126.2, 126.0, 125.7, 117.4, 111.7, 111.5, 56.0, 55.8, 53.7, 48.8, 37.8, 35.7

The hydrochloride salt was prepared by dissolving the product in the minimum amount of Et_2O and treating the solution with ethereal HCl until all products had precipitated. The fluffy off-white crystals were isolated by filtration and dried under reduced pressure. mp. 110 °C dec.

3-(4-bromo-2,5-dimethoxyphenyl)-1-(2-methoxybenzyl)piperidine (4.5)

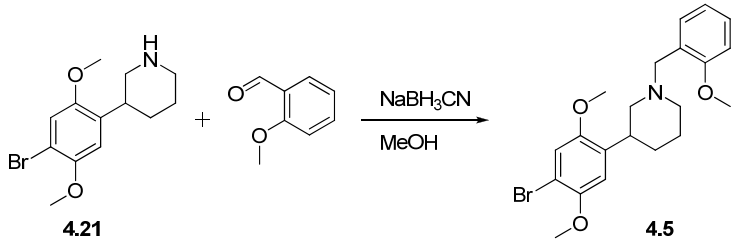

4.21 (0.260 g, 0.866 mmol) was dissolved in dry MeOH and there was added 2-methoxybenzaldehyde (0.104 mL, 0.866 mmol) followed by powdered activated 3Å molecular sieves (0.1 g). The reaction was stirred at room temperature for 45 minutes and then $NaBH_3$ CN (0.087 g, 1.386 mmol) was added in one portion. The reaction was stirred at room temperature for 6 hours and then quenched with 2M NaOH (5 mL). The reaction mixture was partitioned between water (25 mL) and EtOAc (25 mL) and the organic layer was isolated. The aqueous layer was extracted with EtOAc (20 mL) and the organic extracts were pooled and extracted with 1N HCl (3 × 25 mL). The aqueous extracts where made basic (pH>10) with conc. NaOH and extracted with Et_2O (2 × 25 mL) and EtOAc (2 × 25 mL). The combined organic extracts were dried (Na_2SO_4), filtered and evaporated under reduced pressure. The crude product was purified by

flash chromatography (acetone/hexanes 1:20) to give the title compound, **4.5** (0.242 g, 66%).[1]H NMR (300 MHz, $CDCl_3$) δ 7.41 (dd, *J* = 7.4, 1.7 Hz, 1H), 7.21 (ddd, *J* = 8.2, 7.5, 1.7 Hz, 1H), 7.00 (s, 1H), 6.93 (ddd, *J* = 7.4, 7.5, 1.1 Hz, 1H), 6.87 (s, 1H), 6.85 (dd, *J* = 8.2, 1.1 Hz, 1H) 3.83 (s, 3H), 3.80 (s, 3H), 3.74 (s, 3H), 3.59 (s, 2H), 3.28 (tt, *J* = 11.2, 3.4 Hz, 1H), 3.02-2.87 (m, 2H), 2.18-2.02 (m, 2H), 1.88-1.68 (m, 3H), 1.49-1.33 (m, 1H). ^{13}C NMR (75 MHz, $CDCl_3$) δ 157.9, 151.8, 150.1, 133.9, 130.5, 127.9, 126.7, 120.4, 115.9, 112.3, 110.4, 108.7, 59.6, 57.2, 56.5, 56.3, 55.5, 54.1, 35.5, 30.4, 25.7

The hydrochloride salt was prepared by dissolving the product in the minimum amount of MeOH and treating the solution with ethereal HCl. The precipitate was isolated by filtration and redissolved in the minimum amount of MeOH. Et_2O was added until nucleation started and the solution was allowed to crystallize overnight in the freezer. The white crystals were isolated by filtration and dried under reduced pressure. mp. 163 °C dec.

2,5-dimethoxyphenyl)-*N*-methoxy-*N*-methylacetamide (4.13)

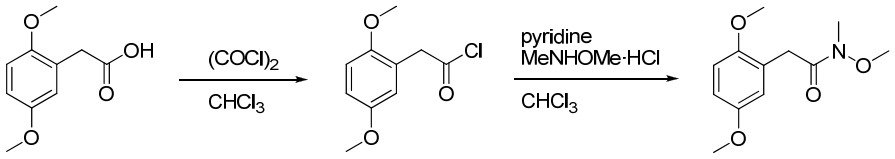

4.12 **4.13**

2-(2,5-dimethoxyphenyl)acetic acid, **4.12** (4.00 g, 20.39 mmol) was dissolved in $CHCl_3$ (100 mL) and cooled to 0 °C. $(COCl)_2$ (3.56 mL, 40.78 mmol) was added dropwise via syringe and the reaction was allowed to reach room temperature. After 1 hour the reaction was concentrated under reduced pressure and the residue was dissolved in $CHCl_3$ and cooled to 0 °C. (1.657 g, 16.99 mmol) was added in one portion and allowed to dissolve. Pyridine (4.11 mL, 50.97 mmol) was added dropwise *via* syringe. The cold bath was removed and the reaction was stirred at room temperature for 1 hour. The reaction mixture was partitioned between Et_2O (120 mL) and 0.1M NaOH (120 mL) and the organic layer was isolated and washed with 0.1M NaOH (120 mL), 0.1M HCl (120 mL) and brine (120 mL). The organic layer was dried ($MgSO_4$), filtered and evaporated under reduced pressure to give a pale yellow oil. Recrystallization from Et_2O/hexanes gave the title compound, **4.13** (3.546 g, 87%) as pale yellow crystals. mp. 58-60 °C. EI-MS: m/z (M^+) 239. ^{1}H-NMR (300 MHz, $CDCl_3$) δ 6.83-6.70 (m, 3H), 3.77 (s, 3H), 3.75 (s, 5H), 3.67 (s, 3H), 3.20 (s, 3H). ^{13}C-NMR (75 MHz, $CDCl_3$) δ 172.6, 153.5, 151.7, 124.9, 117.0, 112.6, 111.5, 61.2, 56.1, 55.7, 33.7, 32.4

tert-butyl 2-(3-(2,5-dimethoxyphenyl)-2-oxopropyl)benzylcarbamate (4.14)

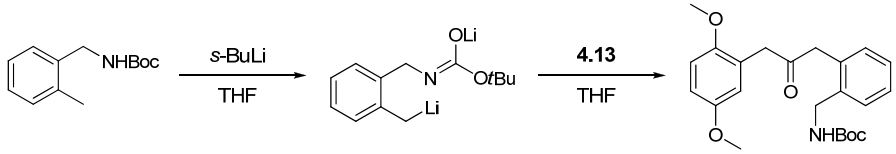

4.11 4.14

A flame-dried flask was charged with a solution **4.11** (0.114 g, 0.515 mmol) in dry THF (5 mL). The solution was cooled to -40 °C. *s*-BuLi (1.3 M in cyclohexane) was added drop wise until the color changed from yellow to orange/red. At this point an additional 1.1 eq. of *s*-BuLi (0.567 g, 0.44 mL) was added. The deep red solution was stirred for 15 minutes at -40 °C and then cooled to -65 °C. A solution of **4.13** (0.112 g, 0.468 mmol) in dry THF (2 mL) was added *via* syringe to the cooled solution and the red color disappeared. The reaction was allowed to reach room temperature over a couple of hours and then quenched by addition of saturated NH_4Cl (1 mL). The mixture was partitioned between water (10 mL) and EtOAc (10 mL) and the organic layer was isolated. The aqueous layer was extracted with EtOAc (10 mL) and the combined organics were dried ($NaSO_4$), filtered and evaporated under reduced pressure. The residue was purified by flash chromatography (EtOAc/hexanes 1:4) to give the title compound, **4.14** (0.071 g, 38%) as white needles. mp. 63-65 °. ESI-MS: m/z ($M+Na^+$) 422. ^{1}H-NMR (300 MHz, $CDCl_3$) δ 7.36-7.30 (m, 1H), 7.28-7.17 (m, 2H), 7.08-7.02 (m, 1H), 6.84-6.76 (m, 2H), 6.74-6.70 (m, 1H), 4.95 (br s, 1H), 4.19 (br d, *J* = 6.7 Hz, 2H), 3.83 (s, 2H), 3.76 (s, 3H), 3.75 (s, 3H), 3.73 (s, 2H), 1.45 (s, 9H). ^{13}C-NMR (75 MHz, $CDCl_3$) δ 206.4, 155.9, 153.6, 151.6, 137.7, 132.9, 131.0, 129.5, 127.8, 127.7, 124.3, 117.5, 113.0, 111.4, 79.4, 55.9, 55.8, 46.3, 44.9, 42.5, 28.5 (3C).

3-(2,5-dimethoxybenzyl)-1,2,3,4-tetrahydroisoquinoline (4.16)

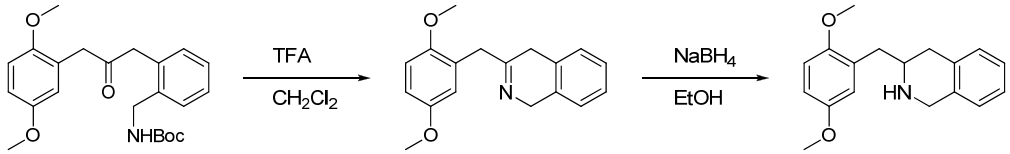

4.14 4.15 4.16

To a stirred solution of **4.14** (0.473 g, 1.184 mmol) in DCM (15 mL) there was added TFA (8 mL, 107.7 mmol). The reaction was stirred at room temperature for 30 minutes and then concentrated under reduced pressure. The residue was dissolved in EtOH (15 mL) and cooled to 0 °C. $NaBH_4$ (0.157 g, 4.144 mmol) was added in small portions and the reaction was stirred for 1 hour at room temperature. The reaction was quenched by addition of 1M HCl (3 mL) and basified with conc. NH_4OH. The mixture was partitioned between brine (10 mL) and DCM (20 mL) and the organic layer was isolated. The aqueous layer was extracted with DCM (2 × 10 mL) and the combined organics were dried ($NaSO_4$), filtered and evaporated under reduced pressure. The crude product was purified by flash chromatography (DCM/MeOH/NH_4OH 95:4:1) to give the title compound, **4.16** (0.252 g, 75%) as a colorless oil. ESI-MS: m/z (M+H) 284. ^{1}H-NMR (300 MHz, $CDCl_3$) δ 7.13-7.98 (m, 4H), 6.85-6.72 (m, 3H), 4.04 (s, 2H), 3.78 (s, 6H), 3.27-3.15 (m, 1H), 2.91-2.57 (m, 4H), 1.81 (br s, 1H).^{13}C-NMR (75 MHz, $CDCl_3$) δ 153.3, 152.0, 135.4, 134.8, 129.1, 128.4, 126.0, 125.9, 125.5, 117.3, 111.5, 111.3, 55.8, 55.6, 53.5, 48.6, 37.6, 35.6

2,5-dimethoxyphenylboronic acid (4.18)

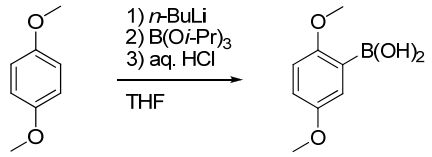

4.17 4.18

To a solution of 1,4-dimethoxybenzene, **4.17** (6.11 g, 44.22 mmol) in dry THF (50 mL) was added 2.5 M *n*-BuLi in hexanes (21.22 mL, 53.06 mmol) over a period of 5 minutes. The solution was stirred at room temperature for 1 hour and then transferred dropwise via cannula to a pre-cooled (-78 °C) solution of B(O*i*Pr)$_3$ (20.79 g, 110.6 mmol) in dry THF (30 mL). The reaction was allowed to reach room temperature over a period of 3 hours (or overnight). To the opaque mixture was added 1M HCl (60 mL) and the mixture was stirred vigorously for 2 hours and then partitioned between water (25 mL) and Et_2O (100 mL). The organic layer was isolated end the aqueous layer was extracted with Et_2O (50 mL). The combined organic layers were washed with water (50 mL), dried ($MgSO_4$), filtered and evaporated under reduced pressure. The solids were recrystallized from EtOAc /hexane to give the title compound, **4.18** (5.55 g, 69%). mp. 96-97 °C. ^{1}H NMR (300 MHz, $CDCl_3$) δ 7.36 (d, *J* = 3.2 Hz, 1H), 6.98 (dd, *J* = 9.2, 3.2 Hz, 1H), 6.85 (d, *J* = 9.2 Hz, 1H), 5.84 (s, 2H), 3.87 (s, 3H), 3.79 (s, 3H)

3-(2,5-dimethoxyphenyl)pyridine (4.19)

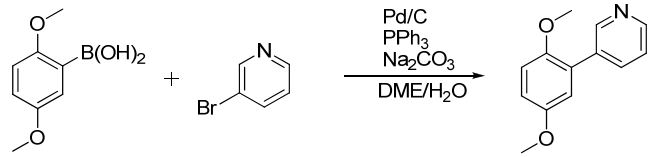

4.18 4.19

To a flame-dried flask was added **4.18** (4.645 g, 25.25 mmol), 3-bromopyridine (2.69 g, 17.02 mmol) and triphenylphosphine (0.893 g, 3.403 mmol). The solids were dissolved in DME (66 mL) and there was added 2M Na_2CO_3 (34 mL, 68.00 mmol) followed by 10% Pd/C (0.905 g). The reaction was stirred overnight at 80 ºC and then cooled to room temperature. The reaction mixture was filtered through a pad of Celite which was washed with EtOAc (100 mL). The filtrate was transferred to a separatory funnel and the organic layer was isolated. The aqueous layer was extracted with EtOAc (2 × 50 mL) and the combined organics were dried (Na_2SO_4), filtered and evaporated under reduced pressure. The dark yellow oil was purified by flash chromatography (EtOAc/hexanes, 2:5) to give the title compound, 4.19 (2.850 g, 78%) as a clear oil. ^{1}H NMR (300 MHz, $CDCl_3$) δ 8.77 (d, *J* = 2.2 Hz, 1H), 8.55 (dd, *J* = 4.8, 1.6 Hz, 1H), 7.85 (ddd, *J* = 7.8, 2.2, 1.6 Hz, 1H), 7.37-7.27 (dd, *J* = 7.8, 4.8 Hz), 6.98-6.87 (m, 3H), 3.80 (s, 3H), 3.76 (s, 3H). ^{13}C NMR (75 MHz, $CDCl_3$) δ 153.9, 150.8, 150.2, 148.1, 136.8, 134.1, 127.9, 122.9, 116.6, 113.9, 112.6, 56.2, 55.9

The hydrochloride salt was prepared by dissolving the product in the minimum amount of Et_2O and treating the solution with ethereal HCl. The precipitate was isolated by filtration and redissolved in the minimum amount of MeOH. Et_2O was added until nucleation started and the solution was allowed to crystallize overnight in the freezer. The pale yellow crystals were isolated by filtration. mp (HCl-salt) 173-175 °C (litt[332]. 170-173 °C)

3-(2,5-dimethoxyphenyl)piperidine (4.20)

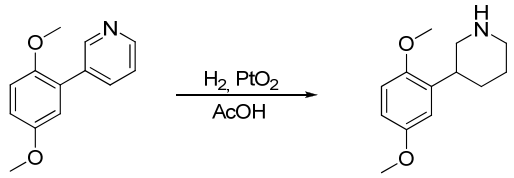

4.19 **4.20**

4.19 (0.924 g, 4.293 mmol) was dissolved in AcOH (22 mL) in a hydrogenation flask. PtO_2 (0.097 g, 0.429 mmol.) was added and the reaction vessel was shaken under H_2-atmosphere (50-70 psi) in a Parr-apparatus until TLC showed full conversion (6 hours). The reaction mixture was filtered through a pad of Celite which was washed with EtOAc (100 mL). The filtrate was basified by addition of 10% aqueous NaOH (150 mL). The organic layer was isolated and the aqueous layer was extracted with EtOAc (2 × 50 mL). The combined organic extracts were dried ($NaSO_4$), filtered and evaporated under reduced pressure to give the title compound, **4.20** (0.833 g, 88%) as an off-white solid. ^{1}H NMR (300 MHz, $CDCl_3$) δ 6.78 (d, *J* = 6.1 Hz, 1H), 6.76 (s, 1H), 6.68 (dd, *J* = 8.6, 3.2 Hz, 1H), 3.77 (s, 3H), 3.76 (s, 3H), 3.19-3.00 (m, 3H), 2.68-2.48 (m, 2H), 1.98-1.87 (m, 1H), 1.81-1.70 (m, 1H), 1.69-1.47 (m, 3H). ^{13}C NMR (75 MHz, $CDCl_3$) δ 153.7, 151.4, 134.5, 113.9, 111.3, 110.3, 56.1, 55.7, 53.0, 46.9, 37.3, 30.9, 27.6

The hydrochloride salt was prepared by dissolving the product in the minimum amount of ether and treating the solution with ethereal HCl. The precipitate was isolated by filtration and redissolved in the minimum amount of MeOH. Et_2O was added until nucleation started and the solution was allowed to crystallize overnight in the freezer. The flaky white crystals were isolated by filtration, and dried under reduced pressure. mp. 167-169 °C

3-(4-bromo-2,5-dimethoxyphenyl)piperidine (4.21)

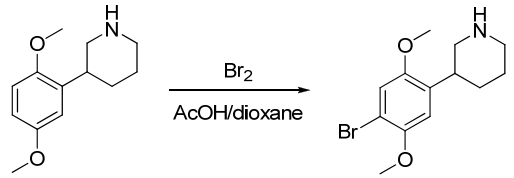

4.20 **4.21**

A flame dried flask containing a solution of the phenylpiperidine, **4.20** (0.380 g, 1.717 mmol) in AcOH/Dioxane 1:1 (13.4 mL) was cooled with magnetic stirring to 0 °C. A 1.0 M solution of Br_2 in AcOH/Dioxane 1:1 (1.8 mL, 1.800 mmol) was added drop wise and the reaction was stirred overnight at room temperature. After 18 hours KOAc (0.200 g) was added to quench excess HBr and the reaction mixture was poured onto ice (ca. 50 mL) and stirred until all ice had melted. Saturated aqueous $NaHSO_3$ (10 mL) was added to quench excess Br_2. The mixture was made basic by addition of conc. NaOH to pH > 10. The mixture was extracted with Et_2O (4 × 50 mL) and the organic extracts were dried (Na_2SO_4), filtered and evaporated under reduced pressure. The crude product was purified by flash chromatography (EtOAc/MeOH/Et_3N 90:9:1) to give bromophenylpiperidine, **4.21** (0.321 g, 62%) as a colorless oil.

The hydrochloride salt was prepared by dissolving the product in the minimum amount of MeOH and treating the solution with ethereal HCl. The precipitate was isolated by filtration and

redissolved in the minimum amount of MeOH. Et_2O was added until nucleation started and the solution was allowed to crystallize overnight in the freezer. The white crystals were isolated by filtration and dried under reduced pressure. mp. 220 °C dec. ^{1}H-NMR (300 MHz, $CDCl_3$) δ 7.03 (s, 1H), 6.67 (s, 1H), 3.82 (s, 3H), 3.75 (s, 3H), 3.59-3.32 (m, 3H), 3.20-3.10 (m, 2H), 2.92-2.81 (m, 1H), 2.20-1.70 (m, 4H). ^{13}C-NMR (75 MHz, $CDCl_3$) δ 151.7, 150.3, 128.7, 116.5, 112.6, 110.6, 57.2, 56.1, 47.2, 44.1, 36.2, 28.2, 22.9

2-chloro-5-(2,5-dimethoxyphenyl)pyridine (4.23)

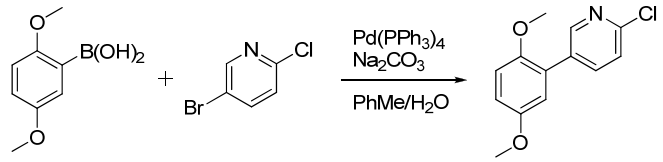

4.18 (2.005 g, 11.02 mmol) was dissolven in toluene (80 mL) and there was added 5-bromo-2-chloropyridine, **4.22** (1.927 g, 10.01 mmol) followed by $Pd(PPh_3)_4$ (0.231 g, 0.20 mmol). 2M Na_2CO_3 (20 mL, 40 mmol) was added and the reaction was stirred at 65 °C overnight. After cooling to room temperature, the reaction mixture was filtered through a pad of Celite which was washed with EtOAc (20 mL). The filtrate was transferred to a separatory funnel and the organic layer was isolated. The aqueous layer was extracted with EtOAc (20 mL) and the combined organic layers were dried (Na_2SO_4), filtered and evaporated under reduced pressure. The residue was purified by flash chromatography (hexanes/acetone 20:1) and recrystallized from hexanes/acetone to give the title compound, **4.23** (1.551 g, 62%) as a white solid. ^{1}H NMR (300 MHz, $CDCl_3$) δ 8.50 (d, *J* = 2.5 Hz, 1H), 7.81 (dd, *J* = 8.3, 2.5, 1H), 7.33 (d, *J* = 8.3, Hz, 1H), 6.96-6.78 (m, 3H), 3.80 (s, 3H), 3.75 (s, 3H). ^{13}C NMR (75 MHz, $CDCl_3$) δ 153.8, 150.7, 150.0, 149.9, 139.6, 133.0, 126.5, 123.5, 116.4, 114.2, 112.7, 56.3, 56.0

5-(2,5-dimethoxyphenyl)-2-(2-methoxyphenyl)pyridine (4.24)

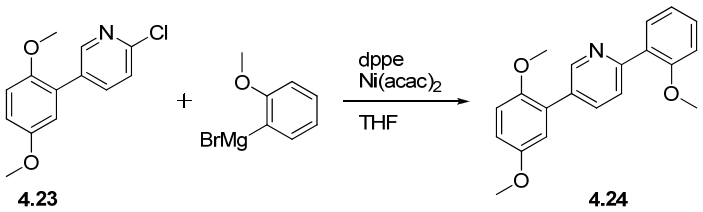

To a well-stirred suspension of Mg-turnings (1.11 g, 45.53 mmol) in dry THF (50 mL) was added 2-bromoanisole (8.51 g, 45.53 mmol) and the reaction was heated at reflux temperature until all the Mg had passed into solution (1 hour). This solution was transferred via cannula to a solution of **4.24** (3.78 g, 15.18 mmol), $Ni(acac)_2$ (0.195 g, 0.769 mmol) and dppe (0.302 g, 0.759 mmol) in dry THF (50 mL). The reaction was stirred overnight at room temperature and then quenched by addition of water (5 mL). The reaction mixture was partitioned between saturated NH_4Cl (100 mL) and Et_2O (100 mL) and the organic layer was isolated. The aqueous layer was extracted with Et_2O (3 × 100 mL) and the combined organic layers were dried (Na_2SO_4), filtered and evaporated under reduced pressure. The residue was purified by flash chromatography (hexanes/EtOAc 10:1) to give the title compound, **4.24** (3.75 g, 77%) as white crystals. ^{1}H NMR (300 MHz, $CDCl_3$) δ 8.85 (dd, *J* = 1.8, 1.4 Hz, 1H), 7.86 (d, *J* = 0.6 Hz, 1H), 7.86 (s, 1H), 7.82 (dd, *J* = 7.6, 1.8 Hz, 1H),

7.35 (ddd, *J* = 8.3, 7.3, 1.8 Hz, 1H), 7.06 (ddd, *J* = 7.5, 7.5, 1.1 Hz, 2H), 6.99 (dd, *J* = 8.2, 1.1 Hz, 1H), 6.94 (dd, *J* = 2.9, 0.6 Hz, 1H), 6.91 (s, 1H), 6.86 (dd, *J* = 8.8, 2.9 Hz, 1H), 3.86 (s, 3H), 3.80 (s, 3H), 3.77 (s, 3H). ^{13}C NMR (75 MHz, $CDCl_3$) δ 157.0, 154.3, 153.8, 150.9, 149.7, 136.4, 131.9, 131.2, 129.8, 128.9, 128.0, 124.3, 121.1, 116.5, 113.8, 112.6, 111.4, 56.3, 55.9, 55.7

Experimental – Chapter 5

2-(4-bromo-2,5-dimethoxyphenyl)-*N*-(2-methoxy-4,5-dimethylbenzyl)ethanamine hydrochloride (5.1)

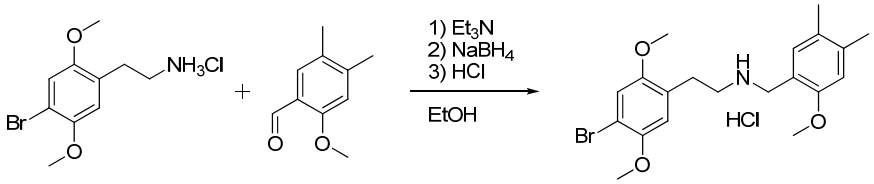

5.11 **5.1**

Obtained from 2C-B·HCl and **5.11** by general procedure A in 71% yield as a colorless solid. mp. 205-206 °C. ^{1}H NMR (300 MHz, DMSO-d_6) δ 9.24 (br s, 2H), 7.22 (s, 1H), 7.17 (s, 1H), 7.00 (s, 1H), 6.87 (s, 1H), 4.01 (t, *J* = 5.2 Hz, 2H), 3.78 (s, 3H), 3.78 (s, 3H), 3.73 (s, 3H), 2.98 (s, 4H), 2.23 (s, 3H), 2.14 (s, 3H). ^{13}C NMR (75 MHz, DMSO-d_6) δ 155.3, 151.3, 149.2, 138.6, 132.3, 127.5, 125.4, 116.3, 115.7, 114.8, 112.3, 108.7, 56.6, 56.2, 55.6, 45.4, 44.4, 26.3, 19.8, 18.4

2-(4-bromo-2,5-dimethoxyphenyl)-*N*-(5-bromo-2-methoxybenzyl)ethanamine hydrochloride, (5.2)

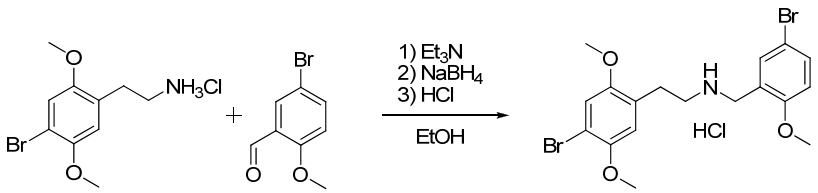

5.13 **5.2**

Obtained from 2C-B·HCl and **5.13** by general procedure A in 73% yield as a colorless solid. mp. 185-186 °C. ^{1}H NMR (300 MHz, DMSO-d_6) δ 9.44 (br s, 2H), 7.74 (d, *J* = 2.5 Hz, 1H), 7.55 (dd, *J* = 8.8, 2.5 Hz, 1H), 7.17 (s, 1H), 7.04 (d, *J* = 8.8 Hz), 7.01 (s, 1H), 4.09 (s, 2H), 3.82 (s, 3H), 3.79 (s, 3H), 3.75 (s, 3H), 3.13-2.94, (m, 4H). ^{13}C NMR (75 MHz, DMSO-d_6) δ 156.6, 151.3, 149.2, 133.5, 132.9, 125.3, 122.2, 115.7, 114.8, 113.3, 111.4, 108.7, 56.6, 56.2, 56.0, 45.7, 43.9, 26.3.

2-(4-bromo-2,5-dimethoxyphenyl)-*N*-(4-bromo-2-methoxybenzyl)ethanamine hydrochloride (5.3)

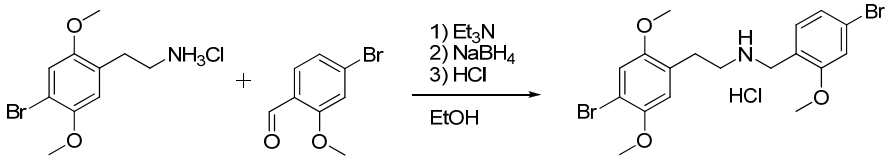

5.16 **5.3**

Obtained from 2C-B·HCl and **5.15** by general procedure A in 74% yield as a colorless solid. mp. 187-188 °C. ^{1}H NMR (300 MHz, DMSO-d_6) δ 9.43 (s, 2H), 7.47 (d, *J* = 8.1 Hz, 1H), 7.26 (d, *J* = 1.8 Hz, 1H), 7.19 (dd, *J* = 8.1, 1.8 Hz, 1H), 7.17 (s, 1H), 4.07 (s, 2H), 3.85 (s, 3H), 3.78 (s, 3H), 3.74 (s, 3H), 3.10-2.93 (m, 4H). ^{13}C NMR (75 MHz, DMSO-d_6) δ 158.1, 151.3, 149.2, 132.9, 125.3, 123.2, 123.0, 119.2, 115.7, 114.8, 114.3, 108.7, 56.6, 56.2, 56.2, 45.6, 44.1, 26.3

2-(4-bromo-2,5-dimethoxyphenyl)-*N*-(2-methoxy-4-methylbenzyl)ethanamine hydrochloride (5.4)

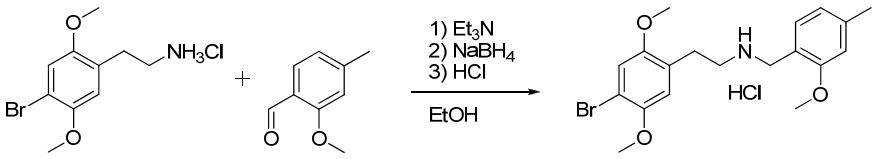

5.19 **5.4**

Obtained from 2C-B·HCl and **5.19** by general procedure A in 68% yield as a colorless solid. mp. 212-213 °C. ^{1}H NMR (300 MHz, DMSO-d_6) δ 9.26 (br s, 2H), 7.35 (d, *J* = 7.6 Hz, 1H), 7.17 (s, 1H), 7.00 (s, 1H), 6.89 (s, 1H), 6.78 (d, *J* = 7.6 Hz, 1H), 4.05 (s, 2H), 3.80 (s, 3H), 3.78 (s, 3H), 3.73 (s, 3H), 3.09-2.92 (m, 4H), 2.32 (s, 3H). ^{13}C NMR (75 MHz, DMSO-d_6) δ 157.2, 151.3, 149.2, 140.4, 131.2, 125.4, 120.7, 116.5, 115.7, 114.8, 111.6, 108.7, 56.6, 56.2, 55.5, 45.5, 44.5, 27.3, 26.3, 21.3

2-(4-bromo-2,5-dimethoxyphenyl)-*N*-(4-ethyl-2-methoxybenzyl)ethanamine hydrochloride (5.5)

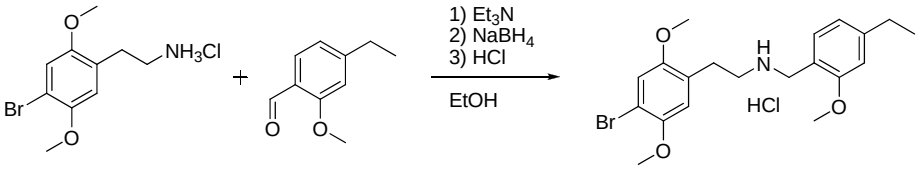

5.24 **5.5**

Obtained from 2C-B·HCl and **5.24** by general procedure A in 56% yield as a colorless solid. mp. 173-174 °C. 1H NMR (300 MHz, DMSO-d6) δ 9.35 (br s, 2H), 7.40 (d, J = 7.6 Hz, 1H), 7.16 (s, 1H), 7.01 (s, 1H), 6.90 (d, J = 1.2 Hz, 1H), 6.81 (dd, J = 7.6, 1.2 Hz, 1H), 4.05 (t, J = 4.9 Hz, 2H), 3.81 (s, 3H), 3.78 (s, 3H), 3.73 (s, 3H), 3.00 (s, 4H), 2.61 (q, *J* = 7.5 Hz, 2H), 1.19 (t, *J* = 7.5 Hz, 3H). ^{13}C NMR (75 MHz, DMSO-d_6) δ 157.3, 151.3, 149.2, 146.7, 131.3, 125.4, 119.4, 116.8, 115.7, 114.8, 110.5, 108.7, 56.6, 56.2, 55.5, 45.5, 44.4, 28.4, 26.3, 15.6

2-(4-bromo-2,5-dimethoxyphenyl)-*N*-(2-methoxy-4-propylbenzyl)ethanamine hydrochloride (5.6)

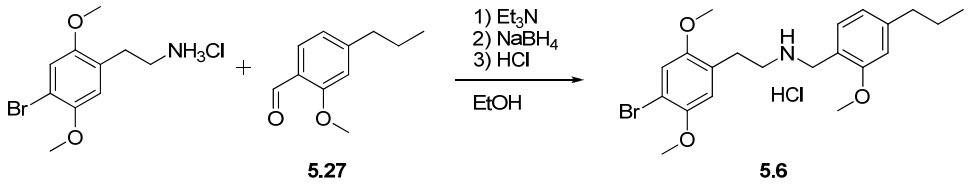

5.27 **5.6**

Obtained from 2C-B·HCl and **5.27** by general procedure A in 68% yield as a colorless solid. mp. 128-129 °C. ^{1}H NMR (300 MHz, DMSO) δ 9.37 (br s, 2H), 7.40 (d, *J* = 7.6 Hz, 1H), 7.16 (s, 1H), 7.01 (s, 1H), 6.88 (d, *J* = 1.2 Hz, 1H), 6.79 (dd, *J* = 7.6, 1.2 Hz, 1H), 4.05 (s, 2H), 3.81 (s, 3H), 3.78 (s, 3H), 3.73 (s, 3H), 3.00 (s, 4H), 2.55 (t, *J* = 7.3 Hz, 2H), 1.59 (sextet, *J* = 7.3 Hz, 2H), 0.89 (t, *J* = 7.3 Hz, 3H). ^{13}C NMR (75 MHz, DMSO) δ 157.2, 151.3, 149.2, 145.1, 131.2, 125.4, 120.1 116.8, 115.7, 114.8, 111.0, 108.7, 56.6, 56.2, 55.5, 45.5, 44.4, 37.4, 26.3, 24.1, 13.7

2-(4-bromo-2,5-dimethoxyphenyl)-*N*-(4-isobutyl-2-methoxybenzyl)ethanamine hydrochloride (5.7)

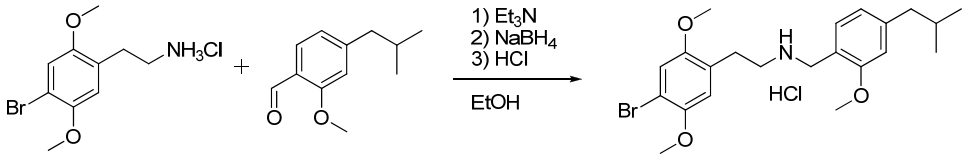

5.30 **5.7**

Obtained from 2C-B·HCl and **5.30** by general procedure A in 68% yield. mp. 144-145 °C. ^{1}H NMR (300 MHz, DMSO) δ 9.34 (br s, 2H), 7.39 (d, *J* = 7.6 Hz, 1H), 7.16 (s, 1H), 7.01 (s, 1H), 6.85 (d, *J* = 1.2 Hz, 1H), 6.76 (dd, *J* = 7.6, 1.2 Hz, 1H), 4.06 (s, 3H), 3.80 (s, 3H), 3.78 (s, 3H), 3.73 (s, 3H), 3.00 (s, 4H), 2.45 (d, *J* = 7.1 Hz, 2H), 1.86 (m, 1H), 0.86 (d, *J* = 6.6 Hz, 6H). ^{13}C NMR (75 MHz, DMSO) δ 157.1, 151.3, 149.2, 144.1, 131.0, 125.4, 120.7, 116.9, 115.7, 114.8, 111.5, 108.7, 56.6, 56.2, 55.5, 45.5, 44.7, 44.5, 29.6, 26.3, 22.2 (2C).

(3-((4-bromo-2,5-dimethoxyphenethylamino)methyl)-4-methoxyphenyl)methanol hydrochloride (5.8)

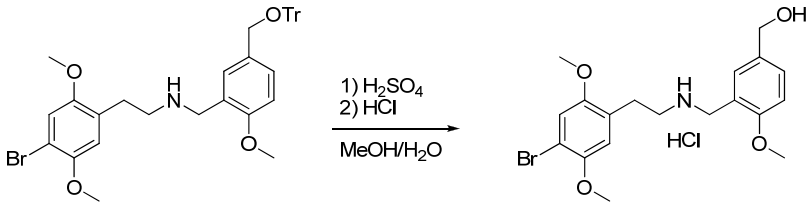

5.38 **5.8**

2-(4-bromo-2,5-dimethoxyphenyl)-*N*-(2-methoxy-5-(trityloxymethyl)benzyl)ethanamine, **5.38** (0.522 g, 0.80 mmol) was suspended in MeOH (20 mL) and there was added 4M aqueous H_2SO_4 (2.0 mL). The reaction was stirred at 50 °C, until TLC showed full conversion (30 minutes). The reaction mixture was neutralized with saturated aqueous $NaHCO_3$ and the MeOH was removed under reduced pressure. The remaining liquid was partitioned between water (20 mL) and CH_2Cl_2 (20 mL) and the organic layer was isolated. The aqueous layer was made basic to pH 11 with conc. NH_3 and extracted with CH_2Cl_2 (2 × 20 mL). The combined organic layers were dried (Na_2SO_4), filtered and evaporated under reduced pressure. The residue was purified by radial chromatography (CH_2Cl_2/2M methanolic ammonia, 98:2 → 90:10) and the free base was precipitated as the hydrochloride salt, **5.8** (0.293 g, 82%). mp. 169-171 °C. ^{1}H NMR (300 MHz, DMSO-d_6) δ 9.26 (br s, 2H), 7.41 (d, *J* = 2.0 Hz, 1H), 7.33 (dd, *J* = 8.4, 2.0 Hz, 1H), 7.17 (s, 1H), 7.02 (d, *J* = 8.4 Hz, 1H), 7.01 (s, 1H), 5.21 (br s, 1H), 4.43 (s, 2H), 4.09 (s, 2H), 3.81 (s, 3H), 3.79 (s, 3H), 3.74 (s, 3H), 3.11-2.93 (m, 4H). ^{13}C NMR (75 MHz, DMSO-d_6) δ 156.1, 151.3, 149.2, 134.3, 129.8, 128.7, 125.4, 119.1, 115.7, 114.8, 110.6, 108.7, 62.2, 56.6, 56.2, 55.7, 45.6, 44.9, 26.3

2-(3-((4-bromo-2,5-dimethoxyphenethylamino)methyl)-4-methoxyphenyl)ethanol hydrochloride (5.9)

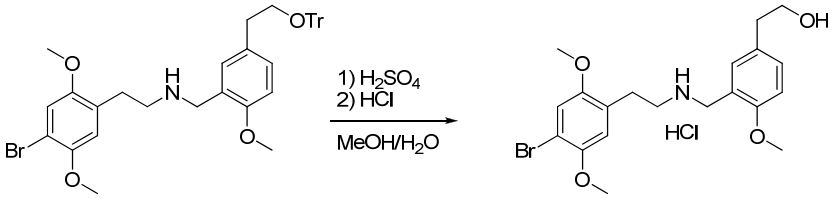

5.39 **5.9**

5.39 (0.570 g, 0.873 mmol) was suspended in MeOH (20 mL) and there was added 4M aqueous H_2SO_4 (2.0 mL). The reaction was stirred at 50 °C, until TLC showed full conversion (30 minutes). The reaction mixture was made basic with 15% aqueous NaOH and transferred to a separatory funnel with CH_2Cl_2 (50 mL) and water (50 mL) and the organic layer was isolated. The aqueous layer was extracted with CH_2Cl_2 (2 × 50 mL) and the combined organic layers were dried (Na_2SO_4), filtered and evaporated under reduced pressure. The residue was purified by radial chromatography (CH_2Cl_2/2M methanolic ammonia, 95:5 → 90:10) and the free base was precipitated as the hydrochloride salt, **5.9** (0.272 g, 68%). mp. 163-165 °C. ^{1}H NMR (300 MHz, DMSO-d_6) δ 9.28 (br s, 2H), 7.35 (d, *J* = 2.1 Hz, 1H), 7.22 (dd, *J* = 8.4, 2.2 Hz, 1H), 7.18 (s, 1H), 7.01 (s, 1H), 6.96 (d, *J* = 8.4 Hz, 1H), 4.69 (br s, 1H), 4.07 (s, 2H), 4.79 (s, 6H), 4.74 (s, 3H), 3.57 (t, *J* = 7.1 Hz, 2H), 3.12-3.93 (m, 4H), 2.66 (t, *J* = 7.1 Hz, 2H). ^{13}C NMR (75 MHz, DMSO-d_6) δ 155.6, 151.3, 149.2, 131.7, 131.2, 130.7, 125.4, 119.2, 115.7, 114.8, 110.8, 108.7, 62.2, 56.6, 56.2, 55.6, 45.7, 44.7, 38.1, 26.3

2-Methoxy-4,5-dimethylbenzaldehyde (5.11)

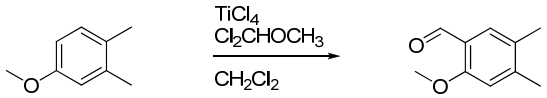

5.10 **5.11**

3,4-dimethylanisole, **5.10** (0.681 g, 5.00 mmol) was dissolved in dry CH_2Cl_2 (15 mL) and cooled to 0 °C. $TiCl_4$ (1.422 g, 7.5 mmol) was added dropwise followed by dichloromethyl methyl ether (0.632 g, 5.5 mmol). The reaction was stirred at 0 °C for 60 minutes and then poured onto ice-water (50 mL). The mixture was extracted with CH_2Cl_2 (2 × 15 mL) and the combined organic layers were dried ($MgSO_4$), filtered and evaporated under reduced pressure to give off-white crystals which were recrystalllized from EtOH/water to afford the title compound, **5.11** (0.755 g, 92%) as shiny off-white crystals. mp. 66-68 °C (Litt.[382] 66-67 °C). ^{1}H NMR (300 MHz, DMSO-d_6) δ 10.23 (s, 1H), 7.41 (s, 1H), 7.01 (s, 1H), 3.86 (s, 3H), 2.28 (s, 3H), 2.17 (s, 3H). ^{13}C NMR (75 MHz, DMSO-d_6) δ 188.2, 159.7, 146.1, 128.4, 127.8, 121.7, 113.5, 55.8, 20.4, 18.3

5-bromo-2-methoxybenzaldehyde (5.13)

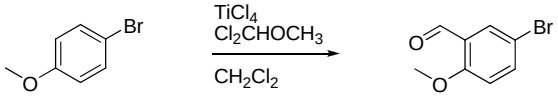

5.12 **5.13**

4-bromoanisole, **5.12** (1.87 g, 10.00 mmol) was dissolved in dry CH_2Cl_2 (30 mL) and cooled to 0 °C. $TiCl_4$ (4.74 g, 25 mmol) was added dropwise followed by dichloromethyl methyl ether (3.45 g,

30 mmol). The reaction was stirred at 0 °C for 90 minutes and then poured onto ice-water (150 mL). The mixture was extracted with CH_2Cl_2 (2 × 50 mL) and the combined organic layers were dried ($MgSO_4$), filtered and evaporated under reduced pressure to give off-white crystals which were recrystalllized from MeOH/water to afford the title compound, **5.13** (1.92 g, 89%) as shiny off-white crystals. mp. 112-114 °C (Litt.[383] 117-118 °C). ^{1}H NMR (300 MHz, $CDCl_3$) δ 10.35 (s, 1H), 7.89 (d, *J* = 2.6 Hz, 1H), 7.60 (dd, *J* = 8.8, 2.6 Hz, 1H), 6.87 (d, *J* = 8.8 Hz, 1H), 3.91 (s, 3H). ^{13}C NMR (75 MHz, $CDCl_3$) δ 188.3, 160.7, 138.29, 131.1, 126.1, 113.8, 113.5, 56.1

4-bromo-2-methoxybenzaldehyde (6.15)

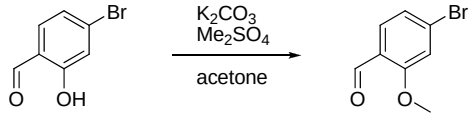

5.14 **5.15**

To a suspension K_2CO_3 (1.38 g, 10.0 mmol) in acetone (25 mL)was added 4-bromo-2-hydroxybenzaldehyde, **5.14** (1.01 g, 5.0 mmol) followed by Me_2SO_4 (0.95 g, 7.5 mmol). The reaction was heated at reflux temperature for 1 hour and then cooled to room temperature. The reaction mixture was filtered and the filter-cake washed thoroughly with acetone. The filtrate was evaporated under reduced pressure and the residue was redissolved in EtOAc (25 mL). The solution was washed with 1 M NaOH (25 mL), 1 M HCl (25 mL) and brine (25 mL), filtered ($MgSO_4$) and evaporated under reduced pressure. The residue was purified by flash chromatography (petroleum ether/EtOAc, 8:1) to give the title compound **5.15** (0.85 g, 79%) colorless oil. ^{1}H NMR (300 MHz, $CDCl_3$) δ 10.36 (s, 1H), 7.66 (d, *J* = 8.0 Hz, 1H), 7.17-7.12 (m, 2H), 3.92 (s, 3H). ^{13}C NMR (75 MHz, $CDCl_3$) δ 188.6, 161.8, 130.6, 129.7, 124.2, 123.7, 115.4, 56.1

Methyl 2-methoxy-4-methylbenzoate (5.17)

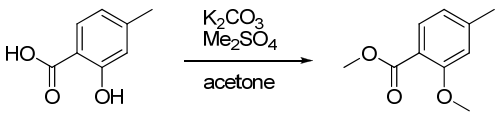

5.16 **5.17**

To a suspension K_2CO_3 (60.0 g, 434 mmol) in acetone (300 mL) was added 2-hydroxy-4-methylbenzoic acid, **5.16** (25.5 g, 168 mmol) followed by Me_2SO_4 (63.4 g, 503 mmol). The reaction was heated at reflux temperature for 4 hours and then cooled to room temperature. The reaction mixture was filtered and the filter-cake washed thoroughly with acetone. The filtrate was evaporated under reduced pressure and the residue was redissolved in EtOAc (300 mL). The solution was washed with 0.2 M NaOH (2 × 150 mL), water (150 mL), dried ($MgSO_4$), filtered and evaporated under reduced pressure. The residue was purified by short-path vacuum distillation and the fraction collected at 80-110 °C (0.2 mmHg) contained the title compound, **5.17** (25.4 g, 84%) as a colorless liquid. ^{1}H NMR (300 MHz, $CDCl_3$) δ 7.70 (d, *J* = 8.2 Hz, 1H), 6.79-6.74 (m, 2H), 3.88 (s, 3H), 3.86 (s, 3H), 2.37 (s, 3H). ^{13}C NMR (75 MHz, $CDCl_3$) δ 166.5, 159.3, 144.6, 131.8, 120.9, 116.9, 112.8, 56.0, 52.0, 22.1

(2-methoxy-4-methylphenyl)methanol (5.18)

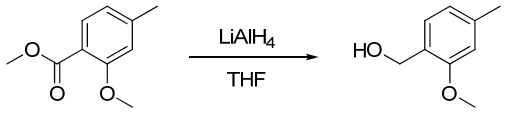

5.17 **5.18**

To a suspension of $LiAlH_4$ (0.683 g, 18.0 mmol) in THF (40 mL) was added **5.17** (1.081 g, 6.00 mmol) as a solution in THF (2 mL). The reaction was stirred at room temperature for 1 hour and then reaction was quenched by successive addition of water (0.7 mL), 15% NaOH (0.7 mL) and water (2.1 mL). The suspension was loosened by addition of Et_2O (20 mL) and filtered. The filter cake was washed thoroughly with Et_2O and the filtrate was evaporated under reduced pressure to give the title compound, **5.18** (0.740 g, 81%) as a colorless oil. ^{1}H NMR (300 MHz, $CDCl_3$) δ 7.11 (d, *J* = 7.4 Hz, 1H), 6.72 (d, *J* = 7.4 Hz, 1H), 6.68 (s, 1H), 4.61 (d, *J* = 6.4 Hz, 2H), 3.83 (s, 4H), 2.38 (d, *J* = 6.4 Hz, 1H), 2.34 (s, 3H). ^{13}C NMR (75 MHz, $CDCl_3$) δ 157.3, 139.1, 128.7, 126.1, 121.1, 111.2, 62.1, 55.3, 21.8

2-Methoxy-4-methylbenzaldehyde (5.19)

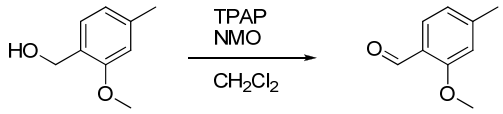

5.18 **5.19**

To a solution of **5.18** (0.700 g, 4.60 mmol) in CH_2Cl_2 (25 mL) was added powdered activated 4Å molecular sieves (2.5 g), TPAP (0.081 g, 0.23 mmol) and NMO (0.862 g, 7.36 mmol). The reaction was stirred for 30 minutes and the crude reaction mixture was poured onto a short column of silica and eluted with petroleum ether/EtOA (3:1). The fractions containing the product were evaporated to give the title compound **5.19** (0.504 g, 73%) as off-white crystals. mp. 45-46 °C (Litt.[384] 42.5-43 °C). ^{1}H NMR (300 MHz, $CDCl_3$) δ 10.36 (d, *J* = 0.6 Hz, 1H), 7.69 (d, *J* = 7.8 Hz, 1H), 6.81 (d, *J* = 7.8 Hz, 1H), 6.76 (s, 1H), 3.89 (s, 3H), 2.39 (s, 3H). ^{13}C NMR (75 MHz, $CDCl_3$) δ 189.3, 161.8, 147.4, 128.5, 122.6, 121.6, 112.2, 55.7, 22.5

1-ethyl-3-methoxybenzene (5.23)

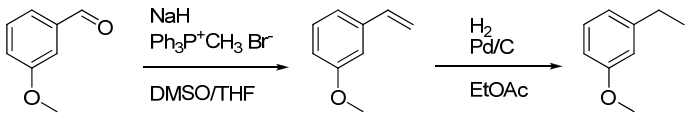

5.21 **5.22** **5.23**

To suspension of NaH (0.90 g, 37.5 mmol, 60% dispersion in oil) in dry DMSO (30 mL) was added methyltriphenylphosphonium bromide (10.71 g, 30.0 mmol) and THF (30 mL). The reaction was stirred at 60 °C for 15 minutes before 3-methoxybenzaldehyde, **5.21** (3.40 g, 25.00 mmol) was added. The reaction was stirred at 60 °C for 30 minutes and then poured into water (250 mL). The mixture was extracted with Et_2O (3 × 75 mL) and the combined organic extracts were washed with water (250 mL) and brine (250 m), dried ($MgSO_4$), filtered and evaporated under reduced pressure. The residue was purified by short-path vacuum-distillation and the fraction collected at 70-100 °C containing the methoxystyrene (**5.22**) was dissolved in EtOAc (30 mL) in a

hydrogenation flask. Pd/C (0.3 g) was added and the mixture was shaken under H_2-atmosphere (50 psi) in a Parr apparatus until GC-MS showed full conversion (ca. 1 hour). The reaction mixture was filtered through a pad of Celite which was washed with EtOAc (30 mL). The combined filtrates were evaporated under reduced pressure to give the title compound, **5.23** (2.70 g, 79%) as a pale yellow oil. ^{1}H NMR (300 MHz, $CDCl_3$) δ 7.17 (t, *J* = 7.7 Hz, 1H), 6.77 (d, *J* = 7.5 Hz, 1H), 6.74-6.67 (m, 2H), 3.78 (s, 1H), 2.62 (q, *J* = 7.6 Hz, 2H), 1.23 (t, *J* = 7.6 Hz, 3H). ^{13}C NMR (75 MHz, $CDCl_3$) δ 159.6, 145.9, 129.2, 120.3, 113.7, 110.8, 55.2, 29.1, 15.7

4-ethyl-2-methoxybenzaldehyde (5.24)

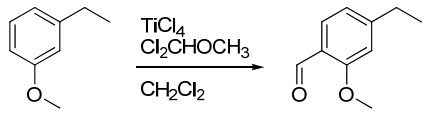

5.23 **5.24**

A solution of **5.23** (0.817 g, 6.00 mmol) in dry CH_2Cl_2 (15 mL) was cooled to 0 °C with stirring and there was added $TiCl_4$ (1.707 g, 9.00 mmol). After 5 minutes dichloromethyl methyl ether (0.828 g, 7.20 mmol) was added and the reaction was stirred at 0 °C for 45 minutes. The reaction mixture was poured into ice-water (50 mL) and extracted with CH_2Cl_2 (3 × 20 mL). The combined organic extracts were dried ($MgSO_4$), filtered and evaporated under reduced pressure. The residue was purified by flash chromatography (petroleum ether/CH_2Cl_2, 3:2) and the third product to elute was collected and evaporated under reduced pressure to give the title compound **5.24** (0.192 g, 20%) as a colorless oil. ^{1}H NMR (300 MHz, $CDCl_3$) δ 10.37 (d, *J* = 0.7 Hz, 1H), 7.72 (d, *J* = 7.9 Hz, 1H), 6.86-6.82 (m, 1H), 6.78 (d, *J* = 1.1 Hz, 1H), 3.90 (s, 3H), 2.68 (q, *J* = 7.6 Hz, 2H), 1.26 (t, *J* = 7.6 Hz, 3H). ^{13}C NMR (75 MHz, $CDCl_3$) δ 189.3, 161.9, 153.6, 128.6, 122.8, 120.4, 111.0, 55.6, 29.8, 15.3

1-methoxy-3-propylbenzene (5.23)

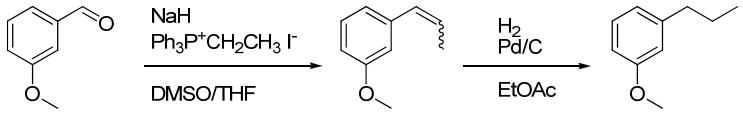

5.21 **5.25** **5.26**

To suspension of NaH (0.60 g, 25.0 mmol, 60% dispersion in oil) in dry DMSO (20 mL) was added ethyltriphenylphosphonium iodide (8.37 g, 20.0 mmol) and THF (20 mL). The reaction was stirred at 60 °C for 15 minutes before 3-methoxybenzaldehyde, **5.21** (2.04 g, 15.00 mmol) was added. The reaction was stirred at 60 °C for 30 minutes and then poured into water (150 mL). The mixture was extracted with Et_2O (3 × 50 mL) and the combined organic extracts were washed with water (2 × 150 mL) and brine (150 mL), dried ($MgSO_4$), filtered and evaporated under reduced pressure. The residue was purified by short-path vacuum-distillation and the fraction collected at 80-120 °C (0.4 mmHg) containing the propenylanisole (**5.25**) was dissolved in EtOAc (20 mL) in a hydrogenation flask. Pd/C (0.2 g) was added and the mixture was shaken under H_2-atmosphere (70 psi) in a Parr apparatus until GC-MS showed full conversion (ca. 90 minutes). The reaction mixture was filtered through a pad of Celite which was washed with EtOAc (30 mL). The combined filtrates were evaporated under reduced pressure to give the title compound, **5.26** (1.62 g, 72%) as a yellow oil. ^{1}H NMR (300 MHz, $CDCl_3$) δ 7.19-7.13 (m, 1H), 6.77-6.72 (m,

1H), 6.72-6.67 (m, 2H), 3.77 (s, 3H), 2.55 (t, *J* = 7.3 Hz, 2H), 1.63 (sextet, 7.3 Hz, 2H), 0.93 (t, *J* = 7.3 Hz, 3H). ^{13}C NMR (75 MHz, $CDCl_3$) δ 159.5, 144.3, 129.2, 121.0, 114.3, 110.9, 55.2, 38.3, 24.7, 14.1

2-methoxy-4-propylbenzaldehyde (5.27)

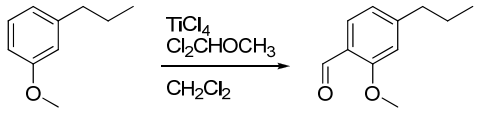

5.26 **5.27**

A solution of **5.26** (1.01 g, 6.72 mmol) in dry CH_2Cl_2 (20 mL) was cooled to 0 °C with stirring and there was added $TiCl_4$ (1.91 g, 10.1 mmol). After 5 minutes dichloromethyl methyl ether (0.927 g, 8.06 mmol) was added and the reaction was stirred at 0 °C for 45 minutes. The reaction mixture was poured into ice-water (75 mL) and extracted with CH_2Cl_2 (3 × 25 mL). The combined organic extracts were dried ($MgSO_4$), filtered and evaporated under reduced pressure. The residue was purified by flash chromatography (petroleum ether/CH_2Cl_2, 3:2) and the third product to elute was collected and evaporated under reduced pressure to give the title compound, **5.27** (0.468 g, 39%) as a pale brown oil. ^{1}H NMR (300 MHz, $CDCl_3$) δ 10.37 (s, 1H), 7.71 (d, *J* = 7.8 Hz, 1H), 6.82 (d, *J* = 7.8 Hz, 1H), 6.76 (s, 1H), 3.90 (s, 3H), 2.61 (t, *J* = 7.3 Hz, 2H), 1.66 (sextet, *J* = 7.3 Hz, 2H), 0.95 (t, *J* = 7.3 Hz, 3H). ^{13}C NMR (75 MHz, $CDCl_3$) δ 189.3, 161.8, 152.1, 128.5, 122.8, 121.0, 111.6, 55.6, 38.8, 24.3, 14.0

1-methoxy-3-(2-methylprop-1-enyl)benzene (5.28)

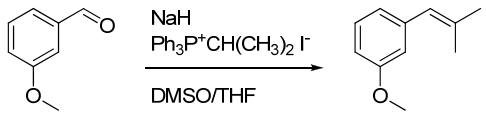

5.21 **5.28**

To suspension of NaH (0.60 g, 25.0 mmol, 60% dispersion in oil) in dry DMSO (20 mL) was added isopropyltriphenylphosphonium iodide (8.37 g, 20.0 mmol) and THF (20 mL). The reaction was stirred at 60 °C for 15 minutes before 3-methoxybenzaldehyde, **5.21** (2.04 g, 15.00 mmol) was added. The reaction was stirred at 60 °C for 30 minutes and then poured into water (150 mL). The mixture was extracted with Et_2O (3 × 50 mL) and the combined organic extracts were washed with water (2 × 150 mL) and brine (150 mL), dried ($MgSO_4$), filtered and evaporated under reduced pressure. The residue was purified by short-path vacuum-distillation and the fraction collected at 80-125 °C (0.4 mmHg) containing the title compound, **5.28** (1.61 g, 66%) as a colorless oil. ^{1}H NMR (300 MHz, $CDCl_3$) δ 7.20 (t, *J* = 7.8 Hz, 1H), 6.82-6.77 (m, 1H), 6.76-6.68 (m, 1H), 6.22 (s, 1H), 3.78 (s, 3H), 1.89 (d, *J* = 1.4 Hz, 1H), 1.86 (d, *J* = 1.4 Hz, 1H). ^{13}C NMR (75 MHz, $CDCl_3$) δ 159.2, 140.1, 135.8, 128.9, 125.0, 121.3, 114.3, 111.3, 55.3, 27.1, 19.7 (2C).

1-isobutyl-3-methoxybenzene (5.29)

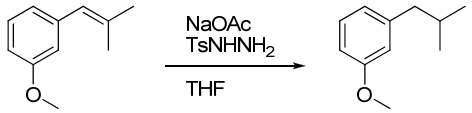

5.28 **5.29**

5.28 (0.85 g, 5.24 mmol) was dissolved in THF (55 mL) and there was added $TsNHNH_2$ (5.86 g, 31.44 mmol) and NaOAc (2.58 g, 31.44 mmol). The reaction was stirred at reflux temperature for 3 days and there was added additional $TsNHNH_2$ (2.93g, 15.72 mmol), NaOAc (1.29 g, 15.72 mmol) and THF (55 mL). The reaction was stirred for another 3 days at reflux temperature and then poured into water (300 mL). The mixture was extracted with Et_2O (2 × 75 mL) and the organic extracts were washed with saturated $NaHCO_3$ (100 mL), water (100 mL) and brine (100 mL). The organic extracts were dried ($MgSO_4$), filtered and evaporated under reduced pressure. The residue was purified by short-path vacuum-distillation and the fraction collected at 95-110 °C (20 mmHg) contained the title compound, **5.29** (0.637 g,74%) as a colorless oil. ^{1}H NMR (300 MHz, $CDCl_3$) δ 7.16 (t, *J* = 7.7 Hz, 1H), 6.74-6.66 (m, 3H), 3.77 (s, 3H), 2.44 (d, *J* = 7.2 Hz, 2H), 1.95-1.76 (m, 1H), 0.90 (d, *J* = 6.6 Hz, 6H). ^{13}C NMR (75 MHz, $CDCl_3$) δ 159.4, 143.4, 129.0, 121.6, 114.9, 110.9, 55.2, 45.7, 30.4, 22.7 (2C).

4-isobutyl-2-methoxybenzaldehyde (5.30)

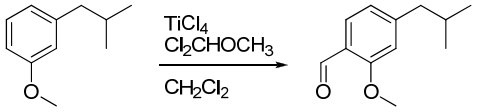

5.29 **5.30**

A solution of **5.29** (0.925 g, 5.632 mmol) in dry CH_2Cl_2 (20 mL) was cooled to 0 °C with stirring and there was added $TiCl_4$ (1.60 g, 8.45 mmol). After 5 minutes dichloromethyl methyl ether (0.777 g, 6.76 mmol) was added and the reaction was stirred at 0 °C for 45 minutes. The reaction mixture was poured into ice-water (100 mL) and extracted with CH_2Cl_2 (3 × 25 mL). The combined organic extracts were dried ($MgSO_4$), filtered and evaporated under reduced pressure. The residue was purified by flash chromatography (petroleum ether/CH_2Cl_2, 4:1 → 3:2) and the third product to elute was collected and evaporated under reduced pressure to give the title compound, **5.30** (0.442 g, 41%) as a pale yellow oil. ^{1}H NMR (300 MHz, $CDCl_3$) δ 10.37 (d, *J* = 0.8 Hz, 1H), 7.71 (d, *J* = 7.8 Hz, 1H), 6.80 (ddd, *J* = 7.8, 1.3, 0.8 Hz, 1H), 6.73 (d, *J* = 1.3 Hz, 1H), 3.90 (s, 3H), 2.51 (d, *J* = 7.2 Hz, 2H), 2.01-1.81 (m, 1H), 0.92 (d, *J* = 6.6 Hz, 6H). ^{13}C NMR (75 MHz, $CDCl_3$) δ 189.4, 161.8, 151.2, 128.4, 122.9, 121.7, 112.2, 55.7, 46.2, 30.3, 22.6 (2C).

((4-methoxybenzyloxy)methanetriyl)tribenzene (5.32)

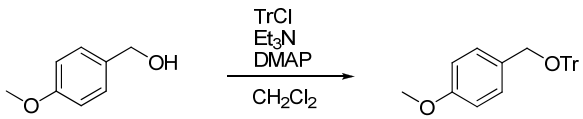

5.31 **5.32**

4-methoxybenzyl alcohol, **5.31** (1.382 g, 10.00 mmol) was dissolved in CH_2Cl_2 (25 mL), and there was added TrCl (2.927 g, 10.50 mmol), Et_3N (1.062 g, 10.50 mmol) and DMAP (0.122 g, 1.00 mmol). The reaction was stirred at room temperature overnight. There was added CH_2Cl_2 (25

mL) and the mixture was washed with water (50 mL), 1M aqueous KH_2PO_4 (50 mL) and brine (50 mL). The organic layer was dried ($MgSO_4$), filtered and evaporated under reduced pressure to give a white solid which was recrystallized from heptane to give the title compound, **5.32** (3.278 g, 86%) as white needles. mp. 135-137 °C (Litt[385]. 132-134). ^{1}H NMR (300 MHz, $CDCl_3$) δ 7.51-7.46 (m, 6H), 7.32-7.17 (m, 11H), 6.89-6.83 (m, 2H), 4.08 (s, 2H), 3.78 (s, 3H). ^{13}C-NMR (75 MHz, $CDCl_3$) δ 158.8, 144.2 (3C), 131.2, 128.8 (6C), 128.5, 127.9 (6C), 127.0 (3C), 113.8, 87.0, 65.6, 55.4

2-methoxy-5-(trityloxymethyl)benzaldehyde (5.33)

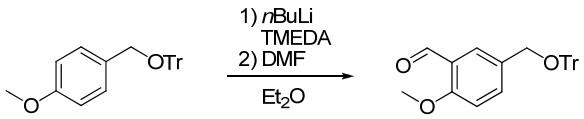

5.32 **5.33**

5.32 (1.141 g, 3.00 mmol) was dissolved in dry Et_2O (100 mL). TMEDA (0.977 g, 8.41 mmol) was added with stirring followed by dropwise addition of *n*-BuLi (8.41 mmol). The reaction was stirred at room temperature for 90 minutes before DMF (1.153 g, 15.77 mmol) was added. Stirring was continued for 30 minutes and the reaction was quenched by addition of saturated aqueous NH_4Cl (50 mL). The biphasic mixture was transferred to a separatory funnel and the organic layer was isolated. The aqueous layer was extracted with EtOAc (2 × 50 mL) and the combined organic layers were dried ($MgSO_4$), filtered and evaporated under reduced pressure. The residue was purified by flash chromatography (petroleum ether/EtOAc, 6:1) and the collected fractions were evaporated and the solids recrystallized from heptane to give the title compound, **5.33** (0.809 g, 66%) as pale yellow crystals. mp. 144-145 °C. ^{1}H NMR (300 MHz, $CDCl_3$) δ 10.47 (s, 1H), 7.78 (d, *J* = 2.3 Hz, 1H), 7.62 (dd, *J* = 8.6, 2.3 Hz, 1H), 7.56-7.48 (m, 6H), 7.37-7.21 (m, 9H), 6.99 (d, *J* = 8.6 Hz, 1H), 4.15 (s, 2H), 3.94 (s, 3H). ^{13}C NMR (75 MHz, $CDCl_3$) δ 189.7, 161.1, 143.9 (3C), 135.0, 131.5, 128.7 (6C), 127.9 (6C), 127.4, 127.1 (3C), 124.5, 111.7, 87.2, 65.1, 55.9

2-(4-methoxyphenyl)ethanol (5.35)

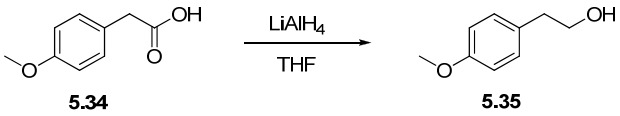

5.34 **5.35**

To a stirred suspension of $LiAlH_4$ (2.30 g, 60.00 mmol) in dry THF (40 mL) at 0 °C was added a solution 2-(4-methoxyphenyl)acetic acid, **5.34** (8.00 g, 48.00 mmol) in dry THF (40 mL). The reaction was heated to 40 °C and stirred for 90 minutes. The reaction was quenched by addition of water (2.3 mL), 15% NaOH (2.3 mL) and water (6.9 mL). The precipitate was removed by filtration, and the filter cake was washed thoroughly with Et_2O. The filtrate was dried (Na_2SO_4), filtered and evaporated under reduced pressure. The residue was purified by short-path vacuum-distillation and the fraction collected at 125-130 °C (0.4 mmHg) contained the title compound, **5.35** (7.245 g, 99%) as a colorless liquid. ^{1}H NMR (300 MHz, C_6D_6) δ 6.97 (d, *J* = 8.6 Hz, 2H), 6.77 (d, *J* = 8.6 Hz, 2H), 3.58 (t, *J* = 6.8 Hz, 2H), 3.34 (s, 3H), 2.62 (t, *J* = 6.8 Hz, 2H), 1.67 (br s, 1H). ^{13}C-NMR (75 MHz, C_6D_6) δ 158.8, 131.2, 130.3 (2C), 114.3 (2C), 64.1, 55.0, 39.0

((4-methoxyphenethoxy)methanetriyl)tribenzene (5.36)

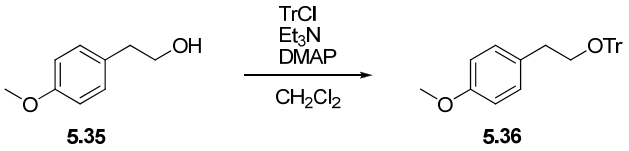

5.35 **5.36**

2-(4-methoxyphenyl)ethanol, **5.35** (3.044 g, 20.00 mmol) was dissolved in CH_2Cl_2 (50 mL) and there was added TrCl (6.133 g, 22.00 mmol), Et_3N (2.530 g, 25.00 mmol) and DMAP (0.305 g, 2.5 mmol). The reaction was stirred at room temperature for 4 hours and then diluted with CH_2Cl_2 (20 mL). The reaction mixture was washed with water (2 × 50 mL), 0.1M KH_2PO_4 (50 mL) and brine (50 mL), dried (Na_2SO_4), filtered and evaporated under reduced pressure. The crude compound was dissolved in hot heptane/toluene (9:1) and hot-filtered. The filtrate was allowed to cool to 5 °C overnight and the title compound, **5.36** (6.179 g, 78%) crystallized as white needles which were collected by filtration. mp. 96-97 °C. ^{1}H-NMR (300 MHz, $CDCl_3$) δ 7.38-7.32 (m, 6H), 7.27-7.14 (m, 9H), 7.08 (d, *J* = 8.5 Hz, 2H), 6.79 (d, *J* = 8.5 Hz, 2H), 3.76 (s, 3H), 3.24 (t, *J* = 6.9 Hz, 2H), 2.82 (t, *J* = 6.9 Hz, 2H). ^{13}C-NMR (75 MHz, $CDCl_3$) δ 158.0, 144.3 (3C), 131.4, 130.1 (2C), 128.7 (6C), 127.8 (6C), 126.9 (3C), 113.7 (2C), 86.7, 65.4, 55.4, 36.0

2-methoxy-5-(2-(trityloxy)ethyl)benzaldehyde (5.37)

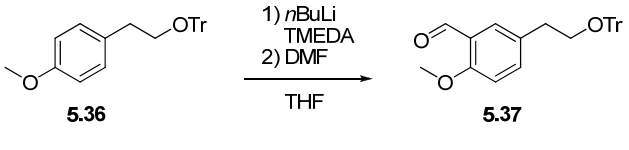

5.36 **5.37**

((4-methoxyphenethoxy)methanetriyl)tribenzene, **5.36** (3.945 g, 10.00 mmol) was dissolved in dry THF (40 mL) and cooled to 0 °C. TMEDA (1.856 g, 16.00 mmol) was added followed by dropwise addition of *n*-BuLi (16.00 mmol). The deep red reaction mixture was stirred at 0 °C for 90 minutes and then DMF (2.924 g, 40.00 mmol) was added. The reaction was allowed to slowly return to room temperature and then quenched with saturated aqueous NH_4Cl. The reaction was partitioned between saturated aqueous NH_4Cl (50 mL) and Et_2O (50 mL). The organic layer was isolated and the aqueous layer was extracted with Et_2O (2 × 50 mL). The combined organic layers were washed with 0.1M KH_2PO_4 (100 mL) and brine (100 mL), dried (Na_2SO_4), filtered and evaporated under reduced pressure. The residue was purified by flash chromatography (petroleum ether /EtOAc, 6:1) and the collected fractions were evaporated to give a pale yellow solid which was recrystallized from MeOH to give the title compound, **5.37** (2.012 g, 49%) as flaky white crystals. mp. 128-129 °C. ^{1}H NMR (300 MHz, $CDCl_3$) δ 10.41 (s, 1H), 7.62 (d, *J* = 2.3 Hz, 1H), 7.37 (dd, *J* = 8.5, 2.3 Hz, 1H), 7.35-7.27 (m, 6H), 7.26-7.14 (m, 9H), 6.87 (d, *J* = 8.5 Hz, 1H), 3.87 (s, 3H), 3.25 (t, *J* = 6.7 Hz, 2H), 2.83 (t, *J* = 6.7 Hz, 2H). ^{13}C NMR (75 MHz, $CDCl_3$) δ 189.8, 160.4, 144.1 (3C), 136.8, 131.8, 128.9, 128.3 (6C), 127.8 (6C), 126.9 (3C), 124.5, 111.6, 86.7, 64.7, 55.9, 35.7

2-(4-bromo-2,5-dimethoxyphenyl)-*N*-(2-methoxy-5-(trityloxymethyl)benzyl)ethanamine (5.38)

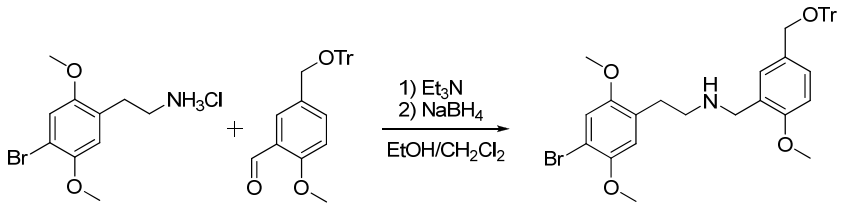

5.33 5.38

2C-B·HCl (0.297 g, 1.00 mmol) and **5.33** (0.490 g, 1.20 mmol) were dissolved in EtOH/CH_2Cl_2 (2:1, 15 mL). There was added Et_3N and the reaction was stirred at room temperature for 3 hours. $NaBH_4$ (0.076 g, 2.00 mmol) was added in one portion and stirring was continued for 1 hour. The reaction mixture was evaporated to dryness and the residue was partitioned between CH_2Cl_2 (20 mL) and water (20 mL). The organic layer was isolated and the aqueous layer was extracted with CH_2Cl_2 (2 × 20 mL). The combined organic layers were dried (Na_2SO_4), filtered and evaporated. The residue was purified by radial chromatography (CH_2Cl_2/2M methanolic NH_3, 98:2) to give the title compound, **5.38** (0.463 g, 71%), as a colorless oil. ^{1}H NMR (300 MHz, $CDCl_3$) δ 7.52-7.43 (m, 6H), 7.32-7.17 (m, 10H), 7.13 (d, *J* = 2.1 Hz, 1H), 6.96 (s, 1H), 6.80 (d, *J* = 8.3 Hz, 1H), 6.71 (s, 1H), 4.06 (s, 2H), 3.78 (s, 2H), 3.75 (s, 3H), 3.74 (s, 3H), 3.67 (s, 3H), 2.83-2.76 (m, 4H), 1.75 (br s, 1H). ^{13}C NMR (75 MHz, $CDCl_3$) δ 156.8, 152.0, 149.8, 144.2 (3C), 130.8, 129.0, 128.9, 128.8 (6C), 128.7, 128.1, 127.9 (6C), 127.0 (3C), 115.9, 114.8, 110.1, 108.7, 87.0, 65.6, 57.0, 56.2, 55.4, 49.5, 48.9, 31.2

2-(4-bromo-2,5-dimethoxyphenyl)-*N*-(2-methoxy-5-(2-(trityloxy)ethyl)benzyl)ethanamine (5.39)

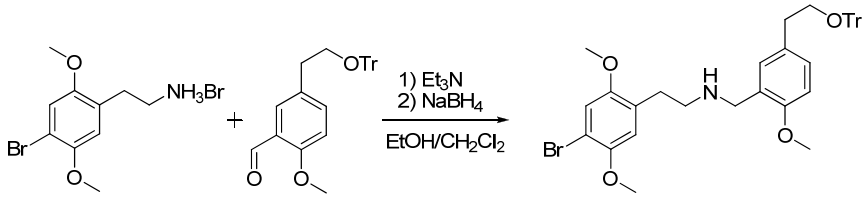

5.37 5.39

2C-B·HCl (0.297 g, 1.00 mmol) and **5.37** (0.465 g, 1.10 mmol) was dissolved in EtOH/CH_2Cl_2 (2:1, 15 mL) and there was added Et_3N (0.101 g, 1.00 mmol). The reaction was stirred for 3 hours at room temperature and then there was added $NaBH_4$ (0.076 g, 2.00 mmol). The reaction was stirred for one hour and then evaporated to dryness. The residue was partitioned between CH_2Cl_2 (20 mL) and water (20 mL). The organic layer was isolated and the aqueous layer was extracted with CH_2Cl_2 (2 × 20 mL). The combined organic layers were dried (Na_2SO_4), filtered and evaporated under reduced pressure. The residue was purified by radial chromatography (CH_2Cl_2/2M methanolic NH_3, 98:2) to give the title compound, **5.39** (0.584 g, 89%) as a colorless oil. ^{1}H NMR (300 MHz, $CDCl_3$) δ 7.38-7.31 (m, 6H), 7.25-7.12 (m, 9H), 7.02-6.97 (m, 2H), 6.95 (s, 1H), 6.72-6.66 (m, 2H), 3.74 (s, 2H), 3.72 (s, 3H), 3.68 (s, 3H), 3.63 (s, 3H), 3.23 (t, *J* = 6.9 Hz, 2H), 2.84-2.72 (m, 6H). ^{13}C NMR (75 MHz, $CDCl_3$) δ 156.0, 152.0, 149.7, 144.2 (3C), 130.9, 130.7, 128.9, 128.6 (6C), 128.5, 128.0, 127.7 (6C), 126.8 (3C), 115.8, 114.8, 110.0, 108.7, 86.6, 65.2, 56.9, 56.1, 55.3, 49.4, 48.8, 35.9, 31.1

Experimental – Chapter 6

tert-butyl 2-hydroxybenzyl(4-iodo-2,5-dimethoxyphenethyl)carbamate (6.11)

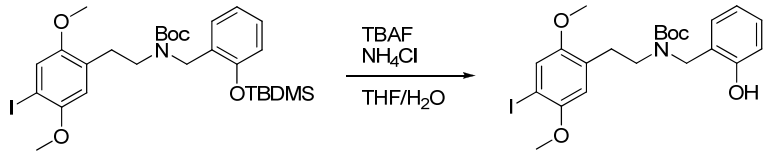

6.24 **6.11**

To a solution of **6.24** (229 mg, 0.36 mmol) in THF (5 mL) was added a 1 M solution of TBAF in THF (1.1 ml, 1.1 mmol) and saturated aqueous NH_4Cl (0.1 mL). The reaction was stirred for 22 hrs at room temperature and the THF removed under reduced pressure. H_2O (20 mL) was added and the mixture extracted with ethyl acetate (3 × 20 mL). The combined organic layers were washed with brine (30 mL), dried ($MgSO_4$) and evaporated under reduced pressure. The residue was purified by flash chromatography (ethyl acetate/heptane 1:20) to yield the title compound, **6.11** (0.150 g, 81%) as a colorless oil solidifying over time. mp. 155.2-155.5 °C. Anal. calc. for $C_{22}H_{28}INO_5$ C, 51.47; H, 5.50; N, 2.73. Found: C, 51.37; H, 5.47; N, 2.67. ^{1}H NMR (300 MHz, $CDCl_3$): δ 9.37 (1H, s), 7.20 (1H, dt, *J* = 8.0, 1.6 Hz), 7.15 (1H, s), 7.05 (1H, dd, *J* = 7.4, 1.7 Hz), 6.89 (1H, dd, *J* = 8.1, 1.1 Hz), 6.77 (1H, dt, *J* = 7.3, 1.2 Hz), 6.37 (1H, s), 4.29 (2H, s), 3.78 (3H, s), 3.67 (3H, s), 3.42 (2H, t, *J* = 6.9 Hz), 2.74 (2H, t, *J* = 6.9 Hz), 1.36 (9H, s).^{13}C NMR (75 MHz, $CDCl_3$): δ 202.8, 156.1, 152.2, 131.2, 129.9, 128.4, 123.0, 121.1, 119.1, 117.3, 113.7, 57.0, 55.9, 48.5, 47.3, 29.7, 28.2.

tert-butyl 2-hydroxy-4-iodo-5-methoxyphenethyl(2-methoxybenzyl)carbamate (6.12)

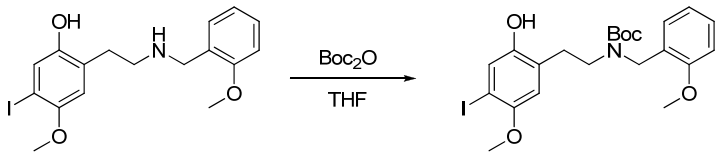

6.35 **6.12**

Obtained from **6.35** using general procedure C in 72% yield as a colorless oil. ^{1}H-NMR (300 Mhz, $CDCl_3$) δ 8.25 (br s, 1H), 7.30-7.21 (m, 1H), 7.24 (s, 1H), 7.13 (d, *J* = 7.2Hz), 6.92 (t, 7.4 Hz, 1H), 6.86 (d, *J* = 8.2 Hz, 1H), 6.39 (s, 1H), 4.46 (s, 2H), 3.83 (s, 3H), 3.74 (s, 3H), 3.33-3.25 (m, 2H), 2.75-2.68 (m, 2H), 1.47 (s, 9H). ^{13}C-NMR (75 MHz, $CDCl_3$) δ 157.2, 157.0, 151.6, 150.5, 128.7, 128.6, 126.0, 125.4, 120.5, 112.9, 110.3, 83.9, 81.1, 57.2, 55.4, 48.2, 47.3, 31.0, 28.6 (3C)

tert-butyl 2-(*tert*-butyldimethylsilyloxy)benzyl(2-hydroxy-4-iodo-5-methoxyphenethyl)carbamate (6.13)

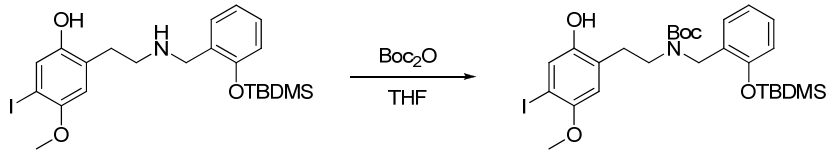

6.36 **6.13**

Obtained from **6.36** using general procedure C in 62% yield as a colorless oil. ^{1}H NMR (300 MHz, $CDCl_3$) δ 8.16 (br s, 1H), 7.29 (s, 1H), 7.16-7.08 (m, 2H), 6.92 (t, *J* = 7.4 Hz, 1H), 6.80 (d, *J* = 7.9 Hz,

1H), 4.47 (s, 2H), 3.73 (s, 3H), 3.33-3.25 (m, 2H), 2.78-2.71 (m, 2H), 1.47 (s, 9H), 1.03 (s, 9H), 0.26 (s, 6H). ^{13}C NMR (75 MHz, $CDCl_3$) δ 157.0, 153.2, 153.1, 151.6, 150.5, 128.3, 128.2 (2C), 127.1, 125.2, 121.5, 118.6, 112.7, 83.9, 81.3, 57.2 48.2, 46.9, 31.2, 28.6 (3C), 26.1 (3C), 18.6, -3.8 (2C)

tert-butyl 2-fluorobenzyl(2-hydroxy-4-iodo-5-methoxyphenethyl)carbamate (6.14).

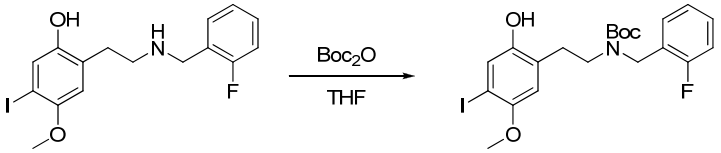

6.37 **6.14**

Obtained from **6.37** using general procedure C in 89% as a colorless oil. ^{1}H NMR (300 MHz, $CDCl_3$) δ 7.97 (br s, 1H), 7.29-7.18 (m, 3H), 7.13-6.97 (m, 2H), 6.43 (s, 1H), 4.48 (s, 2H), 3.75 (s, 3H), 3.34 (t, *J* = 7.4 Hz, 2H), 2.75 (t, *J* = 7.4 Hz, 2H), 1.46 (s, 9H). ^{13}C NMR (75 MHz, $CDCl_3$) δ 160.8 (d, $^1J_{CF}$ = 245.6 Hz), 156.5, 151.7, 150.2, 129.6, 129.2 (d, $^3J_{CF}$ = 8.0 Hz), 126.9, 125.3, 125.0 (d, $^2J_{CF}$ = 14.7 Hz), 124.3 (d, $^4J_{CF}$ = 3.6 Hz), 115.4 (d, $^2J_{CF}$ = 21.6 Hz), 113.0, 83.8, 81.5, 57.2, 48.1, 46.0, 30.8, 28.5 (3C).

tert-butyl benzo[*d*][1,3]dioxol-4-ylmethyl(2-hydroxy-4-iodo-5-methoxyphenethyl)carbamate (6.15)

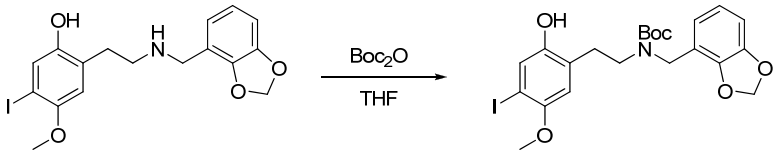

6.38 **6.15**

Obtained from **6.38** using general procedure C in 72% yield as a colorless oil. ^{1}H NMR (300 MHz, $CDCl_3$) δ 8.05 (br s, 1H), 7.29 (s, 1H), 6.84-6.70 (m, 3H), 6.45 (s, 1H), 5.95 (s, 2H), 4.43 (s, 2H), 3.77 (s, 3H), 3.40-3.31 (m, 2H), 2.80-2.73 (m, 2H), 1.49 (s, 9H). ^{13}C NMR (75 MHz, $CDCl_3$) δ 156.5, 151.6, 150.3, 147.3, 145.4, 126.4, 125.3, 121.7, 121.5, 119.5, 113.0, 107.9, 100.9, 83.9, 81.4, 57.2, 48.1, 46.7, 30.8, 28.6 (3C)

tert-butyl 2-(8-bromo-2,3,6,7-tetrahydrobenzofuro[5,6-*b*]furan-4-yl)ethyl(2-hydroxybenzyl)carbamate (6.16)

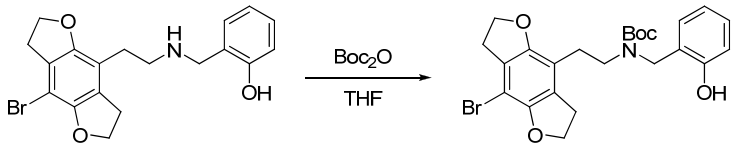

6.41 **6.16**

Obtained from **6.41** using general procedure C in 99% yield as an off-white solid. mp. 140-142 °C. ^{1}H NMR (300 MHz, $CDCl_3$) δ 9.27 (br s, 1H), 7.22-7.15 (m, 1H), 7.01 (dd, *J* = 7.4, 1.5 Hz, 1H), 6.91-6.86 (m, 1H), 6.78-6.71 (m, 1H), 4.60 (t, *J* = 8.6 Hz, 2H), 4.58 (t, *J* = 8.6 Hz, 2H), 4.26 (s, 2H), 3.36 (t, *J* = 7.0 Hz, 2H), 3.14 (t, *J* = 8.6 Hz, 2H), 3.11 (t, *J* = 8.6 Hz, 2H), 2.68 (t, *J* = 7.0 Hz, 2H), 1.42 (s, 9H). ^{13}C NMR (75 MHz $CDCl_3$) δ 157.8, 156.2, 152.9, 150.8, 131.2, 130.0, 126.3, 126.2, 122.9, 119.2, 117.4, 116.4, 97.5, 81.6, 71.8, 71.2, 48.2, 46.0, 31.9, 30.0, 28.4 (3C), 26.7

tert-butyl 4-bromo-2,5-dimethoxyphenethyl(2-hydroxybenzyl)carbamate (6.17)

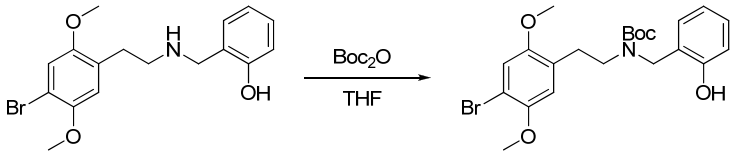

6.42 **6.17**

Obtained from **6.42** using general procedure C in 77% yield as a colorless oil. ^{1}H NMR (300 MHz , $CDCl_3$,) δ 9.28 (br s, 1H), 7.10 (ddd, 8.1, 7.4, 1.7 Hz, 1H), 6.96 (dd, *J* = 7.4, 1.7 Hz, 1H), 6.87 (s, 1H), 6.80 (dd, *J* = 8.1, 1.2 Hz, 1H), 6.68 (ddd, *J* = 7.4, 7.4, 1.2 Hz, 1H), 6.36 (s, 1H), 4.20 (s, 2H), 3.68 (s, 6H), 3.33 (t, *J* = 6.9 Hz, 2H), 2.65, (t, *J* = 6.9 Hz, 2H), 1.27 (s, 9H). ^{13}C NMR (75 MHz, $CDCl_3$) δ 158.2, 156.6, 152.3, 150.2, 131.7, 130.4, 127.8, 123.5, 119.6, 117.8, 115.9, 115.4, 109.7, 81.8, 57.3, 56.4, 49.0, 47.8, 30.0, 28.7 (3C)

tert-butyl 4-chloro-2,5-dimethoxyphenethyl(2-hydroxybenzyl)carbamate (6.18).

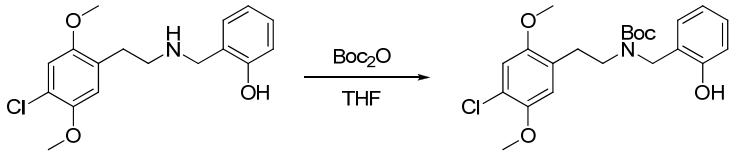

6.43 **6.18**

Obtained from **6.43** using general procedure C in 92% yield as a colorless oil. ^{1}H NMR (300 MHz, $CDCl_3$) δ 9.38 (br. s, 1H), 7.23-7.16 (m, 1H), 7.05 (dd, *J* = 7.4, 1.7 Hz, 1H), 6.89 (dd, *J* = 8.1, 1.1 Hz, 1H), 6.82 (s, 1H), 6.77 (dt, *J* = 7.4, 1.2 Hz, 1H), 6.47 (s, 1H), 4.29 (s, 2H), 3.79 (s, 3H), 3.78 (s, 3H), 3.42 (t, *J* = 6.9 Hz, 2H), 2.75 (t, *J* = 6.9 Hz, 2H), 1.37 (s, 9H). ^{13}C-NMR (75 MHz, $CDCl_3$) δ 157.8, 156.2, 151.6, 148.8, 131.3, 130.0, 126.6, 123.1, 120.4, 119.2, 117.4, 115.2. 112.7, 81.4, 56.9, 56.1, 48.6, 47.5, 29.6, 28.3 (3C)

tert-butyl 2,5-dimethoxy-4-(trifluoromethyl)phenethyl(2-hydroxybenzyl)carbamate (6.19)

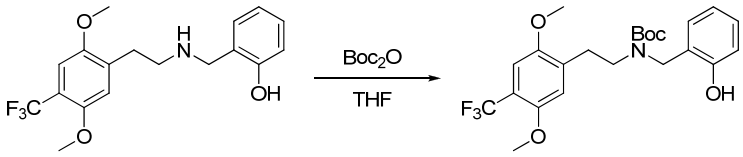

6.44 **6.19**

Obtained from **6.44** using general procedure C in 86% yield as a colorless oil. ^{1}H NMR (300 MHz, $CDCl_3$) δ 9.36 (br s, 1H), 7.20 (ddd, *J* = 8.1, 7.4, 1.7 Hz, 1H), 7.07 (dd, *J* = 7.4, 1.7 Hz, 1H), 6.96 (s, 1H), 6.90 (dd, *J* = 8.1, 1.1 Hz, 1H), 6.78 (ddd, *J* = 7.4, 7.4, 1.1 Hz, 1H), 6.50 (s, 1H), 4.32 (s, 2H), 3.81 (s, 3H), 3.78 (s, 3H), 3.47 (t, *J* = 6.8 Hz, 2H), 2.79 (t, *J* = 6.8 Hz, 2H), 1.33 (s, 9H). ^{13}C NMR (75 MHz, $CDCl_3$) δ 156.3, 151.3 (m), 150.9, 132.6, 131.4, 130.2, 123.6 (q, $^{1}J_{CF}$ = 272 Hz), 123.1, 119.3, 117.5, 115.5, 108.8 (q, $^{3}J_{CF}$ = 5.4 Hz), 81.6, 56.7, 56.0, 48.8, 47.5, 29.9, 28.3 (3C). The quaternary aromatic carbon bearing the CF_3-group was not discernible or obscured by other peaks.

2-(2-hydroxy-4-iodo-5-methoxyphenethyl)isoindoline-1,3-dione (6.20)

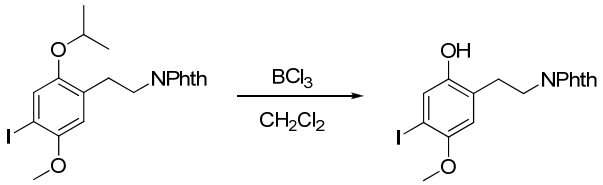

6.47 **6.20**

To a cooled (-78 °C) solution of **6.47** (359 mg, 0.77 mmol) in CH_2Cl_2 (20 mL) was added BCl_3 (1 M in hexanes, 0.93 mL, 0.93 mmol) dropwise via syringe. The reaction was allowed to warm to room temperature and stirred for a further 1 hour before pouring into water (100 mL). The organic layer was isolated and the aqueous phase extracted with CH_2Cl_2 (2 × 25 mL). The combined organic extracts were washed with brine (50 mL), dried (Na_2SO_4) and concentrated under reduced pressure. The residue was recrystallized from EtOAc/petroleum ether to give the title compound, **6.20** (205 mg, 63%) as a light yellow solid. mp. 209-210 °C. ^{1}H NMR (300 MHz, DMSO-d_6) δ 9.20 (s, 1H), 7.83-7.75 (m, 4H), 7.08 (s, 1H), 6.63 (s, 1H), 3.80 (t, J = 6.5 Hz, 2H), 3.55 (s, 3H), 2.83 (t, J = 6.5 Hz, 2H). ^{13}C-NMR (75 MHz, DMSO-d_6) δ 167.5 (2C), 150.6, 150.1, 134.1 (2C), 131.4, 125.8, 124.4, 122.8 (2C), 113.6, 83.1, 56.6, 37.3, 28.8

N-(2-(tert-butyldimethylsilyloxy)benzyl)-2-(4-iodo-2,5-dimethoxyphenyl)ethanamine (6.23)

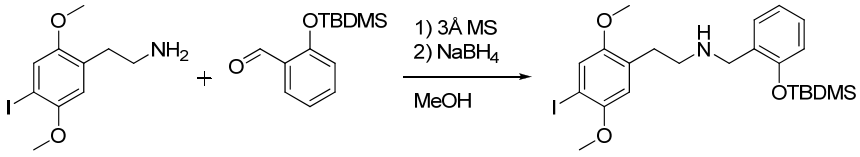

6.22 **6.23**

To a solution of 2-(4-iodo-2,5-dimethoxyphenyl)ethanamine (0.165 g, 0.54 mmol) in dry methanol (5 mL) was added 2-(tert-butyldimethylsilyloxy)benzaldehyde, **6.22** (0.133 g, 0.56 mmol) and 5 pieces of 3Å molecular sieves. The mixture was stirred for 4 hours before adding $NaBH_4$ (0.041 g, 1.08 mmol), the reaction was stirred for a further 30 min, filtered through a plug of Celite and concentrated under reduced pressure. The residue was purified by flash chromatography (ethyl acetate/heptane 1:4 + 1% Et_3N) to give the title compound, **6.23** (149 mg, 53%) as a colorless oil. Anal. Calc. for $C_{23}H_{24}INO_3Si$: C 52.37; H 6.50; N 2.66. Found: C 51.88; H 6.06; N 2.56.^{1}H NMR (300 MHz, $CDCl_3$) δ 7.24-7.20 (1H, m), 7.18 (1H, s), 7.16-7.08 (1H, m), 6.94-6.87 (1H, m), 6.80-6.76 (1H, m), 6.65 (1H, s), 3.79 (3H, s), 3.78 (2H, s), 3.72 (3H, s), 2.82 (4H, s), 1.69 (1H, bs), 0.92 (9H, s), 0.22 (6H, s).^{13}C NMR (75 MHz, $CDCl_3$) δ 153.6, 152.2, 130.5, 129.9, 127.8, 121.5, 120.9, 118.3, 113.5, 82.3, 57.0, 56.1, 49.6, 48.8, 31.4, 25.8 (3C), 18.2, -3.9

tert-butyl 2-(*tert*-butyldimethylsilyloxy)benzyl(4-iodo-2,5-dimethoxyphenethyl)carbamate (6.24)

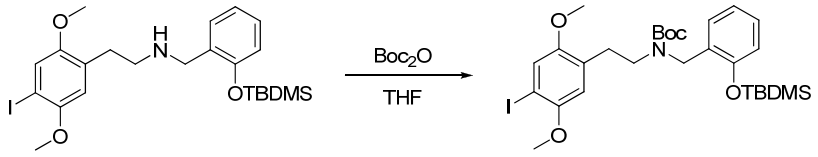

6.23 **6.24**

6.23 (0.121 g, 0.23 mmol) was dissolved in THF (5 mL), di-*tert*-butyl dicarbonate (0.100 g, 0.46 mmol) was added, and the mixture was stirred for 3 hours. The reaction mixture was concentrated under reduced pressure and purified by flash chromatography (ethyl acetate/heptane 1:20) to yield the title compound, **6.24** (291 mg, 90%) as a colorless oil. Anal. Calc. for $C_{28}H_{42}INO_5Si$: C 53.58; H 6.75; N 2.23. Found: C 52.92; H 6.35; N 2.52. ^{1}H NMR (300 MHz, $CDCl_3$) δ 7.20-7.00 (3H, m), 6.91 (1H, t, *J* = 7.4 Hz), 6.78 (1H, d, *J* = 7.9 Hz), 6.67(rot_a)/6.50(rot_b) (1H, s), 4.45(rot_a)/4.31(rot_b) (2H, s), 3.81(rot_a)/3.79(rot_b) (3H, s), 3.72 (3H, s), 3.46(rot_a)/3.34(rot_b) (2H, t, *J* = 7.0 Hz), 2.87(rot_a)/2.77(rot_b) (2H, t, *J* = 7.2 Hz), 1.47(rot_a)/1.41(rot_b) (9H, s), 1.02 (9H, s), 0.24 (6H, s). ^{13}C NMR (75 MHz, $CDCl_3$) δ 155.7, 153.2, 152.2, 152.1, 129.0, 128.9, 128.4, 128.0, 127.5, 127.2, 126.7, 121.1, 118.2, 113.7, 82.5, 79.4, 79.2, 57.0, 55.9, 47.2, 46.9, 46.6, 45.2, 29.8, 29.2, 28.4, 25.8, 18.3, -4.1

1,4-Diiodo-2,5-dimethoxybenzene (6.26)

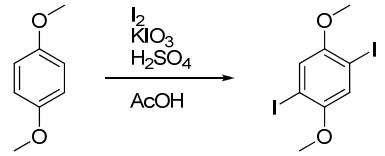

6.25 **6.26**

To a 2 L 3-necked round bottomed flask was added in succession 1.4-dimethoxybenzene (44.0 g, 318 mmol), glacial AcOH (1.0 L), water (45 mL), conc. H_2SO_4 (18 mL, 324 mmol), KIO_3 (69.5 g, 315 mmol) and finally I_2 (89 g, 351 mmol). The reaction was heated to reflux with mechanical stirring. After 3½ hours the reaction was allowed to cool to 60 °C. Water (570 mL) was added and the reaction was allowed to cool to room temperature. The solids were collected by filtration and washed with saturated $Na_2S_2O_3$. The solids were dissolved in completely in $CHCl_3$ and the solution was treated with activated carbon for 30 minutes. The suspension was filtered through a pad of Celite and the filtrate was evaporated under reduced pressure. The pale yellow solid was recrystallized from $CHCl_3$MeOH to give the title compound, 6.26 (78.1 g, 63%). mp. 117 °C (Litt.[386] 115-116°C). ^{1}H NMR (300 MHz, $CDCl_3$) δ 7.17 (s, 2H), 3.82 (s, 6H). ^{13}C NMR (75 MHz, $CDCl_3$) δ 153.3 (2C), 121.6 (2C), 85.6 (2C), 57.4 (2C)

4-iodo-2,5-dimethoxybenzaldehyde (6.27)

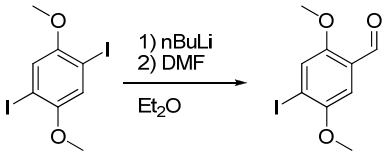

6.26 **6.27**

To a cooled (0 °C) solution of **6.26** (7.797 g, 20.0 mmol) in dry Et_2O (250 mL) was added *n*-butyllithium (20.0 mmol) over a period of 5 minutes. The reaction was stirred at 0 °C for 10 minutes and DMF (3.1 mL, 40.0 mmol) was added. The cooling was removed, and the reaction was stirred for 2 hours and then quenched by the addition of water (100 mL). The organic layer was isolated and the aqueous layer was extracted with Et_2O (2 × 50 mL). The combined organic layers were dried ($MgSO_4$), filtered and evaporated under reduced pressure. The residue was purified by flash chromatography (petroleum ether/CH_2Cl_2, 6:1 → 1:1) to give the title compound, **6.27** (4.26 g, 73%) as white crystals. mp. 140-142 °C.^{1}H NMR (300 MHz, $CDCl_3$) δ 10.38 (s, 1H), 7.46 (s, 1H), 7.21 (s, 1H), 3.90 (s, 3H), 3.88 (s, 3H). ^{13}C NMR (75 MHz, $CDCl_3$) δ 189.0, 156.1, 152.7, 123.7, 108.0, 99.0, 57.1, 56.5

2-hydroxy-4-iodo-5-methoxybenzaldehyde (6.28)

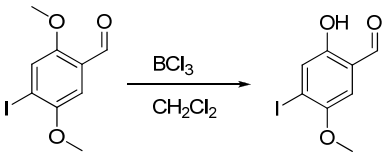

6.27 **6.28**

To a solution of **6.27** (1.51 g, 5.15 mmol) in dry CH_2Cl_2 (40 mL) was added 1.0 M BCl_3 in CH_2Cl_2 (20.6 mmol), and the reaction was stirred overnight at room temperature. The reaction was quenched by the addition of water (40 mL) and saturated aqueous $NaHCO_3$ until neutral pH. The organic layer was isolated and the aqueous layer was extracted with CH_2Cl_2 (2 × 50 mL). The combined organic layers were dried ($MgSO_4$), filtered and evaporated under reduced pressure. The residue was purified by flash chromatography (petroleum ether/ethyl acetate, 9:1) and the solid was recrystallized from *i*Pr_2O to give title compound, **6.28** (1.22 g, 85%) as bright yellow crystals. mp. 107-108 °C. ^{1}H NMR (300 MHz, $CDCl_3$) δ 10.61 (s, 1H), 9.81 (s, 1H), 7.51 (s, 1H), 6.85 (s, 1H), 3.88 (s, 3H). ^{13}C NMR (75 MHz, $CDCl_3$) δ 195.5, 155.5, 151.7, 129.1, 120.1, 112.2, 99.0, 57.1

(*E*)-5-iodo-4-methoxy-2-(2-nitrovinyl)phenol (6.29)

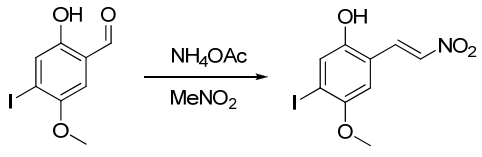

6.28 **6.29**

To a solution of **6.28** (2.50 g, 8.99 mmol) in $MeNO_2$ (30 mL), was added NH_4OAc (0.693 g, 8.99 mmol) and the reaction was stirred at reflux until TLC indicated full conversion (60-80 minutes). Excess $MeNO_2$ was removed under reduced pressure and the residue was dissolved in Et_2O (100

mL). The organic layer was washed with water (2 × 50 mL), dried ($MgSO_4$), filtered and evaporated under reduced pressure. The residue was purified by flash chromatography (petroleum ether/acetone, 9:1) to give the title compound, **6.29** (1.88, 65%) as deep orange crystals. mp. 146 °C dec. ^{1}H NMR (300 MHz, DMSO-d_6) δ 10.64 (s, 1H), 8.25 (d, J = 13.5 Hz), 8.13 (d, J = 13.5 Hz, 1H), 7.38 (s, 1H), 7.29 (s, 1H), 3.78 (s, 3H). ^{13}C NMR (75 MHz, DMSO-d_6) δ 152.5, 151.1, 137.6, 134.6, 126.4, 117.1, 111.6, 93.4, 56.9

2-(2-aminoethyl)-5-iodo-4-methoxyphenol (6.30)

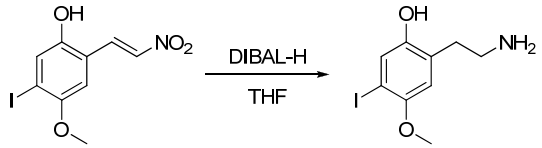

6.29 **6.30**

To a solution of DIBAL-H (4.58 mL, 25.7 mmol) in dry THF (40 mL) was added a solution of **6.29** (1.18 g, 3.67 mmol) in dry THF (20 mL). The reaction was stirred at 60 °C for 2 hours and then cooled to 0°C. The reaction mixture was diluted with Et_2O (60 mL), and there was added in the following order water (1.05 mL), 15% aqueous NaOH (1.05 mL) and water (2.6 mL). The mixture was stirred at room temperature for 30 minutes, anhydrous Na_2SO_4 (10 g) was added, and stirring was continued for 10 minutes. The mixture was filtered and the filtrate was evaporated under reduced pressure. The residue was purified by flash chromatography (CH_2Cl_2/MeOH/NH_3, 95:5:0.05) to give the title compound, **6.30** (0.809 g, 95%) as a pale brown solid. mp. 173-174°C. ^{1}H NMR (300 MHz, DMSO-d_6) δ 7.04 (s, 1H), 6.68 (s, 1H), 5.70 (br s, 3H), 3.69 (s, 3H), 2.78 (t, J = 5.6 Hz, 2H), 2.61 (t, J = 5.6 Hz, 2H). ^{13}C NMR (75 MHz, DMSO-d_6) δ 151.9, 150.0, 128.8, 125.8, 114.2, 82.9, 56.8, 41.4, 35.4

5-iodo-4-methoxy-2-(2-(2-methoxybenzylamino)ethyl)phenol (6.35)

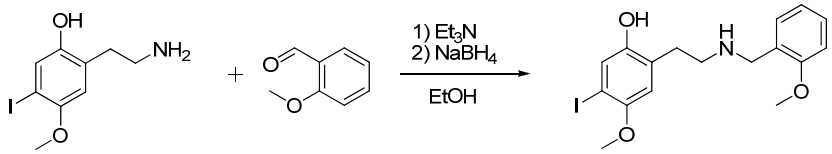

6.30 **6.31** **6.35**

Obtained from **6.30** and 2-methoxybenzaldehyde (**6.31**) using general procedure B in 56% yield as a colorless oil. ^{1}H NMR (300 MHz, $CDCl_3$) δ, 7.30-7.22 (m, 1H), 7.27 (s, 1H), 7.17-7.13 (m, 1H), 6.93-6.83 (m, 2H), 6.46 (s, 1H), 3.83 (s, 5H), 3.76 (s, 3H), 2.88-2.81 (m, 2H), 2.77-2.70 (m, 2H). ^{13}C NMR (75 MHz, $CDCl_3$) δ 157.6, 152.2, 151.0, 130.5, 129.2, 128.6, 128.0, 125.6, 120.6, 113.9, 110.4, 83.9, 57.3, 55.4, 49.1, 48.9, 34.2

2-(2-(2-(*tert*-butyldimethylsilyloxy)benzylamino)ethyl)-5-iodo-4-methoxyphenol (6.36)

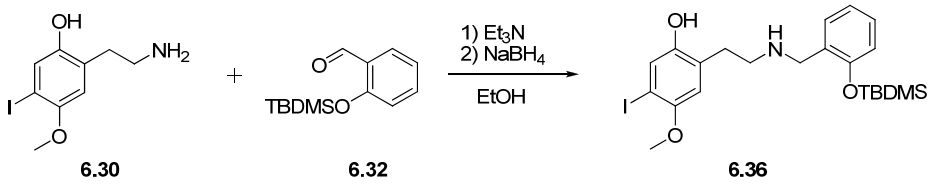

6.30 **6.32** **6.36**

Obtained from **6.30** and 2-(*tert*-butyldimethylsilyloxy)benzaldehyde (**6.32**) using general procedure B in 47% yield as a colorless oil. ^{1}H NMR (300 MHz, $CDCl_3$) δ 7.04 (s, 1H), 7.01-6.86 (m, 2H), 6.71-6.63 (m, 1H), 6.58-6.53 (m, 1H), 6.22 (s, 1H), 3.57 (s, 2H), 3.53 (s, 3H), 2.67-2.62- (m, 2H), 2.53-2.47 (m, 2H), 0.76 (s, 9H), 0.02 (s, 6H). ^{13}C NMR (75 MHz, $CDCl_3$) δ 152.1, 151.1, 130.7, 128.9, 128.5, 128.1, 127.9, 121.4, 118.5, 113.8, 83.9, 57.3, 49.2, 49.1, 34.2, 26.0 (3C), 18.4, -3.8 (2C)

2-(2-(2-fluorobenzylamino)ethyl)-5-iodo-4-methoxyphenol (6.37)

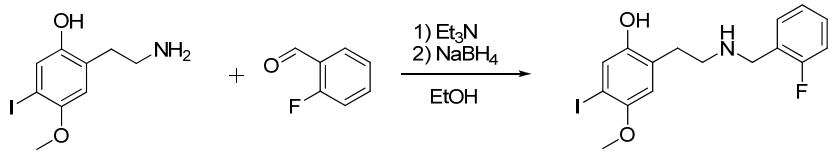

6.30 **6.32** **6.37**

Obtained from **6.30** and 2-fluorobenzaldehyde (**6.33**) using general procedure B in 62% yield as a colorless oil. ^{1}H NMR (300 MHz, $CDCl_3$,) δ 7.30-7.22 (m, 2H), 7.28 (s, 1H), 7.13-6.99 (m, 2H), 6.45 (s, 1H), 3.88 (s, 2H), 3.75 (s, 3H), 2.96-2.90 (m, 2H), 2.76-2.71 (m, 2H). ^{13}C NMR (75 MHz, $CDCl_3$) δ 161.1 (d, $^{1}J_{CF}$ = 245.4 Hz), 151.7, 151.2, 130.7 (d, $^{3}J_{CF}$ = 4.4 Hz), 129.7 (d, $^{3}J_{CF}$ = 8.2 Hz), 128.4, 127.9, 124.6 (d, $^{2}J_{CF}$ = 15.0 Hz), 124.5 (d, $^{4}J_{CF}$ = 3.6 Hz), 115.5 (d, $^{2}J_{CF}$ = 21.6 Hz), 113.8, 83.9, 49.3, 47.0, 34.1

2-(2-(benzo[*d*][1,3]dioxol-4-ylmethylamino)ethyl)-5-iodo-4-methoxyphenol (6.38)

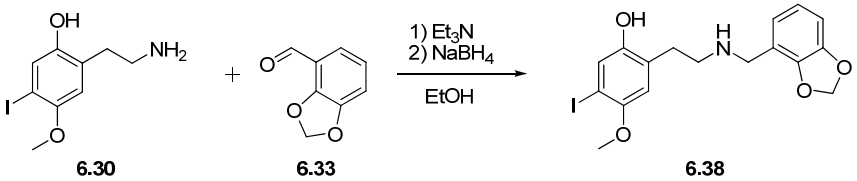

6.30 **6.33** **6.38**

Obtained from **6.30** and 2,3-methylenedioxybenzaldehyde (**6.33**) using general procedure B in 72% yield as a colorless oil. ^{1}H NMR (300 MHz, $CDCl_3$) δ 7.30 (s, 1H), 6.84-6.72 (m, 3H), 6.48 (s, 1H), 5.96 (s, 2H), 3.85 (s, 2H), 3.78 (s, 3H), 2.98-2.93 (m, 2H), 2.78-2.74 (m, 2H). ^{13}C NMR (75 MHz, $CDCl_3$) δ 151.8, 151.2, 147.3, 145.6, 128.4, 128.0, 122.3, 121.9, 119.2, 113.8, 108.2, 101.0, 83.9, 57.3, 49.3, 47.6, 34.2

2-((2-(8-bromo-2,3,6,7-tetrahydrobenzofuro[5,6-*b*]furan-4-yl)ethylamino)methyl)phenol (6.41)

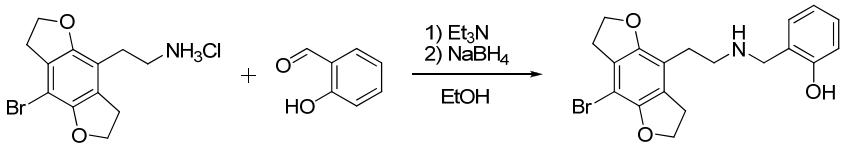

6.39 **6.40** **6.41**

Obtained from **6.39** and salicylaldehyde (**6.40**) using General procedure B in 75% yield as a colorless oil. The compound was characterized as its hydrochloride salt. mp. 230-231°C. ^{1}H NMR (300 MHz, DMSO-d_6) δ 10.31 (s, 1H), 9.28 (br s, 2H), 7.40 (dd, *J* = 7.4, 1.5 Hz, 1H), 7.24-7.17 (m, 1H), 6.99 (dd, *J* = 8.1, 0.9 Hz, 1H), 6.81 (dt, *J* = 7.4, 1.0 Hz, 1H), 4.55 (t, *J* = 8.5 Hz, 2H), 4.07 (m, 2H), 3.22 (t, *J* = 8.5 Hz, 2H), 3.08 (t, *J* = 8.5 Hz, 2H), 3.04-2.81 (m, 4H). ^{13}C NMR (75 MHz, DMSO-d_6) δ 155.9, 151.9, 150.4, 131.5, 130.2, 127.0, 126.1, 118.8, 117.9, 115.3, 114.3, 97.0, 71.5, 70.9, 44.9, 44.7, 31.2, 29.5, 24.1

2-((4-bromo-2,5-dimethoxyphenethylamino)methyl)phenol (6.42).

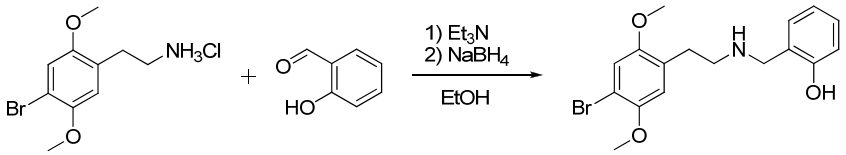

6.40 **6.42**

Obtained from 2C-B·HCl and salicylaldehyde (**6.40**) using general procedure B in 82% yield as a colorless oil. ^{1}H NMR (300 MHz, $CDCl_3$) δ 7.12 (ddd, *J* = 8.1, 7.4, 1.7 Hz, 1H), 7.00 (s, 1H), 6.93 (dd, *J* = 7.4, 1.7 Hz), 6.79 (dd, *J* = 8.1, 1.2 Hz, 1H), 6.73 (ddd, *J* = 7.4, 7.4, 1.2 Hz, 1H), 6.69 (s, 1H), 3.95 (s, 2H), 3.81 (s, 3H), 3.74 (s, 3H), 2.91-2.84 (m, 2H), 2.82-2.76 (m, 2H). ^{13}C-NMR (75 MHz, $CDCl_3$) δ 149.8, 128.6, 128.2, 127.7, 122.5, 118.9, 116.3, 115.8, 114.8, 109.3, 57.0, 56.1, 52.6, 48.3, 30.7

2-((4-chloro-2,5-dimethoxyphenethylamino)methyl)phenol (6.43)

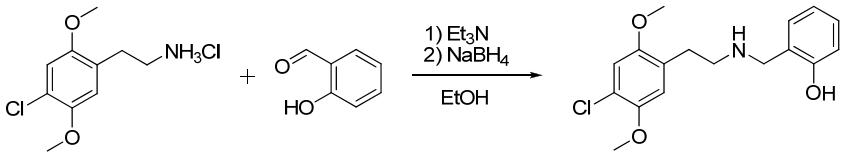

6.40 **6.43**

Obtained from 2C-C·HCl and salicylaldehyde (**6.40**) using general procedure B in 64% yield as a colorless oil. The compound was characterized previously as its hydrochloride salt. mp. 164-167 °C. ^{1}H-NMR (300 MHz, CD_3OD) δ 7.34-7.23 (m, 2H), 7.00 (s, 1H), 6.98 (s, 1H), 6.93-6.84 (m, 2H), 4.23 (s, 2H), 3.83 (s, 3H), 3.78 (s, 3H), 3.27-3.18 (m, 2H), 3.07-2.98 (m, 2H). ^{13}C NMR (75 MHz, CD_3OD) δ 157.2, 152.7, 150.4, 132.5, 132.2, 125.1, 122.5, 120.8, 118.5, 116.3, 116.1, 114.1, 57.3, 56.6, 48.2, 47.8, 28.3

2-((2,5-dimethoxy-4-(trifluoromethyl)phenethylamino)methyl)phenol (6.44)

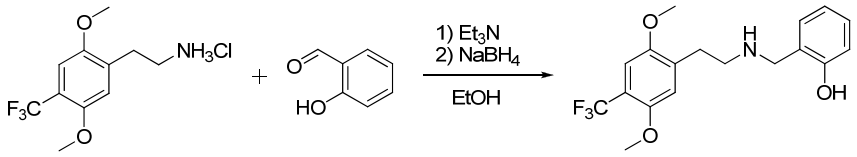

6.40 6.44

Obtained from 2C-TFM·HCl and salicylaldehyde (**6.40**) using general procedure B in 79% yield. The compound was characterized previously as its hydrochloride salt. mp. 209-210 °C. ^{1}H NMR (300 MHz, DMSO-d_6) δ 10.30 (s, 1H), 9.20 (br s, 2H), 7.41 (dd, *J* = 7.5, 1.6 Hz, 1H), 7.21 (ddd, 8.1, 7.4, 1.7 Hz, 1H), 7.15 (s, 1H), 7.11 (s, 1H), 6.98 (dd, *J* = 8.1, 1.1 Hz, 1H), 6.82 (ddd, *J* = 7.5, 7.4, 1.1 Hz, 1H), 4.09 (s, 2H), 3.84 (s, 3H), 3.79 (s, 3H), 3.07 (s, 4H). ^{13}C NMR (75 MHz, DMSO-d_6) δ 155.9, 150,6 (q, $^{3}J_{CF}$ = 1.6 Hz), 150.3, 131.5, 131.1, 130.2, 123.5 (q, $^{1}J_{CF}$ = 271.7 Hz) 115.5, 115.5 (q, $^{2}J_{CF}$ = 30.3 Hz) 115.3, 109.0 (q, $^{3}J_{CF}$ = 5.1 Hz), 56.5, 56.1, 45.5, 44.9, 26.5.

2-(2-isopropoxy-5-methoxyphenethyl)isoindoline-1,3-dione (6.46)

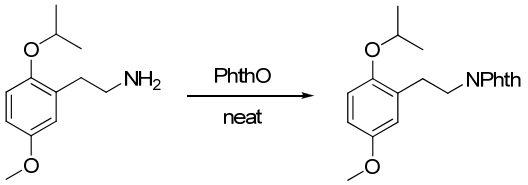

6.45 6.46

2-(2-isopropoxy-5-methoxyphenyl)ethanamine, **6.45** (608 mg, 2.9 mmol) and phthalic anhydride (431 mg, 2.9 mmol) were heated with an open flame until a clear liquid phase was formed. This was allowed to cool and the solid was recrystallized from EtOH to give **6.46** (0.743 g, 75%) as a colorless solid. mp. 79-80°C. ^{1}H NMR (300 MHz, $CDCl_3$) δ 7.81-7.74 (m, 2H), 7.70-7.62 (m, 2H), 6.74 (d, *J* = 8.6 Hz, 1H), 6.71-6.64 (m, 2H), 4.41 (septet, *J* = 6.0 Hz, 1H), 3.92 (t, *J* = 7.4 Hz, 2H), 3.68 (s, 3H), 2.95 (t, *J* = 7.4 Hz, 2H). ^{13}C NMR (75 MHz, $CDCl_3$) δ 168.0 (2C), 153.0, 149.9, 133.5 (2C), 132.1, 128.7, 122.9 (2C), 116.1, 114.2, 112.4, 70.7, 55.6, 38.0, 30.0, 22.2 (2C)

2-(4-iodo-2-isopropoxy-5-methoxyphenethyl)isoindoline-1,3-dione (6.47)

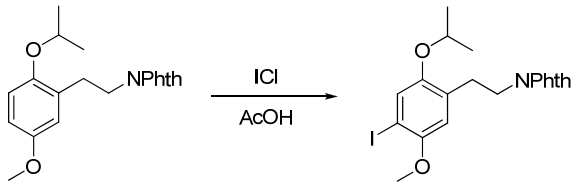

6.46 6.47

To a solution of **6.46** (612 mg, 1.8 mmol) in AcOH (10 mL) was added ICl (0.11 mL, 2.2 mmol). The reaction was stirred at room temperature for 24 hours then quenched with saturated aqueous $Na_2S_2O_3$ and diluted with water (30 mL). The precipitated product was collected by filtration, washed with water and recrystallized from aqueous EtOH to give **6.47** (0.596 g, 71%) as a yellow solid. mp. 134-136 °C. ^{1}H NMR (300 MHz, $CDCl_3$) δ 7.83-7.76 (m, 2H), 7.72-7.64 (m, 2H), 7.19 (s, 1H), 6.62 (s, 1H), 4.40 (septet, *J* = 6.0 Hz, 1H), 3.92 (t, *J* = 7.4 Hz, 2H), 3.71 (s, 3H),

2.95 (t, *J* = 7.4 Hz, 2H), 1.30 (d, *J* = 6.0 Hz, 6H). ^{13}C NMR (75 MHz, $CDCl_3$) δ 168.0 (2C), 152.0, 150.6, 133.7 (2C), 132.0, 128.8, 124.3, 123.0 (2C), 113.3, 83.2, 71.2, 56.9, 37.7, 30.0, 22.1 (2C)

9 References

Reference List

1. Wong, D. T.; Perry, K. W.; Bymaster, F. P. The discovery of fluoxetine hydrochloride (Prozac). *Nature Reviews Drug Discovery* **2005,** *4* (9), 764-774.

2. Jacobs, B. L.; Azmitia, E. C. Structure and Function of the Brain-Serotonin System. *Physiological Reviews* **1992,** *72* (1), 165-229.

3. Nichols, D. E.; Nichols, C. D. Serotonin receptors. *Chemical Reviews* **2008,** *108* (5), 1614-1641.

4. Gaddum, J. H.; Picarelli, Z. P. 2 Kinds of Tryptamine Receptor. *British Journal of Pharmacology and Chemotherapy* **1957,** *12* (3), 323-328.

5. Peroutka, S. J.; Snyder, S. H. Multiple Serotonin Receptors - Differential Binding of [5-Hydroxytryptamine-H-3, [Lysergic-H-3 Acid Diethylamide and [H-3]Spiroperidol. *Molecular Pharmacology* **1979,** *16* (3), 687-699.

6. Kobilka, B. K.; Frielle, T.; Collins, S.; Yangfeng, T.; Kobilka, T. S.; Francke, U.; Lefkowitz, R. J.; Caron, M. G. An Intronless Gene Encoding A Potential Member of the Family of Receptors Coupled to Guanine-Nucleotide Regulatory Proteins. *Nature* **1987,** *329* (6134), 75-79.

7. Fargin, A.; Raymond, J. R.; Lohse, M. J.; Kobilka, B. K.; Caron, M. G.; Lefkowitz, R. J. The Genomic Clone G-21 Which Resembles A Beta-Adrenergic-Receptor Sequence Encodes the 5-HT_{1A} Receptor. *Nature* **1988,** *335* (6188), 358-360.

8. Grailhe, R.; Grabtree, G. W.; Hen, R. Human 5-HT5 receptors: the 5-HT5A receptor is functional but the 5-HT5B receptor was lost during mammalian evolution. *European Journal of Pharmacology* **2001,** *418* (3), 157-167.

9. Hoyer, D.; Hannon, J. P.; Martin, G. R. Molecular, pharmacological and functional diversity of 5-HT receptors. *Pharmacology Biochemistry and Behavior* **2002,** *71* (4), 533-554.

10. Lucas, J. J.; Hen, R. New Players in the 5-HT Receptor Field - Genes and Knockouts. *Trends in Pharmacological Sciences* **1995,** *16* (7), 246-252.

11. Hackler, E. A.; Airey, D. C.; Shannon, C. C.; Sodhi, M. S.; Sanders-Bush, E. 5-HT_{2C} receptor RNA editing in the amygdala of C57BL/6J, DBA/2J, and BALB/cJ mice. *Neuroscience Research* **2006,** *55* (1), 96-104.

12. Sodhi, M. S.; Burnet, P. W. J.; Makoff, A. J.; Kerwin, R. W.; Harrison, P. J. RNA editing of the 5-HT2C receptor is reduced in schizophrenia. *Molecular Psychiatry* **2001,** *6* (4), 373-379.

13. Wang, Q. D.; O'Brien, P. J.; Chen, C. X.; Cho, D. S. C.; Murray, J. M.; Nishikura, K. Altered G protein-coupling functions of RNA editing isoform and splicing variant serotonin(2C) receptors. *Journal of Neurochemistry* **2000,** *74* (3), 1290-1300.

14. Canton, H.; Emeson, R. B.; Barker, E. L.; Backstrom, J. R.; Lu, J. T.; Chang, M. S.; SandersBush, E. Identification, molecular cloning, and distribution of a short variant of the 5-hydroxytryptamine(2C) receptor produced by alternative splicing. *Molecular Pharmacology* **1996,** *50* (4), 799-807.

15. Hoyer, D.; Clarke, D. E.; Fozard, J. R.; Hartig, P. R.; Martin, G. R.; Mylecharane, E. J.; Saxena, P. R.; Humphrey, P. P. A. International Union of Pharmacology Classification of Receptors for 5-Hydroxytryptamine (Serotonin). *Pharmacological Reviews* **1994,** *46* (2), 157-203.

16. Adham, N.; Romanienko, P.; Hartig, P.; Weinshank, R. L.; Branchek, T. The Rat 5-Hydroxytryptamine1B Receptor Is the Species Homolog of the Human 5-Hydroxytryptamine1D-Beta Receptor. *Molecular Pharmacology* **1992,** *41* (1), 1-7.

17. Jin, H.; Oksenberg, D.; Ashkenazi, A.; Peroutka, S. J.; Duncan, A. M.; Rozmahel, R.; Yang, Y.; Mengod, G.; Palacios, J. M.; O'Dowd, B. F. Characterization of the human 5-hydroxytryptamine1B receptor. *Journal of Biological Chemistry* **1992,** *267* (9), 5735-5738.

18. Oksenberg, D.; Marsters, S. A.; Odowd, B. F.; Jin, H.; Havlik, S.; Peroutka, S. J.; Ashkenazi, A. A Single Amino-Acid Difference Confers Major Pharmacological Variation Between Human and Rodent 5-Ht(1B) Receptors. *Nature* **1992,** *360* (6400), 161-163.

19. Hamblin, M. W.; Metcalf, M. A. Primary Structure and Functional-Characterization of A Human 5-HT_{1D}-Type Serotonin Receptor. *Molecular Pharmacology* **1991,** *40* (2), 143-148.

20. Zgombick, J. M.; Schechter, L. E.; Macchi, M.; Hartig, P. R.; Branchek, T. A.; Weinshank, R. L. Human Gene S31 Encodes the Pharmacologically Defined Serotonin 5-Hydroxytryptamine-1e Receptor. *Molecular Pharmacology* **1992,** *42* (2), 180-185.

21. Adham, N.; Kao, H. T.; Schechter, L. E.; Bard, J.; Olsen, M.; Urquhart, D.; Durkin, M.; Hartig, P. R.; Weinshank, R. L.; Branchek, T. A. Cloning of Another Human Serotonin Receptor (5-Ht1F) - A 5Th 5-Ht1 Receptor Subtype Coupled to the Inhibition of Adenylate-Cyclase. *Proceedings of the National Academy of Sciences of the United States of America* **1993,** *90* (2), 408-412.

22. Pritchett, D. B.; Bach, A. W. J.; Wozny, M.; Taleb, O.; Daltoso, R.; Shih, J. C.; Seeburg, P. H. Structure and Functional Expression of Cloned Rat Serotonin 5-HT_2 Receptor. *Embo Journal* **1988,** *7* (13), 4135-4140.

23. Branchek, T.; Adham, N.; Macchi, M.; Kao, H. T.; Hartig, P. R. [H-3] Dob(4-Bromo-2,5-Dimethoxyphenylisopropylamine) and [H-3] Ketanserin Label 2 Affinity States of the Cloned Human 5-Hydroxytryptamine2 Receptor. *Molecular Pharmacology* **1990,** *38* (5), 604-609.

24. Kursar, J. D.; Nelson, D. L.; Wainscott, D. B.; Cohen, M. L.; Baez, M. Molecular-Cloning, Functional Expression, and Pharmacological Characterization of A Novel Serotonin Receptor (5-Hydroxytryptamine2F) from Rat Stomach Fundus. *Molecular Pharmacology* **1992,** *42* (4), 549-557.

25. Julius, D.; Macdermott, A. B.; Axel, R.; Jessell, T. M. Molecular Characterization of A Functional cDNA-Encoding the Serotonin 1C Receptor. *Science* **1988,** *241* (4865), 558-564.

26. Hope, A. G.; Downie, D. L.; Sutherland, L.; Lambert, J. J.; Peters, J. A.; Burchell, B. Cloning and Functional Expression of An Apparent Splice Variant of the Murine 5-Ht(3) Receptor-A Subunit. *European Journal of Pharmacology-Molecular Pharmacology Section* **1993,** *245* (2), 187-192.

27. Gerald, C.; Adham, N.; Kao, H. T.; Olsen, M. A.; Laz, T. M.; Schechter, L. E.; Bard, J. A.; Vaysse, P. J. J.; Hartig, P. R.; Branchek, T. A.; Weinshank, R. L. The 5-Ht4 Receptor - Molecular-Cloning and Pharmacological Characterization of 2 Splice Variants. *Embo Journal* **1995,** *14* (12), 2806-2815.

28. Rees, S.; Dendaas, I.; Foord, S.; Goodson, S.; Bull, D.; Kilpatrick, G.; Lee, M. Cloning and Characterization of the Human 5-Ht5A Serotonin Receptor. *Febs Letters* **1994,** *355* (3), 242-246.

29. Matthes, H.; Boschert, U.; Amlaiky, N.; Grailhe, R.; Plassat, J. L.; Muscatelli, F.; Mattei, M. G.; Hen, R. Mouse 5-Hydroxytryptamine5A and 5-Hydroxytryptamine5B Receptors Define A New Family of Serotonin Receptors - Cloning, Functional Expression, and Chromosomal Localization. *Molecular Pharmacology* **1993,** *43* (3), 313-319.

30. Wisden, W.; Parker, E. M.; Mahle, C. D.; Grisel, D. A.; Nowak, H. P.; Yocca, F. D.; Felder, C. C.; Seeburg, P. H.; Voigt, M. M. Cloning and Characterization of the Rat 5-Ht(5B)Receptor - Evidence That the 5-Ht(5B)Receptor Couples to A G-Protein in Mammalian-Cell Membranes. *Febs Letters* **1993,** *333* (1-2), 25-31.

31. Monsma, F. J.; Shen, Y.; Ward, R. P.; Hamblin, M. W.; Sibley, D. R. Cloning and Expression of A Novel Serotonin Receptor with High-Affinity for Tricyclic Psychotropic-Drugs. *Molecular Pharmacology* **1993,** *43* (3), 320-327.

32. Plassat, J. L.; Amlaiky, N.; Hen, R. Molecular-Cloning of A Mammalian Serotonin Receptor That Activates Adenylate-Cyclase. *Molecular Pharmacology* **1993,** *44* (2), 229-236.

33. Ruat, M.; Traiffort, E.; Arrang, J. M.; Tardivellacombe, J.; Diaz, J.; Leurs, R.; Schwartz, J. C. A Novel Rat Serotonin (5-HT_6) Receptor - Molecular-Cloning, Localization and Stimulation of Camp Accumulation. *Biochemical and Biophysical Research Communications* **1993,** *193* (1), 268-276.

34. Ruat, M.; Traiffort, E.; Leurs, R.; Tardivellacombe, J.; Diaz, J.; Arrang, J. M.; Schwartz, J. C. Molecular-Cloning, Characterization, and Localization of A High-Affinity Serotonin Receptor (5-Ht(7)) Activating Camp Formation. *Proceedings of the National Academy of Sciences of the United States of America* **1993,** *90* (18), 8547-8551.

35. Lovenberg, T. W.; Baron, B. M.; Delecea, L.; Miller, J. D.; Prosser, R. A.; Rea, M. A.; Foye, P. E.; Racke, M.; Slone, A. L.; Siegel, B. W.; Danielson, P. E.; Sutcliffe, J. G.; Erlander, M. G. A Novel Adenylyl Cyclase-Activating Serotonin Receptor (5-Ht7) Implicated in the Regulation of Mammalian Circadian-Rhythms. *Neuron* **1993,** *11* (3), 449-458.

36. Bard, J. A.; Zgombick, J.; Adham, N.; Vaysse, P.; Branchek, T. A.; Weinshank, R. L. Cloning of A Novel Human Serotonin Receptor (5-Ht7) Positively Linked to Adenylate-Cyclase. *Journal of Biological Chemistry* **1993,** *268* (31), 23422-23426.

37. Shen, Y.; Monsma, F. J.; Metcalf, M. A.; Jose, P. A.; Hamblin, M. W.; Sibley, D. R. Molecular-Cloning and Expression of A 5-Hydroxytryptamine7 Serotonin Receptor Subtype. *Journal of Biological Chemistry* **1993,** *268* (24), 18200-18204.

38. Nichols, D. E. Hallucinogens. *Pharmacology & Therapeutics* **2004,** *101* (2), 131-181.

39. Aghajanian, G. K.; Marek, G. J. Serotonin and hallucinogens. *Neuropsychopharmacology* **1999,** *21* (2), S16-S23.

40. Meltzer, H. Y. The Role of Serotonin in Antipsychotic Drug Action. *Neuropsychopharmacology* **1999,** *21* (Supplement), 106-115.

41. Seeman, P. Atypical antipsychotics: Mechanism of action. *Canadian Journal of Psychiatry-Revue Canadienne de Psychiatrie* **2002,** *47* (1), 27-38.

42. Delean, A.; Stadel, J. M.; Lefkowitz, R. J. A Ternary Complex Model Explains the Agonist-Specific Binding-Properties of the Adenylate Cyclase-Coupled Beta-Adrenergic-Receptor. *Journal of Biological Chemistry* **1980,** *255* (15), 7108-7117.

43. Fitzgerald, L. W.; Conklin, D. S.; Krause, C. M.; Marshall, A. P.; Patterson, J. P.; Tran, D. P.; Iyer, G.; Kostich, W. A.; Largent, B. L.; Hartig, P. R. High-affinity agonist binding correlates with efficacy (intrinsic activity) at the human serotonin 5-HT_{2A} and 5-HT_{2C} receptors: Evidence favoring the ternary complex and two-state models of agonist action. *Journal of Neurochemistry* **1999,** *72* (5), 2127-2134.

44. Teitler, M.; Leonhardt, S.; Weisberg, E. L.; Hoffman, B. J. 4-[^{125}I]Iodo-(2,5-Dimethoxy)Phenylisopropylamine and [^{3}H] Ketanserin Labeling of 5-Hydroxytryptamine2 (5-HT_2) Receptors in Mammalian-Cells Transfected with A Rat 5-HT_2 cDNA - Evidence for Multiple States and Not Multiple 5-HT_2 Receptor Subtypes. *Molecular Pharmacology* **1990,** *38* (5), 594-598.

45. Samama, P.; Cotecchia, S.; Costa, T.; Lefkowitz, R. J. A Mutation-Induced Activated State of the β_2-Adrenergic Receptor - Extending the Ternary Complex Model. *Journal of Biological Chemistry* **1993,** *268* (7), 4625-4636.

46. Lefkowitz, R. J.; Cotecchia, S.; Samama, P.; Costa, T. Constitutive Activity of Receptors Coupled to Guanine-Nucleotide Regulatory Proteins. *Trends in Pharmacological Sciences* **1993,** *14* (8), 303-307.

47. Weiss, J. M.; Morgan, P. H.; Lutz, M. W.; Kenakin, T. P. The Cubic Ternary Complex Receptor-Occupancy Model I. Model Description. *Journal of Theoretical Biology* **1996,** *178* (2), 151-167.

48. Weiss, J. M.; Morgan, P. H.; Lutz, M. W.; Kenakin, T. P. The Cubic Ternary Complex Receptor-Occupancy Model II. Understanding Apparent Affinity. *Journal of Theoretical Biology* **1996,** *178* (2), 169-182.

49. Weiss, J. M.; Morgan, P. H.; Lutz, M. W.; Kenakin, T. P. The Cubic Ternary Complex Receptor-Occupancy Model III. Resurrecting Efficacy. *Journal of Theoretical Biology* **1996,** *181* (4), 381-397.

50. Limbird, L. E. The receptor concept: A continuing evolution. *Molecular Interventions* **2004,** *4* (6), 326-336.

51. Kenakin, T. Agonist-Receptor Efficacy .2. Agonist Trafficking of Receptor Signals. *Trends in Pharmacological Sciences* **1995,** *16* (7), 232-238.

52. Urban, J. D.; Clarke, W. P.; von Zastrow, M.; Nichols, D. E.; Kobilka, B.; Weinstein, H.; Javitch, J. A.; Roth, B. L.; Christopoulos, A.; Sexton, P. M.; Miller, K. J.; Spedding, M.; Mailman, R. B. Functional selectivity and classical concepts of quantitative pharmacology. *Journal of Pharmacology and Experimental Therapeutics* **2007,** *320* (1), 1-13.

53. Moya, P. R.; Berg, K. A.; Gutierrez-Hernandez, M. A.; Saez-Briones, P.; Reyes-Parada, M.; Cassels, B. K.; Clarke, W. P. Functional selectivity of hallucinogenic phenethylamine and phenylisopropylamine derivatives at human 5-hydroxytryptamine 5-HT_{2A} and 5-HT_{2C} receptors. *Journal of Pharmacology and Experimental Therapeutics* **2007,** *321* (3), 1054-1061.

54. Zhang, L.; Brass, L. F.; Manning, D. R. The G_q and G_{12} Families of Heterotrimeric G Proteins Report Functional Selectivity. *Molecular Pharmacology* **2009,** *75* (1), 235-241.

55. Mailman, R. B.; Murthy, V. Ligand functional selectivity advances our understanding of drug mechanisms and drug discovery. *Neuropsychopharmacology* **2009,** *35* (1), 345-346.

56. Conn, P. J.; Sanders-Bush, E. Selective 5-HT_2 Antagonists Inhibit Serotonin Stimulated Phosphatidylinositol Metabolism in Cerebral-Cortex. *Neuropharmacology* **1984,** *23* (8), 993-996.

57. Conn, P. J.; Sanders-Bush, E. Serotonin-Stimulated Phosphoinositide Turnover - Mediation by the S_2 Binding-Site in Rat Cerebral-Cortex But Not in Subcortical Regions. *Journal of Pharmacology and Experimental Therapeutics* **1985,** *234* (1), 195-203.

58. Conn, P. J.; Sanders-Bush, E. Regulation of Serotonin-Stimulated Phosphoinositide Hydrolysis - Relation to the Serotonin 5-HT_2 Binding-Site. *Journal of Neuroscience* **1986,** *6* (12), 3669-3675.

59. Nakaki, T.; Roth, B. L.; Chuang, D.; Costa, E. Phasic and Tonic Components in 5-HT_2 Receptor-Mediated Rat Aorta Contraction - Participation of Ca^{++} Channels and Phospholipase C-1. *Journal of Pharmacology and Experimental Therapeutics* **1985,** *234* (2), 442-446.

60. Doyle, V. M.; Creba, J. A.; Ruegg, U. T.; Hoyer, D. Serotonin Increases the Production of Inositol Phosphates and Mobilizes Calcium Via the 5-Ht2 Receptor in A7R5 Smooth-Muscle Cells. *Naunyn-Schmiedebergs Archives of Pharmacology* **1986,** *333* (2), 98-103.

61. Foskett, J. K.; White, C.; Cheung, K. H.; Mak, D.-O. D. Inositol Trisphosphate Receptor Ca^{2+} Release Channels. *Physiological Reviews* **2007,** *87* (2), 593-658.

62. Knauer, C. S.; Campbell, J. E.; Chio, C. L.; Fitzgerald, L. W. Pharmacological characterization of mitogen-activated protein kinase activation by recombinant human 5-HT_{2C}, 5-HT_{2A}, and 5-HT_{2B} receptors. *Naunyn-Schmiedebergs Archives of Pharmacology* **2009,** *379* (5), 461-471.

63. Chong, H.; Vikis, H. G.; Guan, K. L. Mechanisms of regulating the Raf kinase family. *Cellular Signalling* **2003,** *15* (5), 463-469.

64. Whitmarsh, A. J.; Davis, R. J. Transcription factor AP-1 regulation by mitogen-activated protein kinase signal transduction pathways. *Journal of Molecular Medicine-Jmm* **1996,** *74* (10), 589-607.

65. Galetic, I.; Maira, S. M.; Andjelkovic, M.; Hemmings, B. A. Negative regulation of ERK and Elk by protein kinase B modulates c-fos transcription. *Journal of Biological Chemistry* **2003,** *278* (7), 4416-4423.

66. Nichols, C. D.; Sanders-Bush, E. A single dose of lysergic acid diethylamide influences gene expression patterns within the mammalian brain. *Neuropsychopharmacology* **2002,** *26* (5), 634-642.

67. Cussac, D.; Boutet-Robinet, E.; Ailhaud, M. C.; Newman-Tancredi, A.; Martel, J. C.; Danty, N.; Rauly-Lestienne, I. Agonist-directed trafficking of signalling at serotonin 5-HT_{2A}, 5-HT_{2B} and 5-HT_{2C}-VSV receptors mediated $G_{q/11}$ activation and calcium mobilisation in CHO cells. *European Journal of Pharmacology* **2008,** *594* (1-3), 32-38.

68. Garcia, E. E.; Smith, R. L.; Sanders-Bush, E. Role of G_q protein in behavioral effects of the hallucinogenic drug 1-(2,5-dimethoxy-4-iodophenyl)-2-aminopropane. *Neuropharmacology* **2007,** *52* (8), 1671-1677.

69. Parrish, J. C.; Nichols, D. E. Serotonin 5-HT_{2A} receptor activation induces 2-arachidonoylglycerol release through a phospholipase C-dependent mechanism. *Journal of Neurochemistry* **2006,** *99* (4), 1164-1175.

70. Felder, C. C.; Kanterman, R. Y.; Ma, A. L.; Axelrod, J. Serotonin Stimulates Phospholipase-A_2 and the Release of Arachidonic-Acid in Hippocampal-Neurons by A Type-2 Serotonin Receptor That Is Independent of Inositolphospholipid Hydrolysis. *Proceedings of the National Academy of Sciences of the United States of America* **1990,** *87* (6), 2187-2191.

71. Berg, K. A.; Maayani, S.; Clarke, W. P. 5-hydroxytryptamine$_{2C}$ receptor activation inhibits 5-hydroxytryptamine$_{1B}$-like receptor function via arachidonic acid metabolism. *Molecular Pharmacology* **1996,** *50* (4), 1017-1023.

72. Berg, K. A.; Maayani, S.; Goldfarb, J.; Scaramellini, C.; Leff, P.; Clarke, W. P. Effector pathway-dependent relative efficacy at serotonin type 2A and 2C receptors: Evidence for agonist-directed trafficking of receptor stimulus. *Molecular Pharmacology* **1998,** *54* (1), 94-104.

73. Kurrasch-Orbaugh, D. M.; Watts, V. J.; Barker, E. L.; Nichols, D. E. Serotonin 5-hydroxytryptamine(2A) receptor-coupled phospholipase C and phospholipase A_2 signaling pathways have different receptor reserves. *Journal of Pharmacology and Experimental Therapeutics* **2003,** *304* (1), 229-237.

74. Kurrasch-Orbaugh, D. M.; Parrish, J. C.; Watts, V. J.; Nichols, D. E. A complex signaling cascade links the serotonin$_{2A}$ receptor to phospholipase A_2 activation: the involvement of MAP kinases. *Journal of Neurochemistry* **2003,** *86* (4), 980-991.

75. Ahn, S.; Maudsley, S.; Luttrell, L. M.; Lefkowitz, R. J.; Daaka, Y. Src-mediated tyrosine phosphorylation of dynamin is required for β_2-adrenergic receptor internalization and mitogen-activated protein kinase signaling. *Journal of Biological Chemistry* **1999,** *274* (3), 1185-1188.

76. Luttrell, L. M.; Ferguson, S. S. G.; Daaka, Y.; Miller, W. E.; Maudsley, S.; Della Rocca, G. J.; Lin, F. T.; Kawakatsu, H.; Owada, K.; Luttrell, D. K.; Caron, M. G.; Lefkowitz, R. J. beta-arrestin-dependent formation of β_2-adrenergic receptor Src protein kinase complexes. *Science* **1999,** *283* (5402), 655-661.

77. Egan, C. T.; Herrick-Davis, K.; Miller, K.; Glennon, R. A.; Teitler, M. Agonist activity of LSD and lisuride at cloned 5-HT$_{2A}$ and 5HT$_{2C}$ receptors. *Psychopharmacology* **1998,** *136* (4), 409-414.

78. Marona-Lewicka, D.; Kurrasch-Orbaugh, D. M.; Selken, J. R.; Cumbay, M. G.; Lisnicchia, J. G.; Nichols, D. E. Re-evaluation of lisuride pharmacology: 5-hydroxytryptamine$_{1A}$ receptor-mediated behavioral effects overlap its other properties in rats. *Psychopharmacology* **2002,** *164* (1), 93-107.

79. Halberstadt, A. L.; Geyer, M. A. LSD but not lisuride disrupts prepulse inhibition in rats by activating the 5-HT$_{2A}$ receptor. *Psychopharmacology* **2010,** *208* (2), 179-189.

80. White, F. J.; Wang, R. Y. Comparison of the Effects of LSD and Lisuride and A10 Dopamine Neurons in the Rat. *Neuropharmacology* **1983,** *22* (6), 669-676.

81. Adams, L. M.; Geyer, M. A. Patterns of Exploration in Rats Distinguish Lisuride from Lysergic-Acid Diethylamide. *Pharmacology Biochemistry and Behavior* **1985,** *23* (3), 461-468.

82. Gonzalez-Maeso, J.; Yuen, T.; Ebersole, B. J.; Wurmbach, E.; Lira, A.; Zhou, M. M.; Weisstaub, N.; Hen, R.; Gingrich, J. A.; Sealfon, S. C. Transcriptome fingerprints distinguish hallucinogenic and nonhallucinogenic 5-hydroxytryptamine 2A receptor agonist effects in mouse somatosensory cortex. *Journal of Neuroscience* **2003,** *23* (26), 8836-8843.

83. Gonzalez-Maeso, J.; Weisstaub, N. V.; Zhou, M. M.; Chan, P.; Ivic, L.; Ang, R.; Lira, A.; Bradley-Moore, M.; Ge, Y. C.; Zhou, Q.; Sealfon, S. C.; Gingrich, J. A. Hallucinogens recruit specific cortical 5-HT$_{2A}$ receptor-mediated signaling pathways to affect behavior. *Neuron* **2007,** *53* (3), 439-452.

84. Hall, R. A.; Premont, R. T.; Lefkowitz, R. J. Heptahelical receptor signaling: Beyond the G protein paradigm. *Journal of Cell Biology* **1999,** *145* (5), 927-932.

85. Lohse, M. J.; Benovic, J. L.; Codina, J.; Caron, M. G.; Lefkowitz, R. J. β-Arrestin: a protein that regulates beta-adrenergic receptor function. *Science* **1990,** *248* (4962), 1547-1550.

86. Ferguson, S. S. G.; Downey, W. E.; Colapietro, A. M.; Barak, L. S.; Menard, L.; Caron, M. G. Role of beta-arrestin in mediating agonist-promoted G protein-coupled receptor internalization. *Science* **1996,** *271* (5247), 363-366.

87. Luttrell, L. M.; Lefkowitz, R. J. The role of β-arrestins in the termination and transduction of G-protein-coupled receptor signals. *Journal of Cell Science* **2002,** *115* (3), 455-465.

88. Reiter, E.; Lefkowitz, R. J. GRKs and β-arrestins: roles in receptor silencing, trafficking and signaling. *Trends in Endocrinology and Metabolism* **2006,** *17* (4), 159-165.

89. Pierce, K. L.; Lefkowitz, R. J. Classical and new roles of [beta]-arrestins in the regulation of G-PROTEIN-COUPLED receptors. *Nature Reviews Neuroscience* **2001,** *2* (10), 727-733.

90. Schmid, C. L.; Raehal, K. M.; Bohn, L. M. Agonist-directed signaling of the serotonin 2A receptor depends on β-arrestin-2 interactions in vivo. *Proceedings of the National Academy of Sciences of the United States of America* **2008,** *105* (3), 1079-1084.

91. Johnson, M. S.; Robertson, D. N.; Holland, P. J.; Lutz, E. M.; Mitchell, R. Role of the conserved NPxxY motif of the 5-HT_{2A} receptor in determining selective interaction with isoforms of ADP-ribosylation factor (ARF). *Cellular Signalling* **2006,** *18* (10), 1793-1800.

92. Robertson, D. N.; Johnson, M. S.; Moggach, L. O.; Holland, P. J.; Lutz, E. M.; Mitchell, R. Selective interaction of ARF1 with the carboxy-terminal tail domain of the 5-HT_{2A} receptor. *Molecular Pharmacology* **2003,** *64* (5), 1239-1250.

93. Mitchell, R.; McCulloch, D.; Lutz, E.; Johnson, M.; MacKenzie, C.; Fennell, M.; Fink, G.; Zhou, W.; Sealfon, S. C. Rhodopsin-family receptors associate with small G proteins to activate phospholipase D. *Nature* **1998,** *392* (6674), 411-414.

94. Hodgkin, M. N.; Pettitt, T. R.; Martin, A.; Michell, R. H.; Pemberton, A. J.; Wakelam, M. J. O. Diacylglycerols and phosphatidates: which molecular species are intracellular messengers? *Trends in Biochemical Sciences* **1998,** *23* (6), 200-204.

95. Ferguson, S. S. G. Evolving concepts in G protein-coupled receptor endocytosis: The role in receptor desensitization and signaling. *Pharmacological Reviews* **2001,** *53* (1), 1-24.

96. Goodman, O. B.; Krupnick, J. G.; Santini, F.; Gurevich, V. V.; Penn, R. B.; Gagnon, A. W.; Keen, J. H.; Benovic, J. L. beta-arrestin acts as a clathrin adaptor in endocytosis of the β_2-adrenergic receptor. *Nature* **1996,** *383* (6599), 447-450.

97. Kelly, E.; Bailey, C. P.; Henderson, G. Agonist-selective mechanisms of GPCR desensitization. *British Journal of Pharmacology* **2008,** *153* (S1), S379-S388.

98. Glennon, R. A.; Titeler, M.; Young, R. Structure-Activity-Relationships and Mechanism of Action of Hallucinogenic Agents Based on Drug Discrimination and Radioligand Binding-Studies. *Psychopharmacology Bulletin* **1986,** *22* (3), 953-958.

99. Glennon, R. A.; Young, R.; Hauck, A. E.; Mckenney, J. D. Structure-Activity Studies on Amphetamine Analogs Using Drug Discrimination Methodology. *Pharmacology Biochemistry and Behavior* **1984,** *21* (6), 895-901.

100. Glennon, R. A.; Young, R.; Rosecrans, J. A. Antagonism of the Effects of the Hallucinogen DOM and the Purported 5-HT Agonist Quipazine by 5-HT_2 Antagonists. *European Journal of Pharmacology* **1983,** *91* (2-3), 189-196.

101. Vollenweider, F. X.; Leenders, K. L.; Scharfetter, C.; Maguire, P.; Stadelmann, O.; Angst, J. Positron emission tomography and fluorodeoxyglucose studies of metabolic hyperfrontality and psychopathology in the psilocybin model of psychosis. *Neuropsychopharmacology* **1997,** *16* (5), 357-372.

102. Vollenweider, F. X.; Vollenweider-Scherpenhuyzen, M. F. I.; Babler, A.; Vogel, H.; Hell, D. Psilocybin induces schizophrenia-like psychosis in humans via a serotonin-2 agonist action. *Neuroreport* **1998,** *9* (17), 3897-3902.

103. Umbricht, D.; Vollenweider, F. X.; Schmid, L.; Grubel, C.; Skrabo, A.; Huber, T.; Koller, R. Effects of the 5-HT2A agonist psilocybin on mismatch negativity generation and AX-continuous performance task: Implications for the neuropharmacology of cognitive deficits in schizophrenia. *Neuropsychopharmacology* **2003,** *28* (1), 170-181.

104. Hasler, F.; Grimberg, U.; Benz, M. A.; Huber, T.; Vollenweider, F. X. Acute psychological and physiological effects of psilocybin in healthy humans: a double-blind, placebo-controlled dose-effect study. *Psychopharmacology* **2004,** *172* (2), 145-156.

105. Carter, O. L.; Pettigrew, J. D.; Burr, D. C.; Alais, D.; Hasler, F.; Vollenweider, F. X. Psilocybin impairs high-level but not low-level motion perception. *Neuroreport* **2004,** *15* (12), 1947-1951.

106. Carter, O. L.; Pettigrew, J. D.; Hasler, F.; Wallis, G. M.; Liu, G. B.; Hell, D.; Vollenweider, F. X. Modulating the rate and rhythmicity of perceptual rivalry alternations with the mixed 5-HT2A and 5-HT1A agonist psilocybin. *Neuropsychopharmacology* **2005,** *30* (6), 1154-1162.

107. Quednow, B.; Csomor, P. A.; Knappe, B.; Geyer, M. A.; Vollenweider, F. X. The effects of the hallucinogenic 5-HT2A agonist psilocybin on prepulse inhibition of acoustic startle response in healthy human volunteers. *Journal of Psychophysiology* **2006,** *20* (2), 120.

108. Carter, O. L.; Hasler, F.; Pettigrew, J. D.; Wallis, G. M.; Liu, G. B.; Vollenweider, F. X. Psilocybin links binocular rivalry switch rate to attention and subjective arousal levels in humans. *Psychopharmacology* **2007,** *195*, 415-424.

109. Wittmann, M.; Carter, O.; Hasler, F.; Cahn, B. R.; Grimberg, U.; Spring, P.; Hell, D.; Flohr, H.; Vollenweider, F. X. Effects of psilocybin on time perception and temporal

control of behaviour in humans. *Journal of Psychopharmacology* **2007,** *21* (1), 50-64.

110. Vollenweider, F. X.; Hell, D.; Kometer, M. Effects of the hallucinogenic 5-HT2A agonist psilocybin on object completion in humans. *International Journal of Psychophysiology* **2008,** *69* (3), 157.

111. Wackermann, J.; Wittmann, M.; Hasler, F.; Vollenweider, F. X. Effects of varied doses of psilocybin on time interval reproduction in human subjects. *Neuroscience Letters* **2008,** *435* (1), 51-55.

112. Hasler, F.; Quednow, B. B.; Treyer, V.; Schubiger, P. A.; Buck, A.; Vollenweider, F. X. Role of Prefrontal Serotonin-2A Receptors in Self-experience During Psilocybin Induced Altered States. *Neuropsychobiology* **2009,** *59* (2), 2.

113. Green, A. R.; Mechan, A. O.; Elliott, J. M.; O'Shea, E.; Colado, M. I. The Pharmacology and Clinical Pharmacology of 3,4-Methylenedioxymethamphetamine (MDMA, "Ecstasy"). *Pharmacological Reviews* **2003,** *55* (3), 463-508.

114. Roth, B. L.; Baner, K.; Westkaemper, R.; Siebert, D.; Rice, K. C.; Steinberg, S.; Ernsberger, P.; Rothman, R. B. Salvinorin A: A potent naturally occurring nonnitrogenous kappa opioid selective agonist. *Proceedings of the National Academy of Sciences of the United States of America* **2002,** *99* (18), 11934-11939.

115. Bruhn, J. G.; Bruhn, C. Alkaloids and Ethnobotany of Mexican Peyote Cacti and Related Species. *Economic Botany* **1973,** *27* (2), 241-251.

116. Martinez, S. T.; Almeida, M. R.; Pinto, A. C. Natural Hallucinogens: A Flight from Medieval Europe to Brazil. *Quimica Nova* **2009,** *32* (9), 2501-2507.

117. Cao, R. H.; Peng, W. L.; Wang, Z. H.; Xu, A. L. β-Carboline alkaloids: Biochemical and pharmacological functions. *Current Medicinal Chemistry* **2007,** *14* (4), 479-500.

118. McKenna, D. J.; Towers, G. H. N.; Abbott, F. Monoamine oxidase inhibitors in South American hallucinogenic plants: Tryptamine and [beta]-carboline constituents of Ayahuasca. *Journal of Ethnopharmacology* **1984,** *10* (2), 195-223.

119. Mckenna, D. J.; Towers, G. H. N.; Abbott, F. S. Monoamine-Oxidase Inhibitors in South-American Hallucinogenic Plants .2. Constituents of Orally-Active Myristicaceous Hallucinogens. *Journal of Ethnopharmacology* **1984,** *12* (2), 179-211.

120. Guzman, G. Hallucinogenic Mushrooms in Mexico: An Overview. *Economic Botany* **2008,** *62* (3), 404-412.

121. Weil, A. T.; Davis, W. Bufo alvarius: a potent hallucinogen of animal origin. *Journal of Ethnopharmacology* **1994,** *41* (1-2), 1-8.

122. Lyttle, T.; Goldstein, D.; Gartz, J. Bufo toads and bufotenine: Fact and fiction surrounding an alleged psychedelic. *Journal of Psychoactive Drugs* **1996,** *28* (3), 267-290.

123. Brownstein, M. J. A Brief-History of Opiates, Opioid-Peptides, and Opioid Receptors. *Proceedings of the National Academy of Sciences of the United States of America* **1993,** *90* (12), 5391-5393.

124. Hanna, J. M. Coca Leaf Use in Southern-Peru - Biosocial Aspects. *American Anthropologist* **1974,** *76* (2), 281-296.

125. Luqman, W.; Danowski, T. S. Use of Khat (Catha-Edulis) in Yemen Social and Medical Observations. *Annals of Internal Medicine* **1976,** *85* (2), 246-249.

126. Michelot, D.; Melendez-Howell, L. M. Amanita muscaria: chemistry, biology, toxicology, and ethnomycology. *Mycological Research* **2003,** *107*, 131-146.

127. Fabing, H. D. On Going Berserk: A Neurochemical Inquiry. *Scientific Monthly,* **Nov 1, 1954,** p 232.

128. Stoll, A.; Hofmann, A. Partialsynthese von Alkaloiden vom Typus des Ergobasins. (6. Mitteilung über Mutterkornalkaloide). *Helvetica Chimica Acta* **1943,** *26* (3), 944-965.

129. Hofmann, A. Notes and Documents Concerning the Discovery of LSD. *Agents and Actions* **1994,** *43* (3-4), 79-81.

130. Rapport, M. M.; Green, A. A.; Page, I. H. Serum Vasoconstrictor (Serotonin) .3. Chemical Inactivation. *Journal of Biological Chemistry* **1948,** *176* (3), 1237-1241.

131. Rapport, M. M.; Green, A. A.; Page, I. H. Serum Vasoconstrictor (Serotonin) .4. Isolation and Characterization. *Journal of Biological Chemistry* **1948,** *176* (3), 1243-1251.

132. Woolley, D. W.; Shaw, E. A Biochemical and Pharmacological Suggestion about Certain Mental Disorders. *Proceedings of the National Academy of Sciences of the United States of America* **1954,** *40* (4), 228-231.

133. Medicine: Dream Stuff. *Time Magazine,* **Jun 28, 1954**.

134. Medicine: Artificial Psychoses. *Time Magazine,* **Dec 19, 1955**.

135. Medicine: Mushroom Madness. *Time Magazine,* **Jun 16, 1958**.

136. Psychic Research: LSD. *Time Magazine,* **Mar 29, 1963**.

137. Hofmann, A.; Heim, R.; Brack, A.; Kobel, H. Psilocybin, Ein Psychotroper Wirkstoff aus dem Mexikanischen Rauschpilz Psilocybe-Mexicana Heim. *Experientia* **1958,** *14* (3), 107-109.

138. Hofmann, A.; Frey, A.; Ott, H.; Petrzilka, T.; Troxler, F. Konstitutionsaufklarung und Synthese Von Psilocybin. *Experientia* **1958,** *14* (11), 397-399.

139. Hofmann, A.; Heim, R.; Brack, A.; Kobel, H.; Frey, A.; Ott, H.; Petrzilka, T.; Troxler, F. Psilocybin und Psilocin, Zwei Psychotrope Wirkstoffe aus Mexikanischen Rauschpilzen. *Helvetica Chimica Acta* **1959,** *42* (5), 1557-+.

140. Troxler, F.; Seemann, F.; Hofmann, A. Abwandlungsprodukte Von Psilocybin und Psilocin .2. Uber Synthetische Indolverbindungen. *Helvetica Chimica Acta* **1959,** *42* (6), 2073-2103.

141. Stoll, A.; Hofmann, A. Amide der stereoisomeren Lysergsäuren und Dihydro-lysergsäuren. (38. Mitteilung über Mutterkornalkaloide). *Helvetica Chimica Acta* **1955,** *38* (2), 421-433.

142. Hofmann, A. Psychotomimetic Drugs Chemical and Pharmacological Aspects. *Acta Physiologica et Pharmacologica Neerlandica* **1959,** *8* (2), 240-258.

143. Stoll, A.; Troxler, F.; Peyer, J.; Hofmann, A. Mutterkornalkaloide .40. Eine Neue Synthese Von Bufotenin und Verwandten Oxy-Tryptaminen. *Helvetica Chimica Acta* **1955,** *38* (6), 1452-1472.

144. Hoffman, A. J.; Nichols, D. E. Synthesis and LSD-Like Discriminative Stimulus Properties in A Series of N_6-Alkyl Nor-Lysergic Acid N,N-Diethylamide Derivatives. *Journal of Medicinal Chemistry* **1985,** *28* (9), 1252-1255.

145. Nichols, D. E.; Frescas, S.; Marona-Lewicka, D.; Kurrasch-Orbaugh, D. M. Lysergamides of isomeric 2,4-dimethylazetidines map the binding orientation of the diethylamide moiety in the potent hallucinogenic agent N,N-diethyllysergamide (LSD). *Journal of Medicinal Chemistry* **2002,** *45* (19), 4344-4349.

146. Shulgin, A. T.; Shulgin, A. *TIHKAL: The Continuation;* Transform Press: Berkeley, CA, 1997.

147. May, J. A.; Dantanarayana, A. P.; Zinke, P. W.; McLaughlin, M. A.; Sharif, N. A. 1-((*S*)-2-aminopropyl)-1*H*-indazol-6-ol: A potent peripherally acting 5-HT_2 receptor agonist with ocular hypotensive activity. *Journal of Medicinal Chemistry* **2006,** *49* (1), 318-328.

148. May, J. A.; Sharif, N. A.; Chen, H. H.; Liao, J. C.; Kelly, C. R.; Glennon, R. A.; Young, R.; Li, J. X.; Rice, K. C.; France, C. R. Pharmacological properties and discriminative stimulus effects of a novel and selective 5-HT_2 receptor agonist AL-38022A [(*S*)-2-(8,9-dihydro-7*H*-pyrano[2,3-*g*]indazol-1-yl)-1-methylethylamine]. *Pharmacology Biochemistry and Behavior* **2009,** *91* (3), 307-314.

149. Huxley, A. *The Doors of Perception;* Harper & Row: New York, 1954.

150. Heffter, A. Über Cacteenalkaloïde. *Berichte der deutschen chemischen Gesellschaft* **1896,** *29* (1), 216-227.

151. Heffter, A. Über Pellote: Beiträge zur chemischen und pharmakologischen Kenntniss der Cacteen: Zweite Mittheilung. *Naunyn-Schmiedebergs Archives of Pharmacology* **1898,** *40* (5-6), 385-429.

152. Zucker, K. Experiments with mescaline and hallucination. *Zeitschrift fur Die Gesamte Neurologie und Psychiatrie* **1930,** *127,* 108-161.

153. Grace, G. S. The action of mescaline and some related compounds. *Journal of Pharmacology and Experimental Therapeutics* **1934,** *50* (4), 359-372.

154. Guttmann, E. Artificial Psychoses Produced by Mescaline. *Journal of Mental Science* **1936,** *82* (338), 203-221.

155. Stockings, G. T. A Clinical Study of the Mescaline Psychosis, with Special Reference to the Mechanism of the Genesis of Schizophrenic and Other Psychotic States. *Journal of Mental Science* **1940,** *86* (360), 29-47.

156. Jansen, M. P. J. M. beta-2 : 4 : 5-trimethoxyphenylethylamine, an isomer of mescaline. *Recueil des Travaux Chimiques des Pays-Bas* **1931,** *50*, 291-312.

157. Hey, P. The Synthesis of A New Homologue of Mescaline. *Quarterly Journal of Pharmacy and Pharmacology* **1947,** *20* (2), 129-134.

158. Peretz, D. I.; Smythies, J. R.; Gibson, W. C. A New Hallucinogen - 3,4,5-Trimethoxyphenyl-Beta-Aminopropane - with Notes on the Stroboscopic Phenomenon. *Journal of Mental Science* **1955,** *101* (423), 317-329.

159. Shulgin, A. T.; Bunnell, S.; Sargent, T. Psychotomimetic Properties of 3,4,5-Trimethoxyamphetamine. *Nature* **1961,** *189* (476), 1011-&.

160. Shulgin, A. T. Psychotomimetic Agents Related to Mescaline. *Experientia* **1963,** *19* (3), 127-&.

161. Shulgin, A. T. 3-Methoxy-4,5-Methylenedioxy Amphetamine New Psychotomimetic Agent. *Nature* **1964,** *201* (492), 1120-&.

162. Shulgin, A. T.; Sargent, T.; Naranjo, C. Animal Pharmacology and Human Psychopharmacology of 3-Methoxy-4,5-Methylenedioxyphenylisopropylamine (Mmda). *Pharmacology* **1973,** *10* (1), 12-18.

163. Shulgin, A. T. MMDA. *Journal of Psychedelic Drugs* **1976,** *8* (4), 331.

164. Shulgin, A. T. Psychotomimetic Amphetamines - Methoxy 3,4-Dialkoxyamphetamines. *Experientia* **1964,** *20* (7), 366-&.

165. Shulgin, A. T. 6 Trimethoxyphenylisopropylamines (Trimethoxyamphetamines). *Journal of Medicinal Chemistry* **1966,** *9* (3), 445-&.

166. Shulgin, A. T. Ethyl Homologs of 2,4,5-Trimethoxyphenylisopropylamine. *Journal of Medicinal Chemistry* **1968,** *11* (1), 186-&.

167. Shulgin, A. T.; Shulgin, A. *PiHKAL: A Chemical Love Story;* Transform Press: Berkeley, CA, 1991.

168. Snyder, S. H.; Faillace, L.; Holliste, L. 2,5-Dimethoxy-4-Methyl-Amphetamine (STP) - A New Hallucinogenic Drug. *Science* **1967,** *158* (3801), 669-&.

169. Snyder, S. H.; Faillace, L. A.; Weingart, H. Dom (STP) A New Hallucinogenic Drug and Doet - Effects in Normal Subjects. *American Journal of Psychiatry* **1968,** *125* (3), 357-&.

170. Shulgin, A. T.; Sargent, T. Psychotropic Phenylisopropylamines Derived from Apiole and Dillapiole. *Nature* **1967,** *215* (5109), 1494-&.

171. Shulgin, A. T.; Sargent, T.; Naranjo, C. Structure-Activity Relationships of One-Ring Psychotomimetics. *Nature* **1969,** *221* (5180), 537-&.

172. Ho, B. T.; Mcisaac, W. M.; An, R.; Tansey, L. W.; Walker, K. E.; Englert, L. F.; Noel, M. B. Analogs of Alpha-Methylphenethlamine (Amphetamine) .1. Synthesis and Pharmacological Activity of Some Methoxy And/Or Methyl Analogs. *Journal of Medicinal Chemistry* **1970,** *13* (1), 26-&.

173. Ho, B. T.; Tansey, L. W.; Balster, R. L.; An, R.; Mcisaac, W. M.; Harris, R. T. Amphetamine Analogs .2. Methylated Phenethlamines. *Journal of Medicinal Chemistry* **1970,** *13* (1), 134-&.

174. Shulgin, A. T.; Sargent, T.; Naranjo, C. 4-Bromo-2,5-Dimethoxyphenylisopropylamine, A New Centrally Active Amphetamine Analog. *Pharmacology* **1971,** *5* (2), 103-&.

175. Barfknec, C. F.; Nichols, D. E. Potential Psychotomimetics - Bromomethoxyamphetamines. *Journal of Medicinal Chemistry* **1971,** *14* (4), 370-&.

176. Coutts, R. T.; Malicky, J. L. Synthesis of Some Analogs of Hallucinogen 1-(2,5-Dimethoxy-4-Methylphenyl)-2-Aminopropane (DOM). *Canadian Journal of Chemistry-Revue Canadienne de Chimie* **1973,** *51* (9), 1402-1409.

177. Coutts, R. T.; Malicky, J. L. Synthesis of Analogs of Hallucinogen 1-(2,5-Dimethoxy-4-Methylphenyl)-2-Aminopropane (Dom) .2. Some Ring-Methoxylated 1-Aminoindanes and 2-Aminoindanes. *Canadian Journal of Chemistry-Revue Canadienne de Chimie* **1974,** *52* (3), 381-389.

178. Barfknec, C. F.; Nichols, D. E.; Olesen, B.; Engelbre, J. A. Analog of Psychotomimetic Phenylisopropylaminese - 2-Amino-5,8-Dimethoxy-1,2,3,4-Tetrahydronaphthalene. *Pharmacologist* **1971,** *13* (2), 233.

179. Barfknec, C. F.; Nichols, D. E.; Rusterho, D. B.; Long, J. P.; Engelbre, J. A.; Beaton, J. M.; Bradley, R. J.; Dyer, D. C. Potential Psychotomimetics - 2-Amino-1,2,3,4-Tetrahydronaphthalene Analogs. *Journal of Medicinal Chemistry* **1973,** *16* (7), 804-808.

180. Nichols, D. E.; Barfknec, C. F. Potential Psychotomimetics .2. 1 Rigid Analogs of 2,5-Dimethoxy-4-Methylphenylisopropylamine (DOM,STP). *Journal of Medicinal Chemistry* **1974,** *17* (2), 161-166.

181. Walters, G. C.; Cooper, P. D. Alicyclic Analogue of Mescaline. *Nature* **1968,** *218* (5138), 298-&.

182. Cooper, P. D.; Walters, G. C. Stereochemical Requirements of Mescaline Receptor. *Nature* **1972,** *238* (5359), 96-&.

183. Cooper, P. D. Stereospecific synthesis of *cis*- and *trans*-2-(3,4,5-trimethoxyphenyl)-cyclopropylamines. *Canadian Journal of Chemistry-Revue Canadienne de Chimie* **1970,** *48* (24), 3882-3888.

184. Nichols, D. E.; Barfknec, C. F.; Rusterho, D. B. Asymmetric Synthesis of Psychotomimetic Phenylisopropylamines. *Journal of Medicinal Chemistry* **1973,** *16* (5), 480-483.

185. Dyer, D. C.; Nichols, D. E.; Rusterho, D. B.; Barfknec, C. F. Comparative Effects of Stereoisomers of Psychotomimetic Phenylisopropylamines. *Life Sciences* **1973,** *13* (7), 885-896.

186. Shulgin, A. T.; Carter, M. F. Centrally Active Phenethylamines. *Psychopharmacology Communications* **1975,** *1* (1), 93-98.

187. Shulgin, A. T.; Dyer, D. C. Psychotomimetic Phenylisopropylamines .5. 4-Alkyl-2,5-Dimethoxyphenylisopropylamines. *Journal of Medicinal Chemistry* **1975,** *18* (12), 1201-1204.

188. Morin, R. D.; Benington, F.; Mitchell, S. R.; Beaton, J. M.; Bradley, R. J.; Smythies, J. R. Behavioral-Effects of 2,5-Dimethoxy-4-Alkyl Amphetamines. *Experientia* **1975,** *31* (1), 93-95.

189. Shulgin, A. T. Substituted α-methyl-β-phenylethylamines as central nervous system stimulants. GB 1,147,379, Apr 2, 1969.

190. Shulgin, A. T. 4-alkyl-dialkoxy-*alpha*-methyl-phenethylamines and their pharmacologically-acceptable salts. US 3,547,999, Dec 15, 1970.

191. Braun, U.; Shulgin, A. T.; Braun, G.; Sargent, T. Synthesis and Body Distribution of Several ^{131}I Labeled Centrally Acting Drugs. *Journal of Medicinal Chemistry* **1977,** *20* (12), 1543-1546.

192. Cheng, A. C.; Castagnoli, N. Synthesis and Physicochemical and Neurotoxicity Studies of 1-(4-Substituted-2,5-Dihydroxyphenyl)-2-Aminoethane Analogs of 6-Hydroxydopamine. *Journal of Medicinal Chemistry* **1984,** *27* (4), 513-520.

193. Nichols, D. E.; Shulgin, A. T. Sulfur Analogs of Psychotomimetic Amines. *J. Pharm. Sci.* **1976,** *65* (10), 1554-1555.

194. Jacob, P.; Anderson, G.; Meshul, C. K.; Shulgin, A. T.; Castagnoli, N. Monomethylthio Analogs of 1-(2,4,5-Trimethoxyphenyl)-2-Aminopropane. *Journal of Medicinal Chemistry* **1977,** *20* (10), 1235-1239.

195. Jacob, P.; Shulgin, A. T. Sulfur Analogs of Psychotomimetic Agents - Monothio Analogs of Mescaline and Isomescaline. *Journal of Medicinal Chemistry* **1981,** *24* (11), 1348-1353.

196. Jacob, P.; Shulgin, A. T. Sulfur Analogs of Psychotomimetic Agents .2. Analogs of (2,5-Dimethoxy-4-Methylphenyl)Isopropylamine and (2,5-Dimethoxy-4-Ethylphenyl)Isopropylamine. *Journal of Medicinal Chemistry* **1983,** *26* (5), 746-752.

197. Jacob, P.; Shulgin, A. T. Sulfur Analogs of Psychotomimetic Agents .3. Ethyl Homologs of Mescaline and Their Monothio Analogs. *Journal of Medicinal Chemistry* **1984,** *27* (7), 881-888.

198. Nichols, D. E.; Pfister, W. R.; Yim, G. K. W. LSD and Phenethylamine Hallucinogens - New Structural Analogy and Implications for Receptor Geometry. *Life Sciences* **1978,** *22* (24), 2165-2170.

199. Nichols, D. E.; Woodard, R.; Hathaway, B. A.; Lowy, M. T.; Yim, G. K. W. Resolution and Absolute-Configuration of Trans-2-(2,5-Dimethoxy-4-Methylphenyl)Cyclopropylamine, A Potent Hallucinogen Analog. *Journal of Medicinal Chemistry* **1979,** *22* (4), 458-460.

200. Jacob, J. N.; Nichols, D. E. Isomeric Cyclopropyl Ring-Methylated Homologs of Trans-2-(2,5-Dimethoxy-4-Methylphenyl)Cyclopropylamine, An Hallucinogen Analog. *Journal of Medicinal Chemistry* **1982,** *25* (5), 526-530.

201. Mclean, T. H.; Parrish, J. C.; Braden, M. R.; Marona-Lewicka, D.; Gallardo-Godoy, A.; Nichols, D. E. 1-aminomethylbenzocycloalkanes: Conformationally restricted hallucinogenic phenethylamine analogues as functionally selective 5-HT_{2A} receptor agonists. *Journal of Medicinal Chemistry* **2006,** *49* (19), 5794-5803.

202. Dowd, C. S.; Herrick-Davis, K.; Egan, C.; Dupre, A.; Smith, C.; Teitler, M.; Glennon, R. A. 1-[4-(3-phenylalkyl)phenyl]-2-aminopropanes as 5-HT_{2A} partial agonists. *Journal of Medicinal Chemistry* **2000,** *43* (16), 3074-3084.

203. Seggel, M. R.; Yousif, M. Y.; Lyon, R. A.; Titeler, M.; Roth, B. L.; Suba, E. A.; Glennon, R. A. A Structure Affinity Study of the Binding of 4-Substituted Analogs of 1-(2,5-Dimethoxyphenyl)-2-Aminopropane at 5-HT_2 Serotonin Receptors. *Journal of Medicinal Chemistry* **1990,** *33* (3), 1032-1036.

204. Harms, A.; Ulmer, E.; Kovar, K. A. Synthesis and 5-HT_{2A} radioligand receptor binding assays of DOMCI and DOMOM, two novel 5-HT_{2A} receptor ligands. *Archiv der Pharmazie* **2003,** *336* (3), 155-158.

205. Trachsel, D. Synthesis of novel (Phenylalkyl)amines for the investigation of structure-activity relationships. Part 1. Mescalin derivatives. *Helvetica Chimica Acta* **2002,** *85* (9), 3019-3026.

206. Trachsel, D. Synthesis of novel (phenylalkyl)amines for the investigation of structure-activity relationships. Part 2. 4-thio-substituted [2-(2,5-dimethoxyphenyl)ethyl]amines (=2,5-dimethoxybenzeneethanamines). *Helvetica Chimica Acta* **2003,** *86* (7), 2610-2619.

207. Trachsel, D. Synthesis of novel (phenylalkyl)amines for the investigation of structure - Activity relationships - Part 3 - 4-Ethynyl-2,5-dimethoxyphenethylamine (4-Ethynyl-2,5-dimethoxybenzeneethanamine; 2C-YN). *Helvetica Chimica Acta* **2003,** *86* (8), 2754-2759.

208. Trachsel, D.; Nichols, D. E.; Kidd, S.; Hadorn, M.; Baumberger, F. 4-Aryl-Substituted 2,5-Dimethoxyphenethylamines: Synthesis and Serotonin 5-HT_{2A} Receptor Affinities. *Chemistry & Biodiversity* **2009,** *6* (5), 692-704.

209. Nichols, D. E.; Hoffman, A. J.; Oberlender, R. A.; Riggs, R. M. Synthesis and Evaluation of 2,3-Dihydrobenzofuran Analogs of the Hallucinogen 1-(2,5-Dimethoxy-4-Methylphenyl)-2-Aminopropane - Drug Discrimination Studies in Rats. *Journal of Medicinal Chemistry* **1986,** *29* (2), 302-304.

210. Nichols, D. E.; Snyder, S. E.; Oberlender, R.; Johnson, M. P.; Huang, X. M. 2,3-Dihydrobenzofuran Analogs of Hallucinogenic Phenethylamines. *Journal of Medicinal Chemistry* **1991,** *34* (1), 276-281.

211. Monte, A. P.; MaronaLewicka, D.; Parker, M. A.; Wainscott, D. B.; Nelson, D. L.; Nichols, D. E. Dihydrobenzofuran analogues of hallucinogens .3. Models of 4-substituted (2,5-dimethoxyphenyl)alkylamine derivatives with rigidified methoxy groups. *Journal of Medicinal Chemistry* **1996,** *39* (15), 2953-2961.

212. Monte, A. P.; Waldman, S. R.; MaronaLewicka, D.; Wainscott, D. B.; Nelson, D. L.; SandersBush, E.; Nichols, D. E. Dihydrobenzofuran analogues of hallucinogens .4. Mescaline derivatives. *Journal of Medicinal Chemistry* **1997,** *40* (19), 2997-3008.

213. Monte, A. P.; MaronaLewicka, D.; Cozzi, N. V.; Nelson, D. L.; Nichols, D. E. Conformationally restricted tetrahydro-1-benzoxepin analogs of hallucinogenic phenethylamines. *Medicinal Chemistry Research* **1995,** *5* (9), 651-663.

214. Parker, M. A.; Marona-Lewicka, D.; Lucaites, V. L.; Nelson, D. L.; Nichols, D. E. A novel (benzodifuranyl)aminoalkane with extremely potent activity at the 5-HT_{2A} receptor. *Journal of Medicinal Chemistry* **1998,** *41* (26), 5148-5149.

215. Chambers, J. J.; Kurrasch-Orbaugh, D. M.; Parker, M. A.; Nichols, D. E. Enantiospecific synthesis and pharmacological evaluation of a series of super-potent, conformationally restricted 5-$HT_{2A/2C}$ receptor agonists. *Journal of Medicinal Chemistry* **2001,** *44* (6), 1003-1010.

216. Whiteside, M. S.; Kurrasch-Orbaugh, D.; Marona-Lewicka, D.; Nichols, D. E.; Monte, A. Substituted hexahydrobenzodipyrans as 5-$HT_{2A/2C}$ receptor probes. *Bioorganic & Medicinal Chemistry* **2002,** *10* (10), 3301-3306.

217. Schultz, D. M.; Prescher, J. A.; Kidd, S.; Marona-Lewicka, D.; Nichols, D. E.; Monte, A. 'Hybrid' benzofuran-benzopyran congeners as rigid analogs of hallucinogenic phenethylamines. *Bioorganic & Medicinal Chemistry* **2008,** *16* (11), 6242-6251.

218. Heim, R. Synthese und Pharmakologie Potenter 5-HT_{2A}-rezeptoragonisten mit *N*-2-Methoxybenzyl-Partialstruktur. PhD Freie Universität Berlin, Mar 2003.

219. Elz, S.; Klass, T.; Heim, R.; Warnke, U.; Pertz, H. H. Development of highly potent partial agonists and chiral antagonists as tools for the study of 5-HT2A-receptor mediated functions. *Naunyn-Schmiedebergs Archives of Pharmacology* **2002,** *365* (Suppl. 1, Abstract 102), R29.

220. Ratzeburg, K.; Heim, R.; Mahboobi, S.; Henatsch, J.; Pertz, H. H.; Elz, S. Potent partial 5-HT2A-receptor agonism of phenylethan-amines related to mescaline in the rat tail artery model. *Naunyn-Schmiedebergs Archives of Pharmacology* **2003,** *367* (Suppl. 1 Abstract 111), R31.

221. Braden, M. R.; Parrish, J. C.; Naylor, J. C.; Nichols, D. E. Molecular interaction of serotonin 5-HT_{2A} receptor residues Phe339((6.51)) and Phe340((6.52)) with superpotent N-benzyl phenethylamine agonists. *Molecular Pharmacology* **2006,** *70* (6), 1956-1964.

222. Braden, M. R. Towards a Biophysical Understanding of Hallucinogen Action. PhD Purdue University, Oct 2007.

223. Colpaert, F. C.; Niemegeers, C. J. E.; Janssen, P. A. J. Theoretical and Methodological Considerations on Drug Discrimination-Learning. *Psychopharmacologia* **1976,** *46* (2), 169-177.

224. Colpaert, F. C.; Niemegeers, C. J. E.; Janssen, P. A. J. A Drug Discrimination Analysis of Lysergic-Acid Diethylamide (LSD) - Invivo Agonist and Antagonist Effects of Purported 5-Hydroxytryptamine Antagonists and of Pirenperone, A LSD-Antagonist. *Journal of Pharmacology and Experimental Therapeutics* **1982,** *221* (1), 206-214.

225. Glennon, R. A.; Young, R.; Hauck, A. E. Structure-Activity Studies on Methoxy-Substituted Phenylisopropylamines Using Drug Discrimination Methodology. *Pharmacology Biochemistry and Behavior* **1985,** *22* (5), 723-729.

226. Malick, J. B.; Doren, E.; Barnett, A. Quipazine-Induced Head-Twitch in Mice. *Pharmacology Biochemistry and Behavior* **1977,** *6* (3), 325-329.

227. Goodwin, G. M.; Green, A. R.; Johnson, P. 5-HT_2 Receptor Characteristics in Frontal-Cortex and 5-HT_2 Receptor-Mediated Head-Twitch Behavior Following Antidepressant Treatment to Mice. *British Journal of Pharmacology* **1984,** *83* (1), 235-242.

228. Schreiber, R.; Brocco, M.; Audinot, V.; Gobert, A.; Veiga, S.; Millan, M. J. (1-(2,5-Dimethoxy-4 Iodophenyl)-2-Aminopropane)-Induced Head-Twitches in the Rat Are Mediated by 5-Hydroxytryptamine (5-$HT)_{2A}$ Receptors - Modulation by Novel 5-$HT_{2A/2C}$ Antagonists, D_1 Antagonists and 5-HT_{1A} Agonists. *Journal of Pharmacology and Experimental Therapeutics* **1995,** *273* (1), 101-112.

229. Willins, D. L.; Meltzer, H. Y. Direct injection of 5-HT_{2A} receptor agonists into the medial prefrontal cortex produces a head-twitch response in rats. *Journal of Pharmacology and Experimental Therapeutics* **1997,** *282* (2), 699-706.

230. Porter, R. H. P.; Benwell, K. R.; Lamb, H.; Malcolm, C. S.; Allen, N. H.; Revell, D. F.; Adams, D. R.; Sheardown, M. J. Functional characterization of agonists at recombinant human 5-HT2A, 5-HT2B and 5-HT2C receptors in CHO-K1 cells. *British Journal of Pharmacology* **1999,** *128* (1), 13-20.

231. Villalobos, C. A.; Bull, P.; Saez, P.; Cassels, B. K.; Huidobro-Toro, J. P. 4-Bromo-2,5-dimethoxyphenethylamine (2C-B) and structurally related phenylethylamines are potent 5-HT_{2A} receptor antagonists in Xenopus laevis oocytes. *British Journal of Pharmacology* **2004,** *141* (7), 1167-1174.

232. Griffiths, R. R.; Richards, W. A.; McCann, U.; Jesse, R. Psilocybin can occasion mystical-type experiences having substantial and sustained personal meaning and spiritual significance. *Psychopharmacology* **2006,** *187* (3), 268-283.

233. The Heffter Institute . http://www.heffter.org/research-hucla.htm. 2010.
Ref Type: Online Source

234. Moreno, F. A.; Wiegand, C. B.; Taitano, E. K.; Delgado, P. L. Safety, tolerability, and efficacy of psilocybin in 9 patients with obsessive-compulsive disorder. *Journal of Clinical Psychiatry* **2006,** *67* (11), 1735-1740.

235. Dirac, P. A. M. The Quantum Theory of the Electron. *Proceedings of the Royal Society of London. Series A, Containing Papers of a Mathematical and Physical Character* **1928,** *117* (778), 610-624.

236. Anderson, C. D. Free positive electrons resulting from the impact upon atomic nuclei of the photons from ThC ''. *Science* **1933,** *77*, 432.

237. Anderson, C. D. The positive electron. *Phys. Rev.* **1933,** *43* (6), 491-494.

238. Brown, T. F.; Yasillo, N. J. Radiation safety considerations for PET-centers. *Journal of Nuclear Medicine Technology* **1997,** *25* (2), 98-102.

239. Berger, G.; Maziere, M.; Marazano, C.; Comar, D. C-11 Labeling of Psychoactive Drug O-Methyl-Bufotenine and Its Distribution in Animal Organism. *European Journal of Nuclear Medicine* **1978,** *3* (2), 101-104.

240. Laruelle, M. Imaging synaptic neurotransmission with in vivo binding competition techniques: A critical review. *Journal of Cerebral Blood Flow and Metabolism* **2000,** *20* (3), 423-451.

241. Egerton, A.; Mehta, M. A.; Montgomery, A. J.; Lappin, J. M.; Howes, O. D.; Reeves, S. J.; Cunningham, V. J.; Grasby, P. M. The dopaminergic basis of human behaviors: A review of molecular imaging studies. *Neuroscience and Biobehavioral Reviews* **2009,** *33* (7), 1109-1132.

242. Paterson, L. M.; Tyacke, R. J.; Nutt, D. J.; Knudsen, G. M. Measuring endogenous 5-HT release by emission tomography: promises and pitfalls. *Journal of Cerebral Blood Flow and Metabolism* **2010,** *30* (10), 1682-1706.

243. Aznavour, N.; Zimmer, L. [^{18}F]MPPF as a tool fot the in vivo imaging of 5-HT1A receptors in animal and human brain. *Neuropharmacology* **2007,** *52* (3), 695-707.

244. Narendran, R.; Hwang, D. R.; Slifstein, M.; Talbot, P. S.; Erritzoe, D.; Huang, Y. Y.; Cooper, T. B.; Martinez, D.; Kegeles, L. S.; Abi-Dargham, A.; Laruelle, M. In vivo vulnerability to competition by endogenous dopamine: Comparison of the D_2 receptor agonist radiotracer (-)-N-[^{11}C]propyl-norapomorphine ([^{11}C]NPA) with the D_2 receptor antagonist radiotracer [^{11}C]-raclopride. *Synapse* **2004,** *52* (3), 188-208.

245. Seneca, N.; Finnema, S. J.; Farde, L.; Gulyas, B.; Wikstrom, H. V.; Halldin, C.; Innis, R. B. Effect of amphetamine on dopamine D_2 receptor binding in nonhuman primate brain: A comparison of the agonist radioligand [^{11}C]MNPA and antagonist [^{11}C]raclopride. *Synapse* **2006,** *59* (5), 260-269.

246. Cornea-Hebert, V.; Watkins, K. C.; Roth, B. L.; Kroeze, W. K.; Gaudreau, P.; Leclerc, N.; Descarries, L. Similar ultrastructural distribution of the 5-HT_{2A} serotonin receptor and microtubule-associated protein MAP1A in cortical dendrites of adult rat. *Neuroscience* **2002,** *113* (1), 23-35.

247. De-Miguel, F. F.; Trueta, C. Synaptic and extrasynaptic secretion of serotonin. *Cellular and Molecular Neurobiology* **2005,** *25* (2), 297-312.

248. Milak, M. S.; Severance, A. J.; Ogden, R. T.; Prabhakaran, J.; Kumar, J. S. D.; Majo, V. J.; Mann, J. J.; Parsey, R. V. Modeling considerations for [^{11}C]CUMI-101, an agonist radiotracer for imaging serotonin 1A receptor in vivo with PET. *Journal of Nuclear Medicine* **2008,** *49* (4), 587-596.

249. Milak, M. S.; DeLorenzo, C.; Zanderigo, F.; Prabhakaran, J.; Kumar, J. S. D.; Majo, V. J.; Mann, J. J.; Parsey, R. V. In Vivo Quantification of Human Serotonin 1A Receptor Using C-11-CUMI-101, an Agonist PET Radiotracer. *Journal of Nuclear Medicine* **2010,** *51* (12), 1892-1900.

250. Lemoine, L.; Verdurand, M.; Vacher, B.; Blanc, E.; Le Bars, D.; Newman-Tancredi, A.; Zimmer, L. [^{18}F]F15599, a novel 5-HT$_{1A}$ receptor agonist, as a radioligand for PET neuroimaging. *European Journal of Nuclear Medicine and Molecular Imaging* **2010,** *37* (3), 594-605.

251. Berridge, M.; Comar, D.; Crouzel, C.; Baron, J. C. ^{11}C-Labeled Ketanserin - A Selective Serotonin S$_2$ Antagonist. *Journal of Labelled Compounds & Radiopharmaceuticals* **1983,** *20* (1), 73-78.

252. Baron, J. C.; Samson, Y.; Comar, D.; Crouzel, C.; Deniker, P.; Agid, Y. An Invivo Study of Central Serotonin Receptors in Humans Using ^{11}C-Labeled Ketanserin and Positron Tomography. *Revue Neurologique* **1985,** *141* (8-9), 537-545.

253. Lemaire, C.; Cantineau, R.; Guillaume, M.; Plenevaux, A.; Christiaens, L. Fluorine-18-Altanserin: A Radioligand for the Study of Serotonin Receptors with PET: Radiolabeling and In Vivo Biologic Behavior in Rats. *The Journal of Nuclear Medicine* **1991,** *32* (12), 2266-2272.

254. Sadzot, B.; Lemaire, C.; Maquet, P.; Salmon, E.; Plenevaux, A.; Degueldre, C.; Hermanne, J. P.; Guillaume, M.; Cantineau, R.; Comar, D.; Franck, G. Serotonin 5HT$_2$ Receptor Imaging in the Human Brain Using Positron Emission Tomography and A New Radioligand, [^{18}F] Altanserin - Results in Young Normal Controls. *Journal of Cerebral Blood Flow and Metabolism* **1995,** *15* (5), 787-797.

255. Ito, H.; Nyberg, S.; Halldin, C.; Lundkvist, C.; Farde, L. PET imaging of central 5-HT2A receptors with carbon-11-MDL 100,907. *Journal of Nuclear Medicine* **1998,** *39* (1), 208-214.

256. Kristiansen, H.; Elfving, B.; Plenge, P.; Pinborg, L. H.; Gillings, N.; Knudsen, G. M. Binding characteristics of the 5-HT$_{2A}$ receptor antagonists altanserin and MDL 100,907. *Synapse* **2005,** *58* (4), 249-257.

257. Debus, F.; Herth, M. M.; Piel, M.; Buchholz, H. G.; Bausbacher, N.; Kramer, V.; Luddens, H.; Rosch, F. ^{18}F-Labeling and evaluation of novel MDL 100907 derivatives as potential 5-HT$_{2A}$ antagonists for molecular imaging. *Nuclear Medicine and Biology* **2010,** *37* (4), 487-495.

258. Guo, Q.; Brady, M.; Gunn, R. N. A Biomathematical Modeling Approach to Central Nervous System Radioligand Discovery and Development. *Journal of Nuclear Medicine* **2009,** *50* (10), 1715-1723.

259. Pike, V. W. PET radiotracers: crossing the blood-brain barrier and surviving metabolism. *Trends in Pharmacological Sciences* **2009,** *30* (8), 431-440.

260. Nelson, D. L.; Lucaites, V. L.; Wainscott, D. B.; Glennon, R. A. Comparisons of hallucinogenic phenylisopropylamine binding affinities at cloned human 5-HT_{2A}, 5-HT_{2B} and 5-HT_{2C} receptors. *Naunyn-Schmiedebergs Archives of Pharmacology* **1999,** *359* (1), 1-6.

261. Diana, G. D.; Rudewicz, P.; Pevear, D. C.; Nitz, T. J.; Aldous, S. C.; Aldous, D. J.; Robinson, D. T.; Draper, T.; Dutko, F. J.; Aldi, C.; Gendron, G.; Oglesby, R. C.; Volkots, D. L.; Reuman, M.; Bailey, T. R.; Czerniak, R.; Block, T.; Roland, R.; Oppermann, J. Picornavirus Inhibitors - Trifluoromethyl Substitution Provides A Global Protective Effect Against Hepatic-Metabolism. *Journal of Medicinal Chemistry* **1995,** *38* (8), 1355-1371.

262. Henry, L. Formation synthétique d'alcools nitrés. *Comptes Rendus Hebdomadaires des Seances de l'Academie des Sciences* **1895,** *120*, 1265.

263. Skita, A.; Keil, F. Über die Reduktion von Nitro-styrolen zu β-Phenyl-äthylaminen. *Berichte der deutschen chemischen Gesellschaft* **1932,** *65* (3), 424-431.

264. Ramirez, F. A.; Burger, A. The Reduction of Phenolic β-Nitrostyrenes by Lithium Aluminum Hydride. *Journal of the American Chemical Society* **1950,** *72* (6), 2781-2782.

265. Vinogradova, V. I.; Yunusov, M. S.; Kuchin, A. V.; Tolstikov, G. A.; Sagandykov, R. T.; Khalmuratov, K.; Alimov, A. Syntheses based on β-phenylethylamines. I. Preparation of substituted β-phenylethylamines. *Chemistry of Natural Compounds* **1990,** *26* (1), 54-59.

266. Ankner, T.; Hilmersson, G. Instantaneous SmI_2/H2O/amine mediated reduction of nitroalkanes and α,β-unsaturated nitroalkenes. *Tetrahedron Letters* **2007,** *48* (32), 5707-5710.

267. Schiff, H. Mittheilungen aus dem Universitätslaboratorium in Pisa: Eine neue Reihe organischer Basen. *Justus Liebigs Annalen der Chemie* **1864,** *131* (1), 118-119.

268. AbdelMagid, A. F.; Carson, K. G.; Harris, B. D.; Maryanoff, C. A.; Shah, R. D. Reductive amination of aldehydes and ketones with sodium triacetoxyborohydride. Studies on direct and indirect reductive amination procedures. *Journal of Organic Chemistry* **1996,** *61* (11), 3849-3862.

269. Rupe, H.; Hodel, E. Die katalytische Reduktion einiger Nitrile. *Helvetica Chimica Acta* **1923,** *6* (1), 865-880.

270. Leuckart, R. Über die neue Bildungsweise von Tribenzylamin. *Berichte der deutschen chemischen Gesellschaft* **1885,** *18*, 2341-2344.

271. Wallach, O.; Kuthe, M. Über Menthylamin. *Berichte der deutschen chemischen Gesellschaft* **1892,** *25* (2), 3313-3316.

272. Eschweiler, W. Ersatz von an Stickstoff gebundenen Wasserstoffatomen durch die Methylgruppe mit Hülfe von Formaldehyd. *Berichte der deutschen chemischen Gesellschaft* **1905,** *38* (1), 880-882.

273. Clarke, H. T.; Gillespie, H. B.; Weisshaus, S. Z. The Action of Formaldehyde on Amines and Amino Acids. *Journal of the American Chemical Society* **1933,** *55* (11), 4571-4587.

274. Sheehan, J. C.; Hess, G. P. A New Method of Forming Peptide Bonds. *Journal of the American Chemical Society* **1955,** *77* (4), 1067-1068.

275. Joullie, M. M.; Lassen, K. M. Evolution of amide bond formation. *Arkivoc* **2010,** 189-250.

276. Schotten, C. Über die Oxydation des Piperidins. *Berichte der deutschen chemischen Gesellschaft* **1884,** *17* (2), 2544-2547.

277. Anderson, G. W.; Zimmerma, J. E.; Callahan, F. M. A Reinvestigation of Mixed Carbonic Anhydride Method of Peptide Synthesis. *Journal of the American Chemical Society* **1967,** *89* (19), 5012-&.

278. Basha, A.; Lipton, M.; Weinreb, S. M. Mild, General Method for Conversion of Esters to Amides. *Tetrahedron Letters* **1977,** (48), 4171-4174.

279. Nystrom, R. F.; Brown, W. G. Reduction of Organic Compounds by Lithium Aluminum Hydride .3. Halides, Quinones, Miscellaneous Nitrogen Compounds. *Journal of the American Chemical Society* **1948,** *70* (11), 3738-3740.

280. Glennon, R. A.; Dukat, M.; Elbermawy, M.; Law, H.; Delosangeles, J.; Teitler, M.; King, A.; Herrickdavis, K. Influence of Amine Substituents on 5-HT_{2A} Versus 5-HT_{2C} Binding of Phenylalkylamines and Indolylalkylamines. *Journal of Medicinal Chemistry* **1994,** *37* (13), 1929-1935.

281. Walker, E. R. H. The functional group selectivity of complex hydride reducing agents. *Chem. Soc. Rev.* **1976,** *5*, 23-50.

282. Clausen, K.; Thorsen, M.; Lawesson, S.-O. Studies on amino acids and peptides--I : Synthesis of N-benzyloxycarbonylendo-thiodipeptide esters. *Tetrahedron* **1981,** *37* (21), 3635-3639.

283. Kornfeld, E. C. Raney Nickel Hydrogenolysis of Thioamides: A New Amine Synthesis. *The Journal of Organic Chemistry* **1951,** *16* (1), 131-138.

284. Fukuyama, T.; Jow, C. K.; Cheung, M. 2- and 4-Nitrobenzenesulfonamides: Exceptionally versatile means for preparation of secondary amines and protection of amines. *Tetrahedron Letters* **1995,** *36* (36), 6373-6374.

285. Kan, T.; Fukuyama, T. Ns strategies: a highly versatile synthetic method for amines. *Chemical Communications* **2004,** (4), 353-359.

286. Nichols, D. E.; Frescas, S.; Marona-Lewicka, D.; Huang, X. M.; Roth, B. L.; Gudelsky, G. A.; Nash, J. F. 1-(2,5-Dimethoxy-4-(Trifluoromethyl)Phenyl)-2-Aminopropane - A Potent Serotonin 5-$HT_{2A/2C}$ Agonist. *Journal of Medicinal Chemistry* **1994,** *37* (25), 4346-4351.

287. Su, D. B.; Duan, J. X.; Chen, Q. Y. Methyl Chlorodifluoroacetate A Convenient Trifluoromethylating Agent. *Tetrahedron Letters* **1991,** *32* (52), 7689-7690.

288. Langlois, B. R.; Roques, N. Nucleophilic trifluoromethylation of aryl halides with methyl trifluoroacetate. *Journal of Fluorine Chemistry* **2007,** *128*, 1318-1325.

289. Matsui, K.; Tobita, E.; Ando, M.; Kondo, K. A Convenient Trifluoromethylation of Aromatic Halides with Sodium Trifluoroacetate. *Chemistry Letters* **1981,** (12), 1719-1720.

290. Carr, G. E.; Chambers, R. D.; Holmes, T. F.; Parker, D. G. Sodium Perfluoroalkane Carboxylates As Sources of Perfluoroalkyl Groups. *Journal of the Chemical Society, Perkin Transactions 1* **1988,** (4), 921-926.

291. Rodriguez, J. R.; Agejas, J.; Bueno, A. B. Practical synthesis of aromatic ethers by SNAr of fluorobenzenes with alkoxides. *Tetrahedron Letters* **2006,** *47* (32), 5661-5663.

292. Rieche, A.; Gross, H.; Hoft, E. Über Alpha-Halogenäther .4. Synthesen Aromatischer Aldehyde Mit Dichlormethyl-Alkyläthern. *Chemische Berichte-Recueil* **1960,** *93* (1), 88-94.

293. Slocum, D. W.; Book, G.; Jennings, C. A. Rate and Orientation Effect of Tmeda on Directed Lithiation Reactions. *Tetrahedron Letters* **1970,** (39), 3443-&.

294. Slocum, D. W.; Moon, R.; Thompson, J.; Coffey, D. S.; Li, J. D.; Slocum, M. G.; Siegel, A.; Gaytongarcia, R. A Predicative Model for Certain Directed Metalations .1. Applications to the Behavior of Anisole. *Tetrahedron Letters* **1994,** *35* (3), 385-388.

295. Philippo, C. 2-aminoethyl-benzofuran derivatives, preparation thereof and therapeutical use thereof. US 6063810, May 16, 2000.

296. Hertel, L. W.; Xu, Y. Pyrrolidine and pyrroline derivatives having effects on serotonin related systems. US 6353008, May 3, 2002.

297. Bouveault, L. Nouvelle méthode des générale synthétique de préparation des aldéhydes. *Bulletin de Société Chimique de France* **1904,** *31*, 1322-1327.

298. White, A. W.; Almassy, R.; Calvert, A. H.; Curtin, N. J.; Griffin, R. J.; Hostomsky, Z.; Maegley, K.; Newell, D. R.; Srinivasan, S.; Golding, B. T. Resistance-modifying agents. 9. Synthesis and biological properties of benzimidazole inhibitors of the DNA repair enzyme poly(ADP-ribose) polymerase. *Journal of Medicinal Chemistry* **2000,** *43* (22), 4084-4097.

299. Howell, J. R.; Rasmussen, M. Heterocyclic Ambident Nucleophiles .5. Alkylation of Benzimidazoles. *Australian Journal of Chemistry* **1993,** *46* (8), 1177-1191.

300. Hofmann, A. W. Über die Einwirkung des Broms in alkalischer Lösung auf Amide. *Berichte der deutschen chemischen Gesellschaft* **1881,** *14* (2), 2725-2736.

301. Phillips, M. A. CLXXXIII.-The hydrolysis of diacetyl-o-diamines. *Journal of the Chemical Society (Resumed)* **1930,** 1409-1419.

302. Ley, S. V.; Norman, J.; Griffith, W. P.; Marsden, S. P. Tetrapropylammonium Perruthenate, $Pr_4N^+RuO_4^-$, TPAP: A Catalytic Oxidant for Organic Synthesis. *Synthesis* **1994,** *1994* (07), 639,666.

303. Corey, E. J.; Schmidt, G. Useful Procedures for the Oxidation of Alcohols Involving Pyridinium Dichromate in Aprotic Media. *Tetrahedron Letters* **1979,** (5), 399-402.

304. Fatiadi, A. J. Active Manganese-Dioxide Oxidation in Organic-Chemistry .1. *Synthesis* **1976,** (2), 65-104.

305. Sandmeyer, T. Über Isonitrosoacetanilide und deren Kondensation zu Isatinen. *Helvetica Chimica Acta* **1919,** *2* (1), 234-242.

306. Marvel, C. S.; Hiers, G. S. Isatin. *Organic Synthesis* **1925,** *5*, 71.

307. Lamara, K.; Redhouse, A. D.; Smalley, R. K.; Thompson, J. 3*H*-Azepines and Related Systems. Part 5. Photo-induced Ring Expansions of *o*-Azidobenzonitriles to 3-Cyano- and 7-Cyano-3*H*-azepin-2(1*H*)-ones. *Tetrahedron* **1994,** *50* (18), 5515-5526.

308. Reissenweber, G.; Mangold, D. Oxidation of Isatins to Anthranilic Acid-Esters. *Angewandte Chemie-International Edition in English* **1981,** *20* (10), 882-883.

309. Bartsch, R. A.; Yang, I. W. Phase-Transfer Catalyzed Synthesis of Indazoles from Ortho-Alkylbenzenediazonium Tetrafluoroborates. *Journal of Heterocyclic Chemistry* **1984,** *21* (4), 1063-1064.

310. DeHaven-Hudkins, D. L.; Earley, W. G.; Dority Jr, J. A.; Kumar, V.; Subramanyam, C.; Miller, M. S.; Mallamo, J. P. Substituted 6,11-ethano-6,11-dihydrobenzo[*b*]quinolizinium salts and compositions and methods of use thereof. US 5,554,620 A1, Oct 9, 1996.

311. Wang, L. M.; Sheng, J.; Tian, H.; Qian, C. T. An efficient procedure for the synthesis of benzimidazole derivatives using $Yb(OTf)_3$ as catalyst under solvent-free conditions. *Synthetic Communications* **2004,** *34* (23), 4265-4272.

312. Yadagiri, B.; Lown, J. W. Selective Cleavage of Benzoxazoles to Ortho-Hydroxy-N-Substituted Anilines with Sodium Borohydride-Acetic Acid. *Synthetic Communications* **1990,** *20* (2), 175-181.

313. Vit, J. *Eastman Organic Bulletin* **1970,** *42* (3), 1.

314. Malek, J.; Cerny, M. Reduction of Organic Compounds by Alkoxyaluminohydrides. *Synthesis* **1972,** (5), 217-&.

315. Kim, M. S.; Choi, Y. M.; An, D. K. Lithium diisobutyl-t-butoxyaluminum hydride, a new and efficient reducing agent for the conversion of esters to aldehydes. *Tetrahedron Letters* **2007,** *48* (29), 5061-5064.

316. Zondervan, C.; vandenBeuken, E. K.; Kooijman, H.; Spek, A. L.; Feringa, B. L. Efficient synthesis and molecular structure of 2-hydroxyisophthaldehyde. *Tetrahedron Letters* **1997,** *38* (17), 3111-3114.

317. Casey, M. L.; Kemp, D. S.; Paul, K. G.; Cox, D. D. Physical Organic-Chemistry of Benzisoxazoles .1. Mechanism of Base-Catalyzed Decomposition of Benzisoxazoles. *Journal of Organic Chemistry* **1973,** *38* (13), 2294-2301.

318. Li, W.; Li, H. C.; DeVincentis, D.; Mansour, T. S. Oxygen transfer from sulfoxide: formation of aromatic aldehydes from dihalomethylarenes. *Tetrahedron Letters* **2004,** *45* (5), 1071-1074.

319. Augustine, J. K.; Naik, Y. A.; Mandal, A. B.; Chowdappa, N.; Praveen, V. B. A versatile method for the hydrolysis of gem-dibromomethylarenes bearing carboxylate or boronate group into aldehydes. *Tetrahedron* **2008,** *64* (4), 688-695.

320. Gauuan, P. J.; Trova, M. P.; Gregor-Boros, L.; Bocckino, S. B.; Crapo, J. D.; Day, B. J. Superoxide dismutase mimetics: synthesis and structure-activity relationship study of MnTBAP analogues. *Bioorganic & Medicinal Chemistry* **2002,** *10* (9), 3013-3021.

321. Shamblee, D. A.; Gillespie, J. S. Anti-Malarials .4. Trichloronaphthalene Amino-Alcohols. *Journal of Medicinal Chemistry* **1979,** *22* (1), 86-89.

322. Angelini, G.; Giancaspro, C.; Illuminati, G.; Sleiter, G. Electrophilic Heteroaromatic Reactions .3. the α-Side-Chain Bromination of Some Polysubstituted Alpha-Methylpyrroles in the Dark - Evidence for the Formation of Intermediate σ-Adducts. *Journal of Organic Chemistry* **1980,** *45* (10), 1786-1790.

323. Coleman, G. H.; Honeywell, G. E. *p*-Bromobenzaldehyde. *Organic Synthesis* **1937,** *17*, 20.

324. Caijo, F.; Mosset, P.; Gree, R.; Audinot-Bouchez, V.; Boutin, J.; Renard, P.; Caignard, D. H.; Dacquet, C. Synthesis of aromatic analogs of 8(S)-HETE and their biological evaluation as activators of the PPAR nuclear receptors. *European Journal of Organic Chemistry* **2006,** (9), 2181-2196.

325. Trecourt, F.; Marsais, F.; Gungor, T.; Queguiner, G. Improved Synthesis of 2,3-Disubstituted Pyridines by Metalation of 2-Chloropyridine - A Convenient Route to Fused Polyheterocycles. *Journal of the Chemical Society-Perkin Transactions 1* **1990,** (9), 2409-2415.

326. Pictet, A.; Spengler, T. Über die Bildung von Isochinolin-derivaten durch Einwirkung von Methylal auf Phenyl-äthylamin, Phenyl-alanin und Tyrosin. *Berichte der deutschen chemischen Gesellschaft* **1911,** *44* (3), 2030-2036.

327. Bischler, A.; Napieralski, B. Zur Kenntniss einer neuen Isochinolinsynthese. *Berichte der deutschen chemischen Gesellschaft* **1893,** *26* (2), 1903-1908.

328. Clark, R. D.; JAHANGIR; Langston, J. A. Heteroatom-Directed Lateral Lithiation - Synthesis of Isoquinoline Derivatives from N-(Tert-Butoxycarbonyl)-2-Methylbenzylamines. *Canadian Journal of Chemistry-Revue Canadienne de Chimie* **1994,** *72* (1), 23-30.

329. Nahm, S.; Weinreb, S. M. N-Methoxy-N-Methylamides As Effective Acylating Agents. *Tetrahedron Letters* **1981,** *22* (39), 3815-3818.

330. Simonsen, K. B.; Svenstrup, N.; Roberson, M.; Jorgensen, K. A. Development of an unusually highly enantioselective hetero-Diels-Alder reaction of benzaldehyde with activated dienes catalyzed by hypercoordinating chiral aluminum complexes. *Chemistry-A European Journal* **2000,** *6* (1), 123-128.

331. Miyaura, N.; Yanagi, T.; Suzuki, A. The Palladium-Catalyzed Cross-Coupling Reaction of Phenylboronic Acid with Haloarenes in the Presence of Bases. *Synthetic Communications* **1981,** *11* (7), 513-519.

332. Macchia, B.; Macchia, M.; Manera, C.; Martinotti, E.; Nencetti, S.; Orlandini, E.; Rosello, A.; Scatizzi, R. Role of the benzylic hydroxyl group of adrenergic catecholamines in eliciting alpha-adrenergic activity. Synthesis and alpha1- and alpha2-adrenergic activity of 3-phenyl-3-piperidinols and their desoxy analogs. *European Journal of Medicinal Chemistry* **1995,** *30* (11), 869-880.

333. Tamao, K.; Sumitani, K.; Kumada, M. Selective Carbon-Carbon Bond Formation by Cross-Coupling of Grignard-Reagents with Organic Halides - Catalysis by Nickel-Phosphine Complexes. *Journal of the American Chemical Society* **1972,** *94* (12), 4374-&.

334. Sakagami, H.; Kamikubo, T.; Ogasawara, K. Novel reduction of 3-hydroxypyridine and its use in the enantioselective synthesis of (+)-pseudoconhydrine and (+)-N-methylpseudoconhydrine. *Chemical Communications* **1996,** (12), 1433-1434.

335. Palczewski, K.; Kumasaka, T.; Hori, T.; Behnke, C. A.; Motoshima, H.; Fox, B. A.; Le Trong, I.; Teller, D. C.; Okada, T.; Stenkamp, R. E.; Yamamoto, M.; Miyano, M. Crystal structure of rhodopsin: A G protein-coupled receptor. *Science* **2000,** *289* (5480), 739-745.

336. Chambers, J. J.; Nichols, D. E. A homology-based model of the human 5-HT_{2A} receptor derived from an in silico activated G-protein coupled receptor. *Journal of Computer-Aided Molecular Design* **2002,** *16* (7), 511-520.

337. Mclean, T. H.; Chambers, J. J.; Parrish, J. C.; Braden, M. R.; Marona-Lewicka, D.; Kurrasch-Orbaugh, D.; Nichols, D. E. C-(4,5,6-trimethoxyindan-1-yl)methanamine: A mescaline analogue designed using a homology model of the 5-HT2A receptor. *Journal of Medicinal Chemistry* **2006,** *49* (14), 4269-4274.

338. Mclean, T. H.; Parrish, J. C.; Braden, M. R.; Marona-Lewicka, D.; Gallardo-Godoy, A.; Nichols, D. E. 1-aminomethylbenzocycloalkanes: Conformationally restricted hallucinogenic phenethylamine analogues as functionally selective 5-HT2A receptor agonists. *Journal of Medicinal Chemistry* **2006,** *49* (19), 5794-5803.

339. Rasmussen, S. G. F.; Choi, H. J.; Rosenbaum, D. M.; Kobilka, T. S.; Thian, F. S.; Edwards, P. C.; Burghammer, M.; Ratnala, V. R. P.; Sanishvili, R.; Fischetti, R. F.; Schertler, G. F. X.; Weis, W. I.; Kobilka, B. K. Crystal structure of the human β_2 adrenergic G-protein-coupled receptor. *Nature* **2007,** *450*, 383-3U4.

340. Cherezov, V.; Rosenbaum, D. M.; Hanson, M. A.; Rasmussen, S. G. F.; Thian, F. S.; Kobilka, T. S.; Choi, H. J.; Kuhn, P.; Weis, W. I.; Kobilka, B. K.; Stevens, R. C. High-resolution crystal structure of an engineered human β_2-adrenergic G protein-coupled receptor. *Science* **2007,** *318*, 1258-1265.

341. Rosenbaum, D. M.; Cherezov, V.; Hanson, M. A.; Rasmussen, S. G. F.; Thian, F. S.; Kobilka, T. S.; Choi, H. J.; Yao, X. J.; Weis, W. I.; Stevens, R. C.; Kobilka, B. K. GPCR engineering yields high-resolution structural insights into β_2-adrenergic receptor function. *Science* **2007,** *318*, 1266-1273.

342. Murakami, M.; Kouyama, T. Crystal structure of squid rhodopsin. *Nature* **2008,** *453* (7193), 363-U33.

343. Shimamura, T.; Hiraki, K.; Takahashi, N.; Hori, T.; Ago, H.; Masuda, K.; Takio, K.; Ishiguro, M.; Miyano, M. Crystal structure of squid rhodopsin with intracellularly extended cytoplasmic region. *Journal of Biological Chemistry* **2008,** *283* (26), 17753-17756.

344. Warne, T.; Serrano-Vega, M. J.; Baker, J. G.; Moukhametzianov, R.; Edwards, P. C.; Henderson, R.; Leslie, A. G. W.; Tate, C. G.; Schertler, G. F. X. Structure of a β_1-adrenergic G-protein-coupled receptor. *Nature* **2008,** *454* (7203), 486-4U2.

345. Park, J. H.; Scheerer, P.; Hofmann, K. P.; Choe, H. W.; Ernst, O. P. Crystal structure of the ligand-free G-protein-coupled receptor opsin. *Nature* **2008,** *454* (7201), 183-U33.

346. Scheerer, P.; Park, J. H.; Hildebrand, P. W.; Kim, Y. J.; Krauss, N.; Choe, H. W.; Hofmann, K. P.; Ernst, O. P. Crystal structure of opsin in its G-protein-interacting conformation. *Nature* **2008,** *455* (7212), 497-U30.

347. Jaakola, V. P.; Griffith, M. T.; Hanson, M. A.; Cherezov, V.; Chien, E. Y. T.; Lane, J. R.; IJzerman, A. P.; Stevens, R. C. The 2.6 Ångström Crystal Structure of a Human A_{2A} Adenosine Receptor Bound to an Antagonist. *Science* **2008,** *322* (5905), 1211-1217.

348. Ísberg, V.; Balle, T.; Sander, T.; Jørgensen, F. S.; Gloriam, D. A G Protein- and Agonist-bound Serotonin 5-HT2A Receptor Model Activated by Steered Molecular Dynamics Simulations. *Journal of Chemical Information and Modeling* **2010**.

349. Wang, C. D.; Gallaher, T. K.; Shih, J. C. Site-Directed Mutagenesis of the Serotonin 5-Hydroxytrypamine(2) Receptor - Identification of Amino-Acids Necessary for Ligand-Binding and Receptor Activation. *Molecular Pharmacology* **1993,** *43* (6), 931-940.

350. Choudhary, M. S.; Craigo, S.; Roth, B. L. A Single Point Mutation (Phe-340-]Leu-340) of A Conserved Phenylalanine Abolishes 4-[^{125}I]Iodo-(2,5-Dimethoxy)Phenylisopropylamine and [^{3}H] Mesulergine But Not [^{3}H] Ketanserin Binding to 5-Hydroxytryptamine(2) Receptors. *Molecular Pharmacology* **1993,** *43* (5), 755-761.

351. Choudhary, M. S.; Sachs, N.; Uluer, A.; Glennon, R. A.; Westkaemper, R. B.; Roth, B. L. Differential Ergoline and Ergopeptine Binding to 5-Hydroxytryptamine(2A) Receptors - Ergolines Require An Aromatic Residue at Position-340 for High-Affinity Binding. *Molecular Pharmacology* **1995,** *47* (3), 450-457.

352. Johnson, M. P.; Loncharich, R. J.; Baez, M.; Nelson, D. L. Species Variations in Transmembrane Region-V of the 5-Hydroxytryptamine Type 2A Receptor Alter the Structure-Activity Relationship of Certain Ergolines and Tryptamines. *Molecular Pharmacology* **1994,** *45* (2), 277-286.

353. Sealfon, S. C.; Chi, L.; Ebersole, B. J.; Rodic, V.; Zhang, D.; Ballesteros, J. A.; Weinstein, H. Related Contribution of Specific Helix-2 and Helix-7 Residues to Conformational

Activation of the Serotonin 5-HT_{2A} Receptor. *Journal of Biological Chemistry* **1995,** *270* (28), 16683-16688.

354. Braden, M. R.; Nichols, D. E. Assessment of the roles of serines 5.43(239) and 5.46(242) for binding and potency of agonist ligands at the human serotonin 5-HT_{2A} receptor. *Molecular Pharmacology* **2007,** *72* (5), 1200-1209.

355. Kristiansen, K.; Kroeze, W. K.; Willins, D. L.; Gelber, E. I.; Savage, J. E.; Glennon, R. A.; Roth, B. L. A highly conserved aspartic acid (Asp-155) anchors the terminal amine moiety of tryptamines and is involved in membrane targeting of the 5-HT_{2A} serotonin receptor but does not participate in activation via a "salt-bridge disruption" mechanism. *Journal of Pharmacology and Experimental Therapeutics* **2000,** *293* (3), 735-746.

356. Roth, B. L.; Shoham, M.; Choudhary, M. S.; Khan, N. Identification of conserved aromatic residues essential for agonist binding and second messenger production at 5-hydroxytryptamine(2A) receptors. *Molecular Pharmacology* **1997,** *52* (2), 259-266.

357. Murugesan, N.; Gu, Z.; Stein, P. D.; Bisaha, S.; Spergel, S.; Girotra, R.; Lee, V. G.; Lloyd, J.; Misra, R. N.; Schmidt, J.; Mathur, A.; Stratton, L.; Kelly, Y. F.; Bird, E.; Waldron, T.; Liu, E. C. K.; Zhang, R.; Lee, H.; Serafino, R.; Abboa-Offei, B.; Mathers, P.; Giancarli, M.; Seymour, A. A.; Webb, M. L.; Moreland, S.; Barrish, J. C.; Hunt, J. T. Biphenylsulfonamide Endothelin Antagonists: Structure–Activity Relationships of a Series of Mono- and Disubstituted Analogues and Pharmacology of the Orally Active Endothelin Antagonist 2'-Amino-N-(3,4-dimethyl-5-isoxazolyl)-4'-(2-methylpropyl)[1,1'-biphenyl]-2-sulfonamide (BMS-187308). *Journal of Medicinal Chemistry* **1998,** *41* (26), 5198-5218.

358. Li, Z.; Ding, X.; He, C. Nitrene Transfer Reactions Catalyzed by Gold Complexes. *The Journal of Organic Chemistry* **2006,** *71* (16), 5876-5880.

359. Osborn, J. A.; Jardine, F. H.; Young, J. F.; Wilkinson, G. The preparation and properties of tris(triphenylphosphine)halogenorhodium(I) and some reactions thereof including catalytic homogeneous hydrogenation of olefins and acetylenes and their derivatives. *J. Chem. Soc. A* **1966,** 1711-1732.

360. Vilsmeier, A.; Haack, A. The effect of halogen phosphor on alkyl formanilide - A new method for the characterisation of secondary and tertiary p-alkylamino-benzaldehyde. *Berichte der deutschen chemischen Gesellschaft* **1927,** *60*, 119-122.

361. Nicolaou, K. C.; Baran, P. S.; Zhong, Y. L. Selective oxidation at carbon adjacent to aromatic systems with IBX. *Journal of the American Chemical Society* **2001,** *123* (13), 3183-3185.

362. Thiele, J. Über die Einwirkung von Essigsäureanhydrid auf Chinon un auf Dibenzoylstryl. *Berichte der deutschen chemischen Gesellschaft* **1898,** *31* (311), 1247-1251.

363. Etard, M. A. Sur la synthèse des aldéhydes aromatiques; essence de cumin. *Comptes Rendus Hebdomadaires des Seances de l'Academie des Sciences* **1880,** *90*, 534-536.

364. Lin, C. F.; Lu, W. D.; Wang, I. W.; Wu, M. J. Synthesis of 2-(Diarylmethylene)-3-benzofuranones Promoted via Palladium-Catalyzed Reactions of Aryl iodides with 3-Aryl-1-(2- tert-butyldimethylsilyloxy)phenyl-2-propyn-1-ones. *Synlett* **2003,** *2003* (13), 2057,2061.

365. Nichols, D. E.; Frescas, S. P.; Chemel, B. R.; Rehder, K. S.; Zhong, D. S.; Lewin, A. H. High specific activity tritium-labeled *N*-(2-methoxybenzyl)-2,5-dimethoxy-4-iodophenethylamine (INBMeO): A high-affinity 5-HT_{2A} receptor-selective agonist radioligand. *Bioorganic & Medicinal Chemistry* **2008,** *16* (11), 6116-6123.

366. Ettrup, A. Serotonin receptor studies in the pig brain: Pharmacological intervention and positron emission tomography tracer development. PhD University of Copenhagen, Oct 2010.

367. Still, W. C.; Kahn, M.; Mitra, A. Rapid Chromatographic Technique for Preparative Separations with Moderate Resolution. *Journal of Organic Chemistry* **1978,** *43* (14), 2923-2925.

368. Gottlieb, H. E.; Kotlyar, V.; Nudelman, A. NMR chemical shifts of common laboratory solvents as trace impurities. *Journal of Organic Chemistry* **1997,** *62* (21), 7512-7515.

369. Barbasiewicz, M.; Bieniek, M.; Michrowska, A.; Szadkowska, A.; Makal, A.; Wozniak, K.; Grela, K. Probing of the Ligand Anatomy: Effects of the Chelating Alkoxy Ligand Modifications on the Structure and Catalytic Activity of Ruthenium Carbene Complexes. *Adv. Synth. Catal.* **2007,** *349* (1-2), 193-203.

370. Muller, G. W.; Man, H.-W. 5-Substituted Quinazolinone Derivatives and Compositions Comprising and Methods Using the Same. WO2008/39489 A2, 2008.

371. Zhao, H.; Fu, H.; Qiao, R. Copper-Catalyzed Direct Amination of Ortho-Functionalized Haloarenes with Sodium Azide as the Amino Source. *Journal of Organic Chemistry* **2010,** *75* (10), 3311-3316.

372. English, J. P.; Clapp, R. C.; Cole, Q. P.; Halverstadt, I. F.; Lampen, J. O.; Roblin, R. O. Studies in Chemotherapy. IX. Ureylenebenzene and Cyclohexane Derivatives as Biotin Antagonists1. *Journal of the American Chemical Society* **1945,** *67* (2), 295-302.

373. Pavia, M. R.; Moos, W. H.; Hershenson, F. M. Benzo-Fused Bicyclic Imides. *Journal of Organic Chemistry* **1990,** *55* (2), 560-564.

374. Newman, M. S.; Kannan, R. Reactions of 3-methylbenzyne with 2-substituted furans. Steric effects. *Journal of Organic Chemistry* **1976,** *41* (21), 3356-3359.

375. Gripenberg, J. Fungus Pigments XI: 2-Amino-3-Hydroxymethylphenol from Cinnabarin. *Acta Chemica Scandinavica* **2010,** *13*, 1305-1308.

376. Goldstein, S. W.; Dambek, P. J. A facile synthesis of methyl 2-substituted-4-benzoxazolecarboxylates. *Journal of Heterocyclic Chemistry* **1990,** *27* (2), 335-336.

377. Wu, M. T.; Lyle, R. E. Synthesis of some simple actinomycin analogs. *Journal of Heterocyclic Chemistry* **1971,** *8* (6), 989-991.

378. Goldmann, S.; Boshagen, H.; Stoltefuss, J.; Straub, A.; Gross, R.; Hutter, J.; Hebisch, S.; Bechem, M. 2,6-dialkyl-4-(benzothiazol- or benzoxazol-4-yl-1,4-dihydropyridines. US 5200420 A1, Jun 4, 1993.

379. Wayne, E. J.; Cohen, J. B. The aldehydosalicylic acids and their derivatives. *Journal of the Chemical Society, Transactions* **1922,** *121*, 1022-1029.

380. Mallet, M.; Branger, G.; Marsais, F.; Queguiner, G. Migration du lithium en série pyridinique: double catalyse et reformage. Accés aux dérivés de la bromo-2 lithio-3 pyridine et des bromo-4 halogéno-2 lithio-3 pyridines. *Journal of Organometallic Chemistry* **1990,** *382* (3), 319-332.

381. Trecourt, F.; Marsais, F.; Gungor, T.; Queguiner, G. Improved synthesis of 2,3-disubstituted pyridines by metallation of 2-chloropyridine: a convenient route to fused polyheterocycles. *Journal of the Chemical Society, Perkin Transactions 1* **1990,** (9), 2409-2415.

382. Hunsberger, I. M.; Lednicer, D.; Gutowsky, H. S.; Bunker, D. L.; Taussig, P. The Determination of Double-bond Character in Cyclic Systems. III. Indan and o-Xylene. *Journal of the American Chemical Society* **1955,** *77* (9), 2466-2475.

383. Ali Shaikh, T. M.; Emmanuvel, L.; Sudalai, A. NaIO4-Mediated Selective Oxidation of Alkylarenes and Benzylic Bromides/Alcohols to Carbonyl Derivatives Using Water as Solvent. *Journal of Organic Chemistry* **2006,** *71* (13), 5043-5046.

384. Glennon, R. A.; Raghupathi, R.; Bartyzel, P.; Teitler, M.; Leonhardt, S. Binding of Phenylalkylamine Derivatives at 5-HT_{1C} and 5-HT_2 Serotonin Receptors - Evidence for A Lack of Selectivity. *Journal of Medicinal Chemistry* **1992,** *35* (4), 734-740.

385. Jyothi, Y.; Mahalingam, A. K.; Ilangovan, A.; Sharma, G. V. M. Alternative Reagents for the Tritylation of Alcohols. *Synthetic Communications* **2007,** *37* (12), 2091-2101.

386. Kim, I. B.; Erdogan, B.; Wilson, J. N.; Bunz, U. H. F. Sugar–Poly(para-phenylene ethynylene) Conjugates as Sensory Materials: Efficient Quenching by Hg^{2+} and Pb^{2+} Ions. *Chemistry-A European Journal* **2004,** *10* (24), 6247-6254.

Appendix 1 – Full 5-HT receptor screen for Group 1-Compounds

Cmpd	5HT1A	5HT1B	5HT1D	5HT1E	5HT2A	5HT2B	5HT2C	5HT3	5HT4	5HT5A	5HT6	5HT7
2.1	85	3742			2.2	2.3	7			2200	58.1	1670
2.2	>10000	2446	1277		0.7	2.8	1.4			965	111.2	3472
2.3	3673				2.8	19	21			4954	469	
2.4	1351		752		0.6	1.3	22			1858	474.5	4243
2.5	1255		1472		0.7	0.5	1.1			4087	48	
2.6	1953	3437	1412		0.3	8	4.6			2630	63.6	3713
2.7	826	499.8	600	1245	2.7	5.9	18.6				378	2088
2.8	1450	487.5	711	1134	0.6	1.4	11.2			4623	531.1	2714
2.9	2353	2372	1024	5776	1.6	1.1	5.4			4796	36.2	1729
2.10	2852	8113	1104		0.6	8.3	6.2			2536	88.9	2087
2.11	1529	570.2	350	1009	7.6	27	37.6				318.6	1637
2.12	500.3	317.3	182	577	1	8.4	21.6			5454	757	606.8
2.13		6331	5052		3.3	7.5	43.4				79.8	
2.14			2024		4.6	20.7	69.5				414.4	
2.15		2690	3994		56.7	77.2	484.9				552.8	
2.16		2584	2356		12	33.5	257.7				1471	
2.17			5354		2	3.9	5.9				168.9	6744
2.18			2772		1.1	11	12			5892	416.3	1551
2.19		1913	2153		19	50	66.8				2016	4660
2.20	3463	3640			2.6	12	37.4				4477	3375
2.21		3593			0.3	2.2	2.8				148.3	
2.22					0.3	2.2	3.4				214.6	
2.23					2.4	20	26.1				742	
2.24		4181			0.4	4	12				975	
2.25					0.6	20	1.6			5100	140.8	2905
2.26					0.5	4.6	3.1				200	1993
2.27					3.1	1.6	13.2				468.9	
2.28					0.6	5.8	7.4			4129	883.6	2415
2.29		3385			0.5	0.9	7				116.5	
2.30		4770			0.4	1.6	5.1			3384	143.1	
2.31		1628			7.9	14.4	69.6				670.1	
2.32					0.7	2.4	27.4				1415	
2.33					0.6	0.9	2.2				84.9	
2.34		1851	1622			1.9	1.9				68.7	2710
2.35		1467	3579			8.1	23				319.3	
2.36		6099			0.4	1.8	9.2				556.6	
2.37		1902	2176		0.7	2.3	2				68.8	
2.38		5022	1263		0.7	3.9	2.2			2709	157.2	2211
2.39		2725	1967		2.5	13.7	14.5				222.1	
2.40		1685	839.7		1	6.9	8.8			5302	893.5	1881
2.41			1817			1.1	2.7			8128	23.4	5974
2.42	2412					3.5	3.2			2974	23.3	2398
2.43	8629					16	18.2				101.6	5034
2.44			1505			4.5	11.8				245.6	3553
2.45						20.7	56.1				145.2	
2.46					1.3	61.5	131.7			6591	430.8	5256
2.47	>10000				63.3	385.6	633.1				1585	
2.48						109	340.3			>10000	2929	

Appendix 2

Anders Ettrup, Mikael Palner, Nic Gillings, Martin A. Santini, Martin Hansen, Birgitte R. Kornum, Lars K. Rasmussen, Kjell Någren, Jacob Madsen, Mikael Begtrup, and Gitte M. Knudsen.

Radiosynthesis and Evaluation of ^{11}C-CIMBI-5 as a 5-HT_{2A} Receptor Agonist Radioligand for PET.

Journal of Nuclear Medicine **2010**, *51*(11), 1763-1770

Journal of Nuclear Medicine, published on October 18, 2010 as doi:10.2967/jnumed.109.074021

Radiosynthesis and Evaluation of ^{11}C-CIMBI-5 as a 5-HT$_{2A}$ Receptor Agonist Radioligand for PET

Anders Ettrup[1], Mikael Palner[1], Nic Gillings[2], Martin A. Santini[1], Martin Hansen[3], Birgitte R. Kornum[1], Lars K. Rasmussen[3], Kjell Någren[2], Jacob Madsen[2], Mikael Begtrup[3], and Gitte M. Knudsen[1]

[1]Neurobiology Research Unit and Center for Integrated Molecular Brain Imaging (CIMBI), Copenhagen University Hospital, Rigshospitalet, Copenhagen, Denmark; [2]PET and Cyclotron Unit, Copenhagen University Hospital, Rigshospitalet, Copenhagen, Denmark;; and [3]Department of Medicinal Chemistry, Faculty of Pharmaceutical Sciences, University of Copenhagen, Copenhagen, Denmark

PET brain imaging of the serotonin 2A (5-hydroxytryptamine 2A, or 5-HT$_{2A}$) receptor has been widely used in clinical studies, and currently, several well-validated radiolabeled antagonist tracers are used for in vivo imaging of the cerebral 5-HT$_{2A}$ receptor. Access to 5-HT$_{2A}$ receptor agonist PET tracers would, however, enable imaging of the active, high-affinity state of receptors, which may provide a more meaningful assessment of membrane-bound receptors. In this study, we radiolabel the high-affinity 5-HT$_{2A}$ receptor agonist 2-(4-iodo-2,5-dimethoxyphenyl)-*N*-(2-[^{11}C-OCH$_3$]methoxybenzyl)ethanamine (^{11}C-CIMBI-5) and investigate its potential as a PET tracer. **Methods:** The in vitro binding and activation at 5-HT$_{2A}$ receptors by CIMBI-5 was measured with binding and phosphoinositide hydrolysis assays. Ex vivo brain distribution of ^{11}C-CIMBI-5 was investigated in rats, and PET with ^{11}C-CIMBI-5 was conducted in pigs. **Results:** In vitro assays showed that CIMBI-5 was a high-affinity agonist at the 5-HT$_{2A}$ receptor. After intravenous injections of ^{11}C-CIMBI-5, ex vivo rat studies showed a specific binding ratio of 0.77 ± 0.07 in the frontal cortex, which was reduced to cerebellar levels after ketanserin treatment, thus indicating that ^{11}C-CIMBI-5 binds selectively to the 5-HT$_{2A}$ receptor in the rat brain. The PET studies showed that the binding pattern of ^{11}C-CIMBI-5 in the pig brain was in accordance with the expected 5-HT$_{2A}$ receptor distribution. ^{11}C-CIMBI-5 gave rise to a cortical binding potential of 0.46 ± 0.12, and the target-to-background ratio was similar to that of the widely used 5-HT$_{2A}$ receptor antagonist PET tracer ^{18}F-altanserin. Ketanserin treatment reduced the cortical binding potentials to cerebellar levels, indicating that in vivo ^{11}C-CIMBI-5 binds selectively to the 5-HT$_{2A}$ receptor in the pig brain. **Conclusion:** ^{11}C-CIMBI-5 showed a cortex-to-cerebellum binding ratio equal to the widely used 5-HT$_{2A}$ antagonist PET tracer ^{18}F-altanserin, indicating that ^{11}C-CIMBI-5 has a sufficient target-to-background ratio for future clinical use and is displaceable by ketanserin in both rats and pigs. Thus, ^{11}C-CIMBI-5 is a promising tool for investigation of 5-HT$_{2A}$ agonist binding in the living human brain.

Key Words: PET tracer development; agonist; porcine; serotonin receptors

J Nucl Med 2010; 51:1763–1770
DOI: 10.2967/jnumed.109.074021

Serotonin 2A (5-hydroxytryptamine 2A, or 5-HT$_{2A}$) receptors are implicated in the pathophysiology of human diseases such as depression, Alzheimer's disease, and schizophrenia. Also, 5-HT$_{2A}$ receptor stimulation exerts the hallucinogenic effects of recreational drugs such as lysergic acid diethylamide and 1-(2,5-dimethoxy-4-iodophenyl)-2-aminopropane (*1*), and atypical antipsychotics have antagonistic or inverse agonistic effects on the 5-HT$_{2A}$ receptor (*2*).

Currently, there are 3 selective 5-HT$_{2A}$ antagonistic PET ligands—^{18}F-altanserin (*3*), ^{18}F-deuteroaltanserin (*4*), and ^{11}C-MDL100907 (*5*)—in use for mapping and quantifying 5-HT$_{2A}$ receptor binding in the human brain. However, whereas 5-HT$_{2A}$ antagonists bind to the total pool of receptors, 5-HT$_{2A}$ agonists bind only to the high-affinity state of the receptor (*6,7*). Thus, a 5-HT$_{2A}$ receptor agonist ligand holds promise for the selective mapping of 5-HT$_{2A}$ receptors in their functional state; therefore, alterations in agonist binding measured in vivo with PET may be more relevant for assessing dysfunction in the 5-HT$_{2A}$ receptor system in specific patient or population groups. Furthermore, because many of the 5-HT$_{2A}$ receptors are intracellularly localized (*8,9*), combining measurements with antagonist and agonist PET tracers would enable determination of the ratio of the high-affinity, membrane-bound, and active receptors to the low-affinity, intracellular, and inactive receptors (*10*). Thus, quantification of functionally active 5-HT$_{2A}$ receptors in vivo using an agonist PET tracer is hypothesized to be superior to antagonist measurements of total number of 5-HT$_{2A}$ receptors for studying alterations in receptor function in human diseases such as depression.

D$_2$ receptor agonist radiotracers are now known to be superior to antagonist radiotracers in measuring dopamine release in vivo in monkeys (*11*) and mice (*10*). In humans,

Received Jan. 26, 2010; revision accepted Aug. 11, 2010.
For correspondence or reprints contact: Anders Ettrup, Neurobiology Research Unit, Blegdamsvej 9, Rigshospitalet, Bldg. 9201, DK-2100 Copenhagen, Denmark.
E-mail: ettrup@nru.dk

most studies have found that 5-HT_{2A} receptor antagonist PET tracers are not displaceable by elevated levels of endogenous serotonin (5-HT) (*12*). This suggests that agonist PET tracers may be better suited for measuring endogenous competition than antagonist tracers, so that 5-HT_{2A} receptor agonists would be more prone to displacement by competition with endogenously released 5-HT. Monitoring the release of endogenous 5-HT is highly relevant in relation to human diseases such as depression and Alzheimer's disease, which involve dysfunction of the 5-HT system.

2-(4-iodo-2,5-dimethoxyphenyl)-*N*-(2-methoxybenzyl) ethanamine (25I-NBOMe, or CIMBI [Center for Integrated Molecular Brain Imaging]-5) has recently been described as a potent and selective 5-HT_{2A} receptor agonist, and phosphoinositide hydrolysis assays revealed that it has a 12-fold lower half-maximal effective concentration (EC_{50}) than 5-HT itself (*13*). Although this compound has been tritiated (*14*), its in vivo biological distribution and possible PET tracer potential have not been investigated.

Here, we present the synthesis of ^{11}C-labeled CIMBI-5 and biological evaluation of this novel PET tracer. The compound was characterized in vitro, and ^{11}C-CIMBI-5 was investigated after intravenous injection both ex vivo in rats and in vivo in pigs with PET.

MATERIALS AND METHODS

In Vitro Binding and Activation

Inhibition constant (K_i) determinations against various neuro- [**Table 1**] receptors (Table 1) were provided by the Psychoactive Drug Screening Program (PDSP; experimental details are provided at http://pdsp.med.unc.edu/). In our laboratory, competition binding experiments were performed on a NIH-3T3 cell line (GF62) stably transfected with the rat 5-HT_{2A} receptor as previously described (*15*) using 0.2 nM ^{3}H-MDL100907 (kindly provided by Prof. Christer Halldin) and 8 different concentrations of CIMBI-5 (1 μM to 1 pM) in a total of 1 mL of buffer (500 mM Tris base, 1,500 mM NaCl, and 200 mM ethylenediaminetetraacetic acid). Nonspecific binding was determined with 1 μM ketanserin. Incubation was performed for 1 h at 37°C.

TABLE 1
PDSP Screening Result: Inhibition Constants (K_i) for CIMBI-5 Versus Serotonin and Other Receptors

Receptor	K_i (nM)
5-HT_{2A}	2.2 ± 0.1
5-HT_{2B}	2.3 ± 0.2
5-HT_{2C}	7.0 ± 1.0
5-HT_6	58 ± 17
5-HT_{1A}	85 ± 16
D_3	117 ± 14
α_{2C}	348 ± 17
D_4	647 ± 37
Serotonin transporter	1,009 ± 84
α_{2A}	1,106 ± 206
M_5	1,381 ± 231
D_2	1,600 ± 333
5-HT_7	1,670 ± 125
5-HT_{5A}	2,200 ± 385
D_1	3,718 ± 365
5-HT_{1B}	3,742 ± 553
Norepinephrine transporter	4,574 ± 270
Dopamine transporter	5,031 ± 343
D_5	7,872 ± 933

The 5-HT_{2A} receptor activation by CIMBI-5 was measured on GF62 cells using a phosphoinositide hydrolysis assay as previously described (*16*). Briefly, cells were incubated with myo-(*1,2*)-^{3}H-inositol (Amersham) in labeling medium. Subsequently, the cells were washed and incubated at 37°C with CIMBI-5 (1 μM to 0.1 pM). The formed inositol phosphates were extracted and counted with a liquid scintillation counter.

Radiochemical Synthesis of ^{11}C-CIMBI-5

^{11}C-methyl trifluoromethanesulfonate (triflate) produced using a fully automated system was transferred in a stream of helium to a 1.1-mL vial containing 0.3–0.4 mg of the labeling precursor (**3**; Fig. 1) and 2 μL of 2 M NaOH in 300 μL of acetonitrile, and the [**Fig. 1**] resulting mixture was heated at 40°C for 30 s. Subsequently, 250 μL of trifluoroacetic acid:CH_3CN (1:1) were added and the mixture heated at 80°C for 5 min (Fig. 2). After neutralization [**Fig. 2**] with 750 μL of 2 M NaOH, the reaction mixture was purified by high-performance liquid chromatography (HPLC) on a Luna C18 column (Phenomenex Inc.) (250 × 10 mm; 40:60 acetonitrile:25 mM citrate buffer, pH 4.7; and flow rate, 5 mL/min). The chemical synthesis of the labeling precursor is described in detail in the supplemental data (supplemental materials are available online only at http://jnm.snmjournals.org).

The fraction corresponding to the labeled product (~12.5 min) was collected in 50 mL of 0.1% ascorbic acid, and the resulting solution was passed through a solid-phase C18 Sep-Pak extraction column (Waters Corp.), which had been preconditioned with 10 mL of ethanol, followed by 20 mL of 0.1% ascorbic acid. The column was flushed with 3 mL of sterile water. Then, the trapped radioactivity was eluted with 3 mL of ethanol, followed by 3 mL of 0.1% ascorbic acid into a 20-mL vial containing 9 mL of phosphate buffer (100 mM, pH 7), giving a 15 mL solution of ^{11}C-CIMBI-5 with a pH of approximately 7. In a total synthesis time of 40–50 min, 1.5–2.5 GBq of ^{11}C-CIMBI-5 was produced, with radiochemical purity greater than 97% and specific radioactivity in the range 64–355 GBq/μmol. The lipophilicity of CIMBI-5 ($cLogD_{7.4}$ [log of calculated distribution coefficient, octanol/buffer pH 7.4]) was calculated using 2 different programs, which were in good agreement (CSLogD [ChemSilico], $cLogD_{7.4}$ = 3.33; Pallas 3.5 [CompuDrug Inc.], $cLogD_{7.4}$ = 3.21).

Ex Vivo Uptake in Rats

Twenty-two Sprague–Dawley rats (mean weight, 295 ± 53 g; Charles River) were included in the study. All animal experiments were performed in accordance with the European Communities Council Resolves of November 24, 1986 (86-609/ECC), and approved by the Danish State Research Inspectorate (journal no. 2007/561-1320). Rats were maintained on a 12-h light–dark cycle, with free access to food and water.

The ex vivo uptake and brain distribution were evaluated as previously described (*17*). Briefly, rats were injected in the tail vein with ^{11}C-CIMBI-5 (3.9 ± 3.5 MBq/kg; specific radioactivity, 30.9 GBq/μmol). The rats were decapitated at 5 (n = 2), 15 (n = 2), 30 (n = 4), 45 (n = 2), and 60 min (n = 4); the brains were quickly removed, placed on ice, and dissected into frontal cortex

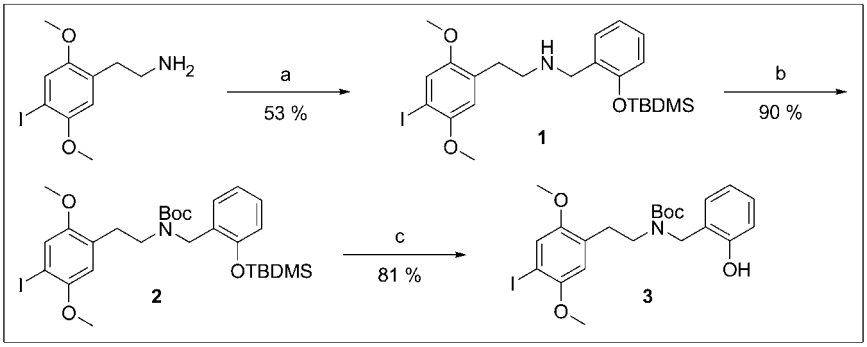

FIGURE 1. Synthesis of labeling precursor for ^{11}C-CIMBI-5 (*3*): (a) 2-(*tert*-butyldimethylsilyloxy)benzaldehyde, $NaBH_4$, MeOH; (b) Boc_2O, THF; and (c) TBAF, NH_4Cl, THF. OTBDMS = t-butyldimethylsiloxy; THF = tetrahydrofuran.

(first 3 mm of the brain) and cerebellum. Blood from the trunk was collected immediately, and plasma was isolated by centrifugation (1,500 rpm, 10 min). All brain tissue samples were collected in tared counting vials and counted for 20 s in a γ-counter (Cobra 5003; Packard Instruments).

For ex vivo blocking studies, rats were divided in vehicle (saline) and ketanserin-treated groups (n = 5–6). Rats were intravenously injected with vehicle or 1 mg/kg of ketanserin (Sigma) 45 min before tracer administration. ^{11}C-CIMBI-5 was injected in the tail vein, and after 30 min, the rats were decapitated. Brain regions and plasma were extracted and counted.

PET in Pigs

Six female Danish Landrace Pigs were used in this study (mean weight, 17.8 ± 1.4 kg). After arrival, animals were housed under standard conditions and were allowed to acclimatize for 1 wk before scanning. On the scanning day, pigs were tranquilized by intramuscular injection of 0.5 mg/kg of midazolam. Anesthesia was induced by 0.1 mL/kg intramuscular injections of Zoletil veterinary mixture (Virbac Animal Health; 125 mg of tiletamine and 125 mg of zolazepam in 8 mL of 5 mg/mL midazolam). After induction, anesthesia was maintained by a 10 mg/kg/h intravenous infusion of propofol (B. Braun Melsugen AG). During anesthesia, animals were endotracheally intubated and ventilated (volume, 250 mL; frequency, 15 per min). Venous access was granted through 2 Venflons (Becton Dickinson) in the peripheral milk veins, and an arterial line for blood sampling measurement was obtained by a catheter in the femoral artery after a minor incision. Vital signs including blood pressure, temperature, and heart rate were monitored throughout the duration of the PET scan. Immediately after scanning, animals were sacrificed by intravenous injection of pentobarbital–lidocaine. All animal procedures were approved by the Danish Council for Animal Ethics (journal no. 2006/561-1155).

PET Protocol

In 5 pigs, ^{11}C-CIMBI-5 was given as intravenous bolus injections, and the pigs were subsequently PET-scanned for 90 min in list mode with a high-resolution research tomography scanner (Siemens AG). Scanning began at the time of injection. After the baseline scan, 3 pigs were maintained in anesthesia and scanned a second time using the same PET protocol. The 5-HT_{2A} receptor antagonist ketanserin tartrate (Sigma) was administered at 30 min before the second scan (3 mg/kg bolus, followed by 1 mg/kg/h infusion for the duration of the scan). For all ^{11}C-CIMBI-5 PET scans, the injected radioactivity was on average 238 MBq (range, 96–418 MBq; n = 9), the specific radioactivity at the time of injection was 75 GBq/μmol (range, 28–133 GBq/μmol; n = 9), the average injected mass was 1.85 μg (range, 0.37–5.49 μg; n = 9), and there were no significant differences in these parameters between the baseline and blocked scans. In 2 pigs, arterial whole-blood samples were taken throughout the entire scan. During the first 15 min after injection, radioactivity in whole blood was continuously measured using an ABSS autosampler (Allogg Technology) counting coincidences in a lead-shielded detector. Concurrently, blood samples were manually drawn at 2.5, 5, 10, 20, 30, 50, 70, and 90 min, and the radioactivity in whole blood and plasma was measured using a well counter (Cobra 5003; Packard Instruments) that was cross-calibrated to the high-resolution research tomography scanner and autosampler. Also, radiolabeled parent compound and metabolites were measured in plasma as in the "HPLC Analysis of Pig Plasma and Pig Brain Tissue" section.

The free fraction of ^{11}C-CIMBI-5 in plasma, f_p, was estimated using an equilibrium dialysis chamber method as previously described (*18*). Briefly, the dialysis was conducted in chambers (Harvard Biosciences) separated by a cellulose membrane with a protein cutoff of 10,000 Da. Small amounts of ^{11}C-CIMBI-5 (~10 MBq) were added to a 5-mL plasma sample from the pig. Plasma (500 μL) was then dialyzed at 37°C against an equal volume of buffer (135 mM NaCl, 3.0 mM KCl, 1.2 mM $CaCl_2$, 1.0 mM $MgCl_2$, and 2.0 mM KH_2PO_4, pH 7.4). Counts per minute in 400 μL of plasma and buffer were determined in a well counter after various dialysis times, and f_p of ^{11}C-CIMBI-5 was calculated as counts per minute in buffer divided by counts per minute in plasma. The samples were taken from the dialysis chambers after equilibrium had been obtained between the 2 chambers.

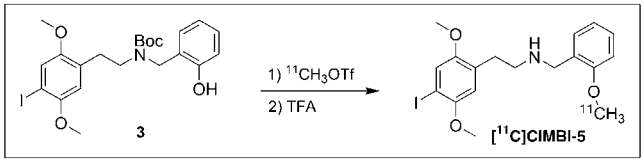

FIGURE 2. Radiochemical synthesis of ^{11}C-CIMBI-5. OTf = triflate; TFA = trifluoroacetic acid.

HPLC Analysis of Pig Plasma and Pig Brain Tissue

Whole-blood samples (10 mL) drawn during PET were centrifuged (3,500 rpm, 4 min), and the plasma was passed through a 0.45-μm filter before HPLC analysis with online radioactivity detection, as previously described (*19*).

Also, the presence of radioactive metabolites of ^{11}C-CIMBI-5 in the pig brain was investigated. Twenty-five minutes after intravenous injection of approximately 500 MBq of ^{11}C-CIMBI-5, the pig was killed by intravenous injection of pentobarbital and

decapitated, and the brain was removed. At the same time, a blood sample was drawn manually. Within 30 min of decapitation, brain tissue was homogenized in 0.1N perchloric acid (Bie and Bentsen) saturated with sodium–ethylenediaminetetraacetic acid (Sigma) for 2×30 s using a Polytron homogenizer (Kinematica, Inc.). After centrifugation, the supernatant was neutralized using phosphate buffer, filtered (0.45 μm), and analyzed by HPLC. A plasma sample taken at the time of decapitation was analyzed concurrently.

Quantification of PET Data

Ninety-minute high-resolution research tomography, list-mode PET data were reconstructed into 38 dynamic frames of increasing length (6×10, 6×20, 4×30, 9×60, 3×120, 6×300, and 4×600 s). Images consisted of 207 planes of 256×256 voxels of $1.22 \times 1.22 \times 1.22$ mm. A summed image of all counts in the 90-min scan was reconstructed for each pig and used for coregistration to a standardized MRI-based statistical atlas of the Danish Landrace pig brain, similar to that previously reported for the Göttingen minipig (*20*), using the program Register as previously described (*18*). The temporal radioactivity in volumes of interest (VOIs), including the cerebellum, cortex (defined in the MRI-based atlas as entire cortical gray matter), hippocampus, lateral and medial thalamus, caudate nucleus, and putamen, was calculated. Radioactivity in all VOIs was calculated as the average of radioactive concentration (Bq/mL) in the left and right sides. Outcome measure in the time–activity curves was calculated as radioactive concentration in VOI (in kBq/mL) normalized to the injected dose corrected for animal weight (in kBq/g), yielding standardized uptake values (g/mL).

In 1 pig in which full arterial input function, including metabolite correction, was measured, we calculated ^{11}C-CIMBI-5 distribution volumes (V_T) for VOIs based on either 1-tissue- or 2-tissue-compartment models (1TC or 2TC, respectively) using plasma corrected for parent compound as the arterial input function (Supplemental Table 1). Cortical nondisplaceable binding potential (BP_{ND}) was calculated as $BP_{ND} = V_T/V_{ND} - 1$ (*21*), assuming that specific 5-HT_{2A} receptor binding in the cerebellum was negligible and that the nondisplaceable volume of distribution (V_{ND}) was equal to the cerebellar V_T (*3*). For all 5 pigs, BP_{ND} was also calculated with the simplified reference tissue model (SRTM) (*22*), both at baseline and in the ketanserin-blocked condition, with the cerebellum as the reference region (Supplemental Table 1). Kinetic modeling was done with PMOD software (version 3.0; PMOD Technologies Inc.). Goodness of fit was evaluated using the Akaike information criterion.

Statistical Analysis

All statistical tests were performed using Prism (version 5.0; GraphPad Software). *P* values below 0.05 were considered statistically significant. Results are expressed in mean ± SD unless otherwise stated.

RESULTS

Chemistry

The labeling precursor was synthesized in 3 steps (Fig. 1): reductive amination with t-butyldimethylsilyl–protected salicylaldehyde, followed by *tert*-butoxycarbonyl (Boc) protection of the secondary amine and removal of the t-butyldimethylsilyl group, which gave the labeling precursor (**3**). Synthesis of the reference compound has been described previously (*13*).

In Vitro Binding Affinity

CIMBI-5 had the highest affinity for the 5-HT_{2A} receptor, in agreement with previous studies (*14*). Between the subtypes of the 5-HT_2 receptors, CIMBI-5 did not show a higher affinity toward 5-HT_{2A} receptors than it did toward 5-HT_{2B} receptors; however, approximately a 3-fold higher affinity of CIMBI-5 for 5-HT_{2A} receptors than for 5-HT_{2C} receptors was found. Against targets other than 5-HT_2 receptors, CIMBI-5 showed at least a 30-fold lower affinity for any other of the investigated receptors than for 5-HT_{2A} receptors (Table 1). In vitro binding assays conducted in our laboratory determined K_i of CIMBI-5 against 2 nM ^{3}H-MDL100907 at 1.5 ± 0.7 nM, thus confirming nanomolar affinity of CIMBI-5 for 5-HT_{2A} receptors.

In Vitro Functional Characterization

The functional properties of CIMBI-5 toward the 5-HT_{2A} receptor were assessed by measuring its effect on phosphoinositide hydrolysis in GF62 cells overexpressing the 5-HT_{2A} receptor. CIMBI-5 was found to be an agonist with an EC_{50} of 1.02 ± 0.17 nM (Supplemental Fig. 1), in agreement with previous reports (*13*). Pretreatment with 1 μM ketanserin completely inhibited CIMBI-5–induced phosphoinositide hydrolysis (data not shown). Furthermore, CIMBI-5 showed 84.6% ± 1.9% of the 5-HT_{2A} activation achieved by 10 μM 5-HT, demonstrating that CIMBI-5 functioned nearly as a full agonist.

Ex Vivo Distribution in Rats

After injection of ^{11}C-CIMBI-5 in awake rats, the time–activity curves measured as standardized uptake values showed highest uptake in the frontal cortex, whereas uptake in the cerebellum (equivalent to nondisplaceable uptake) was lower and paralleled the plasma time–activity curve. The brain uptake peaked in all regions at 15 min after injection and thereafter slowly declined (data not shown).

The specific binding ratio (SBR) in the frontal cortex region of interest, calculated as SBR = (region of interest − cerebellum)/cerebellum, peaked 30 min after injection, reaching a level of 0.77 ± 0.07, after which the SBR slowly declined (Fig. 3A). Thus, 30 min after injection was chosen as a reference time point and used in the blocking experiment with ketanserin. Ketanserin pretreatment reduced the SBR in the frontal cortex to levels not significantly different from zero (0.076 ± 0.12) (Fig. 3B). [**Fig. 3**]

In Vivo Distribution and Ketanserin Blockade in Pig Brain

^{11}C-CIMBI-5 showed high cortical uptake in vivo in the pig brain with PET, medium uptake in striatal and thalamic regions, and low uptake in the cerebellum (Fig. 4). Furthermore, the time–activity curves demonstrated a substantial separation between the cortical and cerebellar time–activity curves (Fig. 5A). The time–activity curves peaked at approximately 10 min after injection and thereafter decreased, implying that ^{11}C-CIMBI-5 binding is reversible over the 90-min scan time used in this study. [**Fig. 4**] [**Fig. 5**]

jnm074021-pm ■ 10/14/10

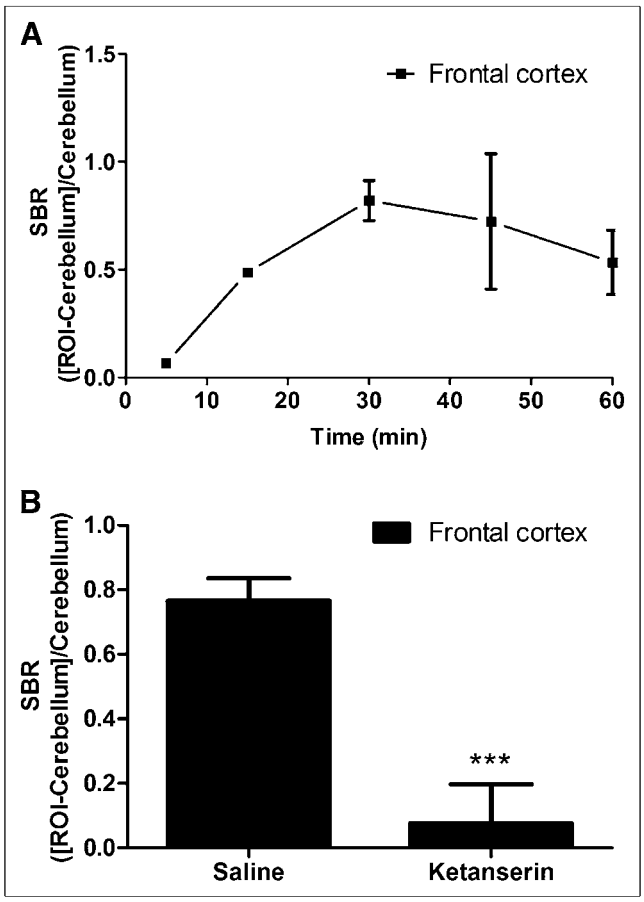

FIGURE 3. Time-dependent ex vivo distribution of ^{11}C-CIMBI-5 and displacement by ketanserin. (A) SBRs in frontal cortex in rats are shown relative to time after injection. (B) After ketanserin pretreatment (1 mg/kg intravenously), SBR in frontal cortex at 30 min after ^{11}C-CIMBI-5 injection is significantly decreased. ***$P < 0.0001$ in Student t test of ketanserin vs. saline. ROI = region of interest.

After ketanserin treatment, the concentration of ^{11}C-CIMBI-5 in the cortex was reduced almost completely to cerebellar levels (Fig. 5A). The cerebellar time–activity curve was unaltered by ketanserin administration (Fig. 5A).

Kinetic Modeling

With the SRTM, baseline cortical BP_{ND} of ^{11}C-CIMBI-5 was 0.46 ± 0.11 (n = 5). After the ketanserin bolus and infusion, the cortical BP_{ND} was significantly decreased by 75% (mean blocked BP_{ND}, 0.11 ± 0.06; n = 3). For the fitted SRTM, no significant difference in goodness of fit was found between baseline and blocked condition (Supplemental Table 1). In 1 pig in which full metabolite-corrected arterial input was measured, V_T was calculated from 1TC and 2TC models. Ratios between V_T in the cortex and cerebellum were 1.57 and 1.61, corresponding to a BP_{ND} of 0.57 and 0.61 with the 1TC and 2TC model, respectively. After ketanserin blockade, cortical ^{11}C-CIMBI-5 BP_{ND} was reduced to 0.13 and 0.11 in the 1TC and 2TC, respectively (Supplemental Table 1).

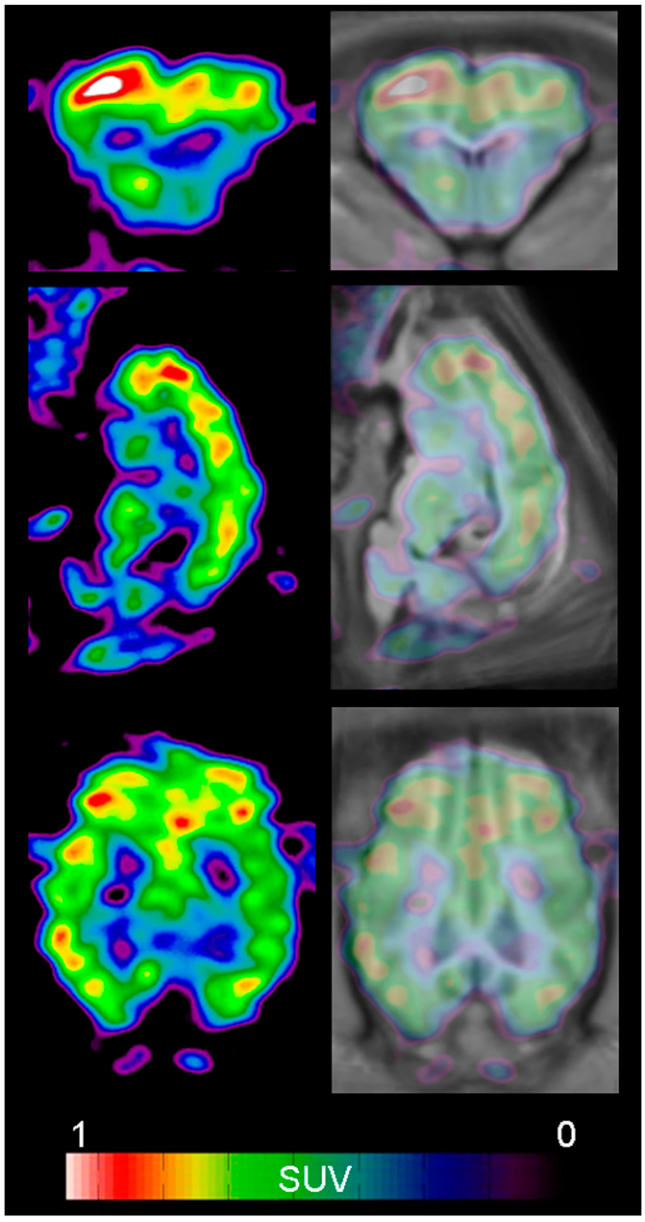

FIGURE 4. Representative coronal (top), sagittal (middle), and horizontal (bottom) PET images summed from 0 to 90 min of scanning showing distribution of ^{11}C-CIMBI-5 in pig brain. Left column shows PET images after 3 × 3 × 3 mm gaussian filtering. Right column shows same PET images aligned and overlaid on a standardized MRI-based atlas of the pig brain after coregistration. SUV = standardized uptake value.

RGB

Radiolabeled Metabolites

In the radio-HPLC analysis, a lipophilic radioactive metabolite accounting for up to 20% of the total plasma radioactivity was found, and it maintained stable plasma levels after 20 min and throughout the scan (Fig. 6). The HPLC retention time of ^{11}C-CIMBI-5 and its metabolite in the HPLC column suggest that the metabolite is slightly less lipophilic than ^{11}C-CIMBI-5 itself (Fig. 7). However, this metabolite was found only in negligible amounts in homogenized pig brain tissue, compared with plasma from the same animal (Fig. 7).

[**Fig. 6**]

[**Fig. 7**]

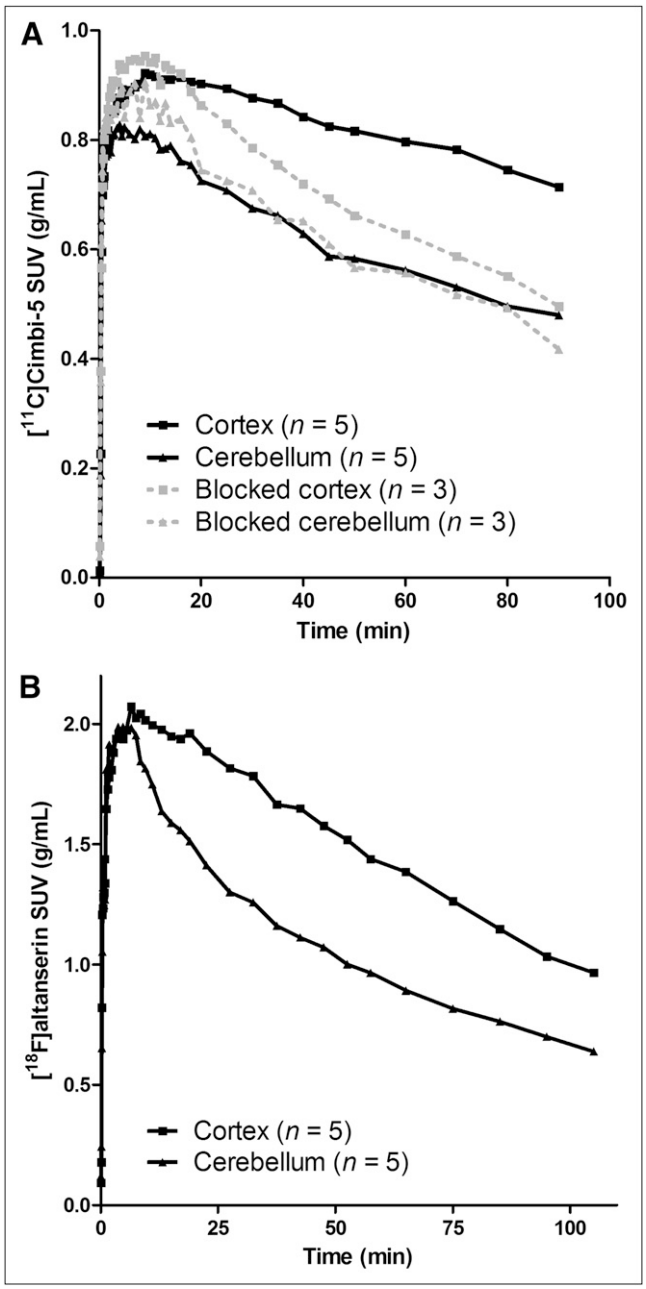

FIGURE 5. Time–activity curves of 5-HT_{2A} agonist and antagonist PET tracers in pig brain. (A) ^{11}C-CIMBI-5 time–activity curves in Danish Landrace pig brain at baseline (black solid line) or after intravenous ketanserin (3 mg/kg bolus, 1 mg/kg/h infusion) blockade (gray dotted line). (B) ^{18}F-altanserin time–activity curves in minipigs. Mean standardized uptake values normalized to injected dose per body weight are shown. SUV = standardized uptake value.

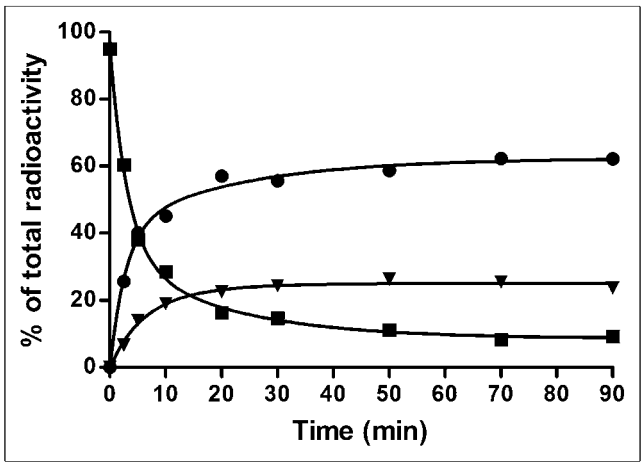

FIGURE 6. HPLC analysis of radioactive metabolites in pig plasma after intravenous injection of ^{11}C-CIMBI-5. ■ = parent compound ^{11}C-CIMBI-5; ▼ = lipophilic metabolite; ● = polar metabolites.

The free fraction of ^{11}C-CIMBI-5 in pig plasma at 37°C was 1.4% ± 0.3% using a dialysis chamber method, in which equilibrium between chambers was reached after 60 min.

DISCUSSION

In the current study, we report the in vitro, ex vivo, and in vivo validation of ^{11}C-CIMBI-5, a novel 5-HT_{2A} receptor agonist PET tracer. To our knowledge, this is the first agonist 5-HT_{2A} receptor PET tracer that has been developed. In vitro assays performed at our laboratory, along with assays performed through the PDSP screening program, confirmed the nanomolar affinity of CIMBI-5 for the 5-HT_{2A} receptor as previously reported (*13,14*). In the current study, the K_i for CIMBI-5 against ^{3}H-MDL100907 was 1.5 ± 0.7 nM, in agreement with the PDSP value of 2.2 nM for K_i of CIMBI-5 against ^{3}H-ketanserin. The somewhat lower value (K_i = 0.15 nM against ^{3}H-ketanserin) previously reported (*13*) may have been because that assay was performed at 25° C, whereas the values reported here were obtained at 37°C. We also confirmed that CIMBI-5 has agonistic properties at the 5-HT_{2A} receptor, with an EC_{50} value of 1.02 ± 0.17 nM, in agreement with previous reports (*13*). In addition, we showed that CIMBI-5 is nearly a full agonist, with 85% of the 5-HT_{2A} activation, compared with 5-HT itself. The data on binding and receptor activation, taken together with the PDSP screening for CIMBI-5 (Table 1), show that CIMBI-5 is a high-affinity agonist for 5-HT_{2A} receptors. CIMBI-5 had an affinity similar to that of the 5-HT_{2A} and the 5-HT_{2B} receptors and a 3-fold lower affinity to 5-HT_{2C} receptor. The eventual presence and distribution of 5-HT_{2B} receptors in the brain is still questionable, and specific 5-HT_{2B} receptor binding in the brain has to our knowledge not yet been demonstrated. For 5-HT_{2C} receptors, density of this subtype of receptors in cortical areas, compared with density of 5-HT_{2A} receptors, is negligible (*23,24*). Therefore, the cortical ^{11}C-CIMBI-5 binding signal stems from its 5-HT_{2A} receptor binding.

^{11}C-CIMBI-5 uptake and distribution in the rat brain after ex vivo dissection were similar to those in previous rat studies with ^{18}F-altanserin (*25*), showing high uptake in the frontal cortex and no displaceable binding in the cerebellum. Also, the specific uptake in the frontal cortex of the rat brain was blocked by ketanserin pretreatment, indicating that ^{11}C-CIMBI-5 binding is selective for the 5-HT_{2A} receptor. Similarly, ^{11}C-CIMBI-5 distributed in the pig

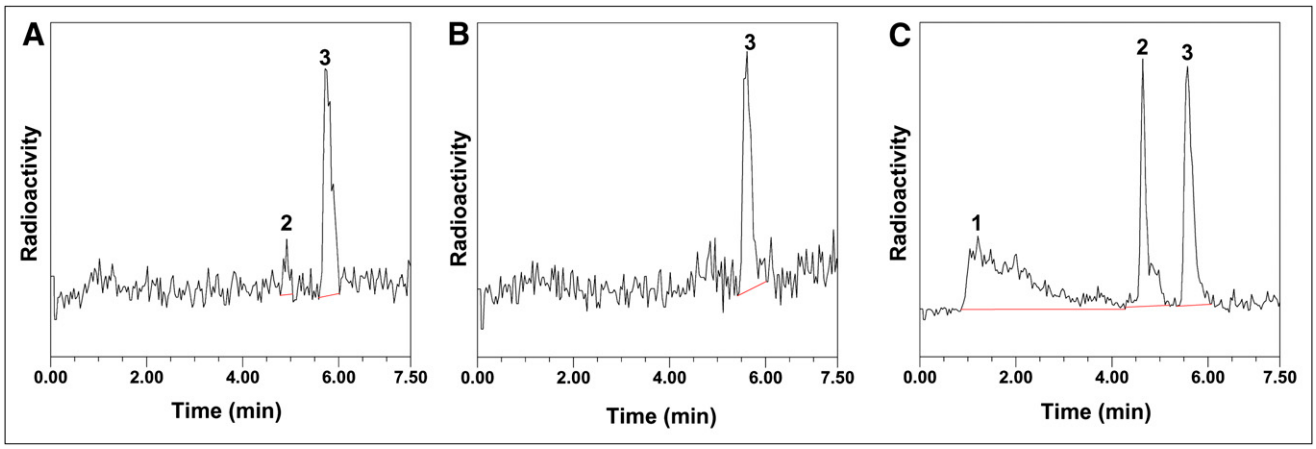

RGB

FIGURE 7. HPLC analysis of brain extracts and plasma at 25 min after injection of ^{11}C-CIMBI-5: frontal cortex (A), cerebellum (B), and plasma (C). Peaks: 1 = polar metabolites, 2 = lipophilic metabolites, and 3 = parent compound.

brain in a pattern resembling the 5-HT_{2A} receptor distribution as measured with 5-HT_{2A} receptor antagonist PET tracers in pigs (*25*) and in humans (*5,26*), with high cortical uptake and low cerebellar uptake. Further, the 5-HT_{2A} selectivity of in vivo cortical ^{11}C-CIMBI-5 binding in the pig was confirmed in the blocking study in which cortical ^{11}C-CIMBI-5 binding was decreased by a ketanserin bolus and infusion, whereas the cerebellar uptake was unaffected.

BP_{ND} for ^{11}C-CIMBI-5 with the cerebellum as a reference region was calculated using compartmental models, reference tissue approaches, and noninvasive Logan methods (Supplemental Table 1). For 5-HT_{2A} receptor antagonist PET tracers, such as ^{18}F-altanserin, the cerebellum is generally regarded as a valid reference region (*3*). Also, because negligible amounts of 5-HT_{2A} receptors are present in the cerebellum, compared with cortical areas, the preferential binding of a 5-HT_{2A} receptor PET ligand, as measured, for example, by the SRTM BP_{ND}, is indicative of the target-to-background ratio of 5-HT_{2A} PET ligands. At baseline, ^{11}C-CIMBI-5 showed an average SRTM BP_{ND} of 0.46. Given that an agonist PET tracer, compared with the antagonist, would bind only a high-affinity subpopulation of 5-HT_{2A} receptors, the maximum number of binding sites for such an agonist tracer would be lower than the antagonist, and—given that the radioligand affinities are comparable—it is anticipated that a lower BP_{ND} for an agonist tracer would be found. When compared with human data from 5-HT_{2A} receptor antagonist PET tracers (*5,26*), the cortical binding potential of ^{11}C-CIMBI-5 was indeed lower, but further studies are required to explore whether the somewhat low binding potential measured in pigs will translate to humans.

To compare the time–activity curves for ^{11}C-CIMBI-5 to a known 5-HT_{2A} antagonist PET tracer in the same animal species, we compared it to ^{18}F-altanserin pig data obtained from our laboratory (*25*). ^{11}C-CIMBI-5 and ^{18}F-altanserin in pigs showed similar cortex-to-cerebellum uptake and equal SRTM BP_{ND}, 0.46 ± 0.11 and 0.47 ± 0.10, respectively. Thus, in the pig brain ^{11}C-CIMBI-5 and ^{18}F-altanserin have similar target-to-background binding ratios, and ^{11}C-CIMBI-5 therefore holds promise for clinical use.

After injection of ^{11}C-CIMBI-5, a radiolabeled metabolite only slightly less lipophilic than ^{11}C-CIMBI-5 appeared in the pig plasma. On the basis of previous studies describing the metabolism of the 5-HT_{2A} receptor agonist compound 1-(2,5-dimethoxy-4-iodophenyl)-2-aminopropane (*27*) in rats, we speculated that this metabolite is the result of *O*-demethylation at a methoxy group in the iododimethoxyphenyl moiety of the tracer. Lipophilic radiolabeled metabolites impose a problem if they cross the blood–brain barrier because their presence will contribute to nonspecific binding. This has been observed for other antagonistic PET tracers in the serotonin system (*3*). Our brain homogenate experiments suggested that the lipophilic metabolite does not enter the pig brain, at least not to any large extent, and consequently the radiolabeled metabolite does not contribute to the nonspecific binding of ^{11}C-CIMBI-5.

Taken together, the results indicate that ^{11}C-CIMBI-5 is a promising tracer for visualization and quantification of high-affinity 5-HT_{2A} receptor agonist binding sites using PET. More specifically, studies of ^{11}C-CIMBI-5 could reveal differences in the number of binding sites measured with an agonist versus antagonist tracer, thus giving insights to whether high- and low-affinity states of 5-HT_{2A} receptors coexist in vivo as is described for the dopamine system (*28*). Optimally, a larger cortical BP_{ND} and higher brain uptake of the PET tracer is preferred. Also, the time–activity curves of ^{11}C-CIMBI-5 suggested relatively slow kinetics, which potentially would be a more pronounced phenomenon in primates and humans complicating quantification. Therefore, it may be worthwhile to pursue development of ^{11}C-CIMBI-5 analogs with modified chemical structures to improve these PET tracer properties.

CONCLUSION

The novel high-affinity 5-HT_{2A} receptor agonist PET tracer ^{11}C-CIMBI-5 distributes in the brain in a pattern compatible with the known 5-HT_{2A} receptor distribution,

and its binding can be blocked by ketanserin treatment. ^{11}C-CIMBI-5 is a promising PET tracer for in vivo imaging and quantification of high-affinity-state 5-HT$_{2A}$ receptors in the human brain.

ACKNOWLEDGMENTS

The study was financially supported by the Lundbeck Foundation, the Faculty of Health Sciences and the Faculty of Pharmaceutical Sciences at the University of Copenhagen, and by the EU 6th Framework program DiMI (LSHB-CT-2005-512146). K_i determinations were generously provided by the NIMH PDSP. A reference sample of CIMBI-5 was kindly provided by David Nichols, Purdue University.

REFERENCES

1. Gonzalez-Maeso J, Weisstaub NV, Zhou M, et al. Hallucinogens recruit specific cortical 5-HT$_{2A}$ receptor-mediated signaling pathways to affect behavior. *Neuron.* 2007;53:439–452.
2. Kim SW, Shin IS, Kim JM, et al. The 5-HT2 receptor profiles of antipsychotics in the pathogenesis of obsessive-compulsive symptoms in schizophrenia. *Clin Neuropharmacol.* 2009;32:224–226.
3. Pinborg LH, Adams KH, Svarer C, et al. Quantification of 5-HT2A receptors in the human brain using [^{18}F]altanserin-PET and the bolus/infusion approach. *J Cereb Blood Flow Metab.* 2003;23:985–996.
4. Soares JC, van Dyck CH, Tan P, et al. Reproducibility of in vivo brain measures of 5-HT2A receptors with PET and [^{18}F]deuteroaltanserin. *Psychiatry Res.* 2001;106:81–93.
5. Ito H, Nyberg S, Halldin C, Lundkvist C, Farde L. PET imaging of central 5-HT2A receptors with carbon-11-MDL 100,907. *J Nucl Med.* 1998;39:208–214.
6. Fitzgerald LW, Conklin DS, Krause CM, et al. High-affinity agonist binding correlates with efficacy (intrinsic activity) at the human serotonin 5-HT2A and 5-HT2C receptors: evidence favoring the ternary complex and two-state models of agonist action. *J Neurochem.* 1999;72:2127–2134.
7. Song J, Hanniford D, Doucette C, et al. Development of homogeneous high-affinity agonist binding assays for 5-HT2 receptor subtypes. *Assay Drug Dev Technol.* 2005;3:649–659.
8. Cornea-Hebert V, Watkins KC, Roth BL, et al. Similar ultrastructural distribution of the 5-HT$_{2A}$ serotonin receptor and microtubule-associated protein MAP1A in cortical dendrites of adult rat. *Neuroscience.* 2002;113:23–35.
9. Peddie CJ, Davies HA, Colyer FM, Stewart MG, Rodriguez JJ. Colocalisation of serotonin2A receptors with the glutamate receptor subunits NR1 and GluR2 in the dentate gyrus: an ultrastructural study of a modulatory role. *Exp Neurol.* 2008;211:561–573.
10. Cumming P, Wong DF, Gillings N, Hilton J, Scheffel U, Gjedde A. Specific binding of [^{11}C]raclopride and *N*-[^{3}H]propyl-norapomorphine to dopamine receptors in living mouse striatum: occupancy by endogenous dopamine and guanosine triphosphate-free G protein. *J Cereb Blood Flow Metab.* 2002;22:596–604.
11. Narendran R, Hwang DR, Slifstein M, et al. In vivo vulnerability to competition by endogenous dopamine: comparison of the D2 receptor agonist radiotracer (−)-*N*-[^{11}C]propyl-norapomorphine ([^{11}C]NPA) with the D2 receptor antagonist radiotracer [^{11}C]-raclopride. *Synapse.* 2004;52:188–208.
12. Pinborg LH, Adams KH, Yndgaard S, et al. [^{18}F]altanserin binding to human 5HT2A receptors is unaltered after citalopram and pindolol challenge. *J Cereb Blood Flow Metab.* 2004;24:1037–1045.
13. Braden MR, Parrish JC, Naylor JC, Nichols DE. Molecular interaction of serotonin 5-HT2A receptor residues Phe339(6.51) and Phe340(6.52) with superpotent *N*-benzyl phenethylamine agonists. *Mol Pharmacol.* 2006;70:1956–1964.
14. Nichols DE, Frescas SP, Chemel BR, Rehder KS, Zhong D, Lewin AH. High specific activity tritium-labeled *N*-(2-methoxybenzyl)-2,5-dimethoxy-4-iodophenethylamine (INBMeO): a high-affinity 5-HT2A receptor-selective agonist radioligand. *Bioorg Med Chem.* 2008;16:6116–6123.
15. Herth MM, Kramer V, Piel M, et al. Synthesis and in vitro affinities of various MDL 100907 derivatives as potential ^{18}F-radioligands for 5-HT2A receptor imaging with PET. *Bioorg Med Chem.* 2009;17:2989–3002.
16. Kramer V, Herth MM, Santini MA, Palner M, Knudsen GM, Rosch F. Structural combination of established 5-HT receptor ligands: new aspects of the binding mode. *Chem Biol Drug Des.* 2010;76:361–366.
17. Palner M, McCormick P, Gillings N, Begtrup M, Wilson AA, Knudsen GM. Radiosynthesis and ex vivo evaluation of (*R*)-(−)-2-chloro-*N*-[1-^{11}C-propyl]n-propylnorapomorphine. *Nucl Med Biol.* 2010;37:35–40.
18. Kornum BR, Lind NM, Gillings N, Marner L, Andersen F, Knudsen GM. Evaluation of the novel 5-HT4 receptor PET ligand [^{11}C]SB207145 in the Gottingen minipig. *J Cereb Blood Flow Metab.* 2009;29:186–196.
19. Gillings N. A restricted access material for rapid analysis of [^{11}C]-labeled radiopharmaceuticals and their metabolites in plasma. *Nucl Med Biol.* 2009;36:961–965.
20. Watanabe H, Andersen F, Simonsen CZ, Evans SM, Gjedde A, Cumming P. MR-based statistical atlas of the Gottingen minipig brain. *Neuroimage.* 2001;14:1089–1096.
21. Innis RB, Cunningham VJ, Delforge J, et al. Consensus nomenclature for in vivo imaging of reversibly binding radioligands. *J Cereb Blood Flow Metab.* 2007;27:1533–1539.
22. Lammertsma AA, Hume SP. Simplified reference tissue model for PET receptor studies. *Neuroimage.* 1996;4:153–158.
23. Kristiansen H, Elfving B, Plenge P, Pinborg LH, Gillings N, Knudsen GM. Binding characteristics of the 5-HT2A receptor antagonists altanserin and MDL 100907. *Synapse.* 2005;58:249–257.
24. Marazziti D, Rossi A, Giannaccini G, et al. Distribution and characterization of [^{3}H]mesulergine binding in human brain postmortem. *Eur Neuropsychopharmacol.* 1999;10:21–26.
25. Syvanen S, Lindhe O, Palner M, et al. Species differences in blood-brain barrier transport of three positron emission tomography radioligands with emphasis on P-glycoprotein transport. *Drug Metab Dispos.* 2009;37:635–643.
26. Adams KH, Pinborg LH, Svarer C, et al. A database of [^{18}F]-altanserin binding to 5-HT$_{2A}$ receptors in normal volunteers: normative data and relationship to physiological and demographic variables. *Neuroimage.* 2004;21:1105–1113.
27. Ewald AH, Fritschi G, Maurer HH. Metabolism and toxicological detection of the designer drug 4-iodo-2,5-dimethoxy-amphetamine (DOI) in rat urine using gas chromatography-mass spectrometry. *J Chromatogr B Analyt Technol Biomed Life Sci.* 2007;857:170–174.
28. Laruelle M. Imaging synaptic neurotransmission with in vivo binding competition techniques: a critical review. *J Cereb Blood Flow Metab.* 2000;20:423–451.

Appendix 3

Anders Ettrup, Martin Hansen, Martin Andreas Santini, James Paine, Nic Gillings, Mikael Palner, Szabolcs Lehel, Matthias M. Herth, Jacob Madsen, Jesper Kristensen, Mikael Begtrup and Gitte Moos Knudsen.

Radiosynthesis and in vivo evaluation of a series of substituted ^{11}C-phenethylamines as 5-HT_{2A} agonist PET tracers.

European Journal of Nuclear Medicine and Molecular Imaging (in press)

Eur J Nucl Med Mol Imaging
DOI 10.1007/s00259-010-1686-8

ORIGINAL ARTICLE

Radiosynthesis and in vivo evaluation of a series of substituted ^{11}C-phenethylamines as 5-HT$_{2A}$ agonist PET tracers

Anders Ettrup · Martin Hansen · Martin A. Santini · James Paine · Nic Gillings · Mikael Palner · Szabolcs Lehel · Matthias M. Herth · Jacob Madsen · Jesper Kristensen · Mikael Begtrup · Gitte M. Knudsen

Received: 26 August 2010 / Accepted: 15 November 2010

Abstract
Purpose Positron emission tomography (PET) imaging of serotonin 2A (5-HT$_{2A}$) receptors with agonist tracers holds promise for the selective labelling of 5-HT$_{2A}$ receptors in their high-affinity state. We have previously validated [^{11}C]Cimbi-5 and found that it is a 5-HT$_{2A}$ receptor agonist PET tracer. In an attempt to further optimize the target-to-background binding ratio, we modified the chemical structure of the phenethylamine backbone and carbon-11 labelling site of [^{11}C]Cimbi-5 in different ways. Here, we present the in vivo validation of nine novel 5-HT$_{2A}$ receptor agonist PET tracers in the pig brain.
Methods Each radiotracer was injected intravenously into anaesthetized Danish Landrace pigs, and the pigs were subsequently scanned for 90 min in a high-resolution research tomography scanner. To evaluate 5-HT$_{2A}$ receptor binding, cortical nondisplaceable binding potentials (BP_{ND}) were calculated using the simplified reference tissue model with the cerebellum as a reference region.
Results After intravenous injection, all compounds entered the brain and distributed preferentially into the cortical areas, in accordance with the known 5-HT$_{2A}$ receptor distribution. The largest target-to-background binding ratio was found for [^{11}C]Cimbi-36 which also had a high brain uptake compared to its analogues. The cortical binding of [^{11}C]Cimbi-36 was decreased by pretreatment with ketanserin, supporting 5-HT$_{2A}$ receptor selectivity in vivo. [^{11}C]Cimbi-82 and [^{11}C]Cimbi-21 showed lower cortical BP_{ND}, while [^{11}C]Cimbi-27, [^{11}C]Cimbi-29, [^{11}C]Cimbi-31 and [^{11}C]Cimbi-88 gave rise to cortical BP_{ND} similar to that of [^{11}C]Cimbi-5.
Conclusion [^{11}C]Cimbi-36 is currently the most promising candidate for investigation of 5-HT$_{2A}$ receptor agonist binding in the living human brain with PET.

Keywords PET tracer development · 5-HT$_{2A}$ · Agonist · Porcine · Serotonin receptors · [^{11}C]Cimbi-36

Electronic supplementary material The online version of this article (doi:10.1007/s00259-010-1686-8) contains supplementary material, which is available to authorized users.

A. Ettrup · M. A. Santini · M. Palner · G. M. Knudsen (✉)
Neurobiology Research Unit, Copenhagen University Hospital, Blegdamsvej 9, Rigshospitalet, building 9201, DK-2100 Copenhagen, Denmark
e-mail: gmk@nru.dk

N. Gillings · S. Lehel · M. M. Herth · J. Madsen
PET and Cyclotron Unit, Copenhagen University Hospital, Rigshospitalet, Copenhagen, Denmark

M. Hansen · J. Paine · J. Kristensen · M. Begtrup
Department of Medicinal Chemistry, Faculty of Pharmaceutical Sciences, University of Copenhagen, Copenhagen, Denmark

A. Ettrup · M. Hansen · M. A. Santini · J. Paine · N. Gillings · M. Palner · M. M. Herth · J. Madsen · J. Kristensen · M. Begtrup · G. M. Knudsen
Center for Integrated Molecular Brain Imaging (Cimbi), Copenhagen University Hospital, Rigshospitalet, Copenhagen, Denmark

Introduction

The serotonin 2A (5-HT$_{2A}$) receptors are implicated in the pathophysiology of human diseases such as depression and schizophrenia, and 5-HT$_{2A}$ receptor stimulation is responsible for the hallucinogenic effects of recreational drugs such as lysergic acid diethylamide (LSD) and 1-(2,5-dimethoxy-4-iodophenyl)-2-aminopropane (DOI) [1], whilst the therapeutic effects of atypical antipsychotics

Published online: 21 December 2010

can be attributed to the antagonistic effects on these receptors [2]. Positron emission tomography (PET) imaging of cerebral 5-HT_{2A} receptors is used to characterize the serotonergic receptor system in disease states, and PET imaging can also be used to measure receptor occupancy by therapeutic drugs, e.g. antipsychotics.

Currently, only antagonistic PET ligands such as [^{18}F] altanserin [3] and [^{11}C]MDL100907 [4] are available to selectively map and quantify 5-HT_{2A} receptor binding in the human brain. However, whereas 5-HT_{2A} receptor antagonists bind to the total pool of receptors, 5-HT_{2A} receptor agonists selectively bind to receptors in their high-affinity state [5, 6]. Thus, a 5-HT_{2A} receptor agonist PET tracer would ideally bind only to 5-HT_{2A} receptors in their functional state. Alterations in agonist binding measured in vivo with PET may be more relevant for assessing dysfunction in the 5-HT_{2A} receptors in specific patient or population groups. Furthermore, since a large fraction of the 5-HT_{2A} receptors are intracellularly localized [7, 8], combining measurements with antagonist and agonist PET tracers would enable in vivo determination of the ratio of the high-affinity, membrane-bound and active receptors to the low-affinity, inactive and intracellular receptors [9]. Thus, quantification of functionally active 5-HT_{2A} receptors in vivo using an agonist PET tracer is hypothesized to be superior to antagonist measurements of total pool of 5-HT_{2A} receptors for studying alterations in receptor function in human diseases such as depression.

In terms of chemical structure, 5-HT_{2A} receptor agonists fall into three classes: tryptamines, ergolines and phenethylamines. Recently, several *N*-benzyl-substituted phenethylamines have been described as superpotent and selective 5-HT_{2A} receptor agonists with EC_{50} values up to 27-fold lower than that of 5-HT itself [10]. One of these compounds, 2-(4-iodo-2,5-dimethoxyphenyl)-*N*-(2-methoxybenzyl)ethanamine (25I-NBOMe, Cimbi-5), was recently tritiated [11], and we have also evaluated [^{11}C]Cimbi-5 as a 5-HT_{2A} receptor agonist PET tracer [12].

Dopamine D_2 receptor agonist radiotracers are superior to antagonist radiotracers for measuring dopamine release in vivo in humans [13], monkeys [14] and mice [9], and since several studies have failed to demonstrate that 5-HT_{2A} receptor antagonist PET tracers are displaceable by elevated levels of endogenous 5-HT [15], it may well be that 5-HT_{2A} receptor agonists would be more prone to displacement by competition with endogenously released 5-HT. Monitoring the release of endogenous 5-HT is highly relevant in relation to human diseases such as depression and Alzheimer's disease which involve dysfunction of the 5-HT system.

Here, we present the synthesis and evaluation of a series of ^{11}C-phenethylamines structurally related to the previously validated lead compound [^{11}C]Cimbi-5. The agonistic properties of the compounds were ascertained in vitro by phosphoinositide (PI) hydrolysis assays and binding assays. To test the suitability of the compounds as PET tracers in vivo, all substituted phenethylamines were labelled with carbon-11, and cerebral uptake, distribution and displacement were investigated in pigs after intravenous (i.v.) injection of PET tracer.

Materials and methods

Chemical synthesis

Synthesis of precursors and radiochemical labelling are summarized in Fig. 1; bold numbers refer to this figure. Experimental conditions, synthesis routes for the precursors, and NMR data for previously unpublished intermediates can be found in the Supplementary material. The precursors for the radiolabelling were, with the exception of **14**, synthesized in two steps from their parent phenethylamines. Reductive amination with the appropriate aldehydes followed by selective Boc-protection of the secondary amines gave the labelling precursors. The syntheses of the parent phenethylamines **1** [16], **2** [16], **3** [17] and **4** [18] have been described elsewhere. The synthesis of **5** was in four steps from 1,4-diiodo-2,5-dimethoxybenzene, and the synthesis of **14** was in 3 steps from 2-(2-isopropoxy-5-methoxyphenyl) ethanamine [11] as described in the Supplementary material. The synthesis of reference compounds except Cimbi-82 have been reported elsewhere [10, 16]. The synthesis of Cimbi-82 is described in the Supplementary material. The lipophilicity of all PET tracers ($cLogD_{7.4}$) was calculated using CSLogD (ChemSilico).

Radiochemical synthesis of ^{11}C-phenethylamines

Radiochemical labelling of all PET tracers is summarized in Fig. 1. All radiolabelled compounds except [^{11}C]Cimbi-88 were prepared as follows. [^{11}C]Methyl triflate was collected in a solution of 0.3–0.4 mg labelling precursor (see Fig. 1) in a mixture of acetonitrile (200 μl) and acetone (100 μl) containing 2 μl 2 M NaOH at room temperature, and the solution was subsequently heated for 30 s at 40°C. Subsequently, 250 μl of a 1:1 mixture of trifluoroacetic acid/CH_3CN was added and the mixture heated at 80°C for 5 min. After neutralization with 750 μl 2 M NaOH and dilution with about 4 ml citrate buffer (25 mM, pH 4.7), the reaction mixture was purified by HPLC (Phenomenex Luna C18(2), 250×10 mm column; 40/60 acetonitrile/25 mM citrate buffer pH 4.7, flow rate 6 ml/min).

The HPLC fraction containing the product was collected in a flask containing 50 ml 0.1% ascorbic acid. This solution was then passed through a C18 SepPak light column which had been preconditioned with 10 ml ethanol

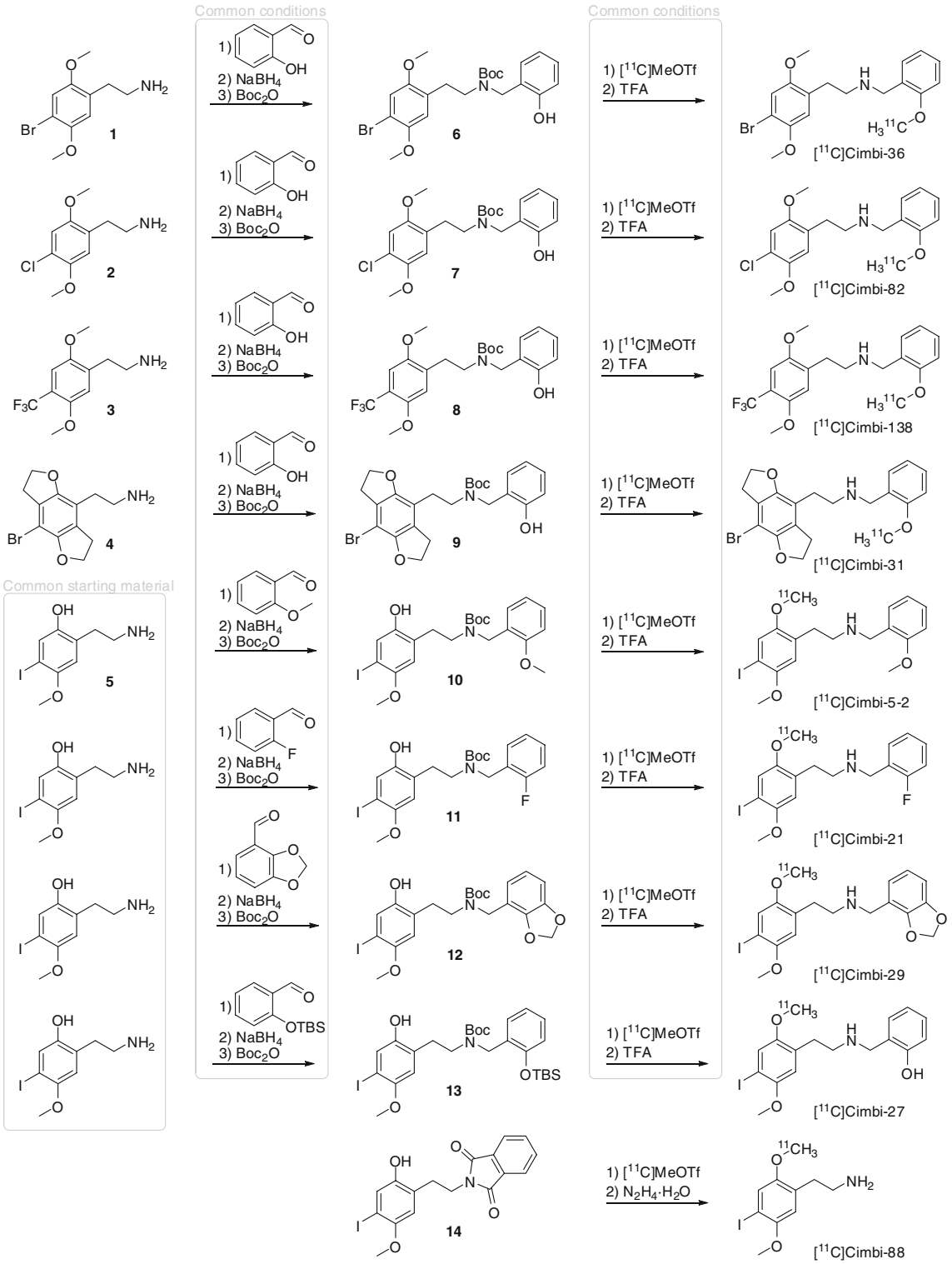

Fig. 1 Chemical synthesis of precursor compounds and radiochemical preparation of PET tracers. For synthesis specifications, refer to the Supplementary material

followed by 20 ml 0.1% ascorbic acid. The column was first flushed with 3 ml sterile water, then the trapped activity was eluted with 3 ml ethanol followed by 3 ml 0.1% ascorbic acid into a 20-ml vial containing 9 ml phosphate buffer (100 mM, pH 7) giving a 15 ml solution of the labelled product. The total synthesis time was 40–50 min. Analysis to determine radiochemical purity and specific radioactivity was performed using HPLC with

online UV and radiodetection (Luna C18(2) 4.6×150 mm column; eluent 40/60 acetonitrile/25 mM citrate buffer pH 4.7; flow rate 2 ml/min, wavelength 300 nm).

[^{11}C]Cimbi-88 was synthesized in an analogous manner to the above except that the deprotection step was performed by addition of hydrazine monohydrate (300 μl) and heating at 120°C for 3 min. The solution was neutralized with 2 ml 3 M HCl, diluted with 2.5 ml citrate buffer (25 mM, pH 4.7) and purified as described above. Radiochemical purity of all radiolabelled compounds was >95% and specific activities at the end of synthesis varied from 14 to 605 GBq/μmol.

In vitro binding

Competition binding experiments against [^{3}H]MDL100907 were performed in a NIH-3T3 cell line (GF62) stably transfected with the rat 5-HT_{2A} receptor as previously described [19] using 0.2 nM [^{3}H]MDL100907 as the radioactive competitor. Eight different concentrations of ligand (from 1 μM to 1 pM) in a total of 1 ml buffer (50 mM Tris-HCl, 150 mM NaCl, 5 mM KCl, 1 mM $CaCl_2$, 1 mM $MgCl_2$, 0.01% ascorbic acid, pH 7.4) including cell homogenate were tested. Nonspecific binding was determined with 1 μM ketanserin. The incubation was terminated after 1 h by filtration using a 24-channel 300-ml cell harvester (Brandel). Tris-HCl buffer was used for washing, and the samples were filtered through a Whatman GF/B filter. The filters were soaked with 1% polyethylenimine prior to filtration in order to reduce and stabilize nonspecific binding to the filters. Radioactive concentrations were determined with a scintillation counter (Packard Instruments), and the K_i values were calculated based on percent binding inhibition of the radioactive ligand. Furthermore, values of K_i against various neuroreceptors were provided by the Psychoactive Drug Screening Program (PDSP; for experimental details refer to the PDSP website http://pdsp.med.unc.edu/).

PI hydrolysis assay

GF62 cells (1.5×10^6 cells/ml) were cultured overnight in Dulbecco's modified Eagle's medium (DMEM) supplemented with 10% fetal bovine serum (FBS), 1 mM sodium pyruvate (Sigma), penicillin (100 U/ml) and streptomycin (100 μg/ml) at 37°C in an atmosphere containing 5% CO_2. Subsequently, cells were incubated overnight with 4 μCi/well of myo-(1,2)-[^{3}H]-inositol (Amersham) in labelling medium (inositol-free DMEM containing 10% FBS and penicillin/streptomycin). The cells were then washed once with incubation buffer (20 mM HEPES, pH 7.4; 20 μM LiCl, 1 mM $MgCl_2$, 1 mM $CaCl_2$) and incubated at 37°C in the same buffer for 30 min in the presence or absence of 1 μM ketanserin. The solutions were removed and test compounds (10 μM to 0.1 pM) or 5-HT (10 μM) were added to the wells for 30 min at 37°C. The formed inositol phosphates were then extracted with 10 mM ice-cold formic acid for 30 min at 4°C. The supernatants were transferred to AG 1-X8 anion exchange resin columns (Bio-Rad) and eluted into Ultima-FLO AF scintillation liquid (Packard) with 2 M ammonium formate/0.1 M formic acid. Accumulated [^{3}H]inositol phosphates were measured with a Tri-Carb 2900TR liquid scintillation counter (Packard Instruments) after 1 h incubation at room temperature.

Animal procedures

Ten female Danish Landrace pigs were used; their mean weight was 20.1±3.8 kg. After arrival, the animals were housed under standard conditions and were allowed to acclimatize for 1 week before scanning. To minimize stress, the animals were provided with straw bedding and environmental enrichment in the form of plastic balls and metal chains. On the scanning day, pigs were tranquilized by intramuscular injection of 0.5 mg/kg midazolam. Anaesthesia was induced by intramuscular injection of a Zoletil veterinary mixture (1.25 mg/kg tiletamin, 1.25 mg/kg zolazepam and 0.5 mg/kg midazolam; Virbac Animal Health). Following induction, anaesthesia was maintained by i.v. infusion of 10 mg/kg propofol per hour (B. Braun Melsugen). During anaesthesia, animals were endotracheally intubated and ventilated (volume 250 ml, frequency 15 per min). Venous access was obtained through two Venflon cannulas (Becton Dickinson) in the peripheral milk veins, and an arterial line for blood sampling was inserted into the femoral artery via a minor incision. Vital signs including blood pressure, temperature and heart rate were monitored throughout the duration of the PET scanning. Immediately after scanning, animals were killed by i.v. injection of pentobarbital/lidocaine. All animal procedures were approved by the Danish Council for Animal Ethics (Journal No. 2006/561-1155).

PET scanning protocol

All PET tracers were evaluated with a single PET scan. On the basis of the pharmacokinetic properties, the best candidate was selected for further investigation including a blocking study in vivo and an examination of metabolites in pig brain tissue. All PET tracers were given as an i.v. bolus injection, and the pigs were subsequently scanned for 90 min in list mode with a high-resolution research tomography (HRRT) scanner (Siemens). Scanning was started at the time of injection (t=0). The injected radioactivities and specific radioactivities at the time of injection are given in Table 2. In all pigs, arterial whole blood

samples were taken throughout the entire scan. During the first 15 min after injection, radioactivity in whole blood was continuously measured using an Allogg ABSS autosampler (Allogg Technology) counting coincidences in a lead-shielded detector. Concurrently, blood samples were manually drawn at 2.5, 5, 10, 20, 30, 50, 70 and 90 min, and radioactivity in whole blood and plasma was measured using a well counter (Cobra 5003; Packard Instruments) that was cross-calibrated to the HRRT scanner and to the autosampler. Also, radiolabelled parent compound and metabolites were measured in plasma as described below.

To test the displaceability of [^{11}C]Cimbi-36 by a known 5-HT$_{2A}$ receptor antagonist in vivo, ketanserin tartrate (10 mg/kg i.v.; Sigma no. S006) was given after a [^{11}C]Cimbi-36 baseline scan 30 min prior to a second scan using the same PET protocol. In these two scans, injected radioactivities were 553 MBq and 590 MBq in the baseline and blocked scan, whereas the specific radioactivities at the time of injection were 175.4 GBq/μmol and 257.0 GBq/μmol.

Quantification of PET data

Data from a 90-min HRRT list mode PET scans were reconstructed using a standard iterative method as previously reported [20] (OSEM3D-OP with point spread function, ten iterations, 16 subsets) into 38 dynamic frames of increasing length (6×10, 6×20, 4×30, 9×60, 3×120, 6×300, 4×600 s). Images consisted of 207 planes of 256×256 voxels of 1.22×1.22×1.22 mm. A summed image of all counts in the 90-min scan time for each pig was reconstructed and used for coregistration to a standardized MRI-based statistical atlas of the Danish Landrace pig brain, similar to that previously reported for the Göttingen minipig [21] using the program Register as previously described [22]. Hereafter, the activity in volumes of interest (VOI), including the cerebellum, cortex (defined in the MRI-based atlas as the entire cortical grey matter), hippocampus, caudate putamen, putamen, dorsal and ventral thalamus, and lateral ventricle, were extracted automatically. Activity in all VOIs was calculated as the average radioactivity concentration (becquerels per cubic centimetre) in the left and right hemispheres. Radioactivity concentrations in the VOIs (kilobecquerels per cubic centimetre) or in parent compound-corrected arterial plasma (kilobecquerels per millilitre) were normalized in time–activity curves to the injected dose (ID) corrected for animal weight, in kilobecquerels per gram, thus yielding the unit grams per cubic centimetre and approximating the amount of uptake in terms of standardized uptake values (SUV).

Arterial input measurements were obtained for all PET tracers, except [^{11}C]Cimbi-88 for which full radiometabolite information was not available, and distribution volumes (V_T) for VOIs were calculated based on the two tissue compartments (2TC) model using parent compound-corrected plasma input function as the arterial input function (Table 2). Assuming the specific 5-HT$_{2A}$ receptor binding in the cerebellum is negligible [3], the non-displaceable binding potential (BP_{ND}) for all PET tracers were calculated applying the simplified reference tissue model (SRTM) [23]. Kinetic modelling was done in PMOD version 3.0 (PMOD Technologies).

HPLC analysis of pig plasma and brain tissue

Whole-blood samples (10 ml) drawn during PET scanning were centrifuged (1,500×*g*, 7 min at ambient temperature), and the plasma was filtered through a 0.45 μm filter (13 mm or 25 mm PVDF syringe filter; Whatman GD/X) before HPLC analysis with online radioactivity detection, as previously described [24].

Additionally, the presence of radioactive metabolites of [^{11}C]Cimbi-36 in the brain was investigated in two pigs. The pigs were killed by i.v. injection of pentobarbital 25 and 60 min after i.v. injection of about 500 MBq [^{11}C]Cimbi-36, and the brains were removed. Within 30 min of pentobarbital injection, brain tissue was homogenized in 0.1 N perchloric acid (Bie and Bentsen) saturated with sodium-EDTA (Sigma) for 2×30 s using a Polytron homogenizer. After centrifugation (1,500×*g*, 7 min at ambient temperature), the supernatant was neutralized using phosphate buffer, filtered (0.45 μm), and analysed by HPLC as described above. A plasma sample from blood taken at the time of decapitation was also analysed.

Statistical analysis

All statistical tests were performed using Prism version 5.0 (GraphPad software). *P* values below 0.05 were considered statistically significant. Results are expressed in means ± standard deviation (SD) unless otherwise stated.

Results

In vitro binding characterization

Affinities of the test compounds towards the 5-HT$_{2A}$ receptor were measured against 0.2 nM [^{3}H]MDL100907 on GF62 cells stably transfected with the rat 5-HT$_{2A}$ receptor, and the K_i values of the test compounds are given in Table 1. All tested compounds showed nanomolar affinity towards the 5-HT$_{2A}$ receptor. Of the tested compounds, Cimbi-31 and Cimbi-138 showed the highest affinities for the 5-HT$_{2A}$ receptor, and Cimbi-21 and Cimbi-88 showed the lowest

Table 1 In vitro 5-HT_{2A} receptor binding affinities and activation of PET tracer compounds

Compound	5-HT_{2A} antagonist binding[a]	5-HT_{2A} activation[b]	Intrinsic activity (%)[c]
Cimbi-5	1.49±0.35	1.02±0.08	91
Cimbi-21	12.5±3.11	50.7±12.3	86
Cimbi-27	1.12±0.08	0.19±0.03	99
Cimbi-29	1.36±0.37	29.7±2.82	93
Cimbi-31	0.16±0.04	1.06±0.19	83
Cimbi-36	1.01±0.17	0.51±0.19	87
Cimbi-82	2.89±1.05	2.31±0.11	88
Cimbi-88	47.2±16.3	6.39±0.97	84
Cimbi-138	0.35±0.05	0.96±0.18	92

[a] K_i (nM ± SEM) measured against [^{3}H]MDL100907 at GF-62 cells overexpressing rat 5-HT_{2A} receptors.

[b] ED_{50} values (nM ± SEM) for 5-HT_{2A} activation at GF-62 cells.

[c] Mean maximal activation by test compound compared to 10 μM 5-HT.

affinities. PDSP screening results were obtained to determine whether the compounds had significant affinities for other neuroreceptors. According to the PDSP data, the K_i for Cimbi-36 against human 5-HT_{2A} receptors was 0.5±0.1 nM. Thus, Cimbi-36 was threefold more selective over 5-HT_{2C} (K_i 1.7±0.1 nM). At other targets tested by PDSP, Cimbi-36 was at least 120-fold more selective for 5-HT_{2A} receptors. The third highest affinity of Cimbi-36 was at Sigma 2 receptors (K_i 62 nM). The full PDSP screening results are given in Table S1 in the Supplementary material.

In vitro functional characterization

The functional properties of the compounds at the 5-HT_{2A} receptor were assessed by measuring their effect on PI hydrolysis in GF62 cells overexpressing the 5-HT_{2A} receptor. All investigated compounds were found to be highly potent agonists at the 5-HT_{2A} receptor with EC_{50} values in the nanomolar range (0.19–50.7 nM). For compounds previously tested, EC_{50} values are in agreement with reported data [10]. For all compounds, pretreatment with 1 μM ketanserin completely inhibited the induced PI hydrolysis (data not shown). Furthermore, the degree of 5-HT_{2A} receptor activation achieved by the compounds was compared to the maximum effect of 5-HT (10 μM) in the same assays and reported as percentage of intrinsic activation. All compounds acted as full or nearly full agonists at the 5-HT_{2A} receptor, giving rise to 83–99% of the activation evoked by 10 μM 5-HT. The full results of in vitro activation are given in Table 1.

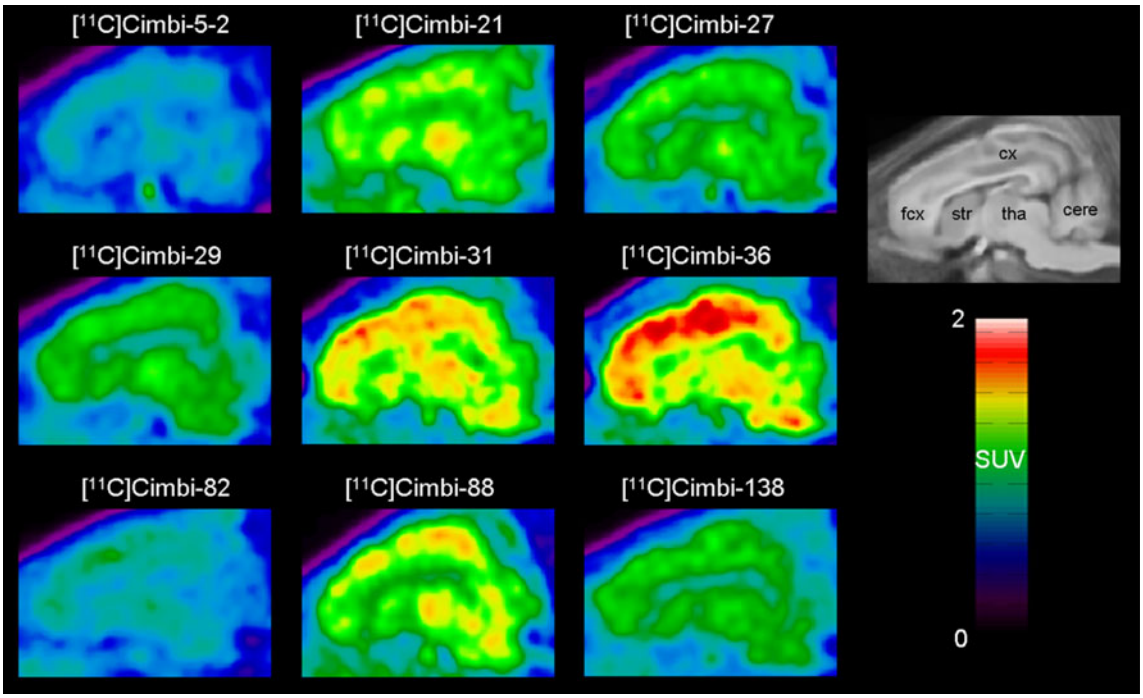

Fig. 2 Colour-coded sagittal PET images showing the average distribution of radioactivity in the pig brain from 10 to 90 min after i.v. injection of tracers. *Right insert* shows the corresponding sagittal view of the MRI-based average atlas of the pig brain with structures labelled: *fcx* frontal cortex, *cx* cerebral cortex, *tha* thalamus, *cere* cerebellum, *str* striatum

In vivo biodistribution in pig brain

All ^{11}C-phenethylamines showed significant uptake in the pig brain as demonstrated in Fig. 2, and for all PET tracers, time–activity curves showed higher uptake in the cortex than in the cerebellum (Fig. 3). The peak cortical uptake varied among the tracers: [^{11}C]Cimbi-36 and [^{11}C]Cimbi-31 showed the highest uptake with a peak around 2.2 SUV, while [^{11}C]Cimbi-5-2 and [^{11}C]Cimbi-82 showed an uptake of only around 0.8 SUV and 1.2 SUV. The cortex-to-cerebellum uptake ratios, as measured by cortical SRTM BP_{ND}, are given in Table 2. Of the nine tested PET tracers, [^{11}C]Cimbi-21 and [^{11}C]Cimbi-88 showed the lowest cortex-to-cerebellum ratios with a cortical SRTM BP_{ND} value of 0.17. PET scanning with [^{11}C]Cimbi-5-2, [^{11}C]Cimbi-27, [^{11}C]Cimbi-31 and [^{11}C]Cimbi-82 gave cortical SRTM BP_{ND} values similar to that found with [^{11}C]Cimbi-5 (0.46±0.11). [^{11}C]Cimbi-36, and [^{11}C]Cimbi-138 showed the highest cortical-to-cerebellum uptake ratios with cortical SRTM BP_{ND} values of 0.60 and 0.82, indicative of high target-to-background ratios with these tracers. For all regional time–activity curves, the peak radioactivity concentration occurred 10–20 min after injection and thereafter declined, implying that binding was reversible over the 90-min scan time. The time–activity curves showed that regional activity of [^{11}C]Cimbi-5-2 and [^{11}C]Cimbi-88 in the pig brain declined at a slower rate than that of the other PET tracers. [^{11}C]Cimbi-21, [^{11}C]Cimbi-31, [^{11}C]Cimbi-36 and [^{11}C]Cimbi-82 showed a more rapid decline in regional brain radioactivity indicating faster kinetics with these tracers. V_T was calculated using the 2TC model with metabolite-corrected arterial plasma radioactivity as input function

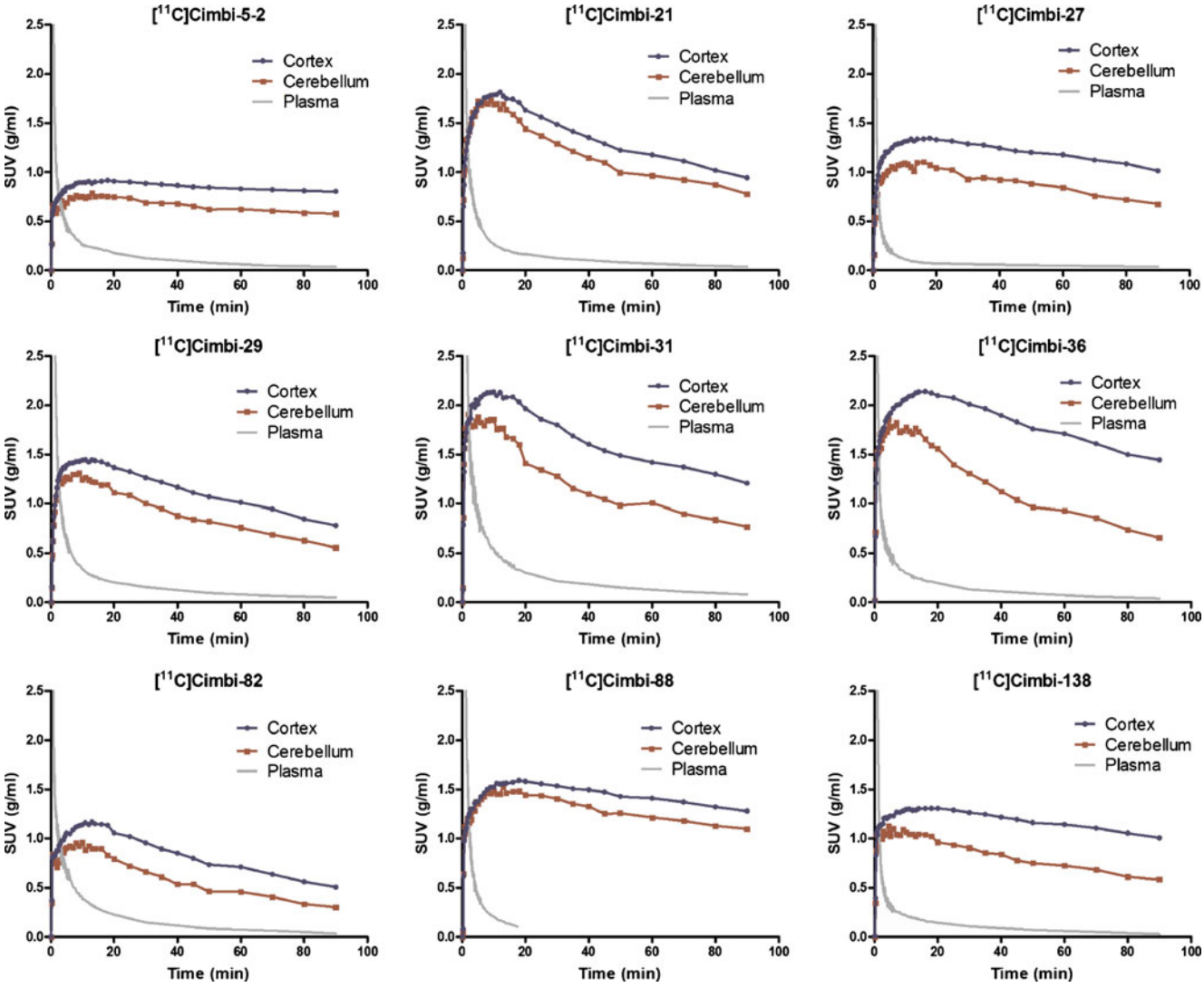

Fig. 3 Regional time–activity curves of ^{11}C- phenethylamines in the pig brain (*blue circles* cortex, *red squares* cerebellum. *grey solid lines* parent compound-corrected plasma). Standardized uptake values (SUV) in pig brain are shown for each tracer

Table 2 PET tracers in pig brain: injection data, cLogD values, free fraction and in vivo biodistribution as calculated by kinetic modelling

Tracer	Injected dose (MBq)[a]	Specific activity (GBq/μmol)[a]	cLogD[b]	Plasma free fraction (%)	2TC distribution volumes		SRTM
					Cortex	Cerebellum	Cortical BP_{ND}
[^{11}C]Cimbi-5-2	682	122.7	3.33	0.4	10.93	6.88	0.32
[^{11}C]Cimbi-21	627	9.6	3.86	0.8	7.24	5.73	0.17
[^{11}C]Cimbi-27	434	21.6	2.94	0.7	16.79	11.00	0.45
[^{11}C]Cimbi-29	710	45.2	3.35	0.4	5.15	3.57	0.32
[^{11}C]Cimbi-31	390	36.3	2.87	1.0	dnf	dnf	0.43
[^{11}C]Cimbi-36	506	210.4	3.42	1.1	13.42	6.76	0.82
[^{11}C]Cimbi-82	578	445.5	3.49	0.7	4.51	2.82	0.49
[^{11}C]Cimbi-88	462	231.2	-0.24	6.5	n.d.	n.d.	0.17
[^{11}C]Cimbi-138	589	455.6	4.40	1.2	13.85	6.19	0.60

dnf did not fit kinetic model, *n.d.* not determined.

[a] At time of injection.

[b] Calculated using CSLogD (ChemSilico).

(Table 2). Due to missing radiometabolite data, 2TC V_T could not be calculated for [^{11}C]Cimbi-82, while the [^{11}C]Cimbi-31 data did not fit the 2TC model.

Ketanserin blockade of [^{11}C]Cimbi-36 in vivo

In a single pig, the effect of pretreatment with ketanserin on [^{11}C]Cimbi-36 binding was examined. In this baseline scan, the cortical SRTM BP_{ND} of [^{11}C]Cimbi-36 was 0.70. Following i.v. administration of 10 mg/kg ketanserin 30 min prior to a second scan, BP_{ND} was decreased to 0.26. Also, the time–activity curves indicated that pretreatment with ketanserin decreased cortical [^{11}C]Cimbi-36 binding (Fig. 5). However, the ketanserin blockade was not complete as indicated by the persistent difference between the cortical and cerebellar radioactivity concentrations in the blocked time–activity curves (Fig. 5).

Radiolabelled metabolites

For all compounds with full metabolite data, the relative amount of parent compound in plasma declined exponentially at similar rates, and 5–9% remained in plasma 90 min after injection (see Fig. 6 for an example). In the radio-HPLC chromatograms of pig plasma taken 30 min after i.v. injection of the PET tracers, a distinct peak was seen for most of the PET tracers eluting prior to the parent compound (Fig. 4). This lipophilic radiolabelled metabolite reached a maximum in plasma at around 20–40 min after injection and then dropped off slightly up to 90 min (see Fig. 6 for an example). In the HPLC analysis of homogenized pig brain tissue taken 20 min after [^{11}C]Cimbi-36 injection, only negligible amounts of this metabolite were found in frontal cortex tissue compared to plasma obtained at the same time (Fig. 7). The brain tissue obtained 60 min after i.v. injection of [^{11}C]Cimbi-36 contained insufficient radioactivity for reliable HPLC analysis.

Discussion

We present here the radiosynthesis and biological evaluation of a series of substituted phenethylamines as 5-HT_{2A} receptor agonist PET tracers. Based on an in vivo screening approach involving a HRRT PET scan with each tracer, we identified [^{11}C]Cimbi-36 as the most promising candidate and conducted further studies with this compound. [^{11}C]Cimbi-36 had a higher brain uptake and improved target-to-background binding ratio over the previously validated candidate [^{11}C]Cimbi-5 (cortical SRTM BP_{ND} 0.46±0.11) [12]. We used SRTM BP_{ND} to evaluate the target-to-background binding ratios of the PET tracers since cerebellum generally is a valid reference region for quantification of 5-HT_{2A} receptor binding [3, 25]. Time–activity curves from [^{11}C]Cimbi-36 showed the highest brain uptake (peak cortical SUV 2.2), and the greatest separation between cortical and cerebellar uptake (cortical SRTM BP_{ND} 0.82) of the nine tested compounds. Thus, the target-to-background ratio of [^{11}C]Cimbi-36 was higher than those of both [^{11}C]Cimbi-5 and the eight other tested PET tracers. Although [^{11}C]Cimbi-138 also displayed promising PET tracer properties with a SRTM BP_{ND} of 0.60 and a peak cortical uptake of 1.4, [^{11}C]Cimbi-36 was superior to [^{11}C]Cimbi-138 in both measures. 5-HT_{2A} receptor blocking with ketanserin resulted in a reduction in the cortical SRTM BP_{ND} from 0.70 to 0.26, supporting the view that [^{11}C]Cimbi-36

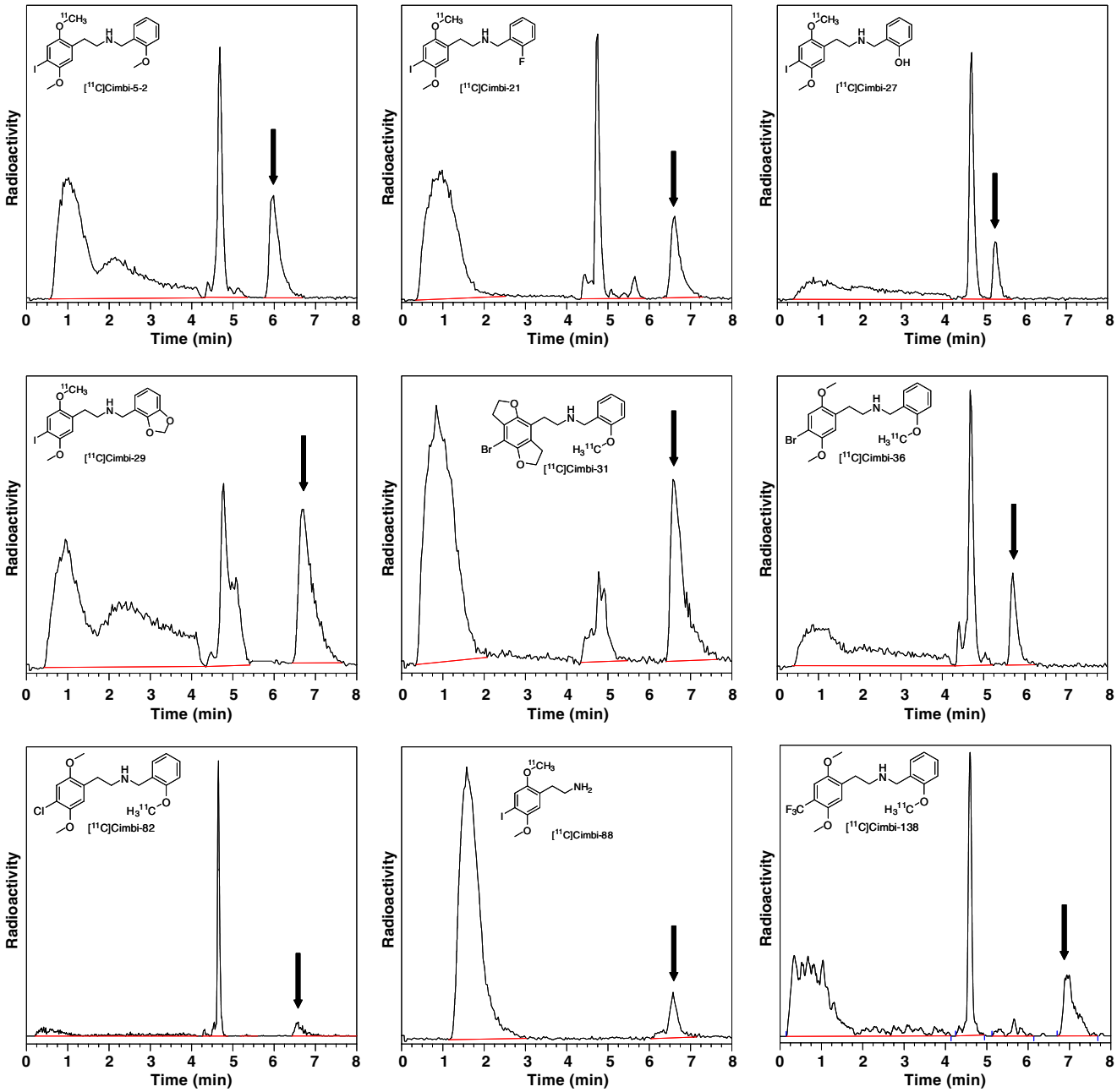

Fig. 4 HPLC radiochromatograms of pig plasma 30 min after injection (10 min for [^{11}C]Cimbi-88); *black arrows* indicate parent compounds. Eluent compositions were adjusted so that each parent compound eluted at 5–7 min retention time

binding in the pig cortex represents 5-HT_{2A} receptor binding. Furthermore, the PDSP screening results confirmed that Cimbi-36 was highly selective over non-5-HT_2 targets. Although Cimbi-36 was only threefold selective for 5-HT_{2A} receptors over 5-HT_{2C} receptors, cortical [^{11}C]Cimbi-36 signal could be attributed to 5-HT_{2A} receptor binding since the density 5-HT_{2C} receptors is negligible compared to the density of 5-HT_{2A} receptors in the cortical areas [26, 27].

PET tracers such as [^{11}C]Cimbi-21 and [^{11}C]Cimbi-88 were discarded for further studies based on their low target-to-background binding ratio in the screening procedure. The cortical SRTM BP_{ND} of these PET tracers were lower in the pig brain than that of the previously validated candidate [^{11}C]Cimbi-5. It should be noted that the [^{11}C]Cimbi-21 scan was conducted with lower specific radioactivity than the scans with the other compounds and [^{11}C]Cimbi-21 target-to-background binding ratio may have

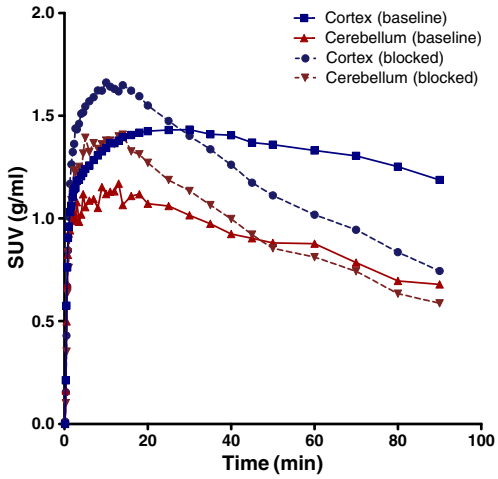

Fig. 5 Cortical and cerebellar time–activity curves of [^{11}C]Cimbi-36 from a pig brain at baseline (*blue*) and following pretreatment with 10 mg/mg ketanserin (*red*). The SUVs are normalized to injected dose per body weight. Cortical SRTM BP_{ND} of [^{11}C]Cimbi-36 was 0.70 at baseline and 0.26 after ketanserin pretreatment

been lower due to this, but it is unlikely that improving the specific radioactivity in a repeat scan with this tracer would have improved cortical BP_{ND} to the level of [^{11}C]Cimbi-36. [^{11}C]Cimbi-5-2, [^{11}C]Cimbi-27, [^{11}C]Cimbi-29, [^{11}C]Cimbi-31 and [^{11}C]Cimbi-82 showed similar brain uptake and cortical SRTM BP_{ND} as the previously labelled candidate PET tracer. Given the close structural resemblance between these compounds, it is perhaps not surprising that they showed similar properties in vivo in the pig brain.

The regional time–activity curves for [^{11}C]Cimbi-36 clearly declined over the 90 min scanning time meaning that [^{11}C]Cimbi-36 shows reversible binding to 5-HT_{2A} receptor during PET scanning. The time-activity curves of [^{11}C]Cimbi-36 also seemed more reversible than, for example, [^{11}C]Cimbi-5-2, [^{11}C]Cimbi-27 and [^{11}C]Cimbi-138. Reversible binding kinetics is advantageous for quantification [28], and the faster kinetics of [^{11}C]Cimbi-36 may prove important when moving into clinical studies in humans where kinetics are usually slower.

The in vitro binding results confirmed that all compounds tested as PET tracers had high affinity for the 5-HT_{2A} receptor and that all compounds, as expected based on their phenethylamine structure, activated 5-HT_{2A} receptors with EC_{50} values in the nanomolar range, and thus are indeed 5-HT_{2A} receptor agonists. This is in agreement with previous data showing that Cimbi-5, Cimbi-27, Cimbi-29 and Cimbi-36 are selective and high-affinity agonists [10]. Cimbi-21 and Cimbi-88 had the lowest 5-HT_{2A} receptor affinity and lower EC_{50} values than most of the other tested compounds, and they also showed the lowest target-to-background binding ratios in the in vivo studies. Since the binding potential of a PET tracer is proportional to its affinity [28], it is not surprising that the compounds with the lowest affinity also gave the lowest cortical SRTM BP_{ND}. However, Cimbi-31 showed the highest 5-HT_{2A} receptor affinity, and in this respect, it is perhaps somewhat surprising that [^{11}C]Cimbi-31 did not seem to bind receptors more irreversibly as compared to some of the other tracers as indicated by rate of washout from the cortical region. However, this testifies to the complexity of the binding in the living brain as compared to affinity constants measured in vitro. The in vivo properties of a PET tracer are influenced by several factors, including brain uptake and transport, binding kinetics and very prominently non-specific binding. We report here roughly similar in vitro binding and activation properties of Cimbi-36, Cimbi-5, Cimbi-27, Cimbi-29 and Cimbi-82, yet [^{11}C]Cimbi-36 was a markedly better PET tracer with higher target-to-background ratios compared to all these compounds.

Thus, in this series of substituted ^{11}C-phenethylamines we demonstrated that minor structural changes may alter the PET tracer properties of a compound without greatly changing its in vitro properties. With these nine tested PET tracers there was no apparent relationship between calculated LogD values and nonspecific uptake as determined by cerebellum V_T. This indicates that the nonspecific binding for phenethylamine PET tracers is dependent on factors other than just lipophilicity, and that lipophilicity alone is not a solid predictor of the level of nonspecific binding of a PET tracer in vivo, which has also been suggested previously [29].

Most of the tested *N*-benzyl substituted ^{11}C-phenethylamines gave rise to a distinct lipophilic radiolabelled metabolite. We were unable to determine the identity of these labelled metabolites in pig plasma based on the retention time on the radiochromatograms alone. It is proposed that they result from an *O*-demethylation at the 2- or 5-methoxy position in the phenethylamine moiety. Several lines of evidence support this speculation. Firstly, DOI has been shown to be metabolized through demethylation at either or both methoxy groups [30]. Further, the radiochromatograms for [^{11}C]Cimbi-31 (which has no methoxy groups in the

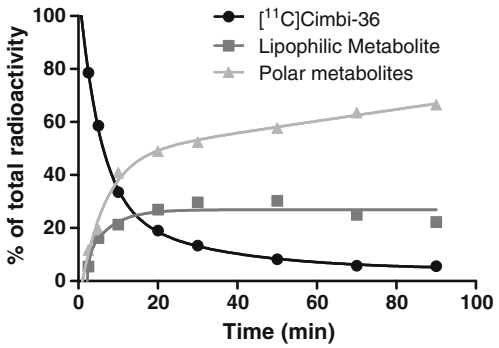

Fig. 6 HPLC analysis of radioactive metabolites in pig plasma after i.v. injection of [^{11}C]Cimbi-36. The amounts of parent compound (*circles*), lipophilic metabolite (*squares*) and polar metabolites (*triangles*) are shown as percent of total radioactivity

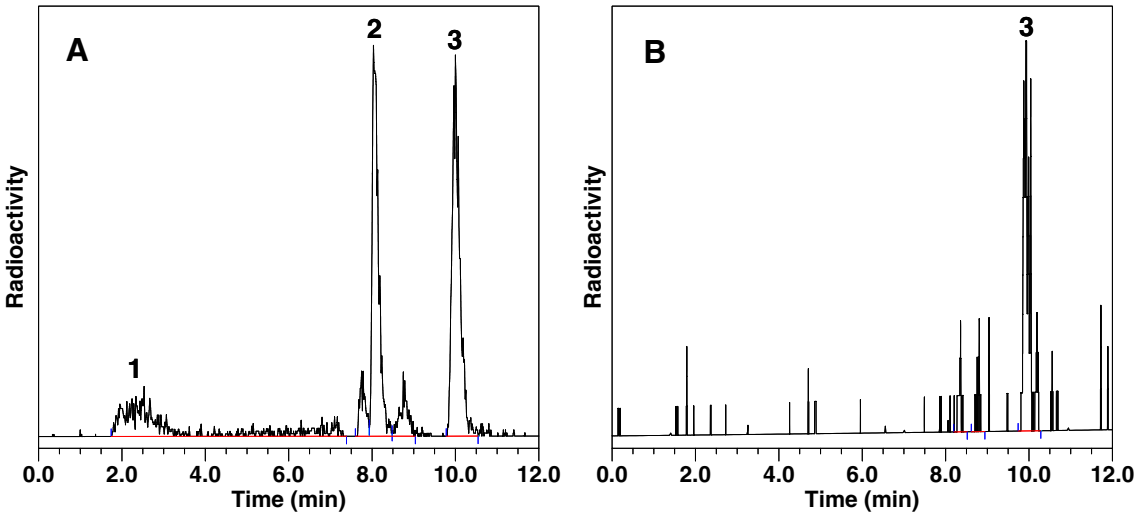

Fig. 7 HPLC analysis of plasma (**a**) and frontal cortex extract (**b**) 20 min after injection of [^{11}C]Cimbi-36. Peaks: *1* polar metabolites, *2* lipophilic metabolites, *3* parent compound

phenethylamine moiety) only showed small amounts of lipophilic metabolites. Also, the demethylation products of [^{11}C]Cimbi-88 would be rather polar and therefore would be expected to elute with polar metabolites, as was the case. The metabolism of Cimbi-88 has also been reported to involve demethylation at both the 2- and 5-methoxy positions [31]. Changing the 4-substituent from iodine to bromine, chlorine or trifluoromethyl in the phenethylamine moiety had a considerable effect on the amount of radiolabelled metabolite in plasma. Since the parent compound in plasma declined similarly over time for all compounds ([^{11}C]Cimbi-5-2, [^{11}C]Cimbi-36, [^{11}C]Cimbi-82 and [^{11}C]Cimbi-138), this difference is probably caused by variation in the rate of further metabolism of the lipophilic metabolites. However, further studies would be needed to uniquely identify the in vivo metabolic route of these substituted phenethylamines.

Given that a radiolabelled metabolite of [^{11}C]Cimbi-36 was present in pig plasma, we investigated the possible presence of the metabolite in pig brain. Although a substantial amount of radiometabolite was present in plasma 20 min after i.v. injection of [^{11}C]Cimbi-36, the radiometabolite was barely detectable in frontal cortex tissue from the same pig (Fig. 7). This suggests that the radiometabolite of [^{11}C]Cimbi-36 does not enter the brain to any extent that would interfere with the [^{11}C]Cimbi-36 signal or decrease the binding potential in vivo. Based on our data, however, we cannot firmly dismiss the presence of some radiometabolites in pig brain since some small peaks were observed in the radiochromatograms which concurrently were noisy due to the dilution of the tissue needed for homogenization. In contrast, plasma is loaded directly to the HPLC without dilution, and thus the chromatogram was less noisy. Although on the basis of the present results we cannot rule out the presence of radiolabelled metabolites in pig brain, a much lower fraction was clearly present in brain compared to plasma, and the small amounts in brain implied by the tissue radiochromatogram may have been derived from blood present in the vascular compartments of the brain tissue.

All the *N*-benzyl-substituted ^{11}C-phenethylamines had a low free fraction in pig plasma (0.4–1.5%); a low free plasma fraction should theoretically impair brain uptake. However, since many of these compounds with similar free fractions showed different degrees of brain uptake as measured by peak SUV, it seems that the level of brain uptake is not markedly influenced by the fraction of free tracer in plasma. The only non-*N*-benzyl-substituted compound, [^{11}C]Cimbi-88, had a higher free fraction in pig plasma (6.5%) which is in accordance with this compound being less lipophilic than the *N*-benzyl-substituted tracers. However, brain uptake of [^{11}C]Cimbi-88 was lower than that of [^{11}C]Cimbi-36, [^{11}C]Cimbi-27 and [^{11}C]Cimbi-31.

Two PET scans were performed with [^{11}C]Cimbi-36 and [^{11}C]Cimbi-82 at relatively low specific radioactivities (6.9 and 9.0 GBq/μmol, respectively; data not shown). In these scans, lower cortical BP_{ND} were found for both tracers, suggesting that tracer doses for 5-HT_{2A} receptor agonist binding were exceeded. Thus, future PET studies with [^{11}C]Cimbi-36 should be conducted with an injected mass of <10 μg cold dose.

Conclusion

Our in vivo screening of phenethylamine 5-HT_{2A} receptor agonist PET tracers led to the identification of [^{11}C]Cimbi-36 as the most promising PET tracer for further investigations. [^{11}C]Cimbi-36 showed the highest target-to-background

binding ratio of all compounds tested, and it was also displaceable by ketanserin in vivo, supporting its 5-HT_{2A} receptor selectivity. In vitro studies confirmed that [^{11}C]Cimbi-36 is a highly potent, high-affinity and selective 5-HT_{2A} receptor agonist. Thus, [^{11}C]Cimbi-36 is currently the most promising PET tracer for imaging cerebral 5-HT_{2A} receptor agonist binding in the living brain.

Acknowledgments The technical assistance of Letty Klarskov, Mette Værum Olesen, Bente Dall and Jack Frausing Nielsen is gratefully acknowledged. This study was financially supported by the Lundbeck Foundation, University of Copenhagen, Faculty of Health Sciences, the Toyota Foundation, the John and Birthe Meyer Foundation, and by the EU 6th Framework program DiMI (LSHB-CT-2005-512146). [^{3}H]MDL100907 was kindly provided by Prof. Christer Halldin, Karolinska Institute, Sweden. K_i determinations at neuroreceptors were generously provided by the National Institute of Mental Health's Psychoactive Drug Screening Program, Contract no. HHSN-271-2008-00025-C (NIMH PDSP). The NIMH PDSP is directed by Bryan L. Roth, MD PhD, at the University of North Carolina at Chapel Hill, and Project Officer Jamie Driscol at NIMH, Bethesda MD, USA.

Conflicts of interest None.

References

1. Gonzalez-Maeso J, Weisstaub NV, Zhou M, et al. Hallucinogens recruit specific cortical 5-HT(2A) receptor-mediated signaling pathways to affect behavior. Neuron. 2007;53:439–52.
2. Abbas A, Roth BL. Pimavanserin tartrate: a 5-HT2A inverse agonist with potential for treating various neuropsychiatric disorders. Expert Opin Pharmacother. 2008;9:3251–9.
3. Pinborg LH, Adams KH, Svarer C, et al. Quantification of 5-HT2A receptors in the human brain using [18F]altanserin-PET and the bolus/infusion approach. J Cereb Blood Flow Metab. 2003;23:985–96.
4. Ito H, Nyberg S, Halldin C, Lundkvist C, Farde L. PET imaging of central 5-HT2A receptors with carbon-11-MDL 100,907. J Nucl Med. 1998;39:208–14.
5. Fitzgerald LW, Conklin DS, Krause CM, et al. High-affinity agonist binding correlates with efficacy (intrinsic activity) at the human serotonin 5-HT2A and 5-HT2C receptors: evidence favoring the ternary complex and two-state models of agonist action. J Neurochem. 1999;72:2127–34.
6. Song J, Hanniford D, Doucette C, et al. Development of homogeneous high-affinity agonist binding assays for 5-HT2 receptor subtypes. Assay Drug Dev Technol. 2005;3:649–59.
7. Cornea-Hebert V, Watkins KC, Roth BL, et al. Similar ultrastructural distribution of the 5-HT(2A) serotonin receptor and microtubule-associated protein MAP1A in cortical dendrites of adult rat. Neuroscience. 2002;113:23–35.
8. Peddie CJ, Davies HA, Colyer FM, Stewart MG, Rodriguez JJ. Colocalisation of serotonin2A receptors with the glutamate receptor subunits NR1 and GluR2 in the dentate gyrus: an ultrastructural study of a modulatory role. Exp Neurol. 2008;211:561–73.
9. Cumming P, Wong DF, Gillings N, Hilton J, Scheffel U, Gjedde A. Specific binding of [(11)C]raclopride and N-[(3)H]propyl-norapomorphine to dopamine receptors in living mouse striatum: occupancy by endogenous dopamine and guanosine triphosphate-free G protein. J Cereb Blood Flow Metab. 2002;22:596–604.
10. Braden MR, Parrish JC, Naylor JC, Nichols DE. Molecular interaction of serotonin 5-HT2A receptor residues Phe339(6.51) and Phe340(6.52) with superpotent N-benzyl phenethylamine agonists. Mol Pharmacol. 2006;70:1956–64.
11. Nichols DE, Frescas SP, Chemel BR, Rehder KS, Zhong D, Lewin AH. High specific activity tritium-labeled N-(2-methoxybenzyl)-2,5-dimethoxy-4-iodophenethylamine (INBMeO): a high-affinity 5-HT2A receptor-selective agonist radioligand. Bioorg Med Chem. 2008;16:6116–23.
12. Ettrup A, Palner M, Gillings N, Santini MA, Hansen M, Kornum BR, et al. Radiosynthesis and evaluation of 11C-CIMBI-5 as a 5-HT2A receptor agonist radioligand for PET. J Nucl Med. 2010;51:1763–70.
13. Narendran R, Mason NS, Laymon CM, et al. A comparative evaluation of the dopamine D(2/3) agonist radiotracer [11C](-)-N-propyl-norapomorphine and antagonist [11C]raclopride to measure amphetamine-induced dopamine release in the human striatum. J Pharmacol Exp Ther. 2010;333:533–9.
14. Narendran R, Hwang DR, Slifstein M, et al. In vivo vulnerability to competition by endogenous dopamine: comparison of the D2 receptor agonist radiotracer (-)-N-[11C]propyl-norapomorphine ([11C]NPA) with the D2 receptor antagonist radiotracer [11C]-raclopride. Synapse. 2004;52:188–208.
15. Paterson LM, Tyacke RJ, Nutt DJ, Knudsen GM. Measuring endogenous 5-HT release by emission tomography: promises and pitfalls. J Cereb Blood Flow Metab. 2010;30:1682–706.
16. Shulgin A, Shulgin A. PIHKAL, a chemical love story. Berkeley, CA: Transform Press; 1991. p. 1–978.
17. Nichols DE, Frescas S, Marona-Lewicka D, et al. 1-(2,5-Dimethoxy-4-(trifluoromethyl)phenyl)-2-aminopropane: a potent serotonin 5-HT2A/2C agonist. J Med Chem. 1994;37:4346–51.
18. Monte AP, Marona-Lewicka D, Parker MA, Wainscott DB, Nelson DL, Nichols DE. Dihydrobenzofuran analogues of hallucinogens. 3. Models of 4-substituted (2,5-dimethoxyphenyl) alkylamine derivatives with rigidified methoxy groups. J Med Chem. 1996;39:2953–61.
19. Herth MM, Kramer V, Piel M, et al. Synthesis and in vitro affinities of various MDL 100907 derivatives as potential 18F-radioligands for 5-HT2A receptor imaging with PET. Bioorg Med Chem. 2009;17:2989–3002.
20. Sureau FC, Reader AJ, Comtat C, et al. Impact of image-space resolution modeling for studies with the high-resolution research tomograph. J Nucl Med. 2008;49:1000–8.
21. Watanabe H, Andersen F, Simonsen CZ, Evans SM, Gjedde A, Cumming P. MR-based statistical atlas of the Gottingen minipig brain. Neuroimage. 2001;14:1089–96.
22. Kornum BR, Lind NM, Gillings N, Marner L, Andersen F, Knudsen GM. Evaluation of the novel 5-HT4 receptor PET ligand [11C]SB207145 in the Gottingen minipig. J Cereb Blood Flow Metab. 2009;29:186–96.
23. Lammertsma AA, Hume SP. Simplified reference tissue model for PET receptor studies. Neuroimage. 1996;4:153–8.
24. Gillings N. A restricted access material for rapid analysis of [11C]-labeled radiopharmaceuticals and their metabolites in plasma. Nucl Med Biol. 2009;36:961–5.
25. Meyer PT, Bhagwagar Z, Cowen PJ, Cunningham VJ, Grasby PM, Hinz R. Simplified quantification of 5-HT2A receptors in the human brain with [11C]MDL 100,907 PET and non-invasive kinetic analyses. Neuroimage. 2010;50:984–93.
26. Kristiansen H, Elfving B, Plenge P, Pinborg LH, Gillings N, Knudsen GM. Binding characteristics of the 5-HT2A receptor antagonists altanserin and MDL 100907. Synapse. 2005;58:249–57.
27. Marazziti D, Rossi A, Giannaccini G, et al. Distribution and characterization of [3H]mesulergine binding in human brain postmortem. Eur Neuropsychopharmacol. 1999;10:21–6.

28. Innis RB, Cunningham VJ, Delforge J, et al. Consensus nomenclature for in vivo imaging of reversibly binding radioligands. J Cereb Blood Flow Metab. 2007;27:1533–9.
29. Guo Q, Brady M, Gunn RN. A biomathematical modeling approach to central nervous system radioligand discovery and development. J Nucl Med. 2009;50:1715–23.
30. Ewald AH, Fritschi G, Maurer HH. Metabolism and toxicological detection of the designer drug 4-iodo-2,5-dimethoxy-amphetamine (DOI) in rat urine using gas chromatography-mass spectrometry. J Chromatogr B Analyt Technol Biomed Life Sci. 2007;857:170–4.
31. Theobald DS, Putz M, Schneider E, Maurer HH. New designer drug 4-iodo-2,5-dimethoxy-beta-phenethylamine (2C-I): studies on its metabolism and toxicological detection in rat urine using gas chromatographic/mass spectrometric and capillary electrophoretic/mass spectrometric techniques. J Mass Spectrom. 2006;41:872–86.